THE DEVELOPMENT OF DETAILED CHEMICAL KINETICS MODELS FOR *n*-HEPTANE AND TOLUENE COMBUSTION

R.P. Lindstedt and L.Q. Maurice

Department of Mechanical Engineering,
Imperial College of Science, Technology and Medicine,
Exhibition Road, London SW7 2BX, UK

JUNE 1994

THERMOFLUIDS REPORT NUMBER TF/94/22

REPORT DOCUMENTATION PAGE

Form Approved OMB No. 0704-0188

1. AGENCY USE ONLY (Leave blank)	2. REPORT DATE	3. REPORT TYPE AND DATES COVERED
	June 1994	Final Report

4. TITLE AND SUBTITLE

The Development of Detailed Chemical Kinetics Models for n-Heptane and Toluene Combustion

5. FUNDING NUMBERS

F6170894W0153

6. AUTHOR(S)

Dr. R. Peter Lindstedt and L.Q. Maurice

7. PERFORMING ORGANIZATION NAME(S) AND ADDRESS(ES)

Imperial College of Science, Technology and Medicine
Mechanical Engineering Dept
Exhibition Road
London SW7 2BX UK

8. PERFORMING ORGANIZATION REPORT NUMBER

TF/94/22

9. SPONSORING/MONITORING AGENCY NAME(S) AND ADDRESS(ES)

EOARD
PSC 802 BOX 14
FPO 09499-0200

10. SPONSORING/MONITORING AGENCY REPORT NUMBER

SPC-94-4014

11. SUPPLEMENTARY NOTES

12a. DISTRIBUTION/AVAILABILITY STATEMENT

Approved for public release; distribution is unlimited.

12b. DISTRIBUTION CODE

A

13. ABSTRACT (Maximum 200 words)

Detailed chemical kinetics mechanisms for the combustion of n-heptane, a toluene/n-heptane blend and toluene have been assembled and validated against counterflow diffusion flame and stirred reactor data. To our knowledge, this is the first published comprehensive data of n-heptane, toluene/n-heptane and toluene diffusion flame structures using detailed chemistry and the first reported successful effort at predicting intermediate species in the structures of these flames.

14. SUBJECT TERMS

15. NUMBER OF PAGES

181

16. PRICE CODE

17. SECURITY CLASSIFICATION OF REPORT	18. SECURITY CLASSIFICATION OF THIS PAGE	19. SECURITY CLASSIFICATION OF ABSTRACT	20. LIMITATION OF ABSTRACT
UNCLASSIFIED	UNCLASSIFIED	UNCLASSIFIED	UL

TABLE OF CONTENTS

TABLE OF CONTENTS (CONCLUDED)

LIST OF FIGURES

LIST OF FIGURES (CONTINUED)

LIST OF FIGURES (CONCLUDED)

LIST OF TABLES

LIST OF TABLES (CONTINUED)

LIST OF TABLES (CONTINUED)

LIST OF TABLES (CONTINUED)

LIST OF TABLES (CONTINUED)

LIST OF TABLES (CONCLUDED)

ABSTRACT AND ACKNOWLEDGEMENTS

Detailed chemical kinetics mechanisms for the combustion of *n*-heptane, a toluene/*n*-heptane blend and toluene have been assembled and validated against counterflow diffusion flame and stirred reactor data. To our knowledge, this is the first published comprehensive data of *n*-heptane, toluene/*n*-heptane and toluene diffusion flame structures using detailed chemistry and the first reported successful effort at predicting intermediate species in the structures of these flames.

Analytical predictions of temperature and major and intermediate species profiles for *n*-heptane counterflow diffusion flames show excellent agreement with the experimental data of two independent researchers. The *n*-heptane kinetics mechanism was also used to reproduce stirred reactor experimental data with agreement equal to or better than previously reported in the literature.

The structure of a toluene/*n*-heptane diffusion flame is also predicted with excellent quantitative agreement of temperature, major and minor species profiles. The predicted temperature and species profiles for a pure toluene diffusion flame are presented as well. Detailed experimental data was not available to validate the pure toluene diffusion flame model, however, results are shown to be sensible based on limited experimental data and the successful prediction of the toluene/*n*-heptane flame structure. The toluene mechanism is also validated against stirred reactor data.

The authors would like to thank Professor K. Seshadri of the University of California, San Diego, for providing *n*-heptane, toluene and toluene/*n*-heptane diffusion flame data. We also wish to thank Professor A. Burcat of the Technion for providing thermochemical data and Charles Westbrook of Lawrence Livermore National Laboratory for providing many useful references.

This work was partially funded by the Aero Propulsion and Power Directorate, Wright Laboratory, Wright-Patterson Air Force Base, Ohio, United States Air Force, under Contract F6170894W0153, administered by the European Office of Aerospace Research and Development (EOARD), London, United Kingdom.

1.0 INTRODUCTION

Endothermic fuels, typically hydrocarbon liquids which undergo heat absorbing chemical reactions, have been established as one of the most promising fuel candidates for air breathing engines capable of operating at high supersonic flight speeds due to their high heat sink potential [1,2]. The bulk of endothermic fuel research to date has been aimed at developing catalysts and heat exchangers/reactors to optimise the available heat sink of selected fuel candidates. The most promising near term fuel candidates identified are methyl-cyclohexane (C_7H_{14}) and *n*-heptane (C_7H_{16}). Toluene and hydrogen are the main fuel components resulting from the dehydrogenation of the former and ethylene and hydrogen are the primary constituents of thermal cracking of the latter [3,4]. To date, experiments aimed at studying the combustion characteristics of endothermic fuels and their decomposition products [5,6,7,8,9,10] have been limited to measurements of flame speeds and auto ignition temperatures in simplified geometries. However, a programme aimed at studying the combustion properties of these fuels in high speed propulsion devices, such as ram burners and turbo ramjet after burners, is currently underway [11]. The aim of the companion analytical programme conducted at Imperial College is to accurately model the chemistry and physics of the combustion processes of these fuel components.

In most detailed combustor flow field studies, the general practice is to assume "fast chemistry" or to replace the chemical kinetics of the fuel consumption process with a few global steps. This approach is sensible and justifiable in many combustor systems where the combustion processes are mixing, rather than kinetically, controlled. However, in high speed propulsion systems, many important phenomena are kinetically limited. Ignition delay, flame speed, blowout and relight at high altitude, product distribution, engine efficiency and pollutant emissions are just some of the issues that must be addressed through kinetic studies [12]. It is readily recognised that the introduction of detailed chemical reaction mechanisms into complex multi-dimensional fluid dynamics problems is computationally prohibitive. The detailed chemical kinetics of even a simple fuel such as hydrogen in air must be modelled with a scheme involving 9 species and around 50 elementary reactions [13]. Thus, simplified reaction mechanisms which have been thoroughly validated must be developed in order to address realistic combustor configurations. Many reduced reaction mechanisms currently in use are generally formulated via educated guesses and trial and error techniques. The goals of the research currently being performed at Imperial College are to develop full chemical kinetics reaction mechanisms for endothermic fuels, verify their validity in both premixed and diffusion flame configurations, and to subsequently reduce the mechanisms to manageable proportions via systematic methods. The resulting simplified mechanisms will subsequently be applied to configurations of relevance to the experimental programme [11]. Whereas detailed reaction mechanisms for many fuels have been extensively developed and validated, detailed mechanisms for C_7 hydrocarbons have not been thoroughly addressed. This interim report covers the development and validation of a detailed chemical reaction mechanism for *n*-heptane and toluene.

Several studies have been conducted to verify the chemical reaction mechanisms of C_1-C_6 hydrocarbon fuels [14-24]. However, the development of detailed mechanisms for C_7 hydrocarbons has been generally limited to studies of premixed systems such as stirred reactors

and shock tubes [25-37]. A numerical study of an *n*-heptane diffusion flame was undertaken by Bui-Pham and Seshadri [38]. However, a very simplified reaction mechanism for the *n*-heptane consumption consisting of only three radical attack steps to form the heptyl (C_7H_{15}) radical and a single pyrolysis step to decompose the heptyl radical to the methyl radical (CH_3) and propene (C_3H_6) was used. The overall mechanism [38] consisted of 96 elementary reactions. Temperature and major species profiles were predicted with reasonable accuracy but comparisons of intermediate species were not provided. Recently, Darabiha *et al* [39] have analysed a laminar counterflow spray diffusion flame using a mechanism featuring 28 elementary reactions to model the *n*-heptane decomposition. However, no comparisons of either major or intermediate species were reported.

In the present study two detailed chemical kinetics mechanisms for *n*-heptane combustion were assembled and validated. The first high temperature mechanism comprises of 481 elementary reactions and 86 species. Of these, 123 elementary reactions and 14 species are specific to the *n*-heptane sub-mechanism. This mechanism has been validated using literature data for *n*-heptane counterflow diffusion flames [40-43]. A more extensive intermediate to high temperature mechanism featuring 93 species and 582 elementary reactions was used to model *n*-heptane combustion in a stirred reactor. Experimental data suitable for validation of this mechanism has been obtained by Chakir *et al* [32]. The influence of the additional 8 species and 101 elementary reactions on the *n*-heptane combustion process was assessed and resulted in the formulation of a more general scheme also for diffusion flames. This mechanism features 485 reactions and 87 species. The *n*-heptane sub-mechanisms were added to the extensively validated cyclic C_6 and C_1-C_4 mechanism developed by Lindstedt and co-workers [19-24] for premixed and diffusion flames. Comparisons between experimental and computational results for *n*-heptane combustion are presented in Section 3. The full mechanisms are provided in Appendix A.

Additionally, a detailed mechanism for the combustion of *n*-heptane and toluene fuel blends was developed. This mechanism did not include as much detail as the full *n*-heptane or toluene sub-mechanisms assembled. Rather, path analyses of the combustion processes of pure *n*-heptane and toluene diffusion flames were performed. Only those elementary reactions shown to dominate the production and consumption of each individual specie were included in the dual fuel sub-mechanism. The omissions made are outlined below. The final *n*-heptane/toluene combustion sub-mechanism consists of 441 elementary reactions and 91 species. It was validated using literature data for a 60% toluene/40% *n*-heptane counterflow diffusion flame [42, 43]. Comparisons between experimental and computational results are shown in Section 4. The dual fuel sub-mechanism is included in Table D1 in Appendix D.

Finally, a detailed sub-mechanisms for the combustion of toluene was developed. This mechanism is based primarily on the work of Emdee *et al* [29] and features 437 elementary reactions and 86 species. The toluene decomposition sub-mechanism comprises of 80 elementary reactions and 14 species. Sufficient experimental data in toluene diffusion flames was not available to permit a comprehensive validation, though attempts were made to compare computational results to the experiments of Hamins and Seshadri [42] and Hamins [43]. The mechanism was then modified to include 447 elementary reactions and 87 species and validated against stirred reactor experimental data [44-46]. This resulted in a more general mechanism also for diffusion flames. Results of

these comparisons are presented in Section 5.0 and the toluene combustion sub-mechanisms are shown in Tables D2 and D3 in Appendix D.

A final mechanism for all cases has been assembled and is provided in Appendix H.

2.0 MODELLING APPROACH

2.1 DIFFUSION FLAMES

The counterflow diffusion flames were computed using a numerical model, LACDIF [47], developed by Lindstedt at Imperial College. The model employs a similarity transformation coordinate system to solve the momentum, species transport and energy equations along a stagnation point stream line. The temperature and density fields are evaluated subsequently following the solution of an energy enthalpy equation. The time dependent initial value problem is initiated from the flame structure of a previously converged flamelet, the new boundary conditions are specified and the solution is allowed to march in time until steady-state temperature and species profiles are obtained. The code includes a kinetics model for soot formation and can account for radiative heat loss caused by soot. The radiative heat loss model is based on the work of Kent and Honnery [48], and the appropriate constants for predicting heat loss due to soot were developed by Leung *et al* [49].

The development of the governing equations for counterflow diffusion flames in a similarity transformed coordinate system has been thoroughly documented by several authors [15, 16, 50]. For completeness, the equations are repeated below:

$$\frac{\partial V}{\partial \eta} + \Phi' = 0$$

$$\frac{1}{a}\frac{\partial \Phi'}{\partial t} + V\frac{\partial \Phi'}{\partial \eta} = \frac{\partial}{\partial \eta}\left\{\mu'\frac{\partial \Phi'}{\partial \eta}\right\} + \left\{\frac{1}{\rho'} - \Phi'\right\}$$

$$\frac{1}{a}\frac{\partial Y_k}{\partial t} + V\frac{\partial Y_k}{\partial \eta} = -\frac{\partial J_k}{\partial \eta} + \frac{R_k M_k}{\rho a}$$

$$\frac{1}{a}\frac{\partial h}{\partial t} + V\frac{\partial h}{\partial \eta} = \frac{\partial}{\partial \eta}\left\{\frac{\mu'}{\sigma_{\mathrm{Pr}}}\frac{\partial h}{\partial \eta}\right\} + \frac{\partial}{\partial \eta}\left\{\sum_{k=1}^{nsp} h_k\left\{-J_k - \frac{\mu'}{\sigma_{\mathrm{Pr}}}\frac{\partial Y_k}{\partial \eta}\right\}\right\}$$

where

$$\Phi' = \frac{u}{u_e}\ ,\quad \mu' = \frac{\rho\mu}{\rho_e\mu_e}\ ,\quad \rho' = \frac{\rho}{\rho_e}\ ,\quad V = \frac{\rho \mathrm{v}}{\sqrt{\rho_e\mu_e a}}\ ,\quad \eta = \sqrt{\frac{a}{\mu_e\rho_e}}\int_0^y \rho dx$$

In these equations the components u and v indicate the velocity components in the x and y directions, ρ is the fluid density, h is the mixture enthalpy, μ is the fluid viscosity, Y_k is the mass

fraction and M_k is the molar mass of species k. The rate of strain is indicated by a and the subscript "e" denotes values prevailing in the potential flow at the "edge" of the boundary layer.

The chemical reaction rate source term is written as,

$$R_k = \sum_{j=1}^{nreac} \Xi_{jk} \left\{ k_j^f \prod_{l=1}^{nsp} \Phi_l^{\xi_{jk}} - k_j^r \prod_{l=1}^{nsp} \Phi_l^{\xi_{jk}} \right\}$$

The expression for the flux term is as proposed by Jones and Lindstedt [51] and for counterflow diffusion flames may be written as,

$$J_k = -\frac{\mu'}{\sigma_{Sc}} \left\{ \frac{\partial Y_k}{\partial \eta} - Y_k \frac{1}{\eta} \frac{\partial \nu}{\partial \eta} \right\} - \frac{\mathrm{v_c}}{\mathrm{v}} V Y_k$$

The transport coefficients are evaluated using the same technique as that used by Jones and Lindstedt [51]. The above equation system was solved using an implicit difference formulation involving two point backward time differencing and central differences for the spatial derivatives. The resulting set of algebraic equations are non-linear and a Newton linearisation was used for the source terms in the species transport equations,

$$R_k' = \sum_{j=1}^{nreac} \Xi_{jk} \left\{ k_j^f \prod_{l=1}^{nsp} \Phi_l^{\xi_{jk}} - k_j^r \prod_{l=1}^{nsp} \Phi_l^{\xi_{jk}} \right\}$$

$$R_k^{\nu+1} = R_k^{\nu} + \sum_{l=1}^{nsp} \frac{\partial R_k'}{\partial \Phi_l} \frac{\partial \Phi_l}{\partial Y_l} \left\{ Y_l^{\nu+1} - Y_l^{\nu} \right\}$$

Additional details regarding the solution procedures may be found in Jones and Lindstedt [52, 53].

The solution of the *n*-heptane and toluene flames was initiated by solving for the structure of a 50% *n*-heptane or toluene and 50% propane counterflow diffusion flame. The applied air side boundary conditions were set to match those of the particular experiment being modelled whereas the initial velocity, enthalpy and species profiles were those for a fully converged propane flamelet. The *n*-heptane or toluene was allowed to diffuse into the boundary until the 50% initial condition was achieved. Thereafter, the boundary was set at 100% *n*-heptane or toluene and the new flamelet allowed to converge. The velocity gradient *2V/R* (rate of strain) was set according to the reported experimental conditions and the fuel injection velocity was adjusted to stabilise the flame in the computational grid. A total of 132 grid points were used and the mesh distribution was adjusted to capture those portions of the flame structure where large gradients in temperature or species concentration occurred. The resulting system of equations was extremely stiff and very small time steps on the order of 1×10^{-6} seconds had to be utilised initially. Once the flame

velocity profile was stabilised in the computational grid, the time step could be increased to values as high as $1x10^{-4}$ seconds. Attempts to further increase this time step were unsuccessful. Full convergence was achieved after integrating the equations forward in time for approximately 20 (adiabatic solution) to 40 milliseconds (soot and radiation heat loss solution). The computations were carried out on a Silicon Graphics Indigo Work Station. The magnitude of the reaction mechanism led to a total computational time of approximately two weeks for each of the initial *n*-heptane or toluene flamelets. Once a converged solution was obtained, parametric analyses of the effects of rates of strain or individual elementary reaction steps could be completed in approximately one day.

The solution of the toluene/*n*-heptane blend flame was achieved by allowing 60% toluene to diffuse into the boundary of a fully converged *n*-heptane flamelet. The computational time for the adiabatic solution was approximately one week and an additional week was needed to achieve a converged solution accounting for soot and radiation heat loss.

2.2 STIRRED REACTORS

The perfectly stirred reactor was modelled via a modified premixed laminar flame numerical code. The code, LAPREM, was also developed by Lindstedt [54]. The model utilises the X-ω coordinate system formulated by Patankar and Spalding [55] to solve the species transport and energy equations.

Since a perfectly stirred reactor is assumed to be spatially uniform, the conservation of mass and energy are simply related to the net generation of chemical species. Only a single point solution is necessary, as opposed to solving for a complete flow field as is necessary to determine the structure of propagating flames. The governing equations for the perfectly stirred reactor are also well documented [31] and thus are only outlined briefly. The equations can be written as:

$$\frac{\partial Y_k}{\partial t} = -\frac{1}{\tau}(Y_k - Y_k^*) + \frac{R_k M_k}{\rho}$$

$$\frac{\partial h}{\partial t} = -\frac{1}{\tau}\sum_{k=1}^{nsp}(Y_k h_k - Y_k^* h_k^*)$$

In the above equations ρ indicates the fluid density, h is the total mixture enthalpy, μ is the fluid viscosity, Y_k is the mass fraction and M_k is the molar mass of species k, τ is the nominal reactor residence time, and V is the reactor volume. The superscript (*) indicates the inlet conditions. The nominal residence time is related to the reactor volume and mass flow rate by,

$$\tau = \frac{\rho V}{m}$$

The reaction rate source term is once more written as for the counterflow diffusion flame case,

$$R_k = \sum_{j=1}^{nreac} \Xi_{jk} \left\{ k_j^f \prod_{l=1}^{nsp} \Phi_l^{\xi_{jk}} - k_j^r \prod_{l=1}^{nsp} \Phi_l^{\xi_{jk}} \right\}$$

The computational procedure involves specifying the temperature and composition of the initial reaction zone and the nominal residence time of the reactor. An initial time step is specified as well, and the algebraic equations describing species concentrations and enthalpy are then solved, marching in time, until a steady state solution is achieved. The initial enthalpy and products distribution were those of the chemical equilibrium solutions for the combustion of *n*-heptane or toluene in O_2/N_2 mixtures as specified in the particular experiment being used for validation. It is crucial that a sufficient amount of radicals be included in this initial profile to initiate and sustain the reaction.

3.0 *n*-HEPTANE COMBUSTION

3.1 *n*-HEPTANE MECHANISMS

3.1.1 DESCRIPTION OF *n*-HEPTANE MECHANISM FOR DIFFUSION FLAMES

The starting block for the *n*-heptane combustion sub-mechanism applied to diffusion flames was the mechanism developed by Leung, Lindstedt and Skevis [20-24] for hydrocarbons up to C_6. The scheme also includes simplified soot formation chemistry [56]. The mechanism consists of 72 species and 358 elementary reactions and has been thoroughly discussed and validated [20-24]. The *n*-heptane combustion sub-mechanism introduced here consists of an additional 14 species and 123 elementary reactions. The reaction rates, temperature dependence and activation energies for the Arrhenius expressions were obtained from recent literature data [31, 32, 57-62]. Preference was given to data reported at conditions relevant to the experimental data available for validation. In some cases, earlier references were consulted when questions arose about the applicability of specific reaction rates [63]. All elementary reactions are assumed reversible with reverse rates computed via the use of equilibrium constants. Whenever possible, thermodynamic data was obtained from literature sources [64-68]. For some species, however, thermochemical data was not available and was generated using Benson's group additivity method [69] as modelled by McBride [70]. Extrapolation to temperatures of interest was accomplished via the use of Wilhoit polynomials as recommended by Burcat [71]. When not available from the literature [66, 72, 73] , transport data were estimated using methods outlined by Reid *et al* [64] and Bird, Stewart and Lightfoot [73]. Thermodynamic and transport data specific to the *n*-heptane sub-mechanism are provided in Appendix B. The structures and heats of formation of the species particular to the *n*-heptane sub-mechanism are as shown in Table 3.1.1.1.

The general approach for building the *n*-heptane sub-mechanism was to incorporate pyrolysis, radical and O_2 attack reactions to model the initial *n*-heptane consumption. Only the two pyrolysis steps identified by Chakir *et al* [32] as dominant under stirred reactor conditions were examined in diffusion flames. All four heptyl isomers were considered. Pyrolysis, along with O_2 attack and rearrangement reactions of the four heptyl radicals were included in the sub-mechanism. All three heptene isomers formed from the heptyl radicals were included. The destruction of the heptene isomers was modelled by pyrolysis reactions. The consumption of both the 1-pentyl radical (formed via the pyrolysis of *n*-heptane and the 1-heptyl radical) and pentenyl radical (formed via the pyrolysis of 3-heptene) was modelled by pyrolysis reactions. The consumption of the *n*-butyl radical (formed via *n*-heptane, 2-heptyl radical and 1-heptene pyrolysis), was modelled via both pyrolysis and O_2 attack reactions. The consumption of 1-butene and 1-butene radical included detailed pyrolysis, radical and O_2 attack reactions. In general, reactions leading to straight chain C_6 species were neglected in the *n*-heptane sub-mechanism for diffusion flames as they are expected to be minor contributors to the overall structure of the flame. The influence of these reactions was, however, considered in the analysis of stirred reactor data.

Table 3.1.1.1
Structures and Heats of Formation of n-Heptane Diffusion Flames Sub-mechanism Species

SPECIE	NAME	STRUCTURE	ΔH_f KJ/mol	Reference
1-C_4H_7	1-Butene Radical	CH_2=CH-CH_2-CH_2·	184.400	pw
1-C_4H_8	1-Butene	CH_2=CH-CH_2-CH_3	-0.540	pw
P-C_4H_9	*n*-Butyl Radical	CH_3-CH_2-CH_2-CH_2·	66.530	pw
C_5H_9	Pentenyl Radical	CH_2=CH-2(CH_2)-CH_2·	159.068	pw
1-C_5H_{10}	1-Pentene	CH_2=CH-2(CH_2)-CH_3	-20.930	pw
1-C_5H_{11}	1-Pentyl Radical	CH_3-3(CH_2)-CH_2·	45.810	pw
1-C_7H_{14}	1-Heptene	CH_2=CH-4(CH_2)-CH_3	-62.329	pw
2-C_7H_{14}	2-Heptene	CH_2-CH=CH-3(CH_2)-CH_3	-75.348	pw
3-C_7H_{14}	3-Heptene	CH_3-CH_2-CH=CH-2(CH_2)-CH_3	-75.348	pw
1-C_7H_{15}	1-Heptyl Radical	CH_3-5(CH_2)-CH_2·	4.380	67
2-C_7H_{15}	2-Heptyl Radical	CH_3-4(CH_2)-C·H-CH_3	1.347	pw
3-C_7H_{15}	3-Heptyl Radical	CH_3-3(CH_2)-C·H-CH_2-CH_3	1.347	pw
4-C_7H_{15}	4-Heptyl Radical	CH_3-2(CH_2)-C·H-2(CH_2)-CH_3	1.347	pw
C_7H_{16}	*n*-Heptane	CH_3-5(CH_2)-CH_3	-187.332	67

The paths of *n*-heptane consumption and the paths for the subsequent decomposition of intermediate species attributable specifically to the *n*-heptane sub-mechanism are discussed below.

The detailed stoichiometry of the elementary reactions, rate constants, temperature dependence and activation energies, as well as the paths for the consumption of C_1 to C_4 and C_6 species, collision efficiencies and the soot formation steps are as shown in Tables A1 and A2 in Appendix A.

3.1.2 PATH ANALYSIS OF *n*-HEPTANE CONSUMPTION IN DIFFUSION FLAMES

Results

The rates of the 123 elementary reactions which comprise the *n*-heptane sub-mechanism for diffusion flames were analysed at strain rates of 50, 80, 100, 125 and 200 sec^{-1} in order to establish the primary reaction path for *n*-heptane combustion. One 50 sec^{-1} strain rate flame was computed with an oxygen depleted (83 mol% N_2/17 mol% O_2) oxidant stream to simulate the experiment of Hamins and Seshadri [42] and Hamins [43]. The remaining flames featured ambient (79 mol% N_2/21 mol% O_2) oxidant streams. Only minor differences were noted in reaction paths as a function of either strain rate or oxidant side boundary conditions. As expected, overall reaction rates varied as a function of temperature and the overall order of reactions was only altered for the less significant paths. A summary of this analysis is shown in Tables 3.1.2.1 to 3.1.2.9 in Appendix C. The flame with a rate of strain of 50 sec^{-1} and oxygen depleted oxidant stream flame is referred to as Flame A. Two flames with rates of strain of 50 and 125 sec^{-1} and ambient oxidant streams are referred to as Flames B and C respectively in these tables.

The analysis revealed that the primary paths of *n*-heptane consumption in diffusion flames are thermal decomposition via C-C bond rupture and H atom abstraction via H and CH_3 radical attack. The maximum rates of all other initiation reactions are one to three orders of magnitude slower. Nonetheless, initiation reactions such as thermal decomposition via C-H bond rupture are important because they are necessary to build the initial pool of radicals for subsequent reactions. The primary *n*-heptane consumption paths can be summarised as follows:

C_7H_{16}			=	$C_3H_7(N)$	+	P-C_4H_9	(410)
C_7H_{16}			=	C_2H_5	+	1-C_5H_{11}	(411)
C_7H_{16}	+	H	=	1-C_7H_{15}	+	H_2	(416)
C_7H_{16}	+	H	=	2-C_7H_{15}	+	H_2	(417)
C_7H_{16}	+	H	=	3-C_7H_{15}	+	H_2	(418)
C_7H_{16}	+	H	=	4-C_7H_{15}	+	H_2	(419)
C_7H_{16}	+	CH_3	=	1-C_7H_{15}	+	CH_4	(428)
C_7H_{16}	+	CH_3	=	2-C_7H_{15}	+	CH_4	(429)
C_7H_{16}	+	CH_3	=	3-C_7H_{15}	+	CH_4	(430)
C_7H_{16}	+	CH_3	=	4-C_7H_{15}	+	CH_4	(431)

Attack by the OH radical is also important, particularly on the fuel lean side of the flame structure. These reactions are:

C_7H_{16} + OH = 1-C_7H_{15} + H_2O (424)

C_7H_{16} + OH = 2-C_7H_{15} + H_2O (425)

C_7H_{16} + OH = 3-C_7H_{15} + H_2O (426)

C_7H_{16} + OH = 4-C_7H_{15} + H_2O (427)

Some of the features of the dominant *n*-heptane consumption reactions are shown in Figure 3.1.2.1 and Table 3.1.2.1. The H and CH_3 radicals diffuse into the fuel rich side of the flame and dominate the structure in this region. Thus, although the rate of the pyrolysis reaction (410) is nearly double that of H attack reaction (416), they are both equally important in computing the overall flame structure. Furthermore, even though the dominant *n*-heptane consumption path is obvious, individual elementary reactions cannot be neglected from the scheme until a systematic sensitivity analysis on the influence of each of these reactions on the product distribution of the intermediate species has been performed.

The consumption of the four isomers of the heptyl radical proceeds primarily via thermal rupture of C-C bonds. Isomerization reactions between the four radicals are significant, as also noted by Chakir *et al* [32]. The rates of H radical and O_2 attack reactions leading to the formation of the three heptene isomers are two to five orders magnitude slower than the dominant heptyl radical consumption reactions. Thus heptene formation is not significant from heptyl radicals consumption and once formed heptene is consumed at approximately the same rate as it is produced.

The thermal decomposition of the 1-pentyl radical formed via reactions (411) and (452) and 1-pentene formed via reaction (455) proceeds very rapidly via reactions (409) and (408) respectively. The overall consumption reaction rates are commensurate with the rates of the reactions leading to the formation of both species.

1-C_5H_{10} = C_2H_5 + C_3H_5(A) (408)

1-C_5H_{11} = C_2H_4 + C_3H_7(N) (409)

C_7H_{16} = C_2H_5 + 1-C_5H_{11} (411)

1-C_7H_{15} = 1-C_5H_{11} + C_2H_4 (452)

4-C_7H_{15} = 1-C_5H_{10} + C_2H_5 (455)

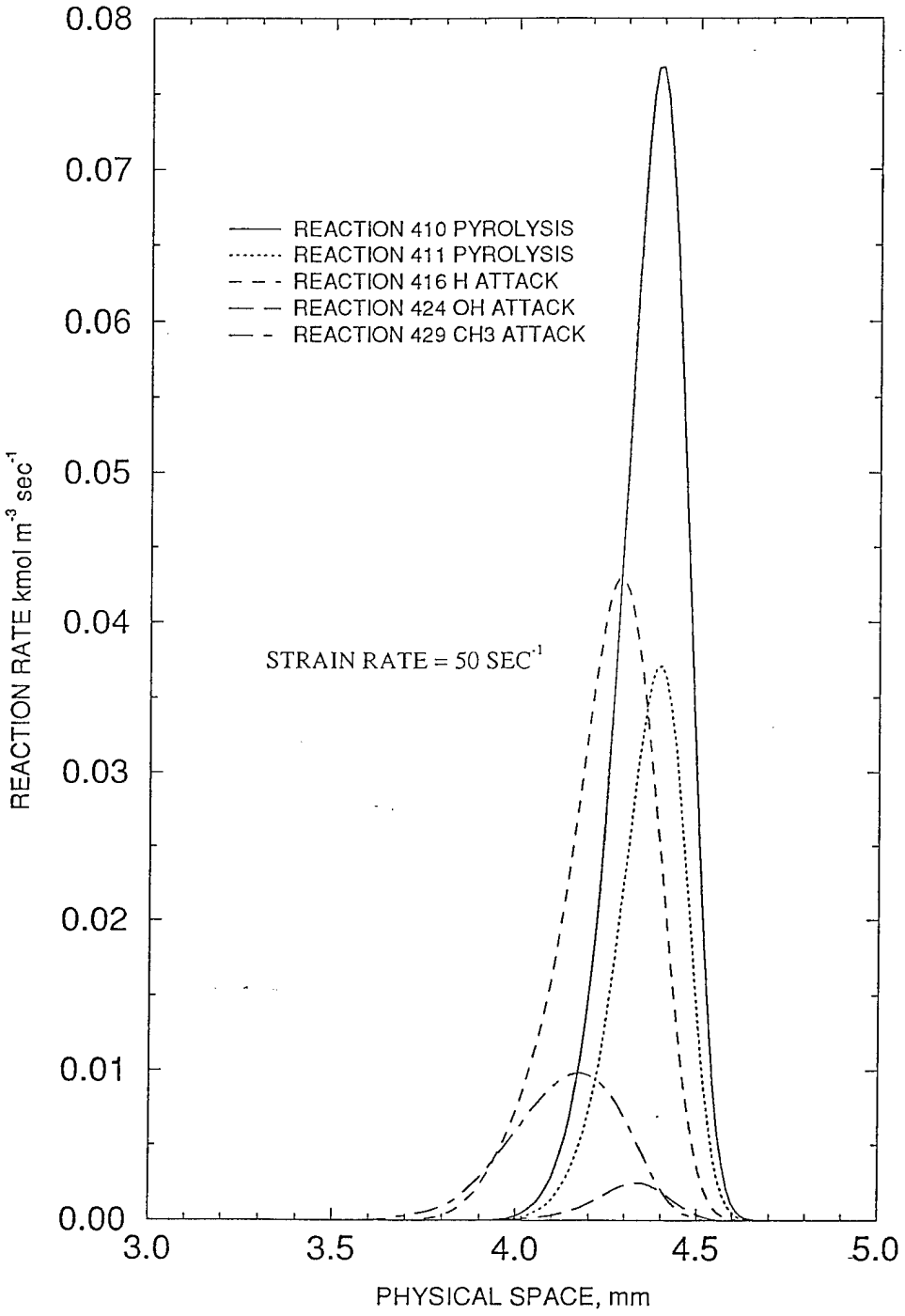

Figure 3.1.2.1
n-Heptane Consumption Reaction Rates in Abdel-Khalik n-Heptane Diffusion Flame

Consumption of the pentenyl radical, formed via heptene pyrolysis reaction (474), exhibits some interesting characteristics. The rate of the pentenyl radical consumption via pyrolysis reaction (405) is identical to its rate of formation via reaction (406). The consumption of the pentenyl radical proceeds through pyrolysis reaction (407).

$$C_5H_9 = C_2H_3 + C_3H_6 \quad (406)$$

$$C_5H_9 = C_4H_6(S) + CH_3 \quad (407)$$

$$3\text{-}C_7H_{14} = C_5H_9 + C_2H_5 \quad (474)$$

The consumption of the *n*-butyl radical, produced via thermal decomposition of *n*-heptane, 1-heptene and 2-heptyl radical via reactions (410), (472) and (453), is dominated by thermal decomposition through C-C bond rupture according to reaction (402). As expected, the rate of *n*-butyl radical consumption by O_2 attack is three orders of magnitude smaller than thermal decomposition.

$$P\text{-}C_4H_9 = C_2H_5 + C_2H_4 \quad (402)$$

$$C_7H_{16} = C_3H_7(N) + P\text{-}C_4H_9 \quad (410)$$

$$2\text{-}C_7H_{15} = C_3H_6 + P\text{-}C_4H_9 \quad (453)$$

$$2\text{-}C_7H_{14} = C_3H_5(A) + P\text{-}C_4H_9 \quad (472)$$

The *n*-butyl radical is also consumed through thermal decomposition of the C-H bond leading to 1-butene formation via reaction (403).

$$P\text{-}C_4H_9 = 1\text{-}C_4H_8 + H \quad (403)$$

The consumption of 1-butene was modelled in some detail via pyrolysis, radical and O_2 attack. It was noted that the production of 1-butene via thermal decomposition of the *n*-butyl radical is not as significant as the pyrolysis of the *n*-butyl radical via C-C bond scission. Thus, only a small amount of 1-butene is produced within the flame. However, methyl radicals are formed via the 1-butene reaction path, leading to methane which is an important intermediate specie. Thus, this path must be included to model the flame structure properly. The consumption of 1-butene was found to occur primarily via thermal decomposition and H radical attack. The two dominant reactions are:

$$1\text{-}C_4H_8 = C_3H_5(A) + CH_3 \quad (389)$$

$$1\text{-}C_4H_8 + H = 1\text{-}C_4H_7 + H_2 \quad (392)$$

The rates of these reactions are between two to five orders of magnitude faster than those of competing reactions as shown in Figure 3.1.2.2. Reaction 389 proceeds in the reverse direction in

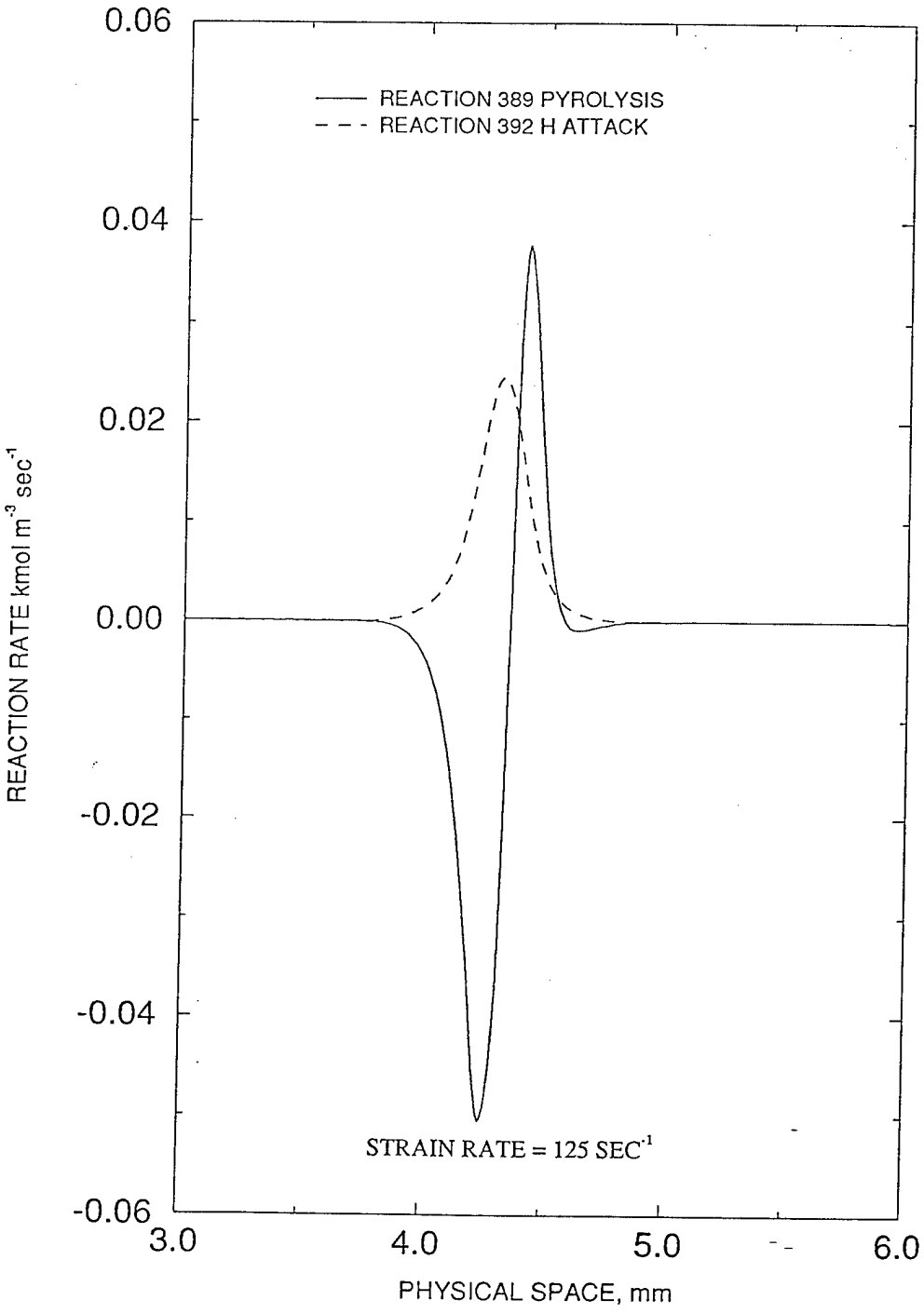

Figure 3.1.2.2
1-Butene Consumption Reaction Rates in Abdel-Khalik n-Heptane Diffusion Flame

the fuel rich part of the flame and competes with 1-butene destruction via reaction 392. In the primary reaction zone both reactions proceed in the forward direction.

Consumption of the 1-butene radical was also modelled in significant detail. Again, this specie is formed via one of the less dominant 1-butene consumption reactions. However, this path generates methane and butadiene. Butadiene in turn generates the C_2H_3 radical leading to acetylene. Thus, modelling this reaction path is important in order to accurately predict intermediate species profiles. The consumption of the 1-butene radical proceeds primarily via thermal decomposition leading to C-H bond rupture and CH_3 radical attack according to:

$$1\text{-}C_4H_7 = C_4H_6(T) + H \quad (378)$$

$$1\text{-}C_4H_7 + CH_3 = C_4H_6(T) + CH_4 \quad (382)$$

Additionally, thermal decomposition via C-C bond rupture and $C_3H_5(A)$ attack are of secondary importance.

$$1\text{-}C_4H_7 = C_2H_4 + C_2H_3 \quad (379)$$

$$1\text{-}C_4H_7 + C_3H_5(A) = C_4H_6(T) + C_3H_6 \quad (386)$$

The rates of other competing reactions are between two to four orders of magnitude less than observed for the principal consumption paths for the 1-butene radical outlined above.

The rates of the additional 358 elementary reactions, not specific to the *n*-heptane sub-mechanism, were analysed for the 50 sec^{-1} strain rate flame with the depleted oxidiser stream flame. The data is tabulated in Table 3.1.2.10 in Appendix C.

In addition to the 1-pentyl and *n*-butyl radicals, the rapid pyrolysis of *n*-heptane yields *n*-propyl and ethyl radicals via reactions (410) and (411) respectively as outlined above. The *n*-propyl radical decomposes to form propene and ethylene whereas the ethyl radical is a precursor to ethylene. The pyrolysis of the four heptyl radicals yields propene via reaction (453), ethane via reaction (452), ethyl radical via reaction (455), and *n*-propyl radicals via reaction (454).

$$1\text{-}C_7H_{15} = C_2H_4 + 1\text{-}C_5H_{11} \quad (452)$$

$$2\text{-}C_7H_{15} = C_3H_6 + P\text{-}C_4H_9 \quad (453)$$

$$3\text{-}C_7H_{15} = C_3H_7(N) + 1\text{-}C_4H_8 \quad (454)$$

$$4\text{-}C_7H_{15} = 1\text{-}C_5H_{10} + C_2H_5 \quad (455)$$

The pool of intermediates is further increased by the pyrolysis of the 1-pentyl radical, 1-pentene and the *n*-butyl radical, producing *n*-propyl radical, ethylene, ethyl and allyl radicals. Consumption of 1-butene and the 1-butene radical gives allyl and methyl radicals, and butadiene

and methane through reactions (389) and (378) respectively as discussed above. The reaction paths of these species in diffusion flames have been thoroughly analysed by Leung and Lindstedt [20]. It is merely noted here that to accurately model the *n*-heptane reactions leading to C_4 and smaller species is crucial in order to properly predict the distribution of intermediate species in the diffusion flame structure. This point is further discussed by comparison of predictions with experimental data provided in Section 3.2.2.

Preliminary analysis of the distribution of intermediate species in *n*-heptane flame structures revealed that methane, ethylene, ethane and propene were consistently over-predicted for all flames. Furthermore, the initial consumption of *n*-heptane occurred more rapidly than experimentally observed and this trend was consistently repeated for all the flames. Since the detailed path analysis indicated that the initial consumption of *n*-heptane via pyrolysis was the dominant mechanism for fuel consumption, reactions (410) and (411) were the subject of some scrutiny. The results of this study are presented in Table 3.1.2.11 in Appendix C and in Figure 3.1.2.3 below.

Decreasing the rate of reactions (410) and (411) in turn by an order of magnitude did produce a reduction in the levels of methane, ethylene, ethane and propene. However, the reduction was much less than expected. Close inspection of Table 3.1.2.10 shows that although reducing the rate of either pyrolysis reaction does in fact result in a decrease in the rate of *n*-heptane consumption, there is a synergistic effect amongst all the *n*-heptane consumption reactions. If one reaction rate is decreased, the overall rates of competing reactions experience an increase, thus producing virtually no variation in the major species profiles. Therefore, it becomes necessary to examine the distribution of intermediate species within the flame structure in order to determine the appropriate levels for fuel consumption rates. The most significant effects were noted in the prediction of methane, ethane and ethylene levels. Each parametric variation yielded a decrease in the peak levels of each of these species, in accordance with experimental predictions. However, the synergistic effect between all the reactions still led to discrepancies with experimental observations. The major points of this discussion are illustrated in Figure 3.1.2.3.

The rates recommended for both pyrolysis reactions by Chakir *et al* [32] were then replaced with the recommendations by Levuch *et al* [63]. However, those rates resulted in an even more severe over-prediction of intermediate species. A total removal of the pyrolysis reactions bypasses an important path of acetylene formation leading to substantial under-prediction of acetylene levels as shown in Figure 3.1.2.3. Thus, it is important that both pyrolysis and radical attack reactions are part of any scheme used to predict the structure of *n*-heptane diffusion flames.

Discussion

Three salient conclusions may be derived from the detailed path analysis of *n*-heptane consumption. First, it appears that most sensible combinations of *n*-heptane consumption reactions will result in reasonable predictions of major species profiles. This is clearly the implication of the work of Bui-Pham and Seshadri [38], who did not include the dominant pyrolysis reactions in their global *n*-heptane initial consumption model, yet they were able to

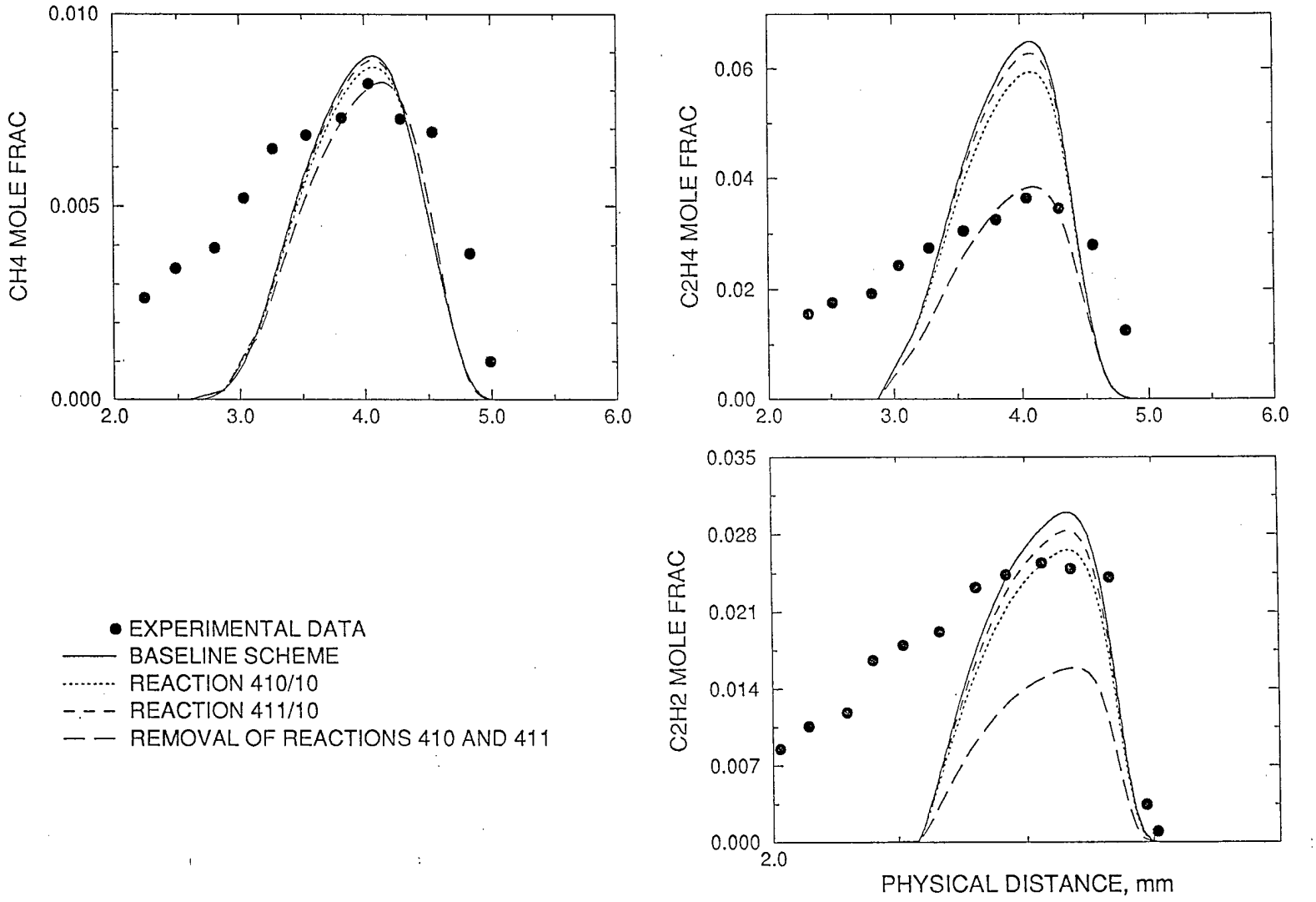

Figure 3.1.2.3
Effect of Pyrolysis Reaction Rates, a=125 sec^{-1}, Forward Stagnation Line Position

predict major species profiles with reasonable accuracy. However, it is clear that pyrolysis reactions must be included in the *n*-heptane kinetics sub-mechanism in order to accurately predict intermediate species. Finally, it is noted that the pyrolysis of *n*-heptane results in the formation of $C_3H_7(N)$, P-C_4H_9, C_2H_5 and 1-C_5H_{11}. All of these species directly decompose to either form ethylene directly or precursors to ethylene formation. If the higher pyrolysis rates proposed by Chakir *et al* [32] are utilised, it has been shown that ethylene is greatly over-predicted. Thus, the rates for *n*-heptane pyrolysis proposed by Chakir *et al* [32] to model stirred reactor experimental results must be reduced by an order of magnitude in order to properly model the chemical features of *n*-heptane diffusion flames. The consequences of this change for the modelling of stirred reactors are discussed in Section 3.1.4 below.

3.1.3 *n*-HEPTANE MECHANISM MODIFICATIONS FOR STIRRED REACTORS

To model low temperature stirred reactors an additional 108 elementary reactions and 8 species [31,32,61,74-79] were added to the *n*-heptane combustion sub-mechanism developed for diffusion flames. The additional reaction paths primarily considered radical attack on the three heptene isomers and formation and consumption of the linear C_6 species. A third elementary reaction for the initial pyrolysis of *n*-heptane to form 1-hexyl radical ($1\text{-}C_6H_{13}$) and CH_3 was also included. Furthermore, the 1-pentene sub-mechanism was augmented to include the formation of 1-pentene via pyrolysis of the 1-pentyl radical as well as the consumption of 1-pentene via radical attack reactions. Finally, elementary reactions considering the formation and destruction of oxygenated species (methyl alcohol, acetaldehyde, acetyl radical and formaldehyde) were included in the stirred reactor *n*-heptane combustion sub-mechanism. The detailed stoichiometry of the additional elementary reactions and the rate constants are listed in Table A3 in Appendix A. Thermodynamic and transport data specific to the *n*-heptane stirred reactor sub-mechanism was assembled using the techniques described in Section 3.1.1 and are tabulated in Appendix B. The structures and heats of formation of the species particular to the *n*-heptane stirred reactor sub-mechanism are as shown in Table 3.1.3.1.

Table 3.1.3.1
Structures and Heats of Formation of n-Heptane Stirred Reactor Sub-mechanism Species

SPECIE	NAME	STRUCTURE	ΔH_f KJ/mol	Reference
CH_3OH	Methyl Alcohol	CH_3-OH	-200.940	67
C_2H_3O	Acetyl Radical	CH_3-·CO	-10.000	67
C_2H_4O	Acetaldehyde	CH_3-HCO	-166.190	67
C_6H_{11}	1-Hexene Radical	CH_2=CH-3(CH_2)-CH_2·	142.324	67
$1\text{-}C_6H_{12}$	1-Hexene	CH_2=CH-3(CH_2)-CH_3	-41.693	67
$1\text{-}C_6H_{13}$	1-Hexyl Radical	CH_3-4(CH_2)-CH_2·	25.100	67
$2\text{-}C_6H_{13}$	2-Hexyl Radical	CH_3-3(CH_2)-C·H-CH_3	24.280	pw
C_7H_{13}	Heptene Radical	CH_2·-4(CH_2)-CH=CH_2	129.111	31

Additional reaction paths in the *n*-heptane sub-mechanism are identical to those discussed in Section 3.1.1. Also, soot formation paths were not included in the stirred reactor computations.

3.1.4 PATH ANALYSIS OF *n*-HEPTANE CONSUMPTION IN STIRRED REACTORS

Results

The rates of the elementary reactions comprising the *n*-heptane combustion sub-mechanism for stirred reactors were analysed in order to determine the principal paths of *n*-heptane combustion in the relatively low temperature environment of a stirred reactor. Emphasis was placed on determining the most critical differences between reaction paths in stirred reactors and diffusion flames. The rates of the elementary reactions were analysed at a temperature of 1000K, a reactor residence time of 180 milliseconds, initial *n*-heptane concentration of 0.2% and a stoichiometric equivalence ratio. In order to determine the relative importance of individual elementary reactions at the higher combustor temperatures encountered in realistic high speed aircraft propulsion systems, the temperature of the stirred reactor model was increased to 2000K and the subsequent effect on reaction paths noted. However, it is clearly understood that a stirred reactor environment is not an adequate representation of a diffusion flame configuration as clearly shown by Bilger [80]. The high temperature stirred reactor path analysis serves merely to either back up the selection of reaction paths used for the counterflow diffusion flame analysis presented in Section 3 or to suggest supplementary elementary reactions for further study in a diffusion flame environment. A summary of this analysis is shown in Tables 3.1.4.1 to 3.1.4.21 in Appendix C. Only species specifically noted occur in significant concentrations in the exhaust of the stirred reactor.

At low temperatures, the principal paths of *n*-heptane consumption are H atom abstractions via OH, H, O, CH_3O and CH_3 radical attack. The largest rate of *n*-heptane thermal decomposition via C-C bond rupture were found to be nearly an order of magnitude slower than those of the principal H atom abstraction reaction rates. The primary *n*-heptane consumption paths at 1000K may be summarised as follows:

$$C_7H_{16} + H = 1\text{-}C_7H_{15} + H_2 \quad (417)$$

$$C_7H_{16} + H = 2\text{-}C_7H_{15} + H_2 \quad (418)$$

$$C_7H_{16} + H = 3\text{-}C_7H_{15} + H_2 \quad (419)$$

$$C_7H_{16} + H = 4\text{-}C_7H_{15} + H_2 \quad (420)$$

$$C_7H_{16} + O = 1\text{-}C_7H_{15} + OH \quad (421)$$

$$C_7H_{16} + OH = 1\text{-}C_7H_{15} + H_2O \quad (425)$$

$$C_7H_{16} + OH = 2\text{-}C_7H_{15} + H_2O \quad (426)$$

$$C_7H_{16} + OH = 3\text{-}C_7H_{15} + H_2O \quad (427)$$

C_7H_{16}	+	OH	=	4-C_7H_{15}	+	H_2O	(428)
C_7H_{16}	+	CH_3	=	2-C_7H_{15}	+	CH_4	(430)
C_7H_{16}	+	CH_3	=	3-C_7H_{15}	+	CH_4	(431)
C_7H_{16}	+	CH_3O	=	3-C_7H_{15}	+	CH_3OH	(454)
C_7H_{16}	+	CH_3O	=	1-C_7H_{15}	+	CH_3OH	(455)

Secondary reaction paths at 1000K include additional H atom abstraction reactions via HO_2 and CH_3 attack according to:

C_7H_{16}	+	CH_3	=	1-C_7H_{15}	+	CH_4	(429)
C_7H_{16}	+	HO_2	=	2-C_7H_{15}	+	H_2O_2	(434)
C_7H_{16}	+	HO_2	=	3-C_7H_{15}	+	H_2O_2	(435)

By contrast, in the higher temperature environment of a diffusion flame, the rates of *n*-heptane consumption via C-C bond rupture were at least twice those of H atom abstraction reactions (Table 3.1.2.1, Appendix C). However, when the stirred reactor temperature is increased to 2000K, it is noted that thermal decomposition reactions again become dominant and their rates are roughly twice those of the H atom abstraction reaction rates. A point of interest is that the rate of the C-C bond rupture reaction which yields 1-hexyl and methyl radicals (412), is nearly equal to that of the C-C bond rupture reaction which yields P-C_4H_9 and C_3H_7(N) radicals (410). In the analysis of *n*-heptane diffusion flames, reaction (412) was not considered, as reactions (410) and (411) were reported to be most probable [32]. The ability to accurately predict both major and minor species in *n*-heptane diffusion flames demonstrated in Section 3.2.2 indicates that neglecting pyrolysis reaction (412) in the analysis of *n*-heptane diffusion flame structures is not too detrimental. Also, 1-C_6H_{13} radical is completely consumed at 2000K. Nonetheless, the effect of reaction 412 on the overall *n*-heptane diffusion flame structure was assessed.

Initially reaction (412) and the subsequent 1-C_6H_{13} consumption reactions were added to the diffusion flame *n*-heptane sub-mechanism using the rates suggested by Chakir *et al* [32]. This resulted in a similar over-prediction of *n*-heptane consumption and intermediate species concentrations as observed when using the higher pyrolysis rates suggested in [32] for reactions (410) and (411). Thus, the rate of reaction (412) was reduced by an order magnitude as was done for reactions (410) and (411) in Section 3.1.2. When equivalent rates were used for all three *n*-heptane pyrolysis reactions, reaction (412) was found to be an order of magnitude and two times slower than reactions (410) and (411) respectively. Furthermore, including these paths in the diffusion flame model yielded no differences in major species profiles. Variations in measured intermediate species concentrations were less than five percent. No significant variations were observed in the profiles of the important radicals. However, differences ranging from 5 to 65 percent were predicted in the concentrations of 1-butene, the *n*-butyl radical, 1-pentene, the

heptyl radicals and the heptene isomers. Thus, reactions (412), (522), (523) and (524) have been included in a more general *n*-heptane mechanism for diffusion flames featuring 485 reactions and 87 species.

$$C_7H_{16} = 1\text{-}C_6H_{13} + CH_3 \quad (412)$$

$$1\text{-}C_6H_{13} = 2\text{-}C_6H_{13} \quad (522)$$

$$1\text{-}C_6H_{13} = C_2H_4 + P\text{-}C_4H_9 \quad (523)$$

$$2\text{-}C_6H_{13} = C_3H_7(N) + C_3H_6 \quad (524)$$

It is also observed that when the stirred reactor temperature was increased to 2000K, the rates of *n*-heptane consumption elementary reactions leading to the production of methyl alcohol become insignificant. Thus, it is arguably sensible to omit these reactions from the *n*-heptane sub-mechanism for diffusion flames.

As for diffusion flames, the consumption of the four isomers of the heptyl radical proceeds primarily via thermal rupture of the C-C bond at both low and high temperatures in the stirred reactor. The rates of isomerization reactions between the four radicals are also significant, as was noted by Chakir *et al* [32] and in the *n*-heptane diffusion flame path analysis (Section 3.1.2) The rates of thermal decomposition reactions via C-H bond rupture leading to the formation of the three heptene isomers were two to three order of magnitude slower than those of the C-C bond rupture reactions. The rates of O_2 and H radical reactions also leading to the formation of the heptene isomers were only one to two orders of magnitude slower than those of the C-C bond rupture reactions. In the diffusion flame, these reactions were two to five orders of magnitude slower than those of the dominant heptyl radical destruction reactions. Thus, including a heptene sub-mechanism to model stirred reactor data appears to be of some importance. However, when the stirred reactor temperature was increased to 2000K, the rates of the H radical and O_2 attack reactions become insignificant.

The rate of C-C bond rupture reaction (464) leading to the formation of $1\text{-}C_6H_{12}$ and CH_3 is approximately an order of magnitude slower than C-C bond rupture reactions (461), (462) and (465). Therefore, neglecting this path from the *n*-heptane diffusion flame analysis is indeed rational.

At the lower temperature, the principal paths of heptene isomer destruction are H atom abstraction via HO_2 radical attack yielding heptene radical. The rates of these reactions are commensurate with the rates of production of the three heptene isomers. At the high temperature, the dominant paths of heptene isomer destruction are thermal decomposition reactions via C-C bond rupture. The decomposition of 3-heptene yields $1\text{-}C_6H_{11}$ radical. However, at high temperature, heptene formation is not significant.

In the 1000K stirred reactor computations, the heptene radical is produced primarily from HO_2 attack on the heptene isomer via reactions (498), (499) and (500) and it is rapidly consumed.

$$1\text{-}C_7H_{14} + HO_2 = C_7H_{13} + H_2O_2 \quad (498)$$

$$2\text{-}C_7H_{14} + HO_2 = C_7H_{13} + H_2O_2 \quad (499)$$

$$3\text{-}C_7H_{14} + HO_2 = C_7H_{13} + H_2O_2 \quad (500)$$

Hexyl radicals are consumed at rates commensurate with their rates of formation at both high and low temperatures. However, as noted previously, the *n*-heptane pyrolysis reaction (414) leading to the formation of 1-hexyl radical appears to be of importance at both high and low temperatures. Therefore, the effect of these reactions on the structure of diffusion flames has been assessed as discussed above.

1-Hexene, formed via the pyrolysis of 3-heptyl radical, was noted as a significant intermediate species in the *n*-heptane stirred reactor experiments of Chakir *et al* [32] conducted in the temperature range of 900 to 1200K. Therefore, the destruction of 1-hexene was modelled in some detail. Originally, the concentration of this specie was under-predicted. Thus, it was necessary to replace the rates of 1-hexene thermal decomposition reactions (525) and (526) used by Chakir *et al* [32] with the slower rates recommended by Tsang [74] in order to accurately predict the concentration of this specie. The principal paths of 1-hexene consumption at 1000K were then found to be H atom abstraction reactions via OH and H radicals attack. The rate of 1-hexene thermal decomposition via C-C bond rupture (Reaction 525) was also of secondary significance at low temperatures. However, at 2000K, only the thermal decomposition reaction (525) was of any importance. The rates of competing reactions were three to thirteen orders of magnitude slower than those of the dominant reaction. As noted above, however, the path of 1-hexene formation is not dominant at high temperature. Thus, the destruction path of this specie is also not of interest in diffusion flames. The 1-hexene radical is rapidly consumed leading predominantly to propene and the C_3H_5(A) radical.

1-Pentene was also a significant intermediate specie noted in the *n*-heptane stirred reactor experiments of Chakir *et al* [32]. Initially, this specie was over-predicted in the stirred reactor computations. In order to improve the correlation, several elementary reactions specific to this specie were included in the *n*-heptane combustion sub-mechanism for stirred reactors. The thermal decomposition reaction of 1-pentyl radical via C-H bond rupture recommended by Westbrook *et al* [75] was found to proceed in the reverse direction at 1000K. This was the most significant path of 1-pentene consumption at low temperatures. Additional important paths of 1-pentene destruction at low temperature were radical abstraction through H and OH radical attack via reactions (545) and (553) and thermal decomposition via C-C bond rupture yielding ethyl and C_3H_5(A) radicals via reaction (408).

$$1\text{-}C_5H_{10} + = C_2H_5 + C_3H_5(A) \quad (408)$$

$$1\text{-}C_5H_{10} + H = C_5H_9 + H_2 \quad (545)$$

$$1\text{-}C_5H_{10} + OH = C_5H_9 + H_2O \quad (553)$$

At 2000K, the only significant 1-pentene destruction path was thermal decomposition reaction (408). At 2000K the thermal decomposition of 1-pentyl radical proceeds in the forward direction. Thus, molecular recombination of H radical and 1-pentene is not a significant path of 1-pentene consumption as predicted at low temperature. In the diffusion flame computations, the only path of 1-pentene consumption considered was thermal decomposition reaction (408). The stirred reactor analysis confirms the validity of this choice.

The principal sources of pentenyl radical production are H atom abstraction via radical attack and thermal decomposition reactions of the heptene isomers and H atom abstraction via radical attack on 1-pentene. None of the paths leading to the formation of the pentenyl radical are significant at either low or high temperatures.

The principal paths of *n*-butyl radical production are thermal decomposition reactions of *n*-heptane and 2-heptyl radical. As found in the path analysis of *n*-heptane consumption in diffusion flames, the consumption of *n*-butyl radical occurs primarily via thermal decomposition through C-C bond rupture. The dominance of this reaction path increases with increasing temperature.

The consumption of 1-butene in the stirred reactor was found to proceed primarily via H and OH radical attack. The thermal decomposition of 1-butene proceeds in the reverse direction at low temperatures, yielding C_3H_5(A) and methyl radicals (reaction 389). Thermal decomposition is the dominant path of 1-butene consumption at high temperature, as was noted in the *n*-heptane diffusion flame path analysis. 1-Butene was experimentally found to be a significant intermediate specie at low temperatures [32] whereas no 1-butene is predicted in the exhaust composition of the high temperature *n*-heptane stirred reactor.

Propane consumption reaction (579) was included in the *n*-heptane combustion stirred reactor sub-mechanism in an attempt to increase the predicted concentration of ethane. However, this reaction is insignificant at low and high temperatures.

$$C_3H_8 + C_2H_5 = C_3H_7(N) + C_2H_6 \qquad (579)$$

Acetaldehyde is primarily formed via radical attack reactions on 1-pentene and 1-butene. The rapid reaction of acetaldehyde with the C_2H_5 radical yields 1-butene and an OH radical. Acetaldehyde is also consumed via radical attack reactions to yield primarily acetyl radical. The acetaldehyde reaction paths are insignificant at high temperatures and thus need not be considered in the analysis of *n*-heptane diffusion flames.

The consumption of ketene by O_2 attack was included in the *n*-heptane combustion sub-mechanism for stirred reactors via reaction (574).

$$C_2H_2O + O_2 = CH_2O + CO_2 \qquad (574)$$

At 1000K the rate of this reaction is between three and seven orders of magnitude greater than those of competing reactions. However, the rate of O_2 attack on ketene is four orders of

magnitude slower than that of the dominant ketene consumption reaction by H and OH radical attack via reactions (130), (131) and (134) at 2000K. Thus O_2 attack on ketene need not be considered in diffusion flames but is an important path in low temperature stirred reactors.

$$C_2H_2O + H = CH_3 + CO \quad (130)$$

$$C_2H_2O + H = C_2HO + H_2 \quad (131)$$

$$C_2H_2O + OH = CH_2O + CHO \quad (134)$$

Methyl alcohol is produced via CH_3O radical attack on *n*-heptane, which is one of the primary *n*-heptane consumption paths at low temperatures. The rate of methyl alcohol production is roughly four times greater than that of the dominant methyl alcohol consumption reaction at 1000K. As expected, the rates of methyl alcohol production and consumption are insignificant at high temperatures and need not be considered in the analysis of *n*-heptane diffusion flame structures.

Formaldehyde consumption via HO_2, CH_3 and CH_3O radical attack via reactions (580), (581) and (582) was considered in the *n*-heptane combustion sub-mechanism for stirred reactors.

$$CH_2O + CH_3O = CH_3OH + CHO \quad (580)$$

$$CH_2O + HO_2 = CHO + H_2O_2 \quad (581)$$

$$CH_2O + CH_3 = CHO + CH_4 \quad (582)$$

The rates of these reactions were an order of magnitude slower than those of the dominant formaldehyde consumption reactions at low temperatures. However, the rates of these reactions exceeded those of formaldehyde consumption via CH and O radicals and O_2 attack and thermal decomposition. The rates of reactions (580), (581) and (582) are between four and nine orders of magnitude slower than those of the dominant formaldehyde consumption reaction at high temperature. Therefore it is not necessary to consider these additional formaldehyde consumption reactions in the analysis of *n*-heptane diffusion flame structures.

Discussion

The path analysis of *n*-heptane combustion in stirred reactors has shown significant differences between dominant reaction paths in the relatively low temperature environment generally encountered in stirred reactors and the high temperature flow fields of diffusion flames. It is thus important that mechanisms validated against stirred reactor data not be applied to high speed propulsion systems without proper validation using experimental flame data.

The high temperature stirred reactor path analysis generally validated the selection of reaction paths used in the *n*-heptane diffusion flame analysis. However, it was noted that the thermal decomposition of *n*-heptane yielding 1-hexyl and methyl radicals was significant at both low and high temperatures. Thus, the influence of this *n*-heptane decomposition path and the subsequent

consumption of 1-hexyl radical on the overall structure of *n*-heptane diffusion flames was assessed. The additional reaction paths did not have a significant effect on the temperature or measured intermediate species profiles. Differences were noted, however, in the concentrations of 1-butene, the *n*-butyl radical, 1-pentene, the heptyl radicals and the heptene isomers. Thus, these reactions were added to a more general *n*-heptane mechanism for diffusion flames.

3.2 *n*-HEPTANE MECHANISM EVALUATION

3.2.1 DESCRIPTION OF EXPERIMENTAL *n*-HEPTANE DIFFUSION FLAMES MODELLED

Available experimental data in the literature for *n*-heptane diffusion flames is scarce [40-43, 81]. To be useful for validating a chemical kinetics mechanism, such data must contain as a minimum temperature, major and intermediate species profiles. It is useful to have profiles for radical species as well; however, such data has not been reported to date for *n*-heptane diffusion flames. Furthermore, when analysing detailed chemical kinetics mechanisms of the magnitude of those reported herein, coflow diffusion flame configurations are not computationally affordable. Thus, based on these criteria, the counterflow *n*-heptane diffusion flames of Hamins and Seshadri [42] and Hamins [43], and Abdel-Khalik *et al* [40] and Abdel-Khalik [41] were selected for kinetic mechanism validation.

Both experimental studies used *n*-heptane in its liquid state. The model chosen to validate the *n*-heptane detailed chemical kinetics mechanism was that of a counterflow diffusion flame formed between two approaching gaseous jets. The importance of the injection and vaporisation process in the case of the Abdel-Khalik flame and the evaporation process in the case of the Hamins and Seshadri flame is readily recognised if attempting to precisely match the overall flow field of the flames. However, the primary aim of this effort was to investigate detailed reaction kinetics. Neglecting the fuel vaporisation process does not affect the overall reaction paths and the sensitivity of the final product distribution to individual elementary reactions. Furthermore, neither researcher obtained detailed velocity measurements for their counterflow diffusion flames and thus accurate modelling of all the features of these flames can not be properly validated against the experimental results.

Hamins and Seshadri studied the counterflow diffusion flame formed in the near wake region above a burning pool of *n*-heptane. Temperature profiles were obtained with Pt versus Pt-10% Rh thermocouples. The accuracy of the measurements is estimated to be ± 50K [42, 82]. The measurements were corrected for radiative heat loss. Species profiles were obtained using gas chromatography. Gas sampling was accomplished with quartz microprobes of 120 μm diameter. Hamins and Seshadri estimated the accuracy in determining the location of the probe tip to be within 0.01 mm. The boundary conditions for the *n*-heptane diffusion flames were 17 mol% O_2 concentration, 41.2 cm/sec air velocity and 1.45 g/cm^2/min burning rate.

In order to assess the overall quality of the species concentration data a mixture fraction analysis was performed. The mixture fraction, *f*, is defined in terms of any conserved property ζ or a linear combination of such properties.

A common expression for mixture fraction is:

$$f = \frac{\zeta_{mixture} - \zeta_{air}}{\zeta_{fuel} - \zeta_{air}}$$

Since the elemental mass of C, H, and O is conserved in a flame a set of mixture fractions may be expressed in terms of these elements as:

$$f_c = \frac{\sum_{k=1}^{nsp} n_{ck} X_k}{\sum_{k=1}^{nsp} X_k M_k} \Bigg/ \frac{n_{cfuel}}{M_{fuel}}$$

$$f_H = \frac{\sum_{k=1}^{nsp} n_{Hk} X_k}{\sum_{k=1}^{nsp} X_k M_k} \Bigg/ \frac{n_{Hfuel}}{M_{fuel}}$$

$$f_o = \left[\frac{n_{Oair}}{M_{air}} - \frac{\sum_{k=1}^{nsp} n_{ok} X_k}{\sum_{k=1}^{nsp} X_k M_k} \right] \Bigg/ \frac{n_{Oair}}{M_{air}}$$

Where n= number of C, H or O atom in a specie

X= the mass fraction of specie k

M = Molecular weight

Additionally, Bilger [83] has suggested the following definition for mixture fraction:

$$f_z = \frac{2Z_C/W_C + Z_H/2W_H + (Z_{Oair} - Z_0)/W_0}{2Z_{Cfuel}/W_C + Z_{Hfuel}/2W_H + Z_{Oair}/W_O}$$

Where Z = elemental mass fraction of C, H, and O

W = atomic mass of the elements C, H, and O

Since mixture fractions are conserved properties, the values of mixture fraction computed via each of the four definitions above should be identical if the species profile data is accurate. The mixture fractions based on all four definitions were computed for the Hamins and Seshadri flame. The mixture fractions based on carbon, hydrogen, and oxygen are plotted versus the mixture fraction defined by Bilger on an X=Y coordinate in Figure 3.2.1.1. In the fuel rich flame zone, excellent agreement is observed amongst the values of mixture fraction computed via each definition. Only a small discrepancy is noted in the mixture fraction value computed based on elemental oxygen in the fuel lean flame zone. Overall, the data appear to be of high quality and well suited for computational validation.

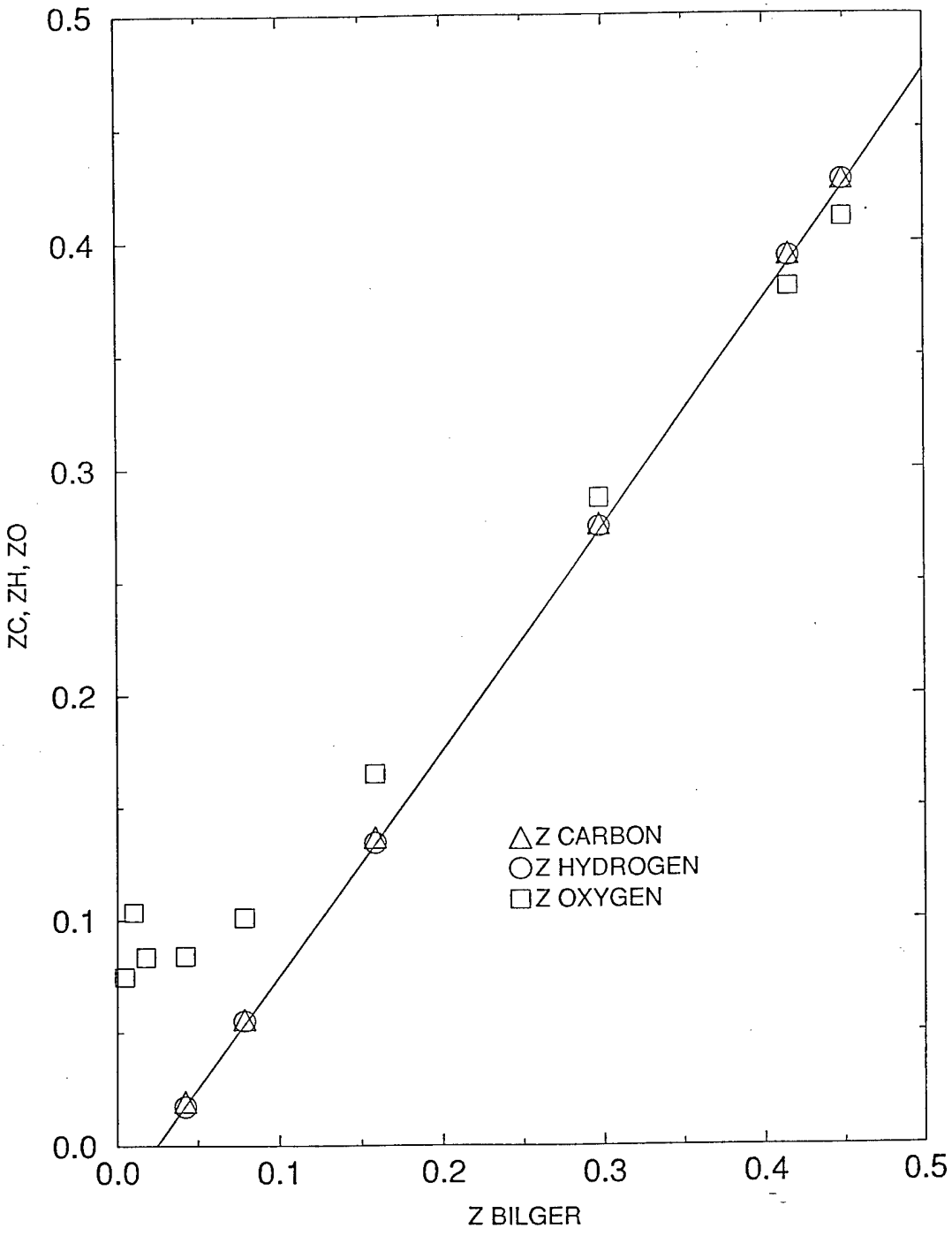

Figure 3.2.1.1
Hamins and Seshadri n-Heptane Diffusion Flame Mass Fraction Comparison

Abdel-Khalik [41] studied counterflow diffusion flames formed around a porous cylinder. Experimental conditions are shown in Table 3.2.1.1. Species profiles were obtained using 5 mm diameter quartz tubes tapered down to 30-50 micron microprobes. The gas samples were analysed using gas chromatography and data were reported on a dry basis. Temperature measurements were obtained using interferometer techniques, relying on the molar refractivity profiles of the measured species and making estimates for the contribution of water. Temperature as well as species profiles were reported along the 0^o, 45^o, 90^o, 135^o, and 180^o radial lines as measured from the forward stagnation line. The forward stagnation line location corresponds to the numerical simulation of the model used in this study and thus these data were used for comparisons.

Table 3.2.1.1

Experimental Conditions for n-Heptane Diffusion Flames [40, 41]

cylinder D, mm	air* velocity cm/sec	Re∞	strain rate ** sec^{-1}
12.80	12	102	37.5
12.80	40	340	125
12.80	64	544	200
6.35	12	51	75
6.35	40	169	252

*Air properties at the boundary: 21 mole % O_2, 79 mole % N_2, T=298K.

**strain rate calculated using Tsuji's recommendation (a=2V/R) [84] for a counterflow diffusion flame in the forward stagnation region of a porous cylinder.

Where V = air velocity
R = cylinder radius

Abdel-Khalik [41] indicated that the effective sampling position and the physical position of the probe tip did not vary by more than 0.25 mm. However, the temperature profiles reported in [40, 41] display some unusual characteristics. The profiles along the $\theta=0^o$ and $\theta=45^o$ positions are identical. The characteristic shape of the Abdel-Khalik flames temperature profiles along the stagnation point for various rates of strain are shown in Figure 3.2.1.2. The shape of the temperature profiles varies markedly from that previously reported for methane and propane diffusion flames formed around a porous cylinder [85, 86]. This observation could be indicative of difficulties with probe positioning. The point is further illustrated in Figure 3.2.1.3. The CO profiles are plotted as a function of physical distance for various strain rates. The width of the CO profile should increase with decreasing rate of strain. It is recognised that the expression proposed by Tsuji [84] to calculate rate of strain for a diffusion flame about a porous cylinder is only an approximation. Nonetheless, a greater difference in the width of the CO profiles should be exhibited between the 37.5 and 200 sec^{-1} strain rate flames about the large cylinder and the 75 and 252 sec^{-1} strain rate flames about the small cylinder.

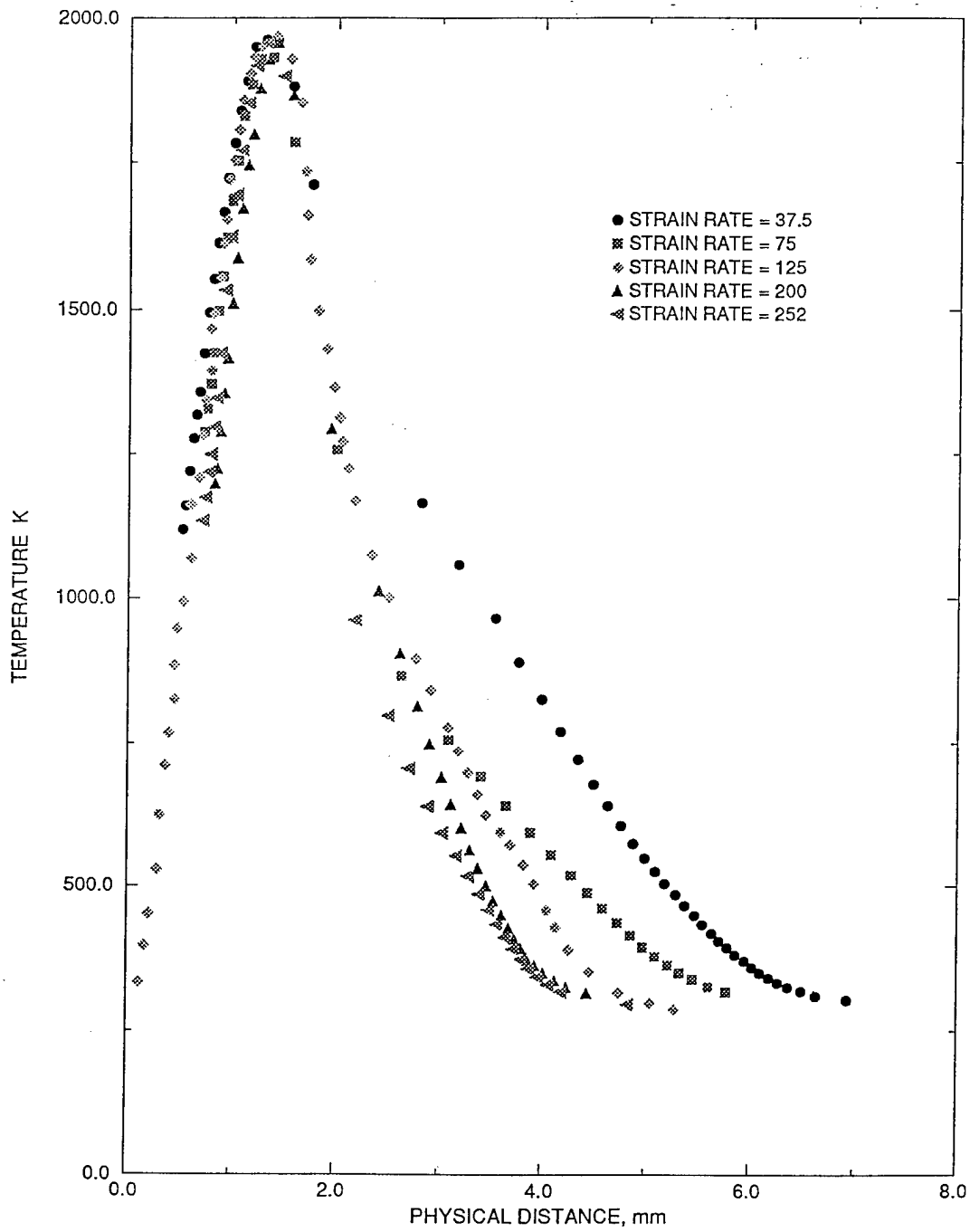

Figure 3.2.1.2
Abdel-Khalik n-Heptane Diffusion Flame Temperature Profiles at Forward Stagnation Line Position

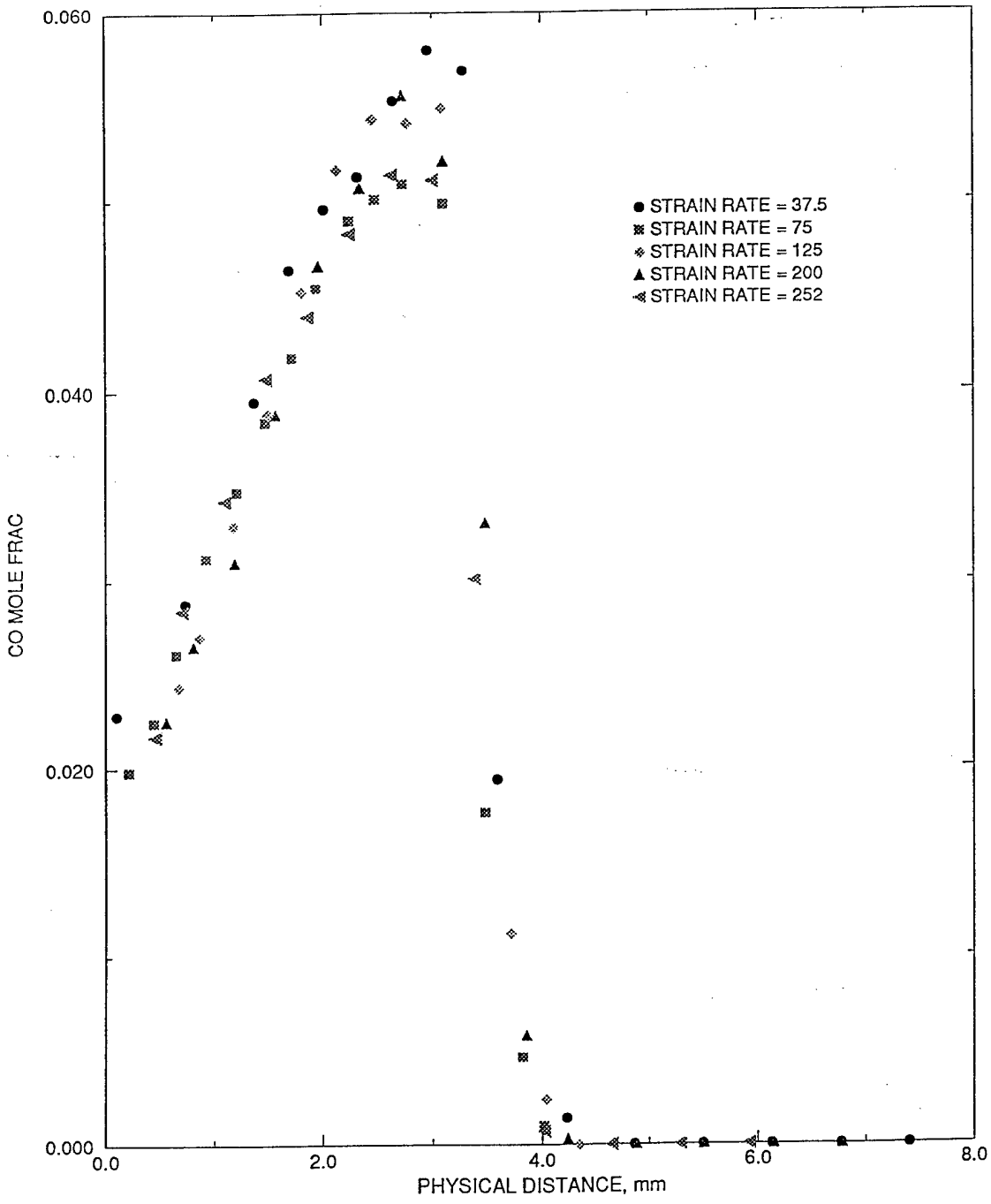

Figure 3.2.1.3
Abdel-Khalik n-Heptane Diffusion Flame CO Profiles at Forward Stagnation Line Position

The species profile data reported for the 12.8 mm diameter cylinder, 40 cm/sec air approach velocity flame were analysed in terms of mixture fraction. Since water and hydrogen measurements were not reported, the mixture fractions calculated in terms of elemental hydrogen and oxygen are not expected to correlate as well, particularly in the fuel lean zone. This trend is indeed observed. However, the values of mixture fraction calculated on the basis of elemental carbon do appear sensible as shown in Figure 3.2.1.4.

Overall, some discrepancies were noted in the *n*-heptane diffusion flame data obtained by Abdel-Khalik in terms of probe positioning. However, the species profile data appear to be of good quality and also well suited for validating the *n*-heptane kinetics mechanism.

3.2.2 *n*-HEPTANE DIFFUSION FLAME RESULTS

The important features of the comparison between experimental and analytical results for the Hamins and Seshadri flame are shown in Figures 3.2.2.1 to 3.2.2.4. A rate of strain of 50 sec^{-1} was found to closely match the width of the temperature profile. This rate of strain is similar to the 30.5 sec^{-1} used by Bui-Pham and Seshadri with global chemistry [38]. No attempt was made to adjust the fuel injection velocity of the calculated flame to match the precise location of the experimental flame. Rather, the two profiles were superimposed to match the peak locations. Such an approach is sufficient to assess the ability of the detailed chemical kinetics mechanism to predict the chemistry of the flame and avoids unnecessary computations.

Figure 3.2.2.1 shows the calculated adiabatic temperature profile as well as that calculated accounting for soot radiation heat losses. The profile incorporating heat losses matches the experimental data well, with the small discrepancy noted attributable to the vaporisation of *n*-heptane. Soot radiation heat loss produced about a 100K temperature drop in peak flame temperature.

Peak concentrations of major species are generally well predicted, as shown in Figure 3.2.2.2. The width and slope of the profiles were not exactly reproduced using a flame strain rate of 50 sec^{-1}. An attempt at improving the correlation was made by decreasing the flame rate of strain to 30 sec^{-1}. This only resulted in marginal improvements in the prediction of the shape of the species profiles but did result in a substantial over-prediction of the width of the temperature profile. All major species, excepting hydrogen, were predicted within a factor of 1.5. The discrepancies observed in CO and CO_2 concentration predictions are well within the bounds of experimental error [87]. Hydrogen concentrations were over-predicted by a factor of 2.5. The peak hydrogen concentration reported by Hamins and Seshadri is around 0.01 mole fraction. This value is substantially lower than values previously reported for methane and propane diffusion flames by Tsuji and [85, 86], which were generally 0.02 to 0.03 mole fraction. In order to assess the likelihood that the mechanism was indeed over-predicting hydrogen concentration, a study was made of the equilibrium composition of the products of combustion of methane, propane, *n*-hexane, *n*-heptane, and *n*-octane burning in air in stoichiometric proportions. The tool used for this study was the well known Chemical Equilibrium code of Gordon and McBride [88]. Results are summarised in Table 3.2.2.1.

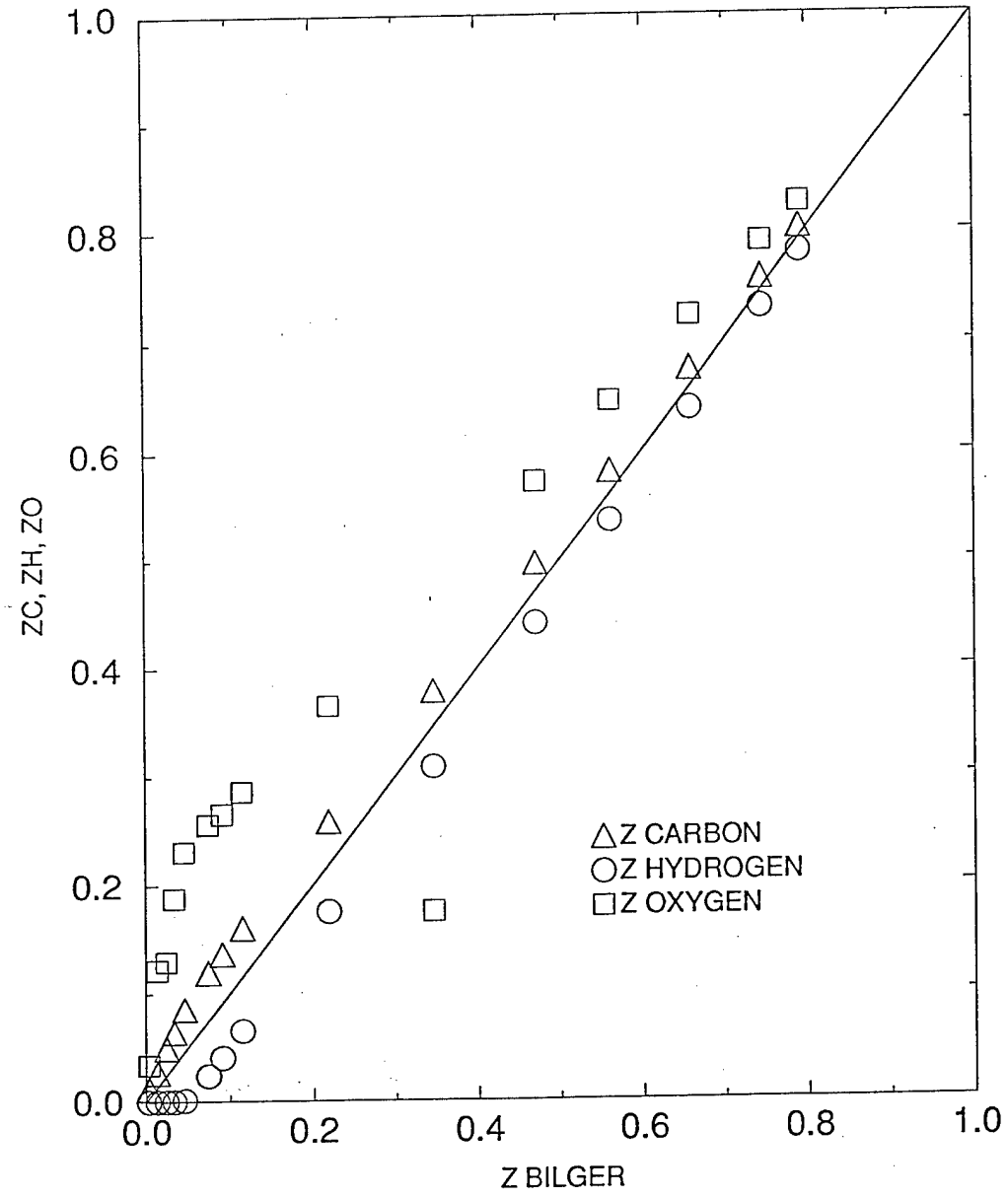

Figure 3.2.1.4
Abdel-Khalik n-Heptane Diffusion Flame Mass Fraction Comparison

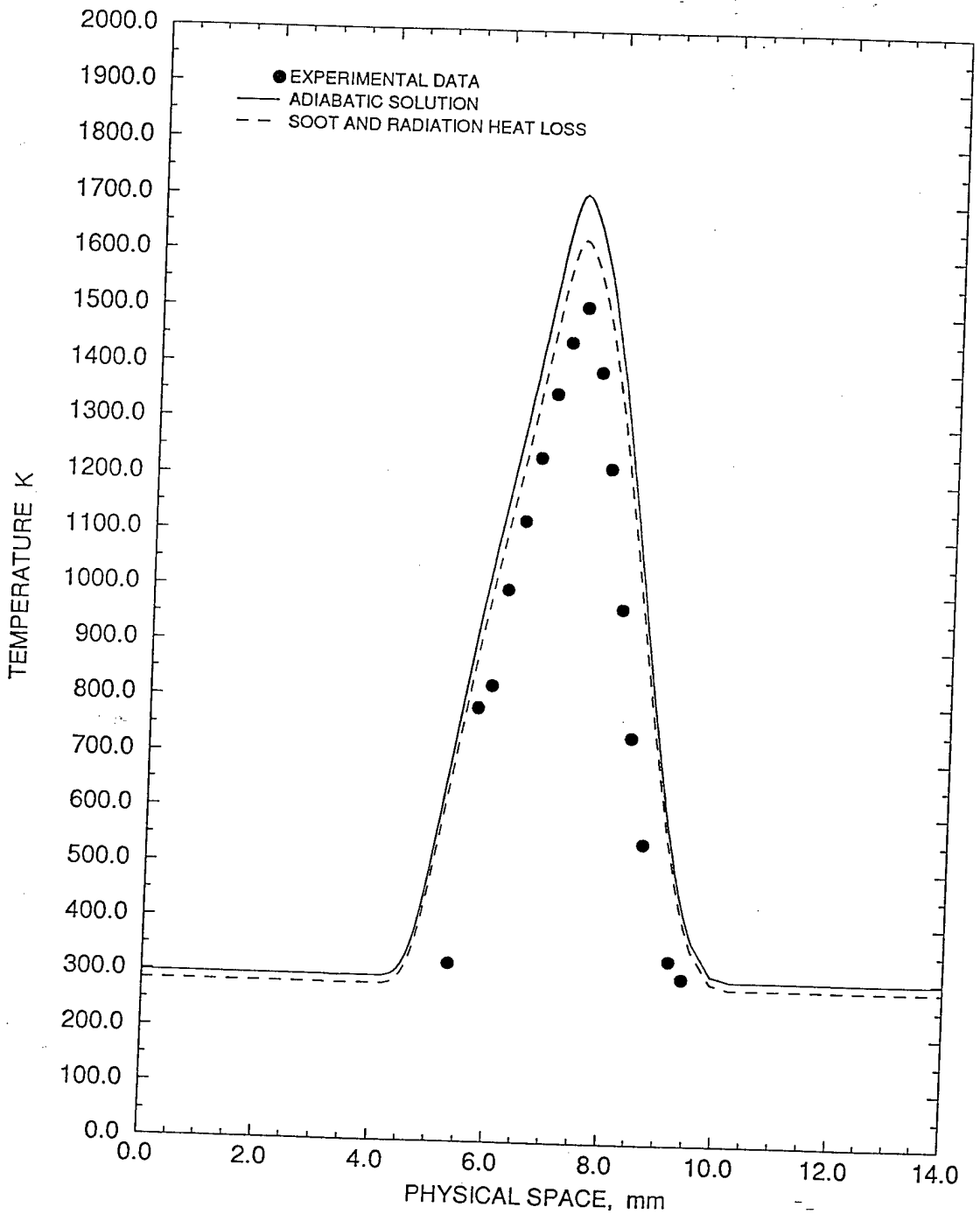

Figure 3.2.2.1
Hamins and Seshadri n-Heptane Diffusion Flame Temperature Measured and Calculated Profiles

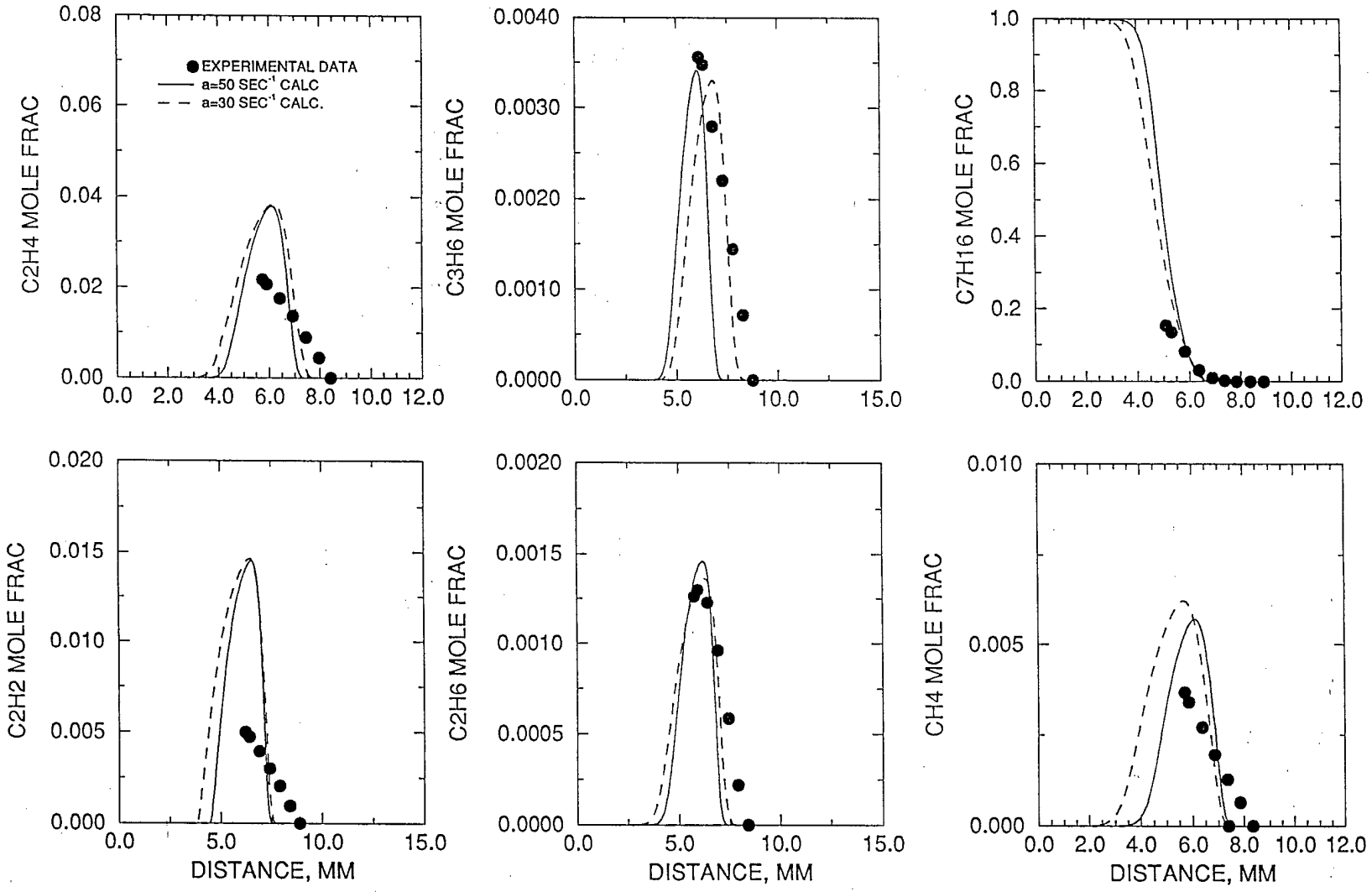

Figure 3.2.2.2
Hamins and Seshadri n-Heptane Diffusion Flame Species Measured and Calculated Profiles

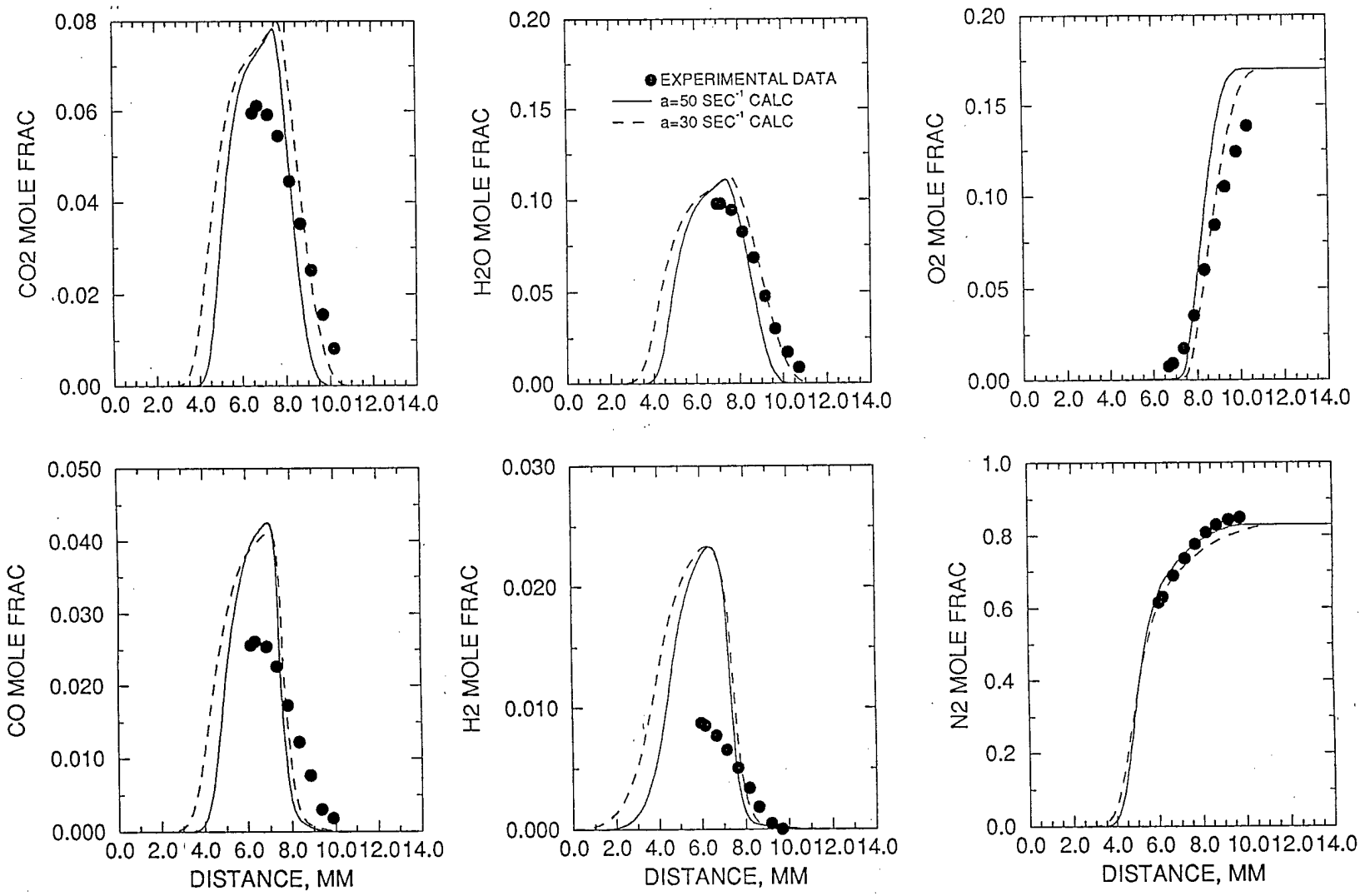

Figure 3.2.2.3
Hamins and Seshadri n-Heptane Diffusion Flame Species Measured and Calculated Profiles

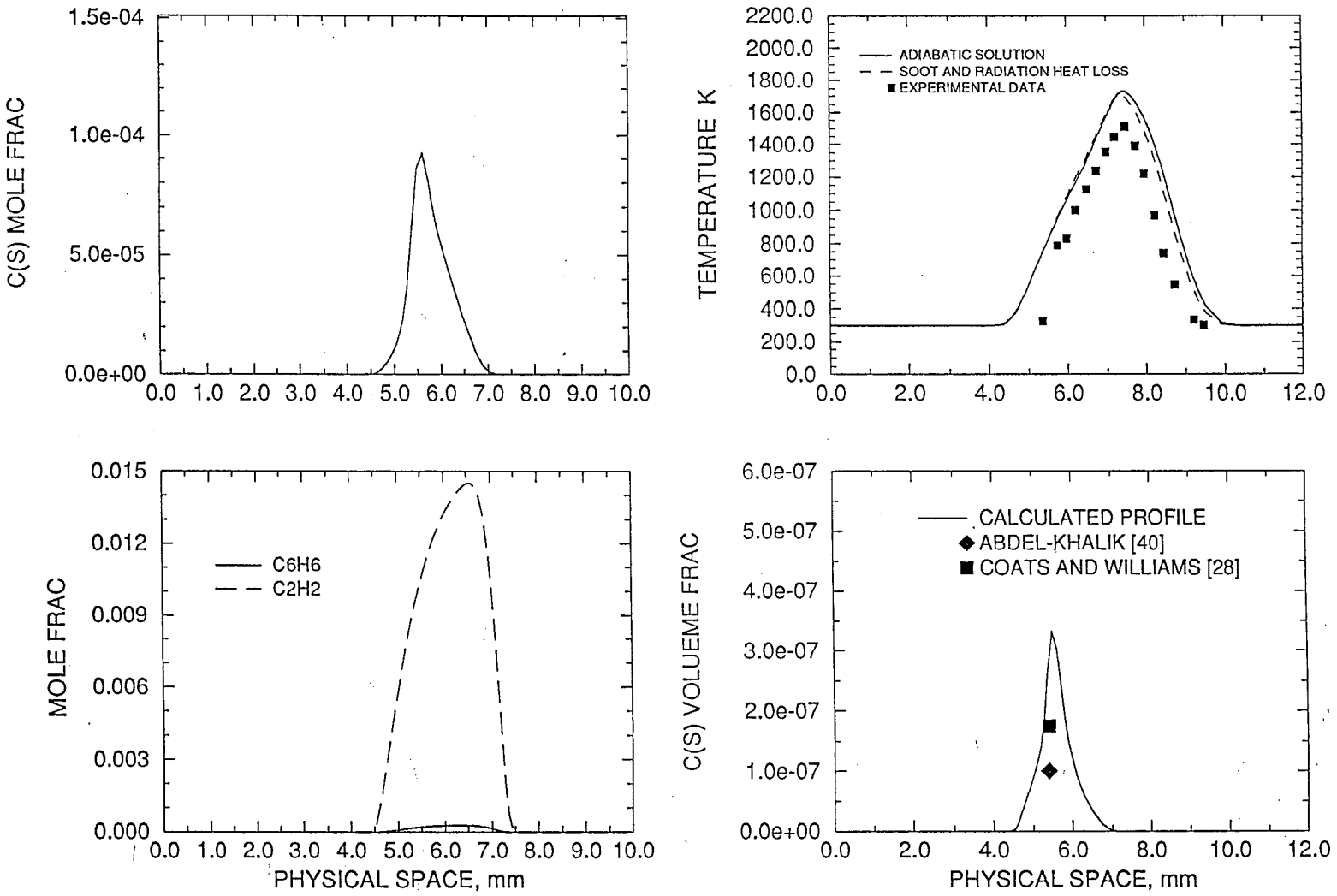

Figure 3.2.2.4
Hamins and Seshadri n-Heptane Diffusion Flame Soot Formation

Table 3.2.2.1

Combustion Efflux Equilibrium Predictions for Various Hydrocarbons

Hydrocarbon	Max Adiabatic Equilibrium Temperature	Equilibrium H_2 Mole Fractions Predicted for Stoichiometric Burning in Air
methane	2116	0.00216
propane	2158	0.00202
n-hexane	2165	0.00190
n-heptane	2166	0.00188
n-octane	2167	0.00187

As expected, the mole fraction of hydrogen present in the efflux decreases with increasing C/H ratio. However, the difference is very small from propane to *n*-octane. Thus, it is likely that the value of 0.01 mole fraction H_2 reported for the Hamins and Seshadri flame is somewhat lower than can be realistically expected. No other hydrogen measurements in pure *n*-heptane diffusion flames have been reported, thus it is impossible to validate either the measured or theoretically predicted result.

As shown in Figure 3.2.2.3, the *n*-heptane consumption profile is modelled with reasonable accuracy. The small discrepancy noted in the fuel rich flame zone is probably the result of the liquid vaporisation process.

The peak concentrations of intermediate species were also very well predicted, with particularly excellent results achieved in the prediction of ethane and propene (Figure 3.2.2.3). Only the peak concentration of ethylene was over-predicted by a factor of 3. Calculated soot mass and volume fraction are also included herein (Figure 3.2.2.4), however there are no direct experimental data available to validate these results. The maximum soot volume fraction computed for the Hamins and Seshadri flame is 3.3E-07. Gulder [89] reported maximum soot volume fractions in toluene/*n*-heptane and benzene/*n*-heptane coflow laminar diffusion flames of 1.12E-05 and 1.25E-05. However, soot formation in these flames was primarily dominated by the heavily sooting aromatic species. Coats and Williams [28] reported a soot volume fraction of 1.75E-07 for rich (ϕ=2) *n*-heptane combustion in a shock tube. This value is within reasonable agreement of that calculated for the Hamins and Seshadri heptane diffusion flame, although the differences in the time scales of the reactions in each device are recognised.

The comparison between analytical predictions and experimental results for the Abdel-Khalik flame are shown in Figures 3.2.2.5 to 3.2.2.12. Results are shown for the 50 and 125 sec^{-1} strain rate flames. Similar trends were observed for all other flames.

Some difficulty was experienced in predicting the shape of the temperature profiles of the Abdel-Khalik flames. As noted in section 3.2.1, the unusual shape of the experimentally derived temperature profiles is likely the result of inaccuracies in probe positioning. Since temperatures were computed on the basis of interferograms coupled with species profiles data, the reported measurements are subject to two sources of error. The peak temperatures accounting for

radiation heat loss were under-predicted by 50 to 100K, well within experimental error. The temperature profiles for each flame are shown in Figures 3.2.2.5 and 3.2.2.9.

The rate of fuel consumption in the 50 sec^{-1} strain rate flame was well predicted. As in the Hamins and Seshadri flame, fuel penetration is over-predicted in the fuel rich flame zone since the effects of vaporisation were neglected in the model. The fuel consumption rate for the 125 sec^{-1} rate of strain flame is not as well predicted. This is likely the result of a discrepancy between the experimental and computational rates of strain. The fuel consumption profiles are shown in Figures 3.2.2.6 and 3.2.2.10.

Major species profiles, shown in Figures 3.2.2.6, 3.2.2.7, 3.2.2.10 and 3.2.2.11, were consistently well predicted. A slight under-prediction of CO_2 and over-prediction of CO are observed. However, as discussed by Colkett *et al* [87] the distribution of CO and CO_2 is one of the most difficult measurements to obtain in a reacting system due to the sensitivity of the distribution of these species to small temperature fluctuations. The observed discrepancy between computational predictions and experimental values is less than a factor of 1.2, which is considered excellent. The humps observed in the CO_2 and N_2 profiles (both computational and experimental) are the result of the data being reported on a dry basis.

The peak concentrations of methane, ethylene and ethane were predicted with impressive accuracy (Figures 3.2.2.7 and 3.2.2.11). For these flames, peak ethylene levels were predicted within factors of 1.1 or better, which markedly differs from the over-prediction of ethylene in the Hamins and Seshadri flame. Ethylene levels were accurately predicted for all five Abdel-Khalik *n*-heptane flames modelled. Thus, it would appear that the detailed chemical kinetics reaction mechanism used herein accurately models this chemical feature of *n*-heptane diffusion flames.

Computed soot and volume fractions for each flame are shown in Figures 3.2.2.8 and 3.2.2.12. As in the Hamins and Seshadri flame, soot radiation results in a temperature drop of about 100K from the adiabatic value. The peak predictions of soot volume fraction for each flame are compared to the values estimated by Abdel-Khalik *et al* [40]. These values were calculated rather than experimentally obtained. Total radiation heat loss was determined from an overall energy balance. The experimentally obtained temperature and composition profiles were used to calculate the radiative heat losses attributable to the gases. The balance was considered to be the result of soot radiation heat loss, and maximum soot volume fractions computed accordingly. The soot volume fractions predicted in this work are approximately four to five times greater than the estimates of Abdel-Khalik *et al* [40]. However, many uncertainties, both experimental and theoretical, prevail.

Overall, the temperature and major and intermediate species profiles of *n*-heptane diffusion flames were very well predicted using the kinetics mechanism assembled herein. The mechanism has been validated against data sets from two experimenters over a wide range of rates of strain, thus proving its versatility.

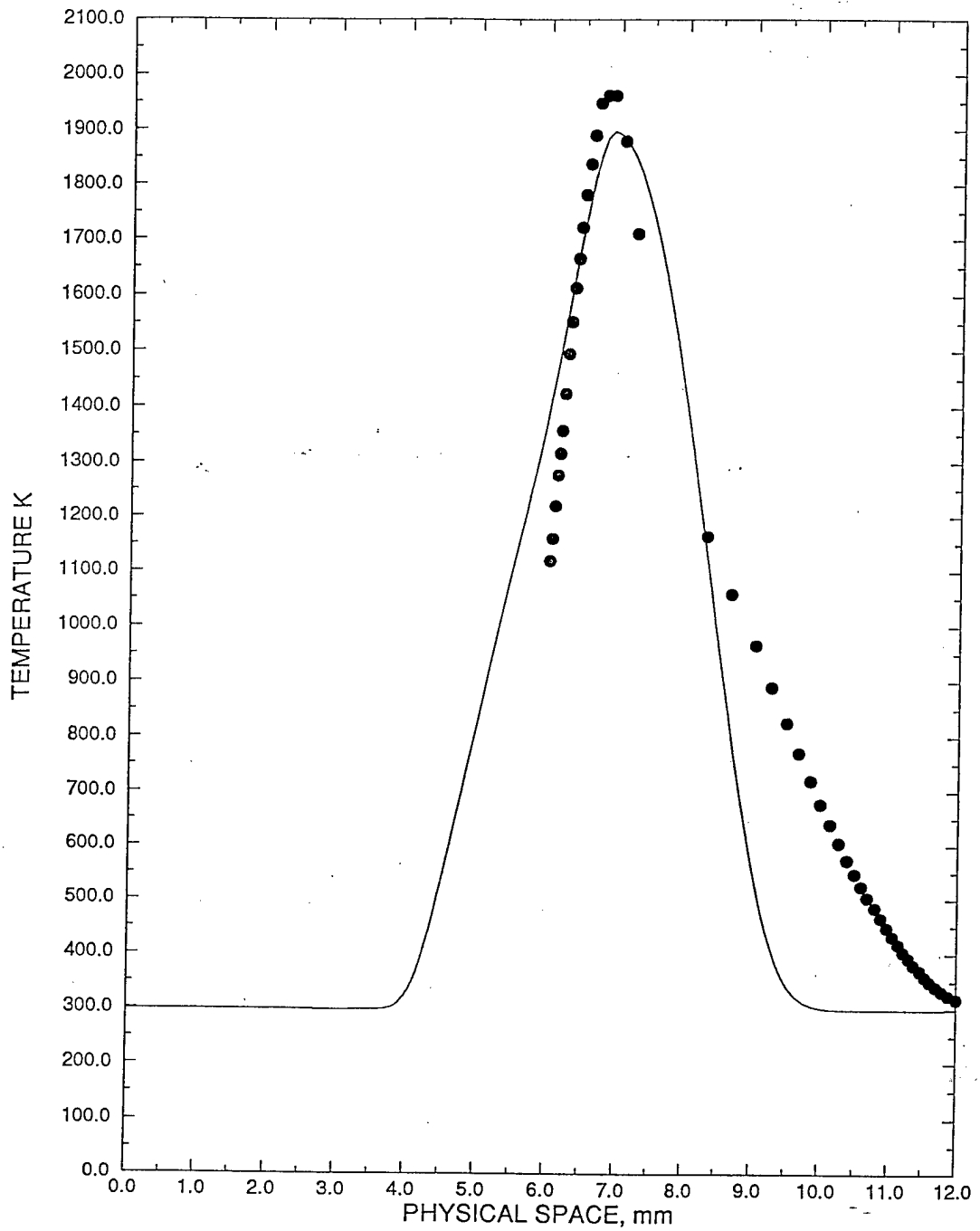

Figure 3.2.2.5
Abdel-Khalik n-Heptane Diffusion Flame
Temperature Measured and Calculated Profiles
a=50 sec^{-1}, Forward Stagnation Line Position

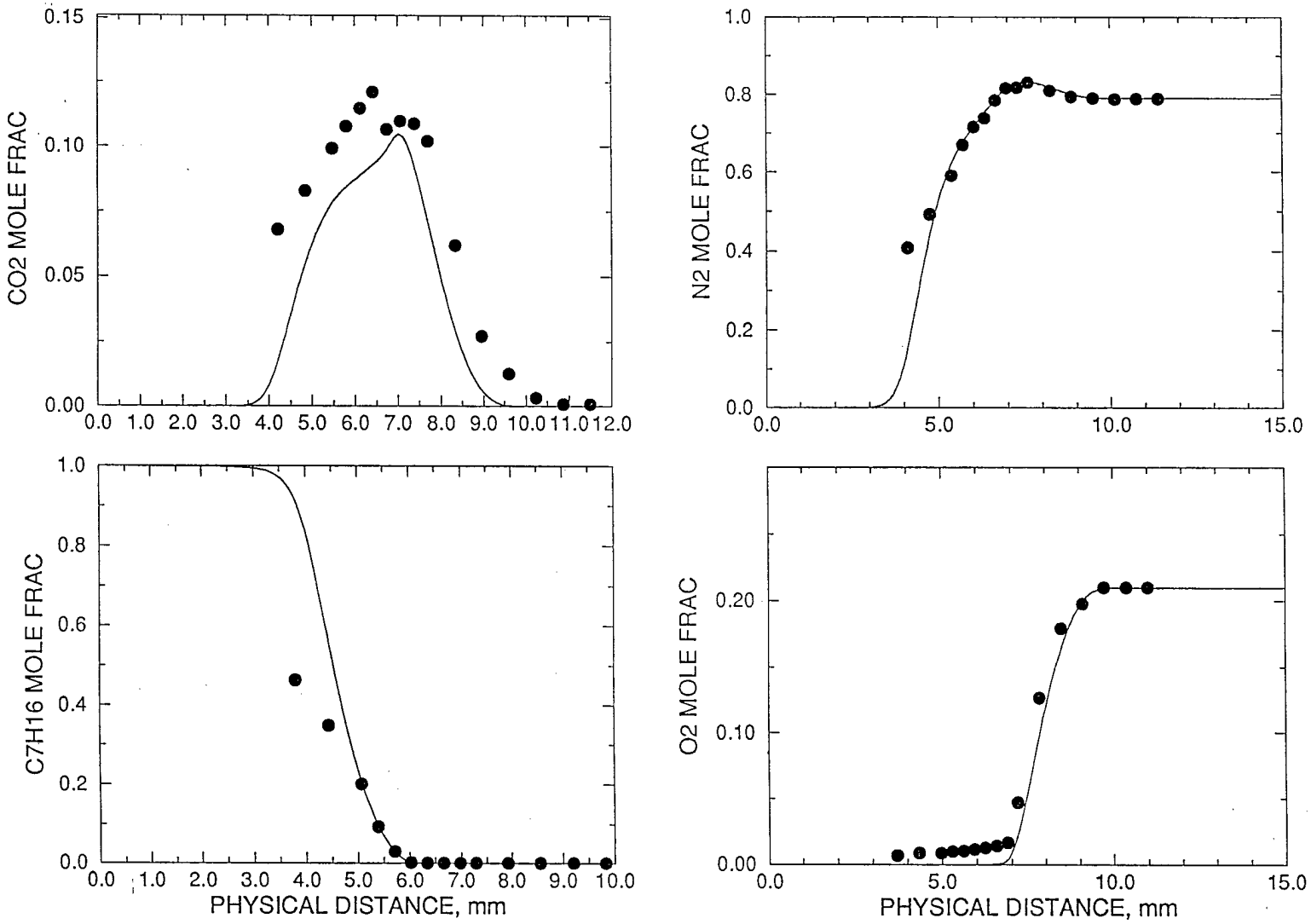

Figure 3.2.2.6
Abdel-Khalik n-Heptane Diffusion Flame Species Measured and Calculated Profiles $a=50\ sec^{-1}$, Forward Stagnation Line Position

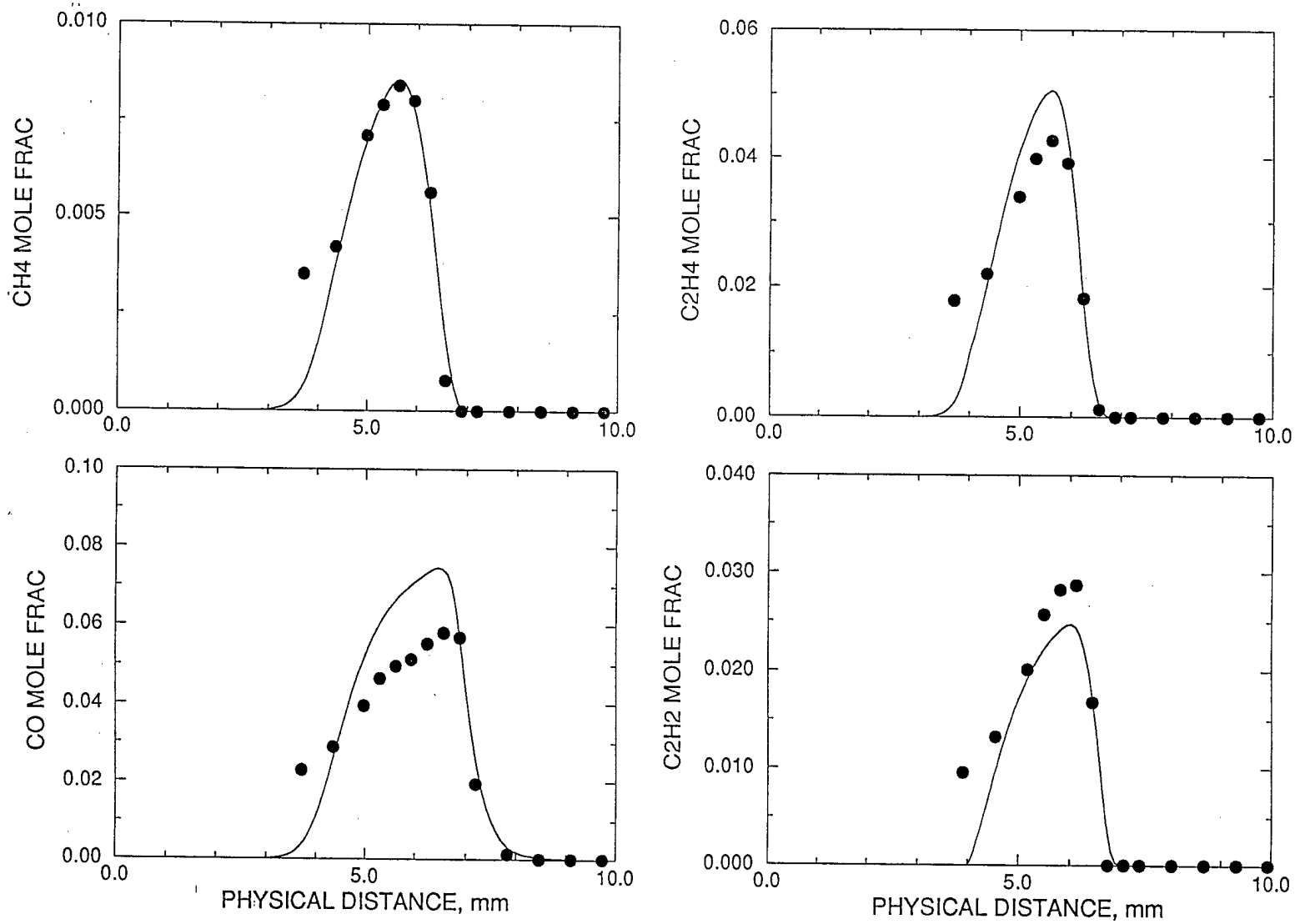

Figure 3.2.2.7
Abdel-Khalik n-Heptane Diffusion Flame Species Measured and Calculated Profiles
a=50 sec^{-1}, Forward Stagnation Line Position

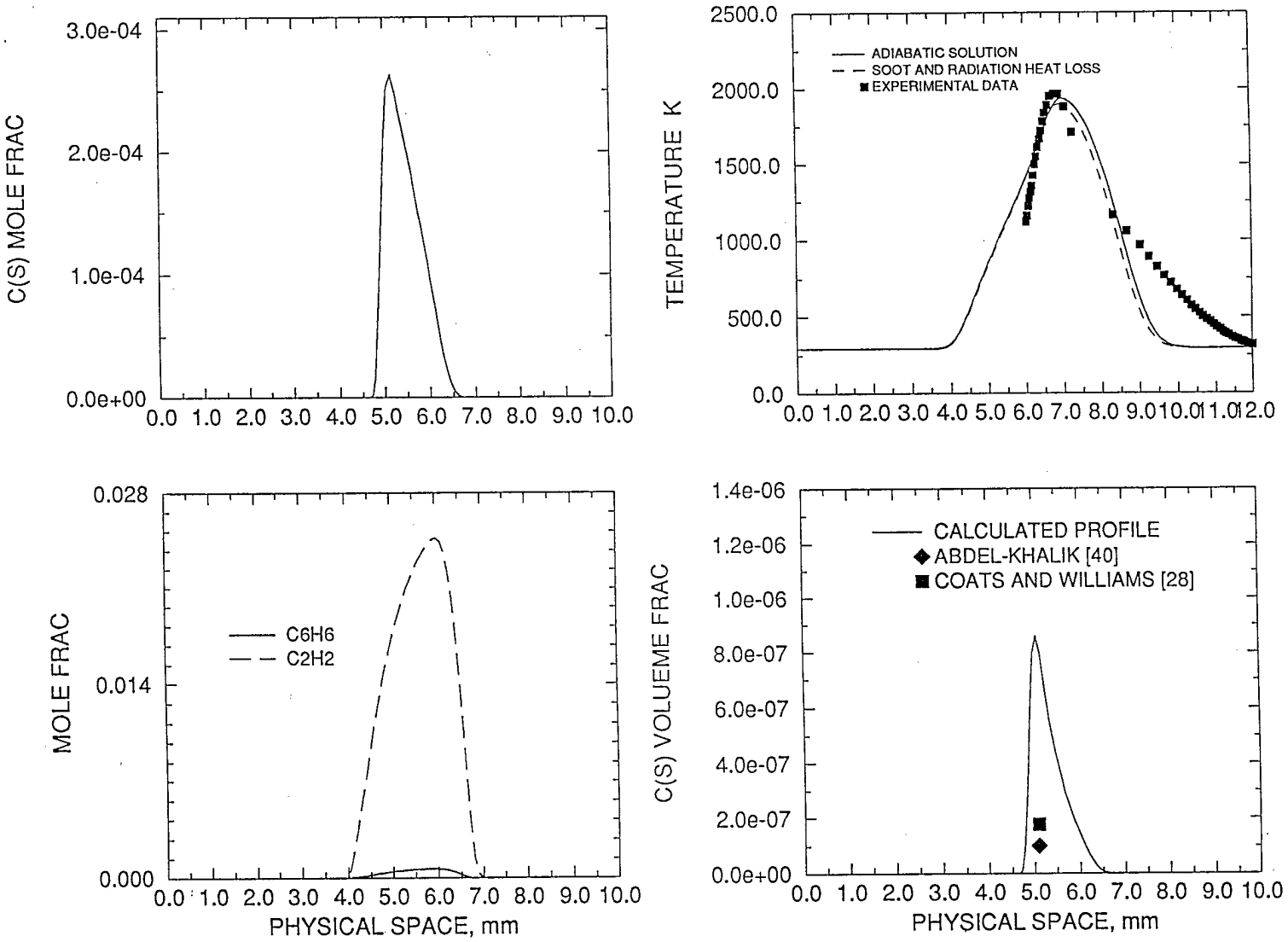

Figure 3.2.2.8
Abdel-Khalik n-Heptane Diffusion Flame Soot Formation
$a=50\ sec^{-1}$, Forward Stagnation Line Position

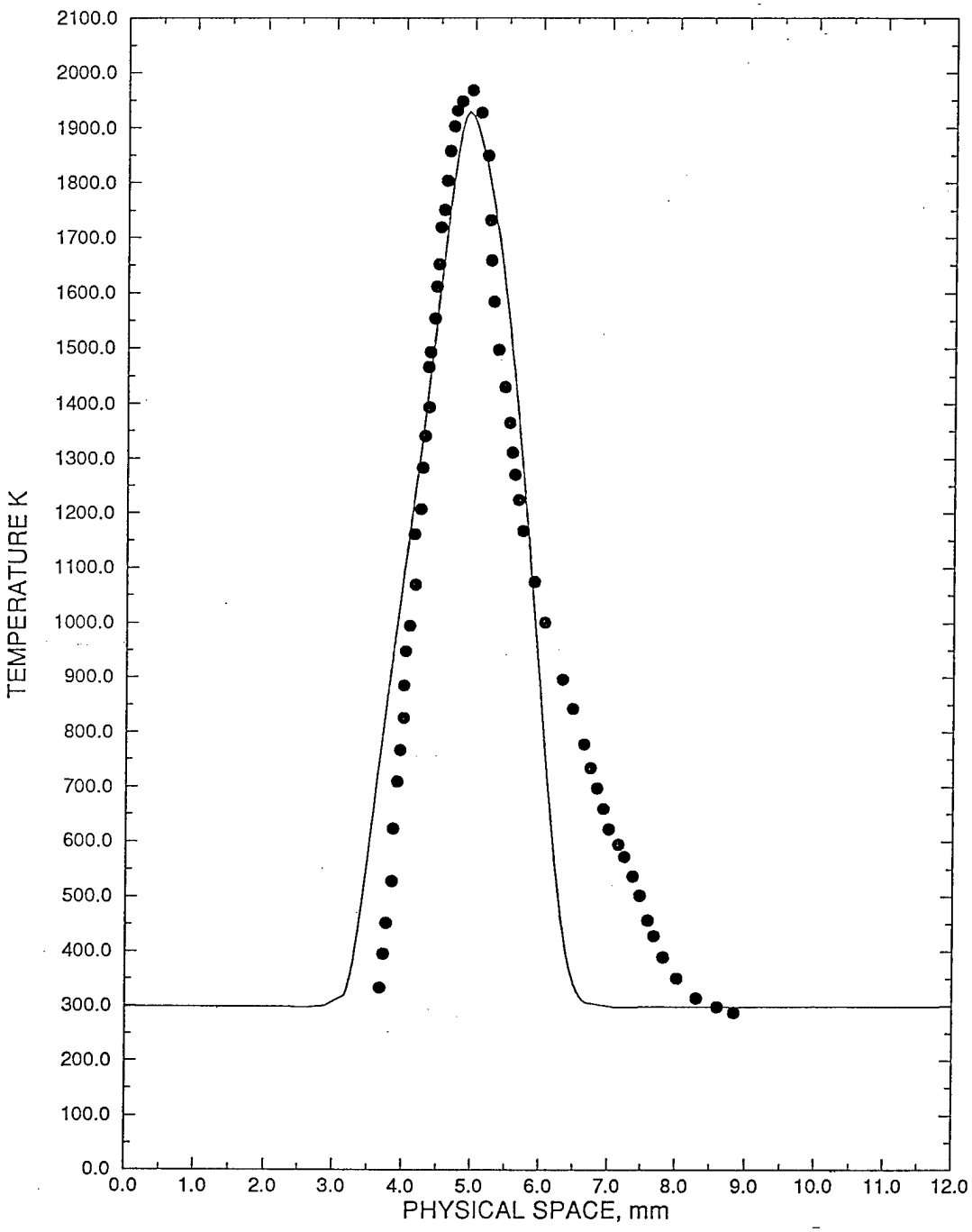

Figure 3.2.2.9
Abdel-Khalik n-Heptane Diffusion Flame
Temperature Measured and Calculated Profiles
$a=125\ sec^{-1}$, Forward Stagnation Line Position

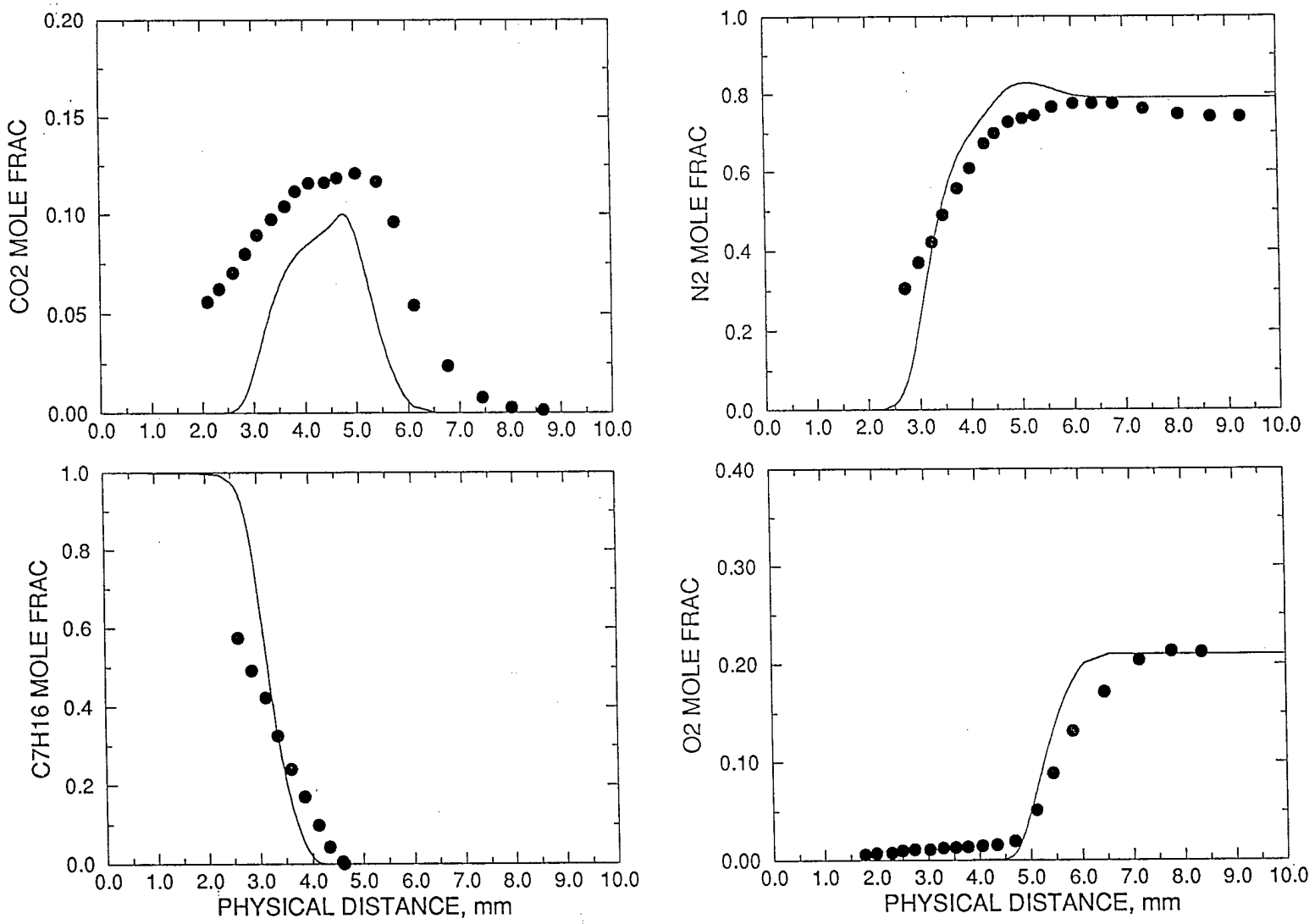

Figure 3.2.2.10
Abdel-Khalik n-Heptane Diffusion Flame Species
Measured and Calculated Profiles
a=125 sec^{-1}, Forward Stagnation Line Position

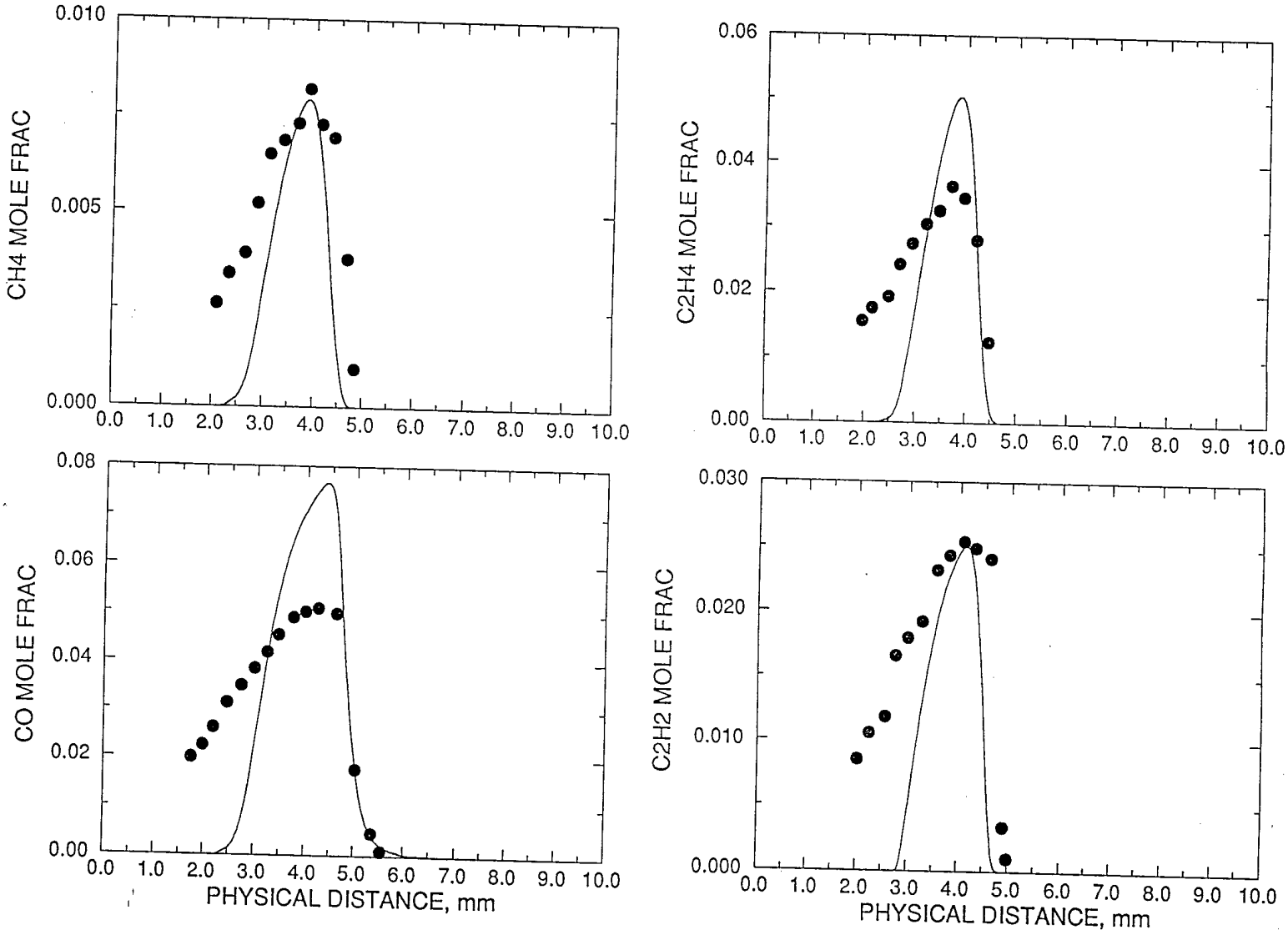

Figure 3.2.2.11
Abdel-Khalik n-Heptane Diffusion Flame Species Measured and Calculated Profiles
a=125 sec^{-1}, Forward Stagnation Line Position

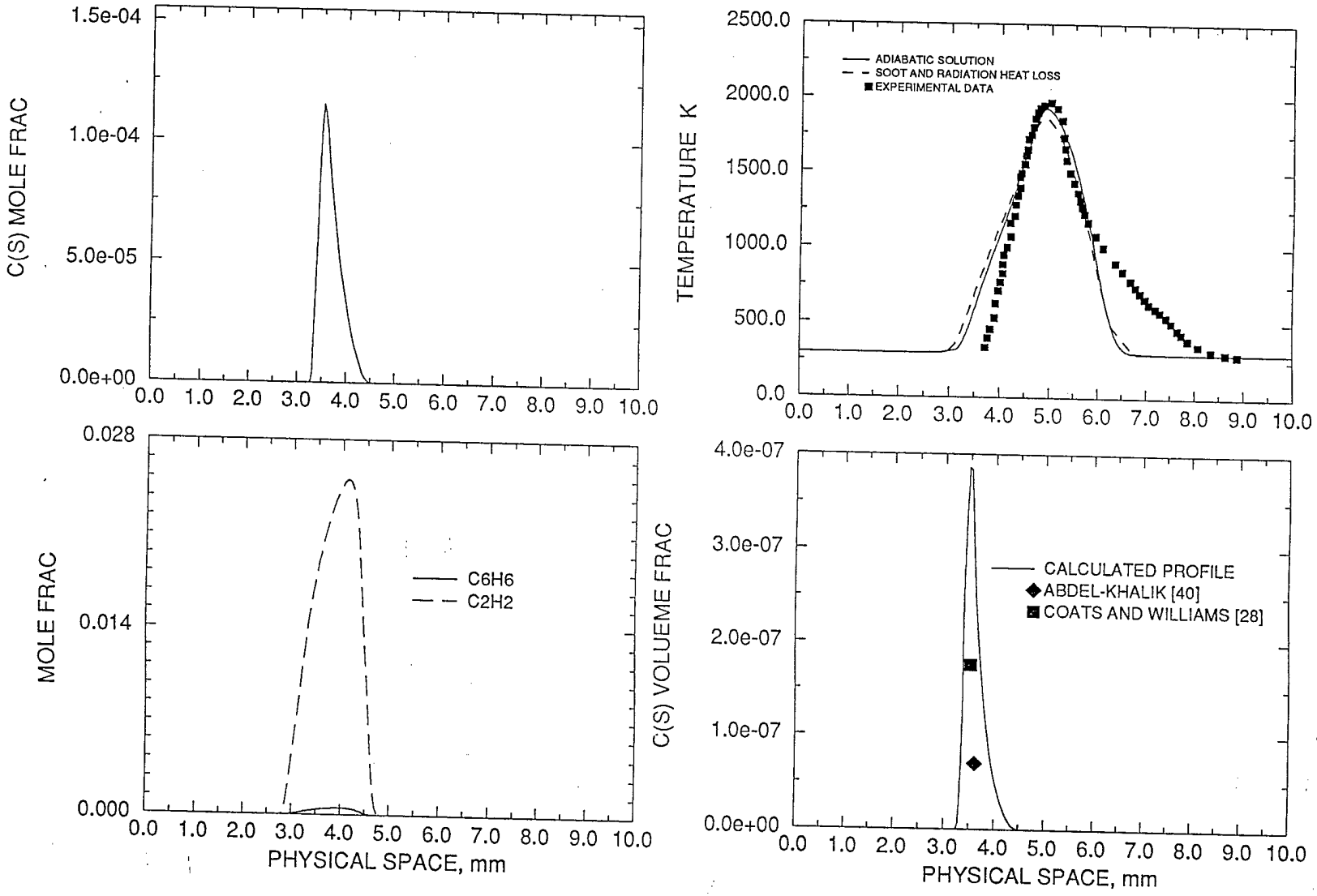

Figure 3.2.2.12
Abdel-Khalik n-Heptane Diffusion Flame Soot Formation
$a=125\ sec^{-1}$, Forward Stagnation Line Position

3.2.3 DESCRIPTION OF *n*-HEPTANE STIRRED REACTOR EXPERIMENT MODELLED

The only available detailed stirred reactor experimental data for *n*-heptane combustion is that of Chakir *et al* [32]. Thus, these results were used to validate the *n*-heptane combustion mechanism for stirred reactors. Aside from validating the reaction paths of the C_7 and linear C_6 species sub-mechanisms, it was also of interest to assess the ability of the C_1-C_4 and cyclic C_6 species sub-mechanism previously developed by Lindstedt and co-workers [19-24] to accurately predict species concentrations in a low temperature environment.

Chakir *et al* studied the combustion of *n*-heptane in a jet-stirred flow reactor over a wide range of temperatures (900-1200K) and fuel-oxygen equivalence ratios (0.2-2). All experiments were at atmospheric pressure. The reactor was a 4 cm diameter sphere made of fused silica which was heated by an electrical resistance system. Experimental procedures were as described by Gueret *et al* [90]. The temperature gradient in the reactor was reported not to exceed 10K [90]. The composition of exhaust products was analysed by gas chromatography and the species found in the exhaust stream included *n*-heptane, CO_2, CO, methane, acetylene, ethylene, ethane, propene, 1,3-butadiene, 1-butene, 1-pentene and 1-hexene.

The *n*-heptane combustion sub-mechanism for stirred reactors was validated at equivalence ratios between of 0.5 and 1 over the complete experimental temperature range reported in [32]. Experimental conditions selected for model validation were as shown in Table 3.2.3.1.

Table 3.2.3.1
n-Heptane Stirred Reactor Computational Conditions

Initial Temperature K	Mean Residence Time milliseconds	Equivalence Ratio	Initial *n*-heptane concentration mol%	Initial O_2 concentration mol%
1000	80-240	1.0	0.20	2.20
900-1170	200	0.5	0.15	3.30

3.2.4 *n*-HEPTANE STIRRED REACTOR RESULTS

The *n*-heptane stirred reactor combustion sub-mechanism was validated against experimental data for a dual purpose. This was to establish the ability of the overall mechanism to predict stirred reactor experimental results as well as to assess the capability of the C_1-C_4 and C_6 mechanism of Lindstedt and co-workers [19-24] to accurately predict species concentrations over a wider temperature range than previously attempted. However, modifications to the C_1-C_4 and cyclic C_6 mechanism of Lindstedt and co-workers [19-24] in order to match stirred reactor experimental data were avoided as this portion of the overall mechanism has been thoroughly validated against experimental data obtained in high temperature regimes. Comparisons between experimental

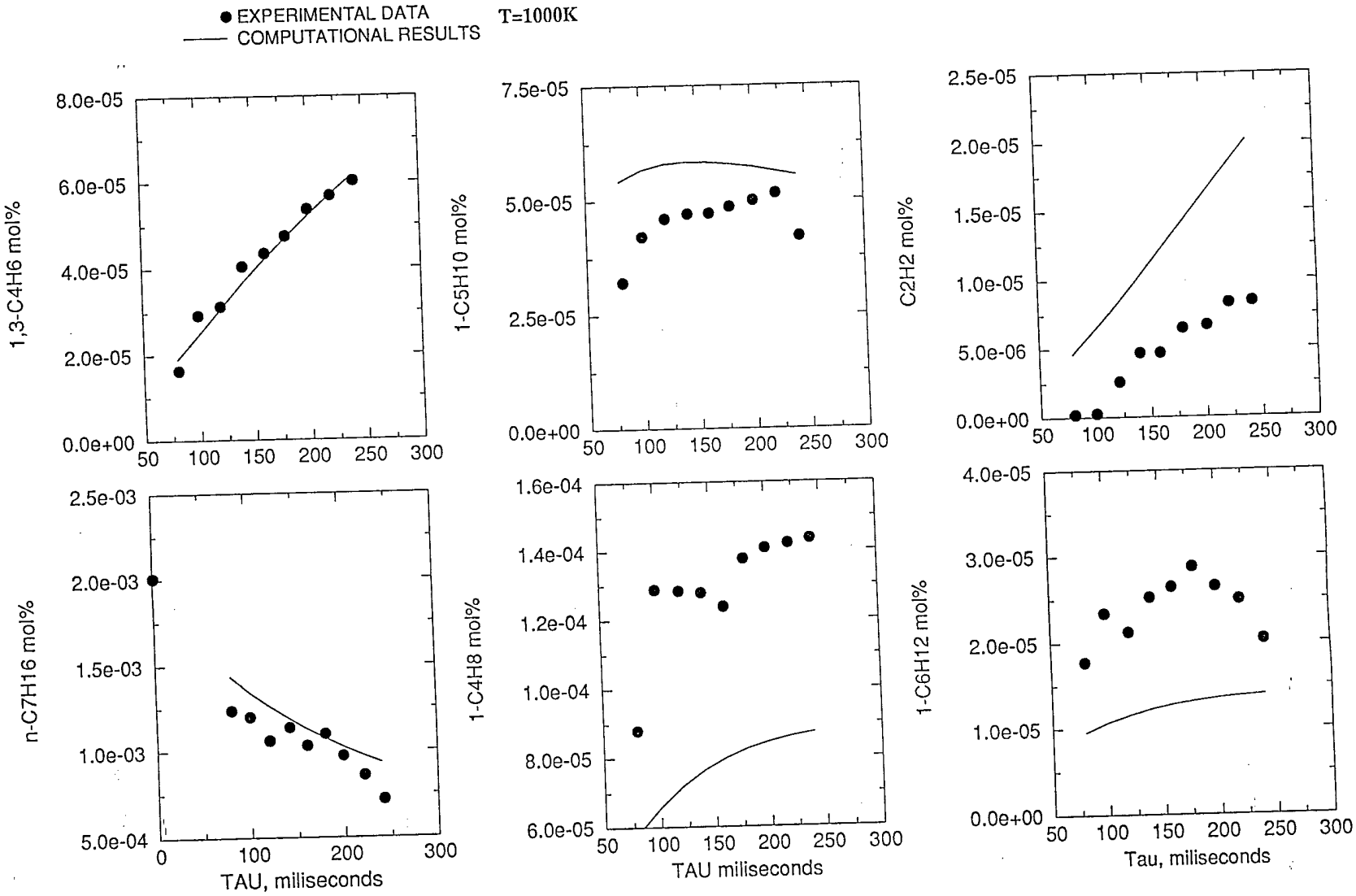

Figure 3.2.4.1
n-Heptane Stirred Reactor Computational Results
Species Concentrations versus Residence Time at 1000K

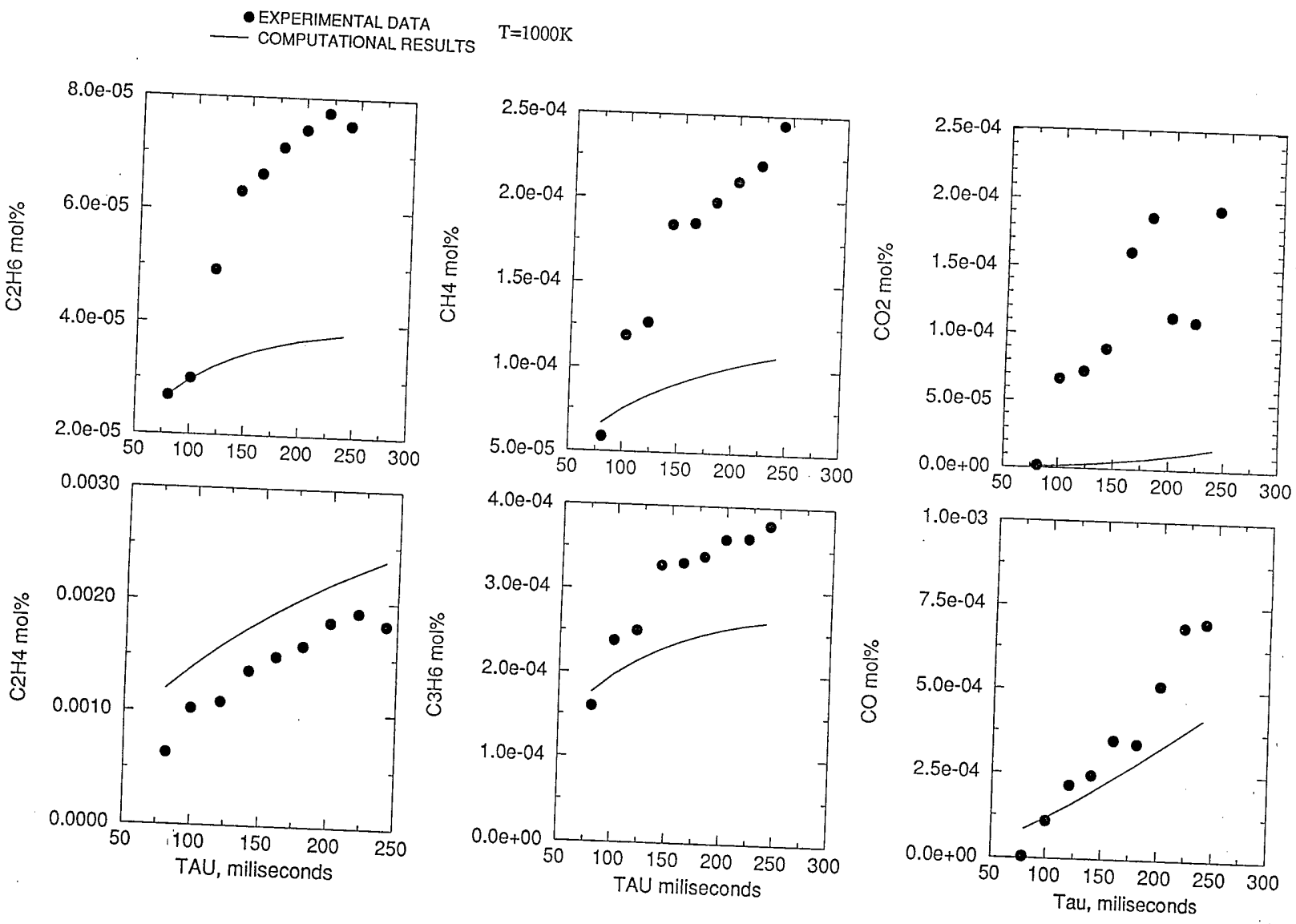

Figure 3.2.4.2
n-Heptane Stirred Reactor Computational Results
Species Concentrations versus Residence Time at 1000K

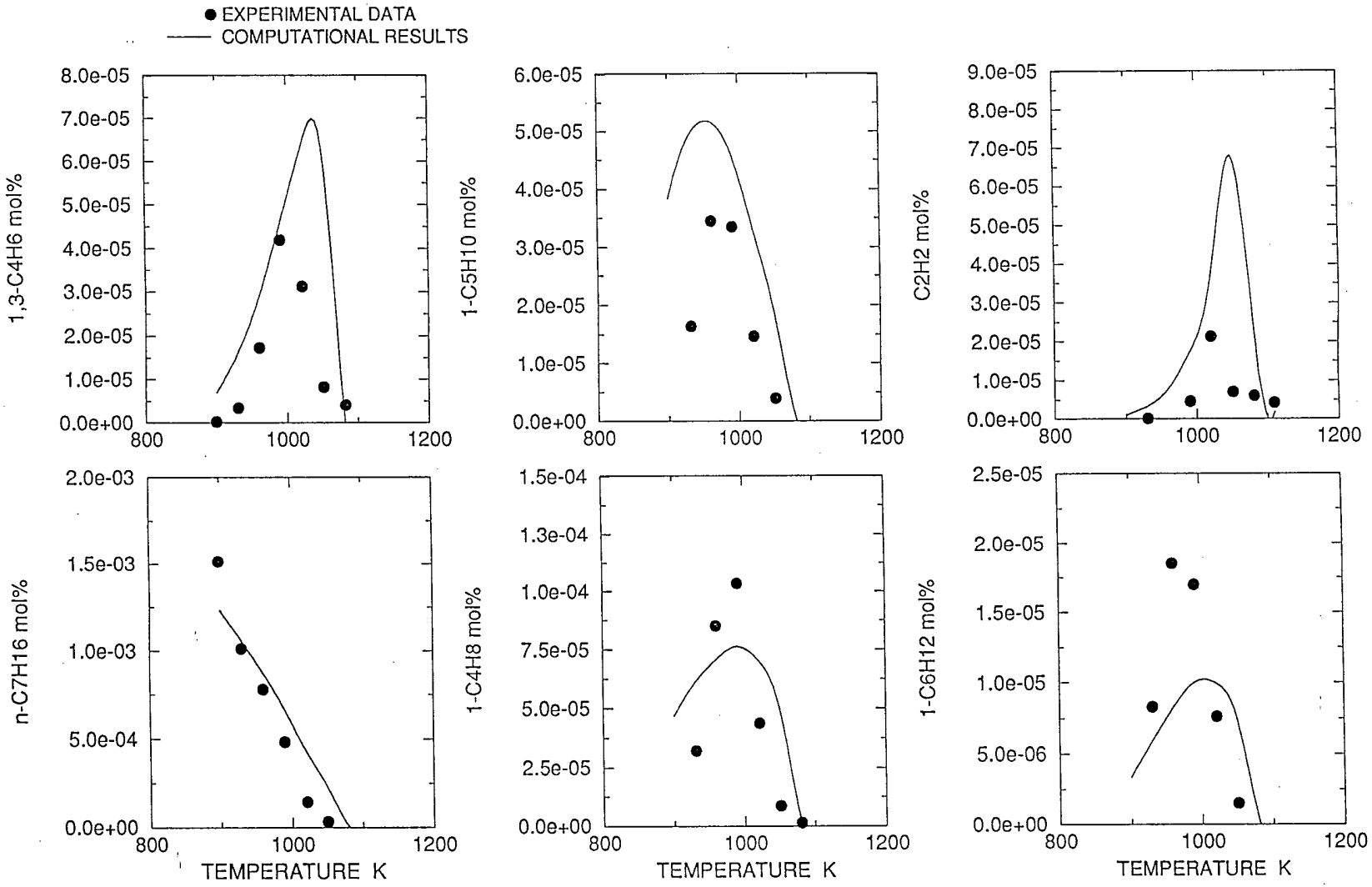

Figure 3.2.4.3
n-Heptane Stirred Reactor Computational Results
Species Concentrations versus Temperature at 200 milliseconds Residence Time

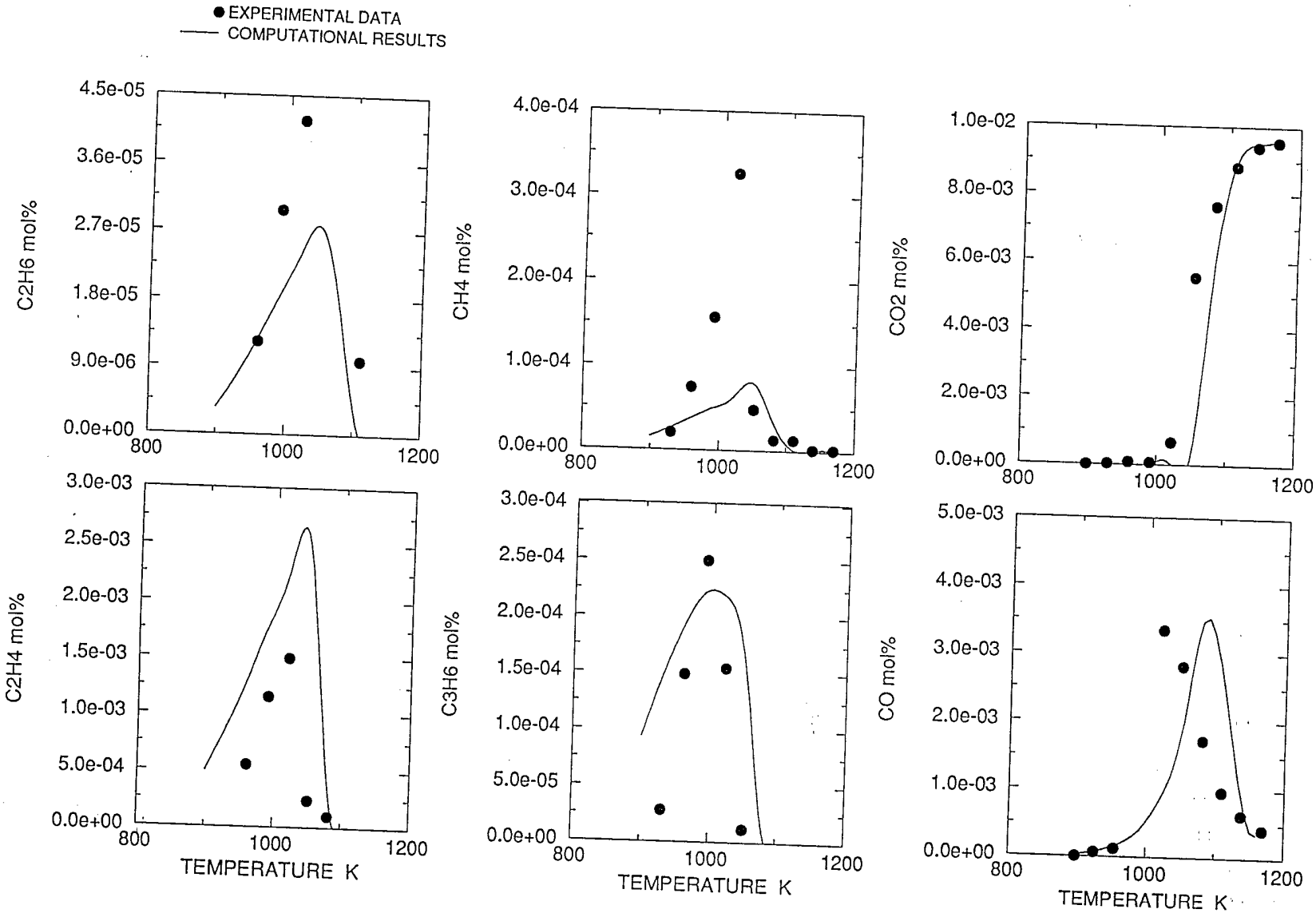

Figure 3.2.4.4
n-Heptane Stirred Reactor Computational Results
Species Concentrations versus Temperature at 200 milliseconds Residence Time

results and predictions for the Chakir *et al* *n*-heptane stirred reactor experiments are shown in Figures 3.2.4.1 to 3.2.4.4.

In general, concentrations of individual species as a function of residence time were well predicted at 1000K (Figures 3.2.4.1 and 3.2.4.2). Predictions were as good or better than those reported by Chakir *et al* [32] As shown in Figure 3.2.4.1, the molar concentration profile of *n*-heptane as a function of residence time was well predicted. Likewise, the molar concentrations of 1,3-butadiene, 1-pentene, 1-hexene, ethylene, propene and CO were predicted with excellent accuracy (a factor of 1.5 or less). Chakir *et al* reported that their mechanism generally over-predicted the concentration profiles of 1,3-butadiene. The mechanism used herein does not experience this difficulty, thus demonstrating the versatility of the high temperature C_1 to C_4 combustion sub-mechanism developed by Lindstedt and co-workers. Molar concentrations of 1-butene, methane, acetylene and ethane were predicted within a factor of two or less, well within the bounds of experimental error. However, the high pressure limit of the following reactions had to be used in order to properly predict the concentrations of ethane and methane at 1000K:

$$CH_3 + CH_3 = C_2H_6 \qquad (81)$$

$$CH_4 = CH_3 + H \qquad (103)$$

The accuracy of these predictions generally decreased with increasing residence time. The only specie concentration not accurately predicted at 1000K was CO_2. Given that the levels of CO were well predicted, it is likely that the source of the disagreement is experimental error. The CO_2 molar concentrations presented by Chakir *et al* [32] were digitized and it was determined that the accuracy of their CO_2 concentration predictions were no better than those shown in Figure 3.2.4.2.

The concentrations of individual species as a function of temperature for a reactor residence time of 200 milliseconds were also generally well predicted as can be seen in Figures 3.2.4.3 and 3.2.4.4. The concentrations of *n*-heptane, 1,3 butadiene, 1-butene, 1-pentene, ethylene, ethane and propene were all predicted within a factor of 1.5 or less. The peak concentration of 1-hexene was under-predicted by a factor of 2 and that of acetylene was over-predicted by a factor of 2.5. Only the over-prediction of acetylene is outside reasonable bounds of experimental error. The source of the acetylene over-prediction is likely to be the fact that soot formation was not included in the model. In the *n*-heptane diffusion flames acetylene levels were over-predicted unless soot formation was included in the computations. Initially, the concentrations of methane and ethane at high temperatures were found to be over-predicted by a factor of 5 when using the high pressure limit of reactions (81) and (103). Using the pressure dependent reaction rates corrected this discrepancy. However, it was not possible to predict the peak concentrations of methane and ethane at 1000K even when using the high pressure limit of reactions (81) and (103). The difficulty of predicting methane concentration has been discussed in the literature [31] and it is recognised that this part of the mechanism could further be enhanced. The rate constants used for the methane reactions are the best available at the moment and are firmly based on published rates and extensive validation of the C_1 to C_4 mechanism in diffusion flames. Finally, the

concentrations of CO and CO_2 were well predicted at high temperatures, as has also been reported by other researchers [31, 32].

In general, the *n*-heptane combustion mechanism for stirred reactors predicts experimental data within accuracy levels as good as or better than those reported by Chakir *et al* [32] and Foelsche *et al* [31]. The ability to accurately predict 1,3-butadiene levels is a particularly significant improvement over the kinetics reaction schemes utilised by these two groups of researchers.

4.0 TOLUENE/*n*-HEPTANE COMBUSTION

4.1 TOLUENE/*n*-HEPTANE MECHANISM

4.1.1 DESCRIPTION OF MECHANISM

Based on the path analysis of *n*-heptane combustion in diffusion flames discussed in 3.1.2 and a similar path analysis performed on a pure toluene diffusion flame to be discussed in Section 5.1.2, a mechanism was assembled to model the combustion of a toluene/*n*-heptane fuel blend in a diffusion flame. Elementary reactions and species determined to be of secondary importance in the pure *n*-heptane and pure toluene diffusion flames were neglected from the dual fuel mechanism. The toluene/*n*-heptane combustion sub-mechanism consisted of 59 elementary reactions and is presented in Table D1, Appendix D. The total mechanism is made up of 441 elementary reactions and 92 species. Thermochemical and physical properties for the individual species are as tabulated in Appendices B and E for the *n*-heptane and toluene sub-mechanisms.

The consumption of C_6 and below species and the soot formation steps proceed via the same elementary steps as in the overall *n*-heptane combustion sub-mechanism as shown in Appendix A.

4.1.2 PATH ANALYSIS OF TOLUENE/*n*-HEPTANE CONSUMPTION IN DIFFUSION FLAMES

Results

The rates of the 82 elementary reactions comprising the C_6 and C_7 sub-mechanism of the toluene/*n*-heptane combustion model were analysed in order to establish the predominant paths of fuel consumption. Emphasis was placed on assessing differences between reaction paths in diffusion flames of the pure components and those in the dual fuel flame. Only a 50 sec^{-1} strain rate flame was analysed, as differences in reactions paths with varying rates of strain have already been shown to be largely insignificant in section 3.1.2. The flame was modelled to simulate the experiment of Hamins and Seshadri [42] and Hamins [43] The boundary conditions for this flame were 18.1 mol% O_2 and 81.9 mol% N_2. The detailed path analysis for the toluene/*n*-heptane diffusion flame is summarised in Figure 4.1.2.1 shown below and Tables 4.1.2.1 to 4.1.2.22 shown in Appendix F.

The most significant features of toluene and *n*-heptane consumption in the dual fuel diffusion flame are shown in Figure 4.1.2.1. Toluene, being the lighter component, diffuses further downstream into the flame structure. The main paths of toluene destruction are H atom abstraction via H and OH radicals attack and cleavage of the methyl side group via H radical attack according to:

$$C_7H_8 + H = C_7H_7 + H_2 \quad (378)$$

$$C_7H_8 + OH = C_7H_7 + H_2O \quad (377)$$

$$C_7H_8 + H = C_6H_6 + CH_3 \quad (389)$$

Important secondary paths are H atom abstraction reactions via O radical attack according to:

$$C_7H_8 + O = C_7H_7 + OH \quad (376)$$

$$C_7H_8 + O = OC_7H_7 + H \quad (384)$$

The toluene pyrolysis reactions (381 and 380) achieve their highest rates in the reverse direction in the primary reaction zone. These reactions do occur at slow rates in the forward direction in the initial pyrolysis zone and must be included in the overall reaction mechanism in order to properly predict the pool of radicals for the subsequent H atom abstraction reactions. The behaviour of toluene consumption in the dual fuel flame is identical to that observed in the pure toluene diffusion flame as discussed in Section 5.1.2 with one notable exception. In the pure toluene diffusion flame, reaction 380 occurred only in the forward direction. In the dual fuel flame, a relatively larger pool of radicals is available earlier in the flame structure due to the initial consumption of *n*-heptane. Thus, radical attack reactions are more dominant than the highly endothermic thermal decomposition steps.

Comparison of the relative order of each initial toluene destruction elementary reaction in the dual fuel and pure toluene diffusion flames only revealed one minor difference. This was in the relative order of the two least dominant reactions, (382) and (383), and is likely attributable to temperature differences and/or differences in the relative concentrations of radicals within the flame structures.

$$C_7H_8 + C_6H_5 = C_7H_7 + C_6H_6 \quad (382)$$

$$C_7H_8 + CH_3 = C_7H_7 + CH_4 \quad (383)$$

Benzyl radical destruction was modelled via only O and OH radicals attack. The relative order of the reactions does not differ between the dual fuel and pure toluene diffusion flames. Linear C_7H_7 radical is produced and consumed at commensurate rates. This was also observed in the pure toluene diffusion flame.

Benzyl alcohol destruction was modelled via H radical attack yielding benzaldehyde. In the pure toluene diffusion flame the rate of this reaction was six to eight orders of magnitude faster than those of all other competing reactions. The rate of benzyl alcohol destruction in the dual fuel diffusion flame is roughly a third slower than predicted in the pure fuel flame as a result of temperature differences.

Benzaldehyde is consumed via pyrolysis and H and OH radical attack at rates slightly exceeding its rate of formation via benzyl alcohol radical abstraction reaction (388). The relative ranking of benzaldehyde destruction reactions is identical for dual fuel and pure toluene diffusion flames. Reaction rates are about three times slower in the dual fuel flame, as was observed in benzyl alcohol destruction.

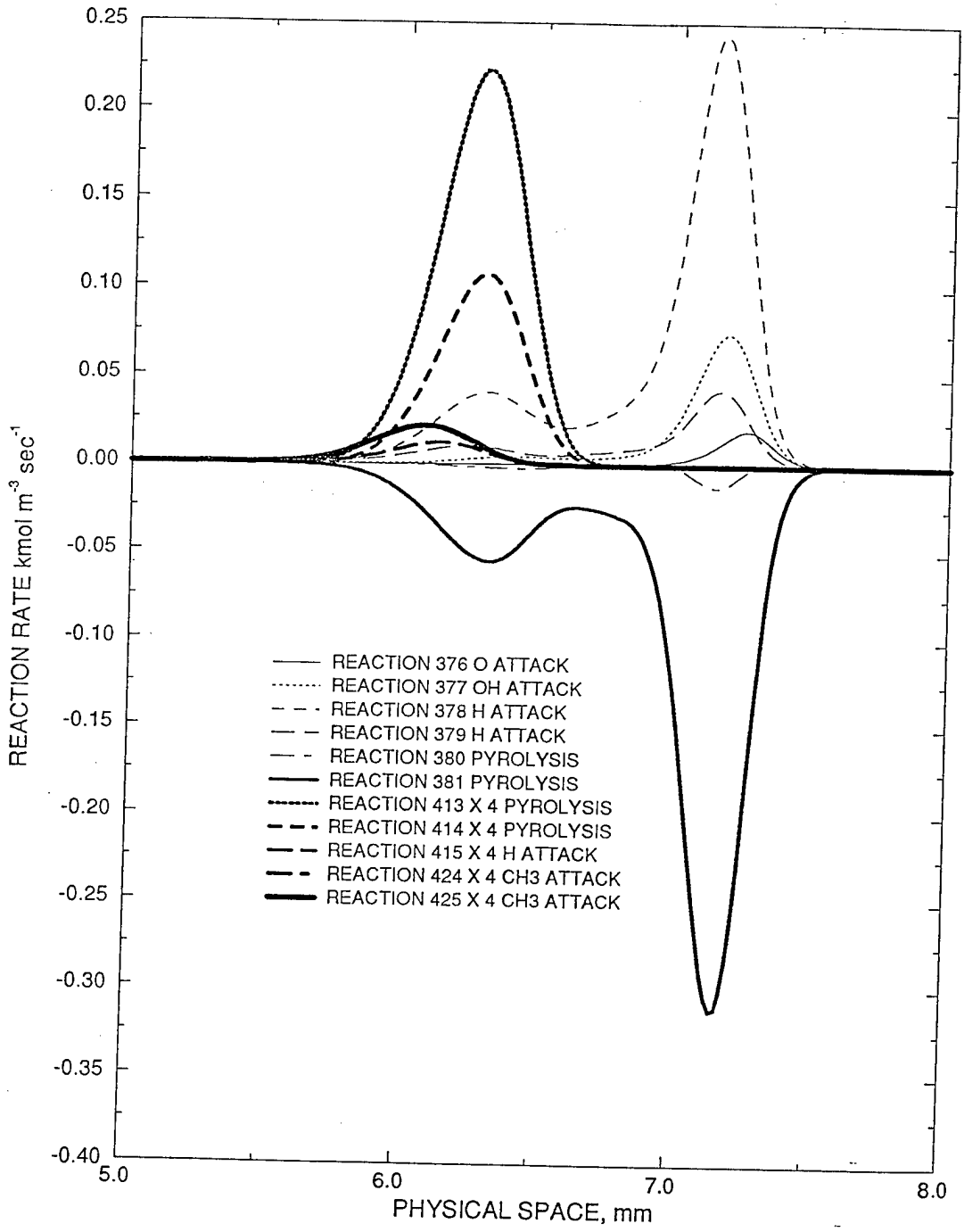

Figure 4.1.2.1

Toluene and n-Heptane Consumption Rates in Hamins and Seshadri Diffusion Flame

Cresoxy radical is consumed two times slower than it is produced via O attack on toluene and two to five times faster than formed via cresol H and OH radical abstraction reactions. The dominant cresoxy radical destruction reaction produces cresol as well, thus cresol is eventually destroyed via thermal decomposition. No differences in the reaction paths of cresoxy radical and cresol were noted between dual fuel and pure toluene diffusion flames.

In the dual fuel diffusion flame, benzene is principally consumed via H, OH and O radical attack. These were also the principal benzene destruction paths identified in the pure toluene diffusion flame. The relative ranking of individual reactions differs somewhat between the dual fuel and pure toluene diffusion flames. This is likely caused by differences in the radical pools between the two flames as a result of the *n*-heptane reactions.

As in the pure toluene diffusion flame, linear C_7H_8 is locally produced at slow rates. However, the primary direction of this reaction is in the forward direction.

The phenyl radical and linear C_6H_5 are observed to be consumed via similar paths as predicted in the pure toluene diffusion flame. The phenyl radical is consumed via OH radical attack and pyrolysis. As in the pure toluene diffusion flame, linear C_6H_5 is formed via rearrangement of the cyclic phenyl radical molecule. In the dual fuel flame linear C_6H_5 is formed via the molecular recombination of two propargyl radicals as well. Linear C_6H_5 is subsequently consumed at a rate an order of magnitude slower than its rate of formation.

As was observed in the pure toluene diffusion flame, phenoxy radical is quickly destroyed to form C_5H_5 and CO at a rate exceeding its rate of formation. In the primary flame zone, phenoxy radical also recombines with H radical to form phenyl alcohol.

Phenyl alcohol is consumed via pyrolysis and H, OH and O radical attack. Some differences are noted in the relative order of the reactions in the pure toluene and dual fuel diffusion flames. The primary path of phenyl alcohol destruction in the dual fuel diffusion flame is via pyrolysis whereas the rates of the radical abstraction reactions are faster in the pure toluene diffusion flame. However, the differences in overall reaction rates are small. Thus, the phenyl alcohol consumption paths can be considered to be similar in the two flames.

The features of the dominant *n*-heptane consumption reactions are also shown in Figure 4.1.2.1. In general, the destruction of *n*-heptane occurs prior to that of toluene in the dual fuel flame. Thus, differences in reaction paths between the dual fuel flame and pure *n*-heptane flame discussed in Section 3.1.2 should not be significant. This can indeed be observed in Figure 4.1.2.1 and Table 4.1.2.16. In the dual fuel flame, *n*-heptane is also primarily destroyed via C-C bond rupture pyrolysis reactions. H and CH_3 radicals diffuse into the fuel rich flame zone and dominate this part of the structure as noted in the pure *n*-heptane diffusion flame. Likewise, the slower OH radical attack reactions are observed to be important in the fuel lean flame zone. The most notable difference in the *n*-heptane reaction paths in the two flames is the relative ranking of the CH_3 and H radicals abstraction reactions. In the dual fuel flame, the CH_3 abstraction reactions are more dominant. This is reasonable, since one of the direct products of toluene

consumption is the CH_3 radical. Therefore the relative concentration of this radical is larger in the dual fuel flame structure and thus this destruction path of *n*-heptane is slightly more dominant.

The rate of heptyl radical consumption via thermal rupture of C-C bonds and of isomerization reactions between the four radicals were shown to be two to five orders of magnitude faster than those of H radical and O_2 attack reactions. Thus, only the pyrolysis and isomerization reactions of the heptyl radicals were considered in the dual fuel diffusion flame model. As shown in Table 4.1.2.17, the relative order of the heptyl radicals destruction reactions is not changed between the two flames. Likewise, the thermal decomposition of the 1-pentyl radical and 1-pentene rapidly proceeds at rates commensurate with their rates of production.

In the dual fuel flame, the destruction of the *n*-butyl radical also occurs primarily via thermal decomposition through C-C bond rupture. The consumption of *n*-butyl radical via C-H bond rupture is not as significant, as was noted in the pure *n*-heptane diffusion flame. Nonetheless, this reaction and the most dominant ensuing destruction paths of 1-butene and 1-butene radical were considered in the dual flame model as these paths generate methyl radical and subsequently methane, an important intermediate specie. No differences were observed in the *n*-butyl radical, 1-butene and 1-butene radical reaction paths in the dual fuel and pure *n*-heptane diffusion flames.

Discussion

The most important conclusion that may be derived from the detailed path analysis of toluene and *n*-heptane consumption in the dual fuel flame is that no critical differences are noted between the reaction paths of each individual fuel component in the dual fuel diffusion flame and those observed in diffusion flames of each pure component. It is very difficult to obtain detailed species concentration data in the fuel rich zone of a pure toluene diffusion flame due to the high soot concentrations encountered in this region [42, 43]. However, since the destruction paths of toluene are shown to be virtually unchanged in a dual fuel flame, it is possible to validate a toluene combustion sub-mechanism for diffusion flames against data obtained for a diffusion flame of a toluene/*n*-heptane fuel blend.

4.2 TOLUENE/*n*-HEPTANE MECHANISM EVALUATION

4.2.1 DESCRIPTION OF TOLUENE/*n*-HEPTANE EXPERIMENTAL DIFFUSION FLAME MODELLED

The only known data sets for toluene/*n*-heptane fuel blend diffusion flames are those of Gulder [89] and Hamins and Seshadri [42] and Hamins [43]. The Gulder flame was a coflow configuration and only peak soot levels were reported in this reference. Hamins and Seshadri did report temperature and major and intermediate species profiles for a counterflow toluene/*n*-heptane diffusion flame. Thus, the Hamins and Seshadri data set was selected for model validation.

The experimental set up and data accuracy for the Hamins and Seshadri toluene/*n*-heptane diffusion flame are identical to those reported for the *n*-heptane diffusion flame and previously described in Section 3.2.1. The reported boundary conditions were 60 mol% toluene and 40 mol% *n*-heptane at the fuel boundary, 18.1 mol% O_2 concentration at the air side boundary, 39.6 cm/sec air velocity and 0.56 g/cm^2/min burning rate. The wide sooting zone observed on the fuel rich side of a pure toluene diffusion flame was not detected in the dual fuel flame. Composition and temperature profiles were thus reported over the entire flame zone.

The species concentration data reported by Hamins and Seshadri were analysed in terms of mixture fraction using the techniques discussed in Section 3.2.1. Results of this analysis are shown in Figure 4.2.1.1. In the fuel rich flame zone, the mixture fraction values calculated using Bilger's definition correlate well with those computed based on elemental carbon, hydrogen and oxygen. As was observed in the Hamins and Seshadri *n*-heptane flame, there is a small discrepancy in the mixture fraction value computed based on elemental oxygen in the fuel lean zone. Overall, these data appear to be of good quality and well suited for kinetic mechanism validation.

4.2.2 TOLUENE/*n*-HEPTANE DIFFUSION FLAME RESULTS

Comparisons between analytical predictions and experimental results for the Hamins and Seshadri toluene/*n*-heptane flame are summarised in Figures 4.2.2.1 to 4.2.2.5. A rate of strain of 50 sec^{-1} was found to accurately match the width of the temperature and major species profiles.

The temperature profile calculated using soot and radiation heat loss is shown in Figure 4.2.2.1. The predicted profile matches the experimental data within 150K, which is outside the bounds of experimental uncertainty by around 50K. Since the heat of vaporisation of toluene is higher than that of *n*-heptane, the discrepancy between analytical temperature predictions and experimental data observed is slightly higher than noted for the pure *n*-heptane flame (Section 3.2.2).

Fuel consumption and major species peak concentrations and overall profiles were predicted with excellent accuracy, as shown in Figures 4.2.2.2 and 4.2.2.3. Only the shape of the O_2 profile shows some discrepancy. The model assumes that no O_2 is present at the fuel side boundary,

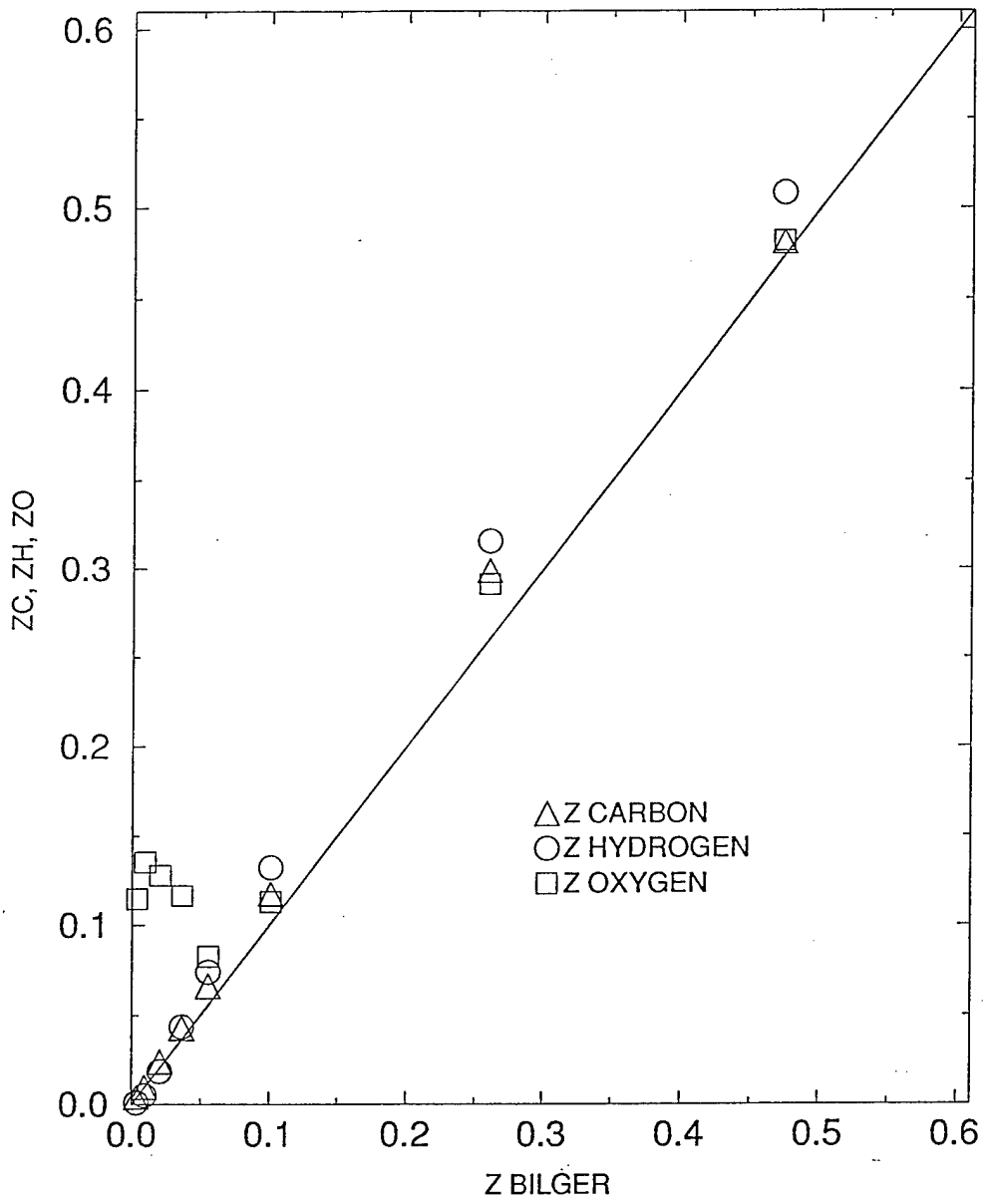

Figure 4.2.1.1
Hamins and Seshadri Toluene/n-Heptane Diffusion Flame Mass Fraction Comparison

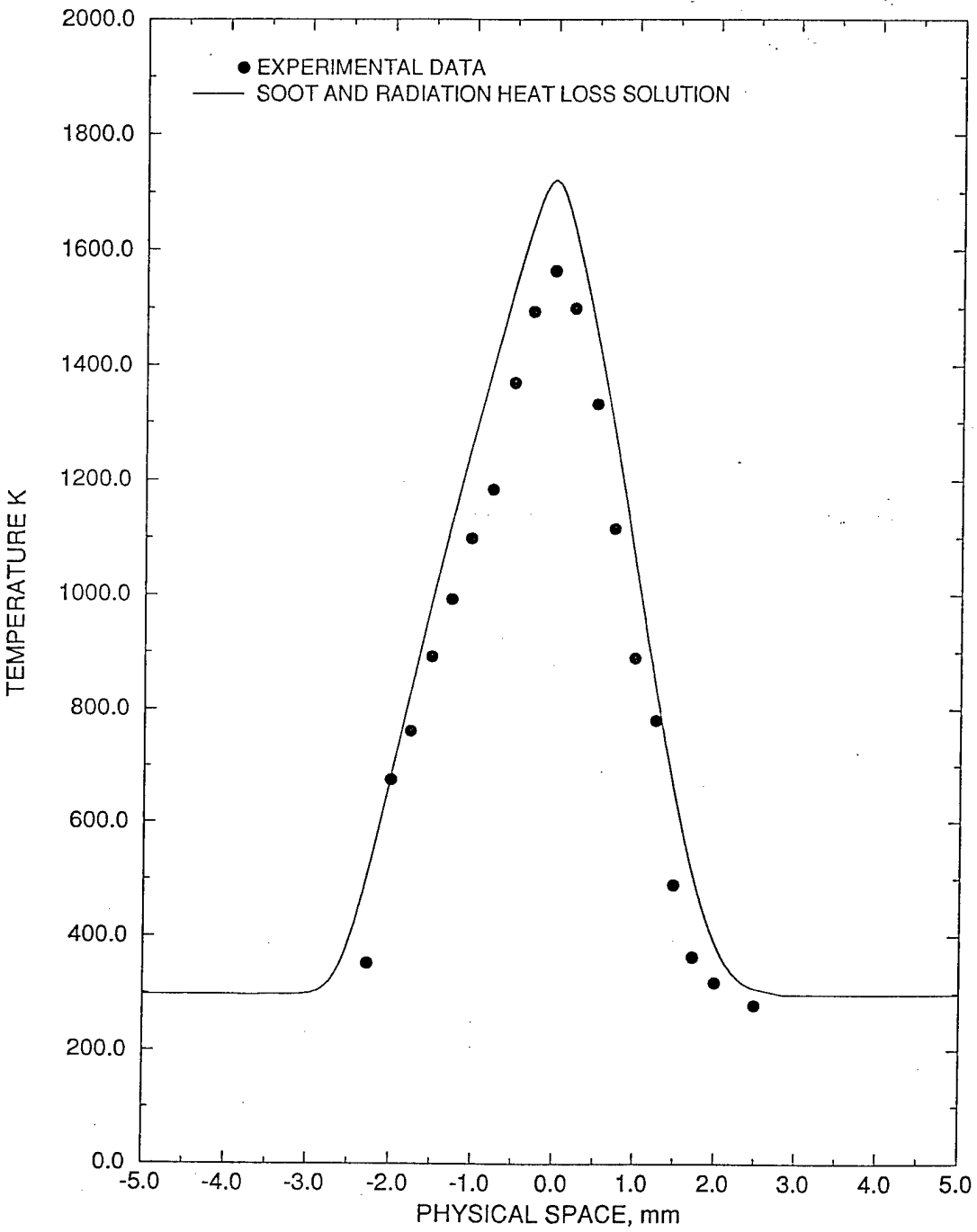

Figure 4.2.2.1
Hamins and Seshadri Toluene/n-Heptane Diffusion Flame Temperature Measured and Calculated Profiles

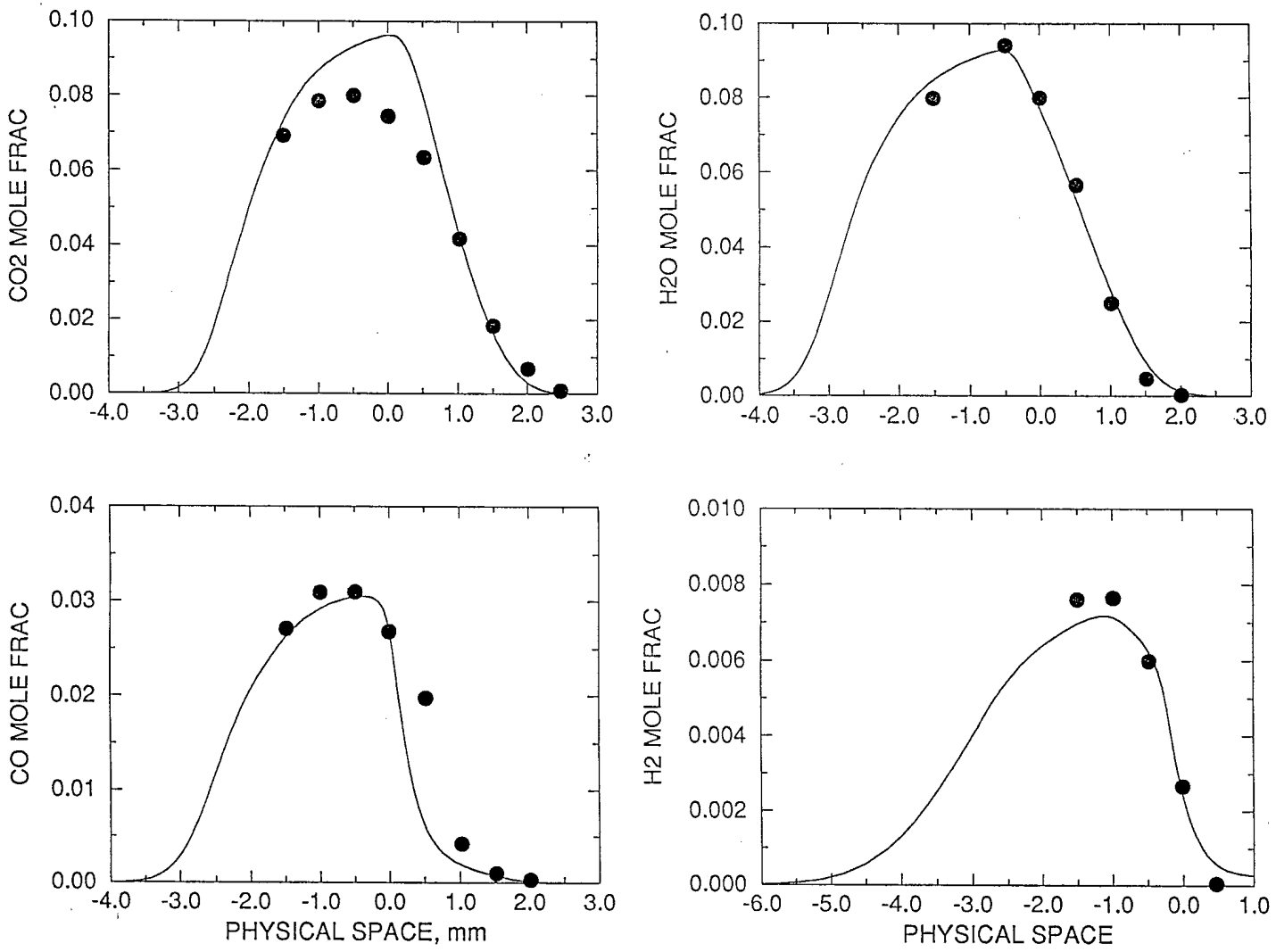

Figure 4.2.2.2
Hamins and Seshadri Toluene/n-Heptane Diffusion Flame Species Measured and Calculated Profiles

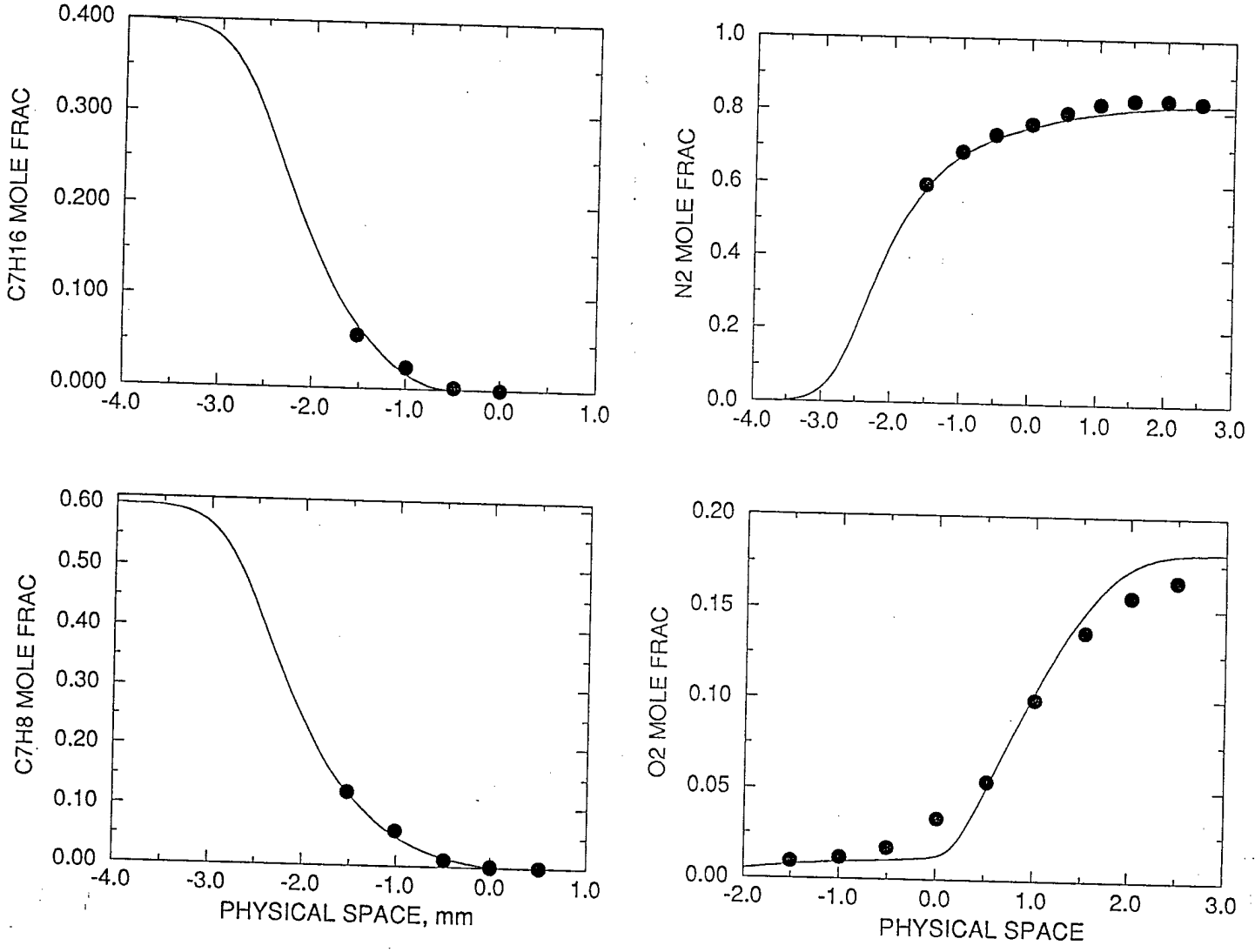

Figure 4.2.2.3
Hamins and Seshadri Toluene/n-Heptane Diffusion Flame Species Measured and Calculated Profiles

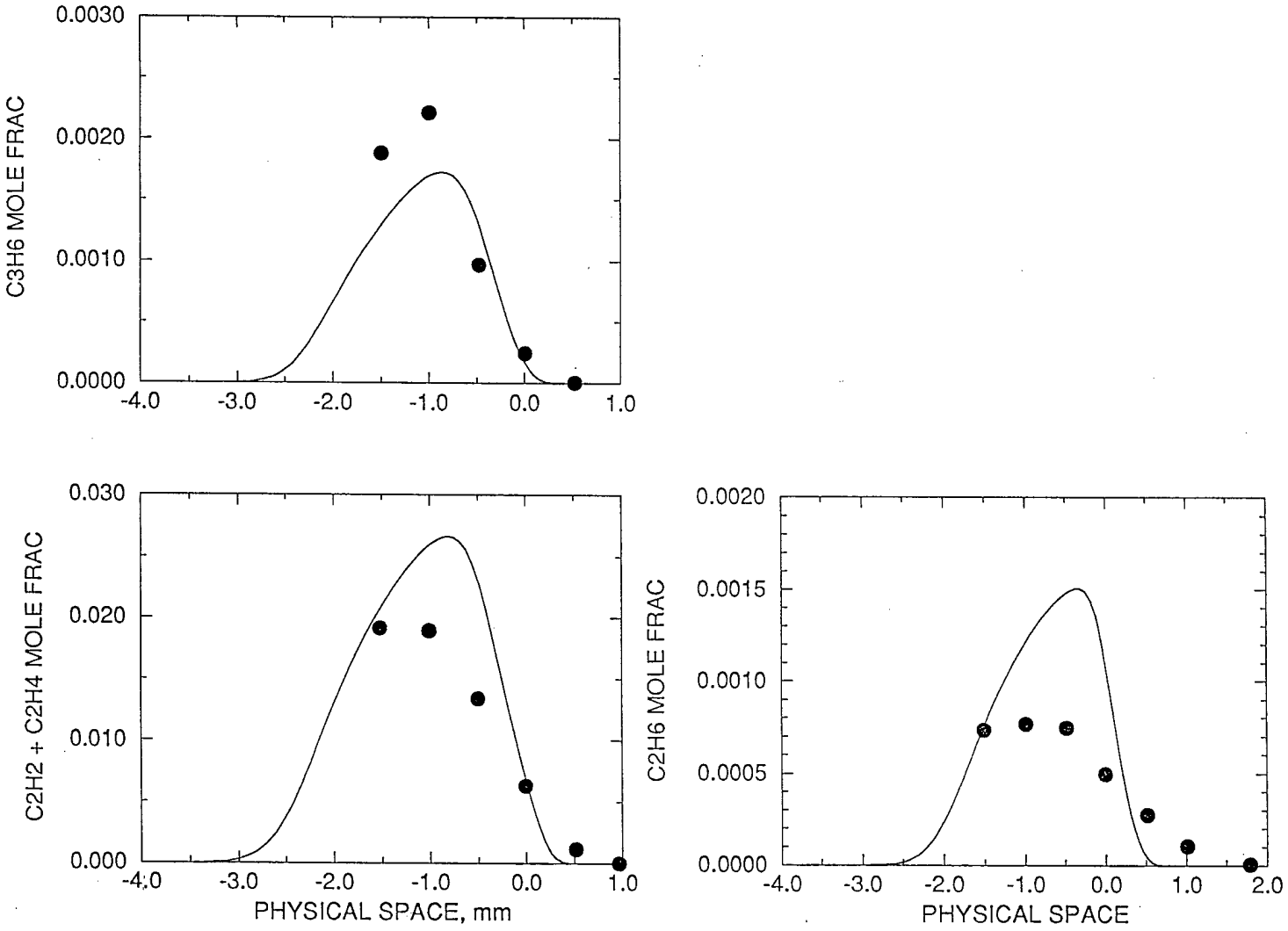

Figure 4.2.2.4
Hamins and Seshadri Toluene/n-Heptane Diffusion Flame Species Measured and Calculated Profiles

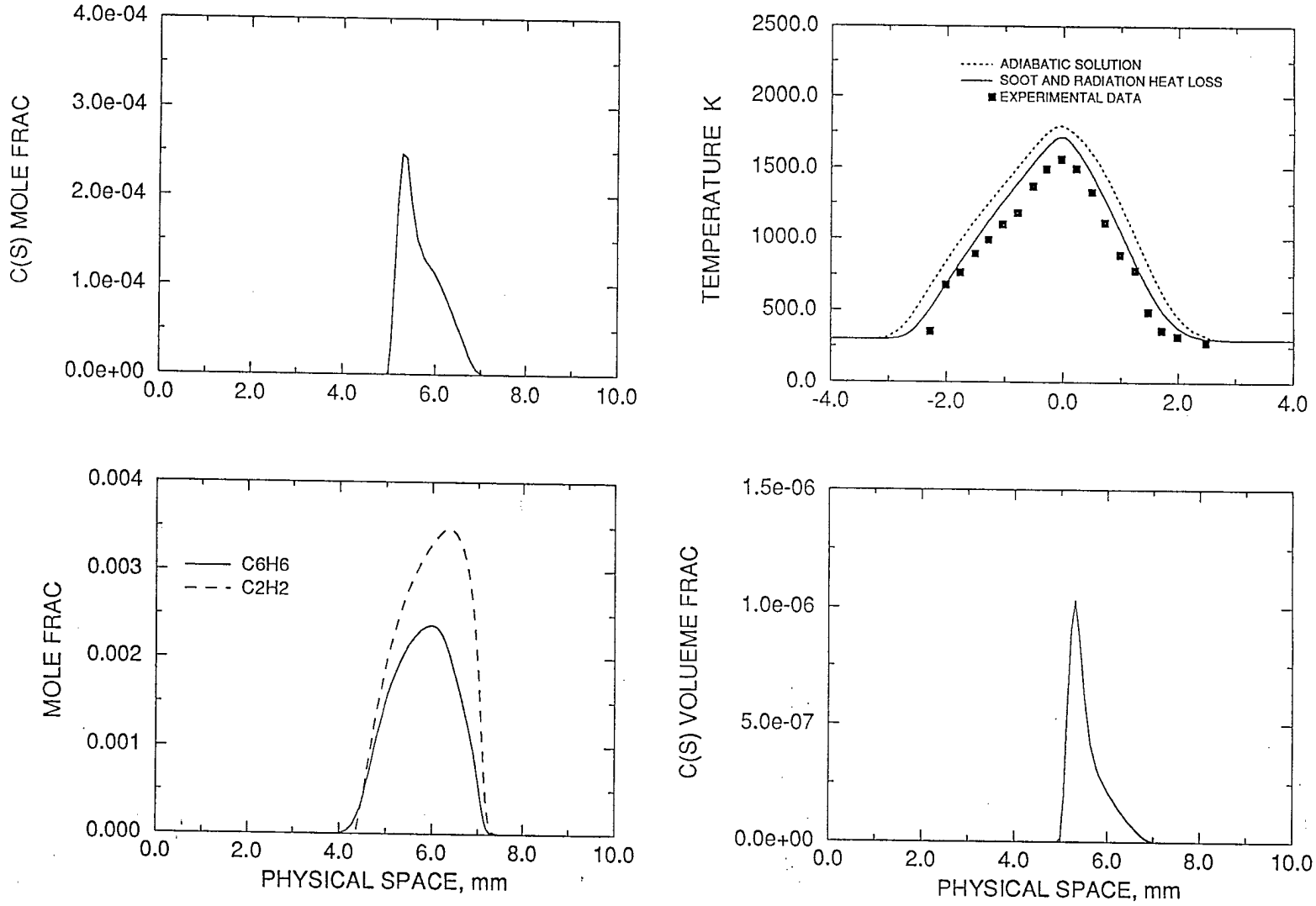

Figure 4.2.2.5
Hamins and Seshadri Toluene/n-Heptane Diffusion Flame Soot Formation

whereas experimentally a small amount of O_2 was detected at this boundary [43]. This is likely the cause of the observed discrepancy.

Hydrogen concentrations, which were over-predicted by a factor of 2.5 for the pure *n*-heptane flame, is precisely predicted in the dual fuel flame. As discussed in Section 3.2.2, the reported hydrogen measurements for the pure *n*-heptane diffusion flame appear low. A hydrogen mole fraction of approximately 0.008 was reported in the dual fuel flame whereas in the pure *n*-heptane flame a value slightly under 0.01 mole fraction was reported. Given that the carbon to hydrogen ratio of *n*-heptane is 2.28 and that of toluene is 1.14, it is reasonable to expect that a higher difference should have been measured in the relative concentrations of these species between the two flames.

Excellent results were achieved in the prediction of peak levels of intermediate species, as shown in Figure 4.2.2.4. Intermediate species levels were predicted within a factor of 1.5. The predictions of acetylene and ethylene concentrations are shown on a cumulative basis, as was reported experimentally. It should also be noted that ethylene levels have been accurately predicted for the five Abdel-Khalik *n*-heptane flames as well as for the Hamins and Seshadri toluene/*n*-heptane flame. Thus, the over-prediction of ethylene by a factor of 3 observed in the Hamins and Seshadri *n*-heptane flame computations can sensibly be attributable to experimental measurement error.

Computed soot and volume fractions as well as other flame sooting characteristics are shown in Figure 4.2.2.5. The soot radiation model resulted in a temperature drop slightly exceeding 100K from the adiabatic value. The peak soot volume fraction predicted for the toluene/*n*-heptane flame was nearly an order of magnitude higher than that predicted for the Hamins and Seshadri *n*-heptane flame (1.37E-06 versus 3.3E-07). This is reasonable, considering the well known sooting tendencies of toluene. The soot and radiation model does result in reasonable predictions of temperature and species profiles without resorting to fictitious heat loss factors. Since soot levels were not reported for the specific flames computed herein, it is not sensible to alter the soot model at this time without further experimental guidance. Once a reduced mechanism is obtained, it would be computationally feasible to model the coflow toluene/*n*-heptane diffusion flame studied by Gulder [89] using detailed chemistry in order to enhance and validate the soot formation model.

5.0 TOLUENE COMBUSTION

5.1 TOLUENE MECHANISM

5.1.1 DESCRIPTION OF MECHANISM

A detailed mechanism consisting of 437 elementary reactions and 86 species was used to model the combustion of toluene in diffusion flames whereas a mechanism consisting of 447 elementary reactions and 87 species was used to model the combustion of toluene in stirred reactors. The differences in the toluene combustion sub-mechanisms were the result of favouring reaction rates at temperatures exceeding 1200K for modelling diffusion flames and including additional oxygenated species reactions and neglecting soot formation paths from the stirred reactor computations. Essentially, the toluene sub-mechanisms encompassed the recommendations of Emdee *et al* [29] as well as of others [30, 91-106]. The formation and consumption of oxygenated species was included in order to thoroughly assess the influence of as many elementary reactions as feasible when the mechanism is eventually reduced via systematic methods. The criteria employed for selecting specific reaction rate constants and techniques used to gather and/or generate thermochemical and physical properties data for unusual species were as described in section 3.1.1 for the *n*-heptane sub-mechanism. The toluene sub-mechanisms are shown in Appendix D and the thermochemical and physical properties for species specific to these sub-mechanisms

Table 5.1.1.1
Structures and Heats of Formation of Toluene Sub-Mechanism Species

SPECIE	NAME	STRUCTURE	ΔH_f KJ/mol	Reference
C_6H_5CO	Benzoyl Radical	ϕ-CO·	109.250	29
C_7H_6O	Benzaldehyde	ϕ-CHO	-36.420	29
C_7H_7	Benzyl Radical	ϕ-CH_2·	210.500	67
C_7H_7L	Linear C_7H_7	CH_2=C=CH-CH=CH-CH=CH·	177.680	19,22
OC_7H_7	Cresoxy radical	·O-ϕ-CH_3	15.190	29
C_7H_7O	Methoxy Phenyl Radical	ϕ-CH_2O	100.690	pw
HOC_7H_7	Cresol	OH-ϕ-CH_3	-128.800	29
C_7H_7OH	Benzyl Alcohol	ϕ-CH_2OH	-100.420	29
C_7H_8	Toluene	ϕ-CH_3	50.020	67
C_7H_8L	Linear C_7H_8	CH_2=C=CH-CH=CH-CH=CH_2	199.695	19,22
C_8H_8	Styrene	ϕ-C_2H_3	148.063	29
C_8H_{10}	Ethyl Benzene	ϕ-C_2H_5	29.930	29
$C_{12}H_{10}$	Biphenyl	ϕ-ϕ	182.453	67
$C_{14}H_{14}$	Bibenzyl	ϕ-CH_2-CH_2-ϕ	143.580	29

ϕ = PHENYL STRUCTURE

The consumption of C_5 and below species and the formation of soot proceeds via the same elementary steps as in the overall *n*-heptane combustion mechanism shown in Appendix A.

5.1.2 PATH ANALYSIS OF TOLUENE CONSUMPTION IN DIFFUSION FLAMES

Results

The rates of the elementary reactions comprising the C_6 and C_7 sub-mechanisms were analysed in order to establish the principal paths of toluene and benzene consumption in pure toluene diffusion flames. A 50 sec^{-1} strain rate flame was analysed, according to the experiment of Hamins and Seshadri [42] and Hamins [43] The oxidiser stream for this flame was 20.2 mol% O_2/79.8 mol% N_2. A summary of the detailed path analysis for the toluene diffusion flames is provided in Figure 5.1.2.1 shown below and Tables 5.1.2.1 to 5.1.2.16 shown in Appendix G.

The principal features of toluene consumption in the diffusion flame structure are shown in Figure 5.1.2.1. The detailed toluene consumption path analysis shows that the main paths of initial toluene destruction in the flame structure are H abstraction via H and OH radical attack according to:

$$C_7H_8 + H = C_7H_7 + H_2 \quad (383)$$

$$C_7H_8 + OH = C_7H_7 + H_2O \quad (381)$$

Important secondary paths for toluene consumption involve cleavage of the methyl side group via H attack and pyrolysis according to:

$$C_7H_8 + H = C_6H_6 + CH_3 \quad (384)$$

$$C_7H_8 = C_6H_5 + CH3 \quad (385)$$

Hydrogen atom abstraction via O radical attack complete the primary reaction paths according to:

$$C_7H_8 + O = C_7H_7 + OH \quad (380)$$

$$C_7H_8 + O = OC_7H_7 + H \quad (389)$$

It is noted that reaction (389) results in the production of cresol at a relatively substantial rate. Thus it appears to be of some interest to include oxygenated species in the analysis of the toluene diffusion flame structure.

The toluene pyrolysis reaction (386) occurs in the reverse direction in the primary reaction zone at a very fast rate. Therefore, toluene is created via H atom recombination with the benzyl radical. However, in the initial fuel rich flame zone, this reaction occurs in the forward direction at a very

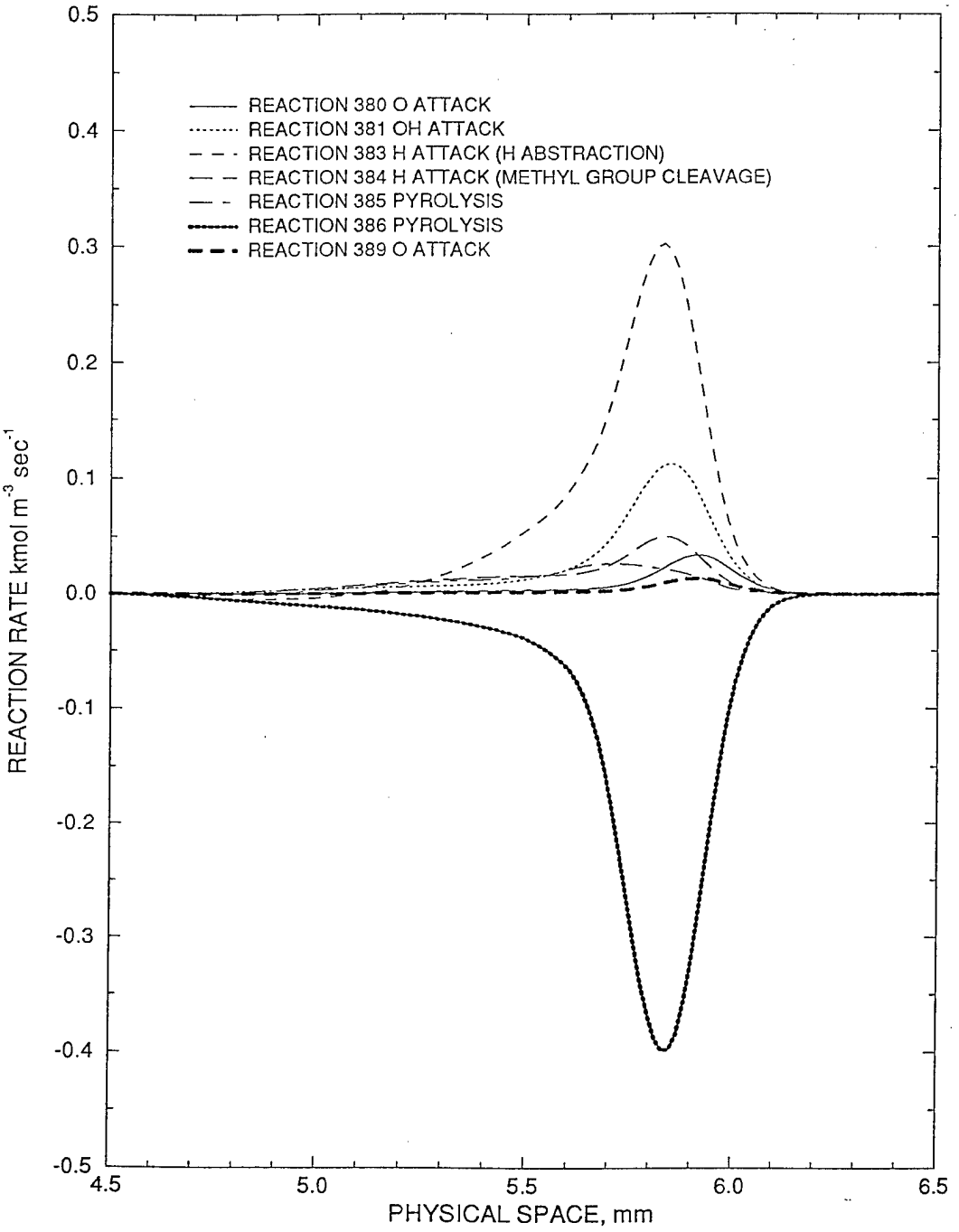

Figure 5.1.2.1
Toluene Consumption Rates in Hamins and Seshadri Diffusion Flame

slow rate thus building the radical pool responsible for the subsequent highly exothermic radical attack reactions during this initial induction period.

Benzyl radical destruction occurs primarily via OH and O attack according to the following reactions:

$$C_7H_7 + OH = C_7H_7OH \quad (398)$$

$$C_7H_7 + O = C_7H_6O + H \quad (392)$$

$$C_7H_7 + O = C_6H_5 + CH_2O \quad (393)$$

A feature of interest is that benzyl alcohol and benzaldehyde are formed at rates greater than the phenyl radical. Bibenzyl, formed through recombination of two benzyl radicals via reaction (396), is formed in the initial reaction zone at a rate one order of magnitude slower as that of the dominant benzyl radicals destruction rates.

$$C_7H_7 + C_7H_7 = C_{14}H_{14} \quad (398)$$

Bibenzyl is subsequently consumed in the primary flame zone at a rate commensurate with its rate of formation. All other competing benzyl radical destruction reaction rates are at least an order of magnitude slower than the rates of the predominant reactions.

Linear C_7H_7 radical is produced at a fairly slow rate. Likewise, linear C_7H_7 radical consumption occurs at rates commensurate with its rate of production.

Benzyl alcohol is consumed primarily via H radical attack to produce benzaldehyde according to reaction (401).

$$C_7H_7OH + H = C_7H_6O + H + H_2 \quad (401)$$

The rates of all other competing reactions are six to eight orders of magnitude slower than the H radical attack reaction rate. All reactions occur in the primary reaction region of the flame zone.

Benzaldehyde is primarily consumed via pyrolysis, and OH, C_7H_7 and H radical attack reactions according to:

$$C_7H_6O = C_6H_5 + CHO \quad (414)$$

$$C_7H_6O + OH = C_6H_5CO + H_2O \quad (406)$$

$$C_7H_6O + C_7H_7 = C_7H_8 + C_6H_5CO \quad (410)$$

$$C_7H_6O + H = C_6H_5CO + H_2 \quad (408)$$

Again, it is observed that the dominant reaction paths lead to the formation of oxygenated species. Competing reaction rates are two to five orders of magnitude slower than those of the dominant reactions.

Ethyl benzene, produced via methyl radical attack on benzyl radical, is consumed at a rate 1.5 times slower than its rate of formation.

Cresoxy radical, formed by O attack on toluene via reaction (389), is consumed via both H attack and pyrolysis reactions. The rates of these reactions are two to six times slower than the rate of cresoxy radical formation via reaction (389).

$$C_7H_8 + O = OC_7H_7OH + H \quad (389)$$

Cresol, formed by H radical attack on cresoxy radical via reaction (418), is produced at a rate two to five times faster than its rate of destruction by OH and H radical attack via reactions (420) and (421). The primary cresol consumption reactions result in cresoxy radical formation as well. Therefore, cresol is eventually consumed by H radical attack forming phenyl alcohol, toluene and CH_3 and OH radicals via reactions (422) and (423).

$$OC_7H_7 + H = HOC_7H_7OH \quad (418)$$

$$HOC_7H_7 + OH = OC_7H_7 + H_2O \quad (420)$$

$$HOC_7H_7 + H = OC_7H_7 + H_2 \quad (421)$$

$$HOC_7H_7 + H = C_7H_8 + OH \quad (422)$$

$$HOC_7H_7 + H = C_6H_5OH + CH_3 \quad (423)$$

Benzoyl radical is rapidly consumed at a rate approximately equal its fastest rate of formation by OH attack on benzaldehyde via reaction (406).

$$C_7H_6O + OH = C_6H_5CO + H_2O \quad (406)$$

Benzene is principally consumed by H atom abstraction through OH and H radical attack via reactions (328) and (325) producing phenyl radical. It is noted that benzene is also rapidly formed via H attack on the phenyl radical according to reaction (324). Secondary benzene consumption paths include O and OH radical attack according to reactions (326) and (332), producing the phenoxy radical and phenyl alcohol respectively.

$$C_6H_6 = C_6H_5 + H \quad (324)$$

$$C_6H_6 + H = C_6H_5 + H_2 \quad (325)$$

$$C_6H_6 + O = C_6H_5O + H \quad (326)$$

$C_6H_6 + OH = C_6H_5 + H_2O$ (328)

$C_6H_6 + OH = C_6H_5OH + H$ (332)

Linear C_7H_8 is produced in some regions of the flame structure at very slow rates. However, the primary direction of this reaction is in the forward formation direction.

Phenyl radicals are primarily consumed via the OH radical attack reaction (321) to form the phenoxy radical and the pyrolysis (310), forming acetylene and the *n*-C_4H_3 radical. The linearisation of the phenyl radical and its destruction via O_2 attack according to reactions (322) and (320) respectively are also locally important within the flame structure.

$C_6H_5 = C_4H_3(N) + C_2H_2$ (310)

$C_6H_5 + O_2 = C_6H_5O + O$ (320)

$C_6H_5 + OH = C_6H_5O + H$ (321)

$C_6H_5L = C_6H_5$ (322)

Linear C_6H_5 is formed at a high rate via rearrangement of the cyclic phenyl radical molecule according to reaction (322) above. This specie is consumed via H attack and pyrolysis at rates of reaction slightly slower than its rate of formation according to reactions (239), (323) and (311).

$C_3H_3 + C_3H_3 = C_6H_5L + H$ (239)

$C_6H_5L = C_6H_4 + H$ (323)

$C_6H_5L = C_4H_3(N) + C_2H_2$ (311)

The phenoxy radical is pyrolised to C_5H_5 and CO according to reaction (336) at a rate slightly exceeding its maximum rate of production within the flame structure. In the primary flame zone, the phenoxy radical is also consumed via H radical attack according to reaction (331) at a rate nearly an order of magnitude less than its rate of consumption via pyrolysis.

$C_6H_5OH + = C_6H_5O + H$ (331)

$C_6H_5O + H = C_5H_5 + CO$ (336)

Phenyl alcohol is produced via H attack on the phenoxy radical as well as OH radical attack on benzene according to reaction (332). It is subsequently consumed via OH, H and O radical attack according to reactions (333), (334) and (335), producing the phenoxy radical. However, the maximum rate of phenyl alcohol consumption via radical attack reactions is an order of magnitude

less than its rate of formation. Phenyl alcohol is further depleted via the pyrolysis reaction (337), yielding C_5H_6 and CO.

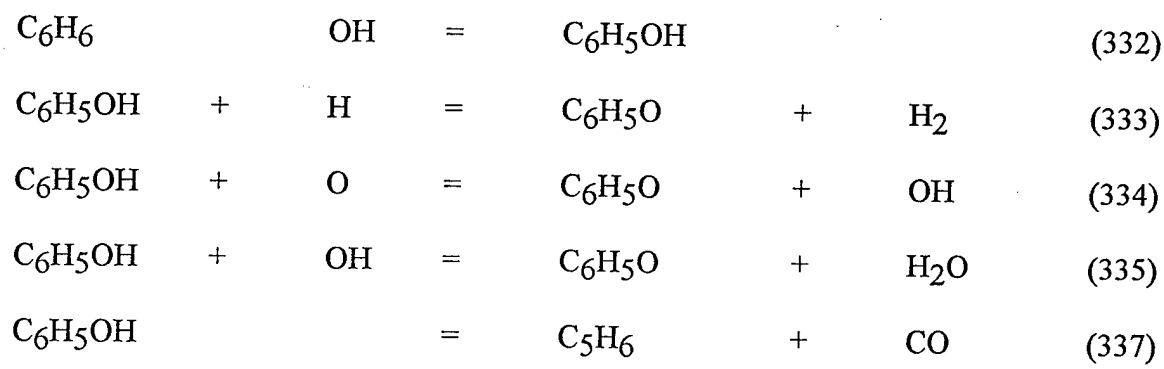

$$C_6H_6 + OH = C_6H_5OH \quad (332)$$

$$C_6H_5OH + H = C_6H_5O + H_2 \quad (333)$$

$$C_6H_5OH + O = C_6H_5O + OH \quad (334)$$

$$C_6H_5OH + OH = C_6H_5O + H_2O \quad (335)$$

$$C_6H_5OH = C_5H_6 + CO \quad (337)$$

Methoxy phenyl radical is produced by OH attack on benzyl alcohol via reaction (400) at an insignificant rate. The rate of methoxy phenyl radical consumption via reaction (430) is eight orders of magnitude faster than its rate of production. Thus, these paths appear to be unimportant in computing the features of toluene diffusion flames.

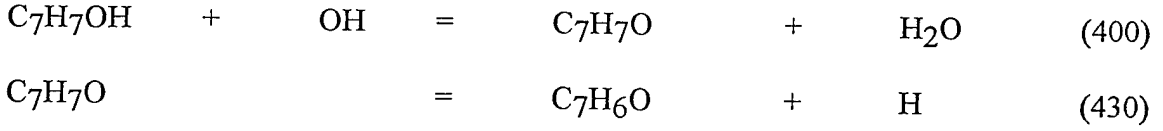

$$C_7H_7OH + OH = C_7H_7O + H_2O \quad (400)$$

$$C_7H_7O = C_7H_6O + H \quad (430)$$

Discussion

The toluene diffusion flame path analysis has primarily served the purpose of establishing the toluene consumption paths within the flame structure according to toluene combustion elementary reactions established in the literature. However, at this time, sufficient experimental data in pure toluene diffusion flames is not available to either validate the analysis or suggest alternative schemes or reaction rates. This initial toluene diffusion flame path analysis was used to establish the primary toluene consumption paths included in the toluene/*n*-heptane combustion sub-mechanism outlined in Section 4.1.1. This sub-mechanism was successfully validated against experimental data and results were presented in Section 4.2.2. Therefore, the principal initial toluene destruction paths and the subsequent destruction paths of other C_7 and C_6 species identified herein for a diffusion flame environment appear sound.

5.1.3 PATH ANALYSIS OF TOLUENE CONSUMPTION IN STIRRED REACTORS

Results

The rates of the elementary reactions comprising the toluene combustion sub-mechanism were analysed for the combustion of toluene in a stirred reactor in order to assess important differences in reaction paths in diffusion flames and stirred reactors. The rates of the elementary reactions were analysed at a temperature of 1188K, reactor residence time of 75 milliseconds, initial toluene concentration of 0.15% and an equivalence ratio of 0.63. A summary of this analysis is shown in Tables 5.1.3.1a to 5.1.3.18 in Appendix G.

Many notable differences were observed in the consumption paths of toluene in the high temperature environment of diffusion flames, as discussed in Section 5.1.2, and the low to intermediate temperature environment of the stirred reactor discussed below. The primary toluene consumption paths common to both combustion environments may be summarised as follows:

$C_7H_8 + OH = C_7H_7 + H_2O$ (381)

$C_7H_8 + H = C_7H_7 + H_2$ (383)

$C_7H_8 + H = C_6H_6 + CH_3$ (384)

$C_7H_8 + O = OC_7H_7 + H$ (389)

As was observed in the diffusion flames, toluene was also created via reaction (386):

$C_7H_7 + H = C_7H_8$ (386)

However, the pyrolysis of toluene via reaction (385), the O radical attack reaction (380) and the O_2 molecular abstraction reaction (382) exhibited significant differences.

$C_7H_8 + O = C_7H_7 + OH$ (380)

$C_7H_8 + O_2 = C_7H_7 + HO_2$ (382)

$C_7H_8 = C_6H_6 + CH_3$ (385)

In the stirred reactor, reaction (380) proceeds rapidly in the reverse direction. Thus, insignificant toluene consumption was predicted until this reaction path was removed from the toluene sub-mechanism. Although reaction (380) was one of the primary toluene consumption paths in diffusion flames, removing this reaction from the toluene sub-mechanism did not have a significant effect in the overall structure of toluene and toluene/*n*-heptane diffusion flames. No differences were noted in the major species profiles and measured intermediate species profiles decreased by

less than five percent. Predicted peak temperatures decreased by approximately 25K, which was closer to experimental measurements.

Although reaction (382) ranks fifth in terms of overall toluene consumption, it has the most significant effect on the predicted toluene profile as was also observed by Emdee *et al* [29]. It was found that the activation energy value of 173,200 Joules/mole recommended by Emdee *et al* [29] for this reaction had to be decreased by 837 Joules/mole in order to properly predict toluene concentrations. Bittker [30] recommends an activation energy value of 159,000 Joules/mole for this reaction, thus the value used in the present work is well within reported uncertainty limits. Since reaction (382) was insignificant in the diffusion flame computations, this change did not affect the toluene diffusion flame structure.

Reaction (385) proceeds in the reverse direction in the stirred reactor whereas in the toluene diffusion flame it is one of the primary toluene consumption paths. This is reasonable, noting the high activation energy for this reaction. When the temperature of the stirred reactor was increased to 2000K, this reaction proceeds in the forward, or thermal decomposition, direction. At 1188K, toluene formation via benzyl radical attack reactions (410) on benzaldehyde and (390) on phenyl alcohol is also important. However, at high temperature, these reactions become insignificant.

In the stirred reactor, benzyl radical destruction occurs primarily via H, O and HO_2 radical attack according to:

$$C_7H_7 + H = C_7H_8 \quad (386)$$

$$C_7H_7 + O = C_7H_6O + H \quad (392)$$

$$C_7H_7 + HO_2 = C_7H_6O + H + OH \quad (394)$$

$$C_7H_7 + HO_2 = C_6H_5 + CH_2O + OH \quad (395)$$

The consumption of the benzyl radical via HO_2 radical attack was faster than predicted in the toluene diffusion flame structure. This is reasonable as the HO_2 radical is produced via O_2 molecular abstraction reaction (382) noted above which is not significant at higher temperatures. Also, the rapid production of benzyl alcohol via the recombination of the benzyl and OH radicals observed in the diffusion flame structure was not significant in the stirred reactor computations. The production and consumption of the linear C_7H_7 was also not important at 1188K. However, when the stirred reactor temperature was increased to 2000K, the rates of these reactions increased by three orders of magnitude.

Benzyl alcohol consumption in the toluene stirred reactor occurs primarily via OH radical attack to yield benzaldehyde according to reaction (400):

$$C_7H_7OH + OH = C_7H_6O + H_2O + H \quad (400)$$

In the diffusion flame structure, benzyl alcohol was primarily destroyed via H radical attack according to reaction (401) noted above also yielding benzaldehyde.

$$C_7H_7OH + H = C_7H_6O + C_6H_6 + H_2 \quad (401)$$

In the stirred reactor computations, however, reaction (401) destroys benzyl alcohol very rapidly. This results in an under-prediction of the benzyl alcohol concentrations measured by Brezinsky and co-workers [44-46] of three orders of magnitude. Removing this reaction from the toluene combustion sub-mechanism results in sensible predictions of benzyl alcohol concentrations and has no effect on the computed toluene diffusion flame structure.

At lower temperatures, benzaldehyde was primarily consumed via the benzyl radical, OH and H attack according to reactions (406), (407) and (410):

$$C_7H_6O + OH = C_6H_5CO + H_2O \quad (406)$$

$$C_7H_6O + H = C_6H_5CO + H_2 \quad (407)$$

$$C_7H_6O + C_7H_7 = C_6H_5CO + C_7H_8 \quad (410)$$

In the diffusion flame structure, benzaldehyde was also consumed via the pyrolysis reaction (414):

$$C_7H_6O = C_6H_5 + CHO \quad (414)$$

In the stirred reactor, however, this reaction resulted in very rapid consumption of benzaldehyde thus under-predicting the measured concentrations. Removing this reaction from the scheme resulted in sensible predictions of benzaldehyde concentrations and no effect on the toluene diffusion flame structure.

In the stirred reactor, ethyl benzene is formed via recombination of the benzyl and CH_3 radicals according to reaction (397) which proceeds in the reverse direction. Ethyl benzene is rapidly consumed via H attack to yield styrene, H_2 and an H radical according to reaction (416).

$$C_8H_{10} = C_7H_7 + CH_3 \quad (397)$$

$$C_8H_{10} + H = C_8H_8 + H_2 + H \quad (416)$$

Emdee *et al* [29] reported accurate predictions of both ethyl benzene and styrene using their kinetics model. In the present work, measured concentrations of styrene were over-predicted by a factor of two, which is within experimental uncertainty. However, measured concentrations of ethyl benzene were under-predicted by a factor of 75. The rate proposed by Mizerka *et al* for reaction (397) was replaced with that recommended by Emdee *et al* [29]. This resulted in an under-prediction of styrene as well as ethyl benzene. Reaction (397) proceeds primarily in the reverse direction whereas reaction (416) is partially equilibrated. Decreasing the rate of reaction (416) by a factor of two only increased the predicted concentrations of ethyl benzene by less than

five percent. Given available rate and thermodynamic data, it is not possible to further adjust this portion of the mechanism at the present without additional corroborating experimental data.

Cresoxy radical is consumed via competing pyrolysis and H attack reactions according to:

$$OC_7H_7 + H = HOC_7H_7 \quad (418)$$

$$OC_7H_7 = C_6H_6 + H + CO \quad (419)$$

The rate for reaction (419) used by Emdee *et al* [29] was based on the rate of the phenoxy radical decomposition measured by Lin and Lin [102]. Lin and Lin [102] reported a great deal of uncertainly in the measurement. Using the rates recommended by Emdee *et al* initially resulted in an under-prediction of the cresols concentrations by a factor of 30. The rate of reaction (419) was then decreased to the lowest value recommended by Lin and Lin [102] and further decreased by a factor of two. This increased the cresols concentrations predictions to within a factor of two of experimental measurements without adversely affecting any of the other measured species profiles. However, a great deal of uncertainty both experimental and theoretical remains in this portion of the mechanism.

The cresols consumption in the toluene stirred reactor proceeded via competing H radical attack reactions (423) and (422) yielding phenyl alcohol and a methyl radical, and toluene and an OH radical respectively.

$$HOC_7H_7 + H = C_7H_8 + OH \quad (422)$$

$$HOC_7H_7 + H = C_6H_5OH + CH_3 \quad (423)$$

In the toluene diffusion flame, cresol was also consumed via OH radical attack reaction (420) noted above. However, this reaction consumed cresol at rates commensurate with its formation in the stirred reactor, which was not experimentally corroborated. Removing reaction (420) from the mechanism improved predictions of the cresols concentrations without an effect on the diffusion flame structure.

Benzene was primarily consumed via O radical attack yielding the phenoxy radical according to reaction (326) and H and OH radical attack yielding the phenyl radical according to reactions (325) and (328):

$$C_6H_6 + H = C_6H_5 + H_2 \quad (325)$$

$$C_6H_6 + O = C_6H_5O + H \quad (326)$$

$$C_6H_6 + OH = C_6H_5 + H_2O \quad (328)$$

The phenyl radical is rapidly consumed via O_2 attack yielding the phenoxy radical and an O radical according to reaction (320):

$$C_6H_5 + O_2 = C_6H_5O + O \quad (320)$$

All other competing reactions are at least two orders of magnitude slower. The formation and destruction of the liner C_6H_5 is insignificant at 1188K. However, the rates of formation and subsequent destruction of the linear C_6H_5 become dominant at 2000K.

The destruction of the phenoxy radical proceeds via competing reactions (331) and (336):

$$C_6H_5O + H = C_6H_5OH \quad (331)$$

$$C_6H_5O + = C_5H_5 + CO \quad (336)$$

The lower limit of the rate recommended by Lin and Lin [102] was used to predict sensible phenyl alcohol concentrations.

As in the toluene diffusion flame, the principal paths of phenyl alcohol destruction yield the phenoxy radical at rates half to an order of magnitude slower than its rate of formation. The principal phenyl alcohol destruction reaction is:

$$C_6H_5OH + OH = C_6H_5O + H_2O \quad (335)$$

At 2000K, the formation and destruction of the phenyl alcohol are not as significant.

In the toluene diffusion flame, formation of the phenoxy radical was not a primary reaction path. In the stirred reactor environment, however, including paths for the formation and destruction of the phenoxy radical appears to be important for the sensible prediction of phenyl alcohol concentrations. However, Lindstedt and Skevis [24] have shown that including reaction (326) in the kinetics mechanism used to predict the structure of low pressure benzene pre-mixed flames results in large over-predictions over the measured concentrations of the phenoxy radical. Therefore, the phenoxy radical formation and destruction paths of the mechanism proposed herein also contains many experimental and theoretical uncertainties yet to be resolved.

The consumption of cyclopentadiene occurs primarily via O_2 molecular abstraction according to:

$$C_5H_6 + O_2 = C_5H_5 + HO_2 \quad (345)$$

Other competing reactions are at least an order of magnitude slower. Cyclopentadiene production and consumption are insignificant at higher temperatures.

The consumption of the cyclopentadienyl radical proceeds according to:

$$C_5H_5 + H = C_5H_6 \quad (338)$$

$$C_5H_5 + O = C_4H_5(T) + CO \quad (339)$$

$$C_5H_5 + HO_2 = C_5H_5O + OH \quad (342)$$

The rate of reaction (339) proposed by Emdee *et al* [32] was estimated based on the methods of Benson [69]. Initial calculations showed that this reaction dominated the consumption of the cyclopentadienyl radical and a subsequent under-prediction of cyclopentadiene was noted. Also, the $C_4H_5(T)$ radical rapidly reacted with H_2 according to reaction (291) to yield 1,3-butadiene and an H radical. Since the concentration of 1,3-butadiene in the stirred reactor computations was also over-predicted, the rate of reaction (339) was reduced by a factor of two. This made the predictions of both cyclopentadiene and 1,3-butadiene concentrations more sensible.

$$C_4H_6(T) + H = C_4H_5(T) + H_2 \quad (291)$$

Furthermore, the rate of the thermal decomposition of $C_4H_5(T)$ yielding acetylene and the C_2H_3 radical via reaction (273) was increased within the bounds of the uncertainty limits, further improving the 1,3-butadiene and acetylene predictions. None of the changes to the mechanism resulted in a notable difference in the calculated species profiles in the toluene and toluene/*n*-heptane diffusion flames structures.

Discussion

The path analysis of toluene combustion in a stirred reactor has also shown significant differences between the dominant reaction paths in the low to intermediate temperature environment of stirred reactors and the high temperature flow fields of diffusion flames. This was also clearly shown in the path analysis of *n*-heptane combustion in stirred reactors discussed in Section 3.1.4. The high temperature stirred reactor path analysis generally validated the observations made in the diffusion flame path analysis.

The toluene stirred reactor path analysis served to identify that the consumption of toluene according to reaction (380), phenyl alcohol according to reaction (401), benzaldehyde according to reaction (414) and cresol according to reaction (420) resulted in significant discrepancies in the predictions of these species in the toluene stirred reactor. These reactions were removed from the toluene diffusion flame sub-mechanism with no significant differences in the computed structure of the toluene and toluene/*n*-heptane diffusion flames. Thus, a more general mechanism for the combustion of toluene in diffusion flames and stirred reactors has been formulated.

Finally, uncertainties both experimental and theoretical, in the production and consumption paths of the phenoxy radical, the cresoxy radical, ethyl benzene and styrene have been observed. Additional experimental rate data and species concentration profiles are needed and continued comparison of analytical predictions in diffusion flames, pre-mixed flames and stirred reactors will be undertaken to further develop and validate this portion of the toluene combustion sub-mechanism.

5.2 TOLUENE MECHANISM EVALUATION

5.2.1 DESCRIPTION OF TOLUENE EXPERIMENTAL DIFFUSION FLAMES

Detailed species concentration data available in the literature for pure toluene diffusion flame structures is even more rare than data for *n*-heptane diffusion flames. Santoro *et al* [107] have studied a number of coflow diffusion flames containing small amounts of toluene. Reported measurements primarily included soot formation levels. Thus, these flames were not appropriate for validating the toluene combustion mechanism. Tesner *et al* [108] conducted detailed studies of toluene/hydrogen diffusion flames. Again, measurements strictly included soot formation parameters. Hamins *et al* [97] studied a methane/toluene laminar diffusion flame in a Wolfhard-Parker burner. Detailed measurements of stable species and the methyl radical were reported in this reference. However, this data set was not selected for model validation because of the massive computational costs of modelling a coflow diffusion flame using detailed kinetics. The only known data set for a pure toluene counterflow diffusion flame including species measurements is that of Hamins and Seshadri [42] and Hamins [43]. Thus, this data set was selected for model validation.

The experimental set up of the Hamins and Seshadri toluene diffusion flame is identical to that used to study *n*-heptane diffusion flames as described in Section 3.2.1. The reported boundary conditions were 20.2 mol% O_2 concentration, 34.6 cm/sec air velocity and 2.28 g/cm^2/min burning rate. A wide sooting zone was observed on the fuel rich side of the flame. Attempts at probing this region of the flame were unsuccessful, as the small microprobes became plugged immediately after insertion into the flow field. Composition profiles were reported for only the fuel lean zone, with the first reported measurement being obtained at a temperature 400 degrees below the peak temperature. A complete temperature profile was reported.

The species concentration data were analysed in terms of mixture fraction using the techniques discussed in Section 3.2.1. Results of this analysis are shown in Figure 5.2.1.1. It is noted that the mixture fraction values calculated using Bilger's definition correlate well with those computed based on elemental carbon and hydrogen. Unfortunately, the mixture fraction values computed based on elemental oxygen do not correlate well. Thus, these data can only be used to establish the reasonableness of the proposed kinetics scheme in predicting peak levels of major and intermediate species rather than for detailed validation.

5.2.2 TOLUENE DIFFUSION FLAME RESULTS

Comparisons between experimental results and predictions for the Hamins and Seshadri toluene diffusion flame are shown in Figures 5.2.2.1 to 5.2.2.4. The temperature profile was well predicted using a 50 sec^{-1} rate of strain after accounting for soot radiation heat losses as shown in Figure 5.2.2.1.

Comparisons to major species profiles are shown in Figures 5.2.2.2 and 5.2.2.3. An unusual shape is noted in the profiles reported for CO, CO_2 and O_2. Given the poor correlation of the mixture fraction values computed based on elemental oxygen with those based on other

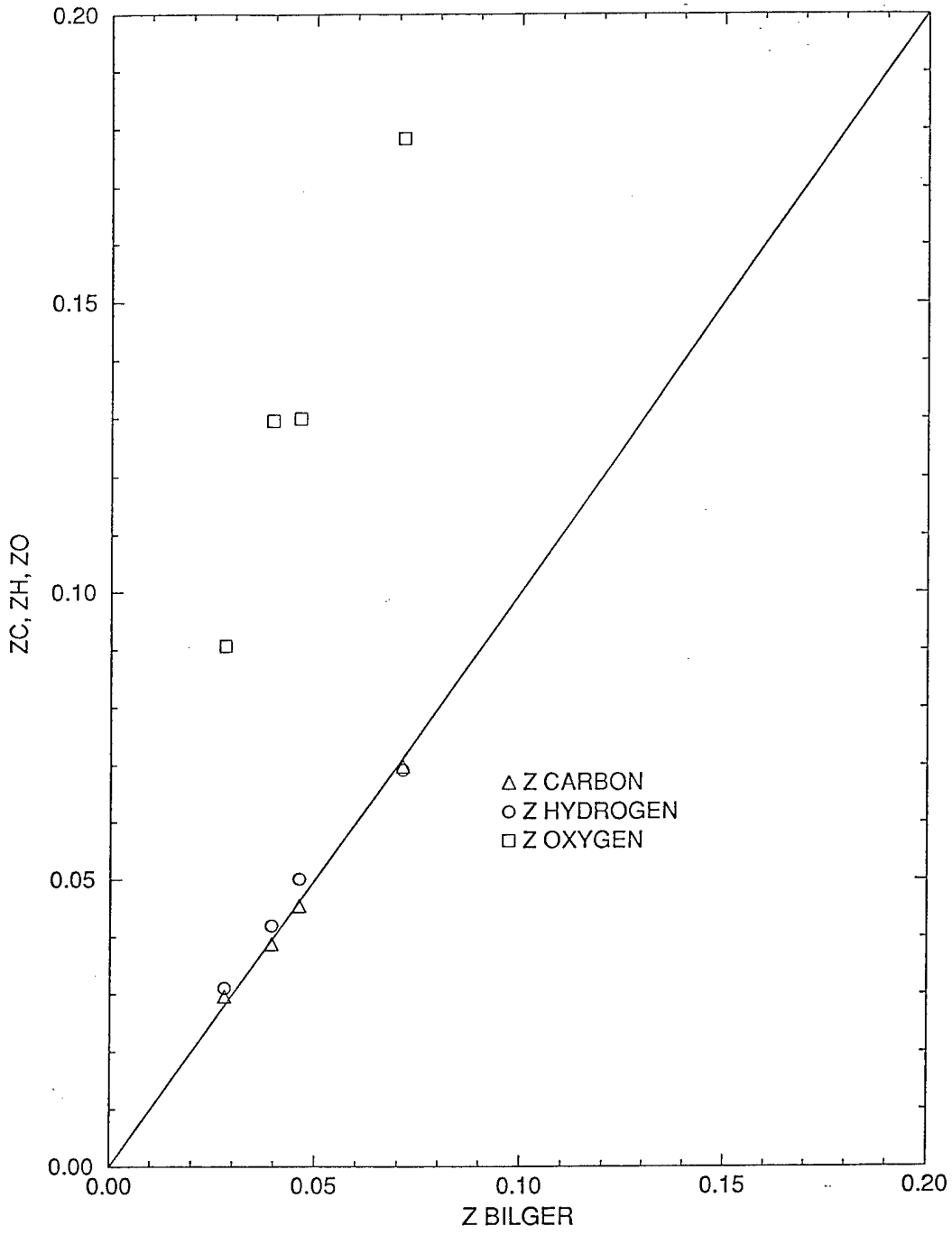

Figure 5.2.1.1
Hamins and Seshadri Toluene Diffusion Flame
Mass Fraction Comparison

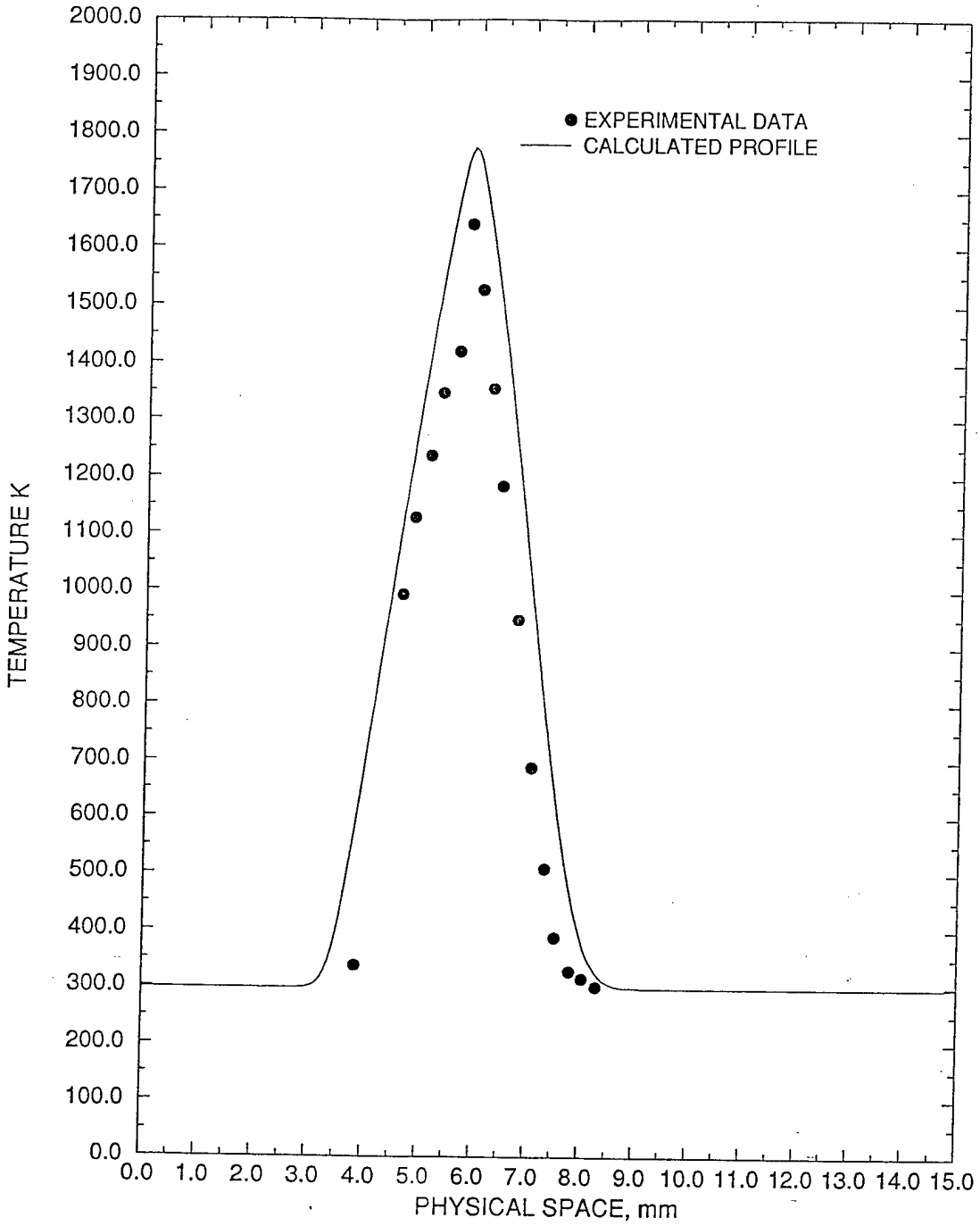

Figure 5.2.2.1
Hamins and Seshadri Toluene Diffusion Flame Temperature Measured and Calculated Profiles

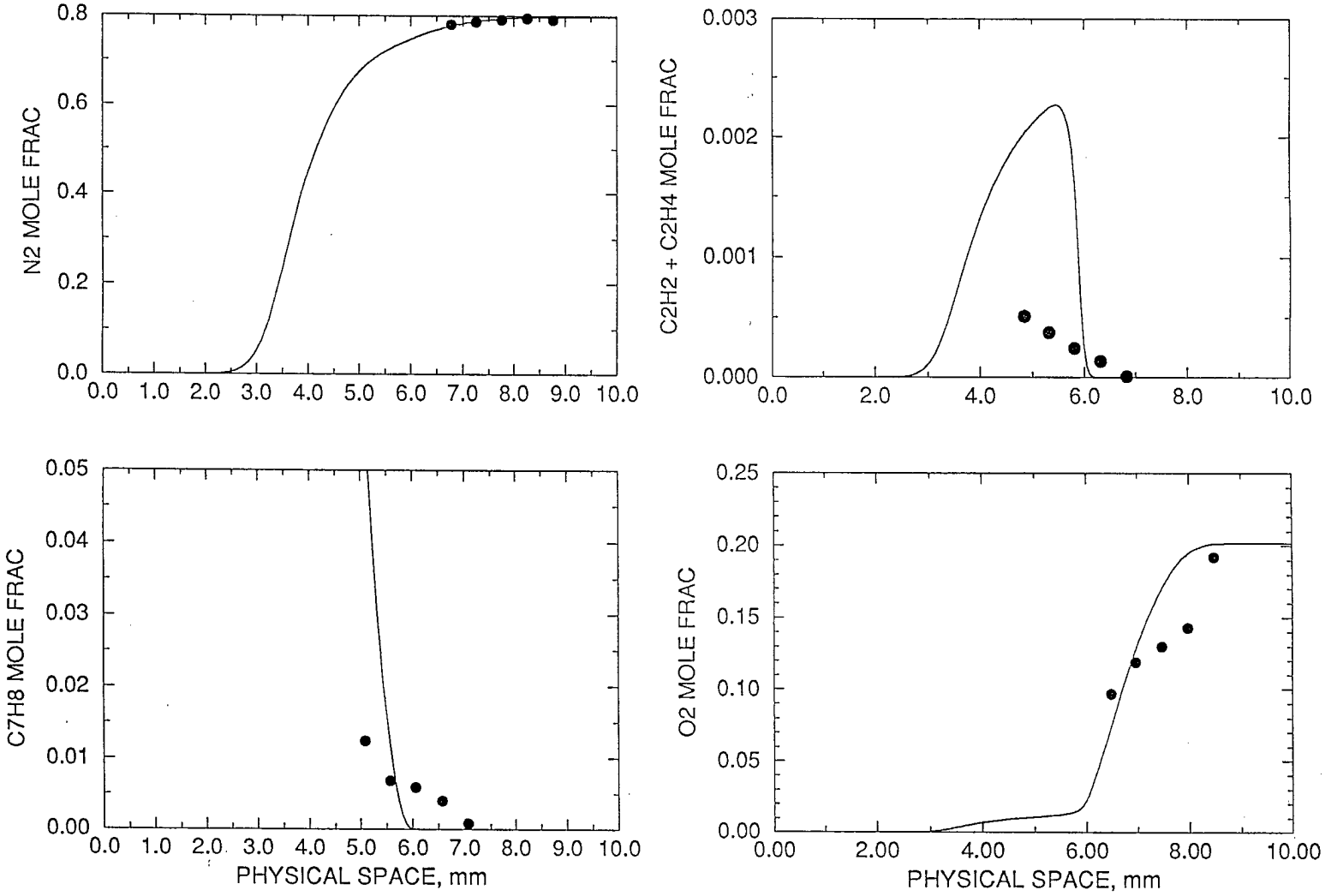

Figure 5.2.2.2
Hamins and Seshadri Toluene Diffusion Flame Species Measured and Calculated Profiles

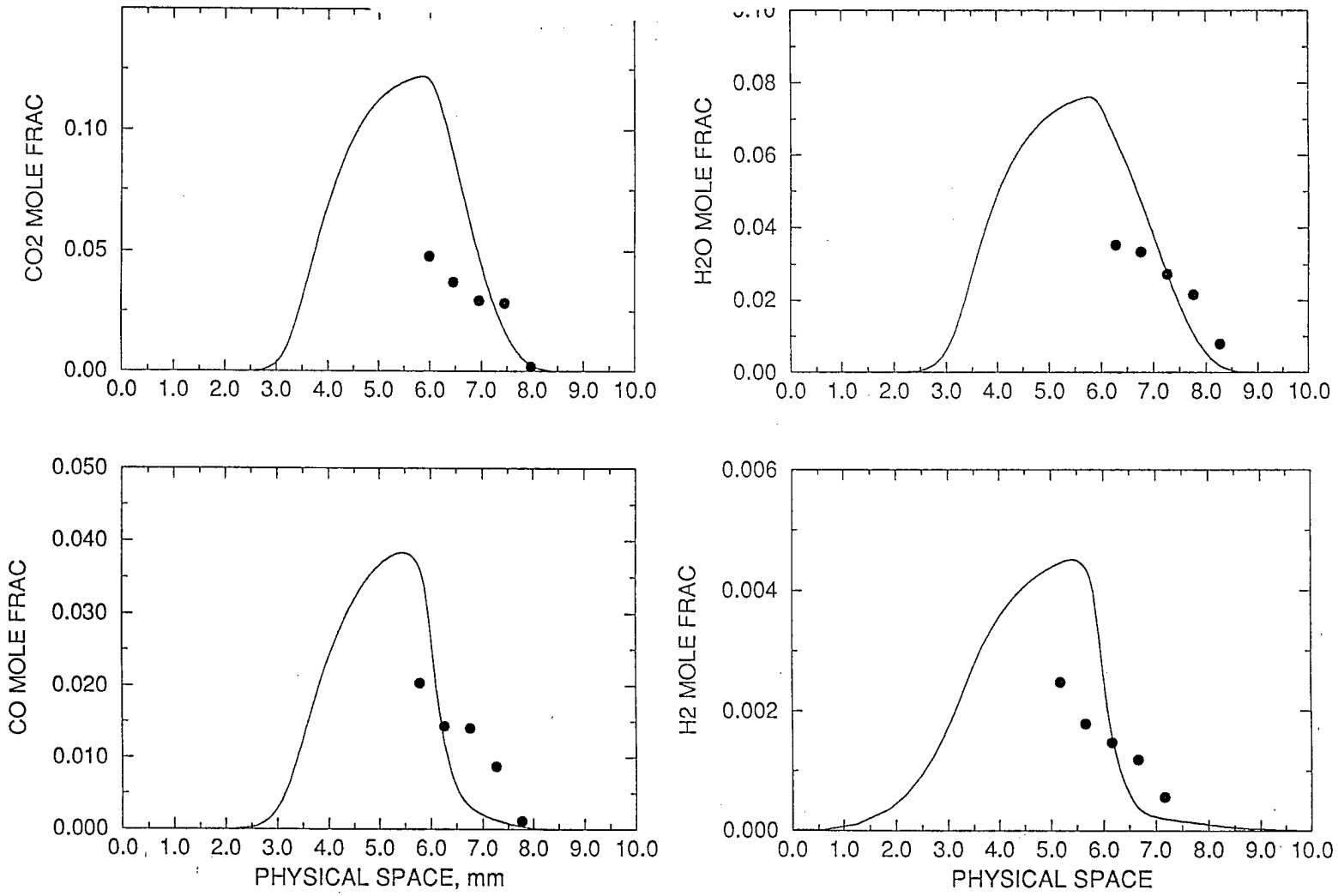

Figure 5.2.2.3
Hamins and Seshadri Toluene Diffusion Flame Species Measured and Calculated Profiles

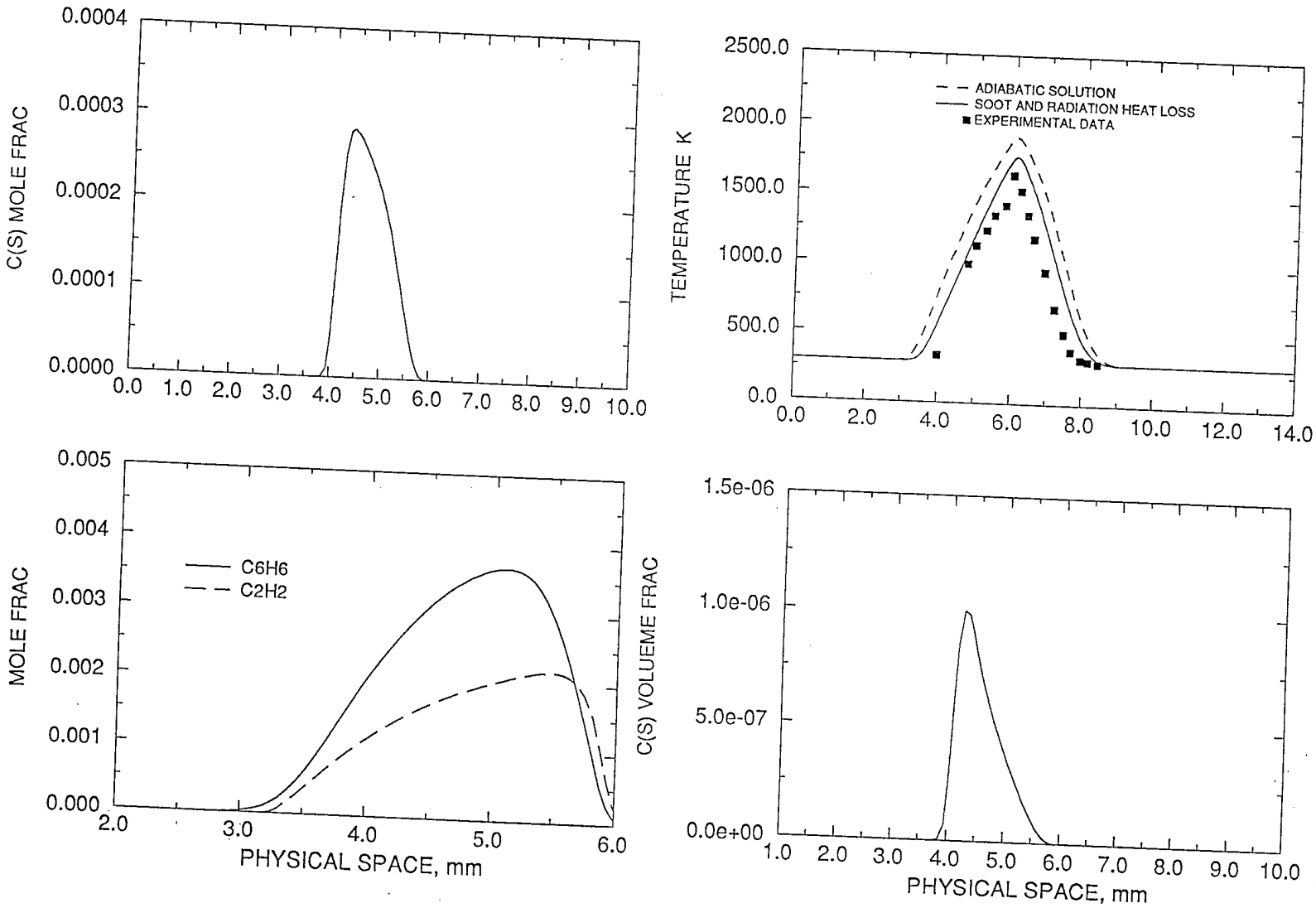

Figure 5.2.2.4
Hamins and Seshadri Toluene Diffusion Flame Soot Formation

definitions, it is reasonable to suspect the accuracy of the data. The comparison does show that predictions for major species profiles are sensible, taking into account that the highest experimental values reported were obtained at a location below their expected peak concentrations. Based on these factors, it is reasonable to expect that peak concentrations are predicted within a factor of 1.5, which is well within the bounds of experimental error.

The only data reported for intermediate species were the concentrations of ethylene and acetylene. Methane concentrations were reported in combination with nitrogen, making it impossible to reach any conclusions about the accuracy of predicting the levels of this specie within the flame structure.

The sooting characteristics of the toluene diffusion flame modelled are shown in Figure 5.2.2.4. As previously reported by many researchers [89, 107-110], high soot levels were indeed predicted. High levels of benzene were also predicted within the flame structure. Soot radiation resulted in a temperature drop slightly over 200K from the peak adiabatic flame temperature. In fact, sensible levels of major or intermediate species could not be predicted unless the soot model was included.

The only conclusion that may be reached from the toluene diffusion flame analytical study is that the proposed mechanism appears to be sensible. However, if these results are coupled with those of the *n*-heptane and toluene/*n*-heptane diffusion flame analyses discussed in Sections 3.2.2 and 4.2.2 respectively the validity of overall toluene mechanism assembled herein is apparent. It is intended to model the toluene/heptane/methanol counterflow diffusion flames also studied by Hamins and Seshadri [42] and Hamins [43] during the next phase of the overall research programme in order to further demonstrate the flexibility of the proposed mechanism for toluene and *n*-heptane combustion in diffusion flames.

5.2.3 DESCRIPTION OF TOLUENE STIRRED REACTOR EXPERIMENT MODELLED

The data sets considered to validate the toluene combustion mechanism in a stirred reactor configuration were the toluene combustion adiabatic flow reactor data of Brezinsky and Dryer [44], Brezinsky [45] and Brezinsky *et al* [46] and the ethylene/toluene gas generator data of Buckley *et at* [111]. The gas generator experiment of Buckley *et al* could be modelled as a stirred reactor and was the only toluene combustion data obtained at high pressure (350 kPa). However, species concentration data was reported for only for one set of experimental conditions and was limited to toluene, benzene, acetylene, ethylene, ethane, methane, carbon dioxide and carbon monoxide concentrations. The data reported by Brezinsky and co-workers [44-46] was obtained at atmospheric pressure and equivalence ratios of 0.63 and 1.4 over a wide range of reactor residence times. Very detailed species concentrations measurements were reported in these references, including toluene, benzene, benzaldehyde, benzyl alcohol, ethyl benzene, bibenzyl, styrene, cresols, phenyl alcohol, C_5H_6, vinyl acetylene, ethane, ethylene, acetylene, methane and carbon monoxide. Thus, the experimental data of Brezinsky and co-workers was selected for initial model validation. Nonetheless, it is intended to model the experiment of

Buckley *et al* [111] at a later date in order to assess the high pressure and fuel rich performance of the mechanism.

Brezinsky and co-workers studied the combustion of toluene in a turbulent adiabatic flow reactor at a nominal temperature of 1200K and fuel-oxygen equivalence ratios of 0.63 and 1.4. All experiments were carried out at atmospheric pressures. The reactor was a 10 cm diameter cylindrical quartz tube as described by Hautman [112]. The temperature gradient in the reactor was reported not to exceed 10K [44]. The composition of exhaust products was analysed by gas chromatography/mass spectrometry [44, 46].

The toluene combustion sub-mechanism was validated against the fuel lean (0.63 equivalence ratio) data set. Experimental conditions used for model validation were as shown in Table 5.2.3.1. Residence times were shifted by 33 milliseconds from the values reported by Brezinsky and Dryer [44] as recommended by Emdee *et al* [29].

Table 5.2.3.1
Toluene Stirred Reactor Computational Conditions

Initial Temperature K	Mean Residence Time milliseconds	Equivalence Ratio	Initial *n*-heptane concentration mol%	Initial O_2 concentration mol%
1188	35-65	0.63	0.15	2.14
1189	75	0.63	0.15	2.14
1193	85	0.63	0.15	2.14
1196	95	0.63	0.15	2.14
1197	105	0.63	0.15	2.14

5.2.4 TOLUENE STIRRED REACTOR RESULTS

As with the validation of the *n*-heptane combustion stirred reactor sub-mechanism, the toluene combustion stirred reactor sub mechanism was validated for the purposes of establishing the validity of the overall sub-mechanism as well as assessing the high temperature performance of the C_1-C_4 and cyclic C_6 sub-mechanism of Lindstedt and co-workers [19-24]. Again, only very minor modifications to the C_1-C_4 sub-mechanism were undertaken to match experimental results as this portion of the mechanism has been extensively validated against high temperature experimental data. Comparisons between the experimental data of Brezinsky and co-workers [44-46] and analytical predictions are shown in Figures 5.2.4.1 to 5.2.4.3.

In general, concentrations of toluene, benzene, benzaldehyde, the cresols, phenyl alcohol and benzyl alcohol as a function of residence time were predicted within a factor of two or less, which is within the bounds of experimental error. However, although these predictions appear sensible, the accuracy decreased with increasing residence time. The predictions of phenyl alcohol and the cresols show an improvement over those reported by Emdee *et al* [29].

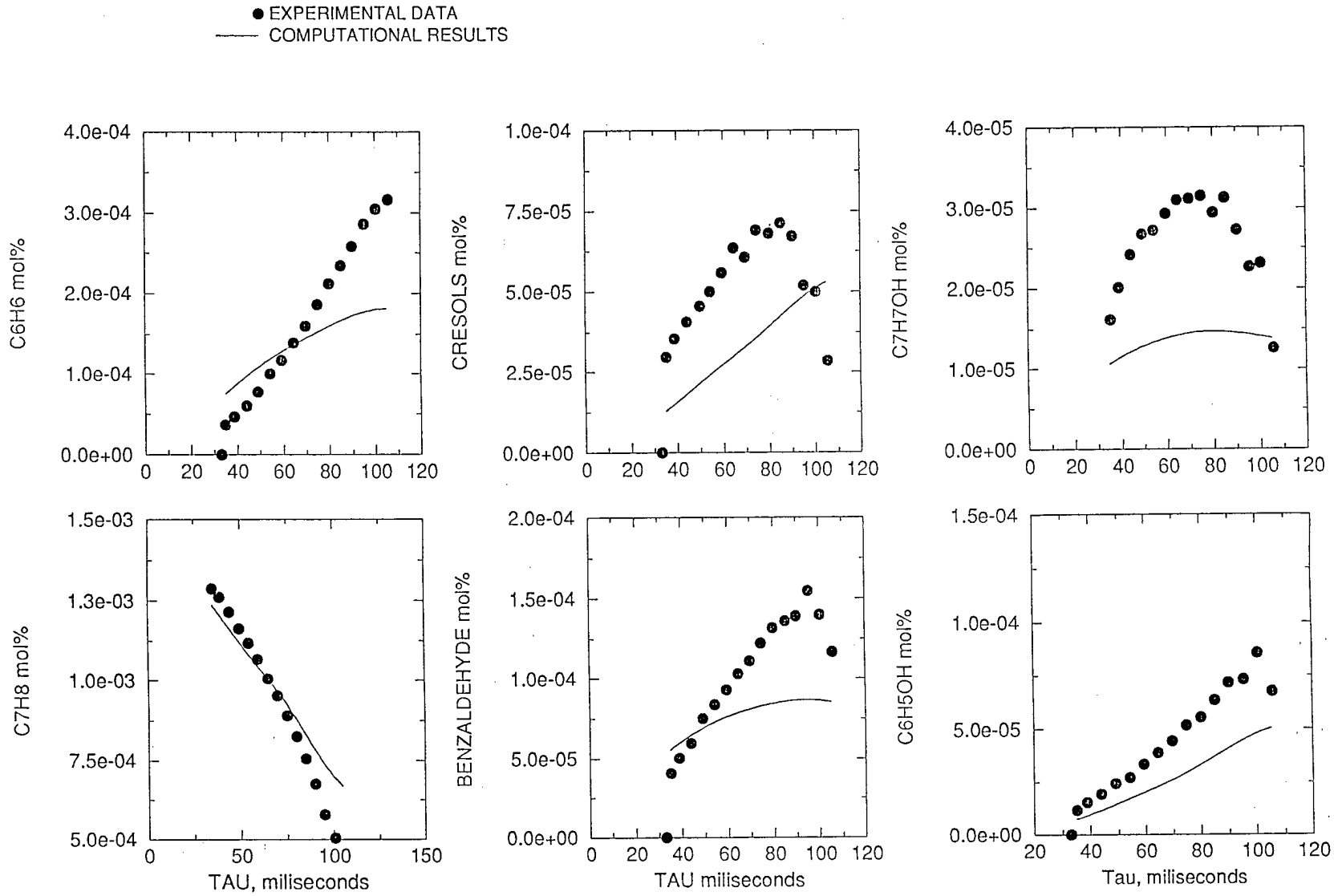

Figure 5.2.4.1
Toluene Stirred Reactor Computational Results
Major Products

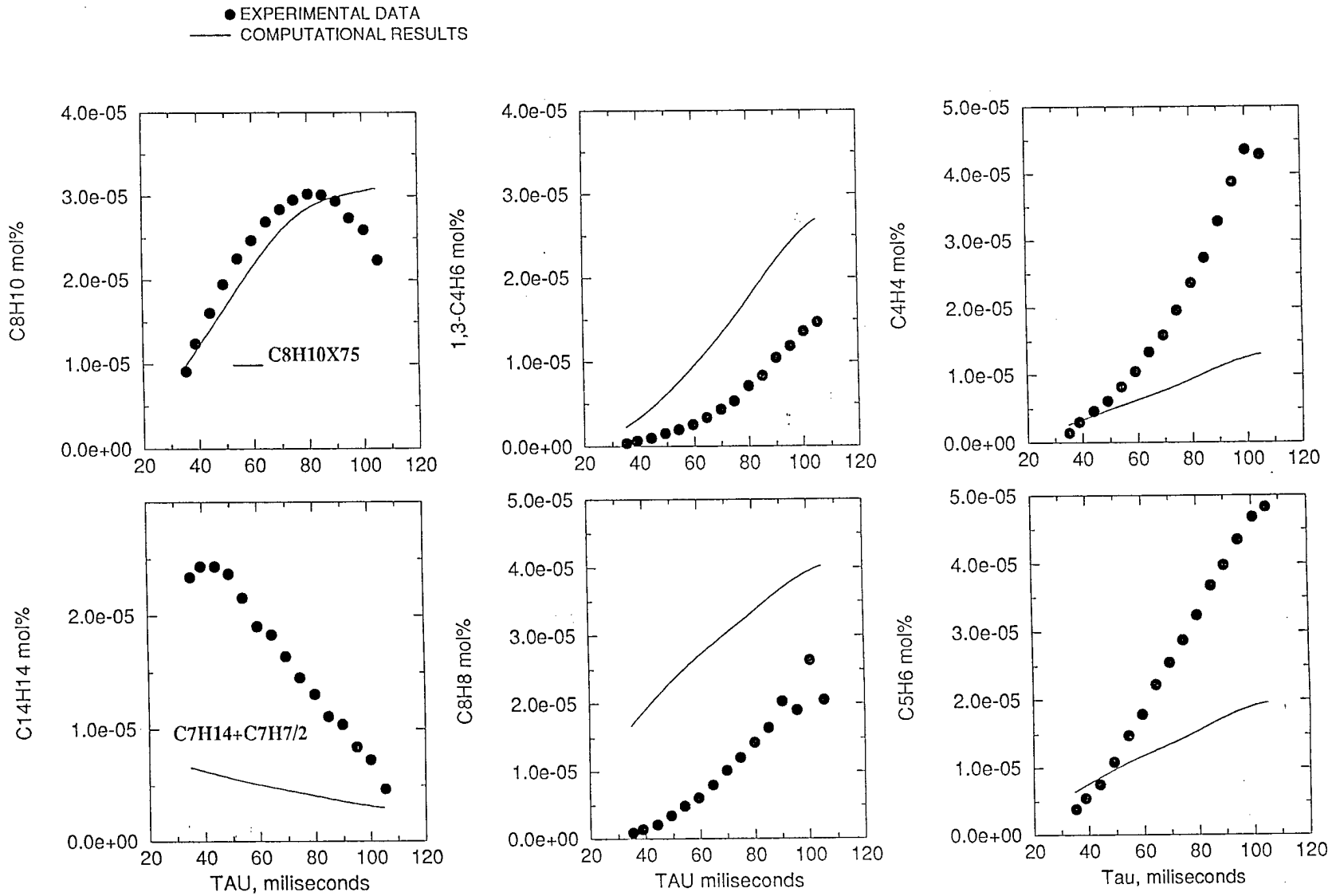

Figure 5.2.4.2
Toluene Stirred Reactor Computational Results
Large Hydrocarbons

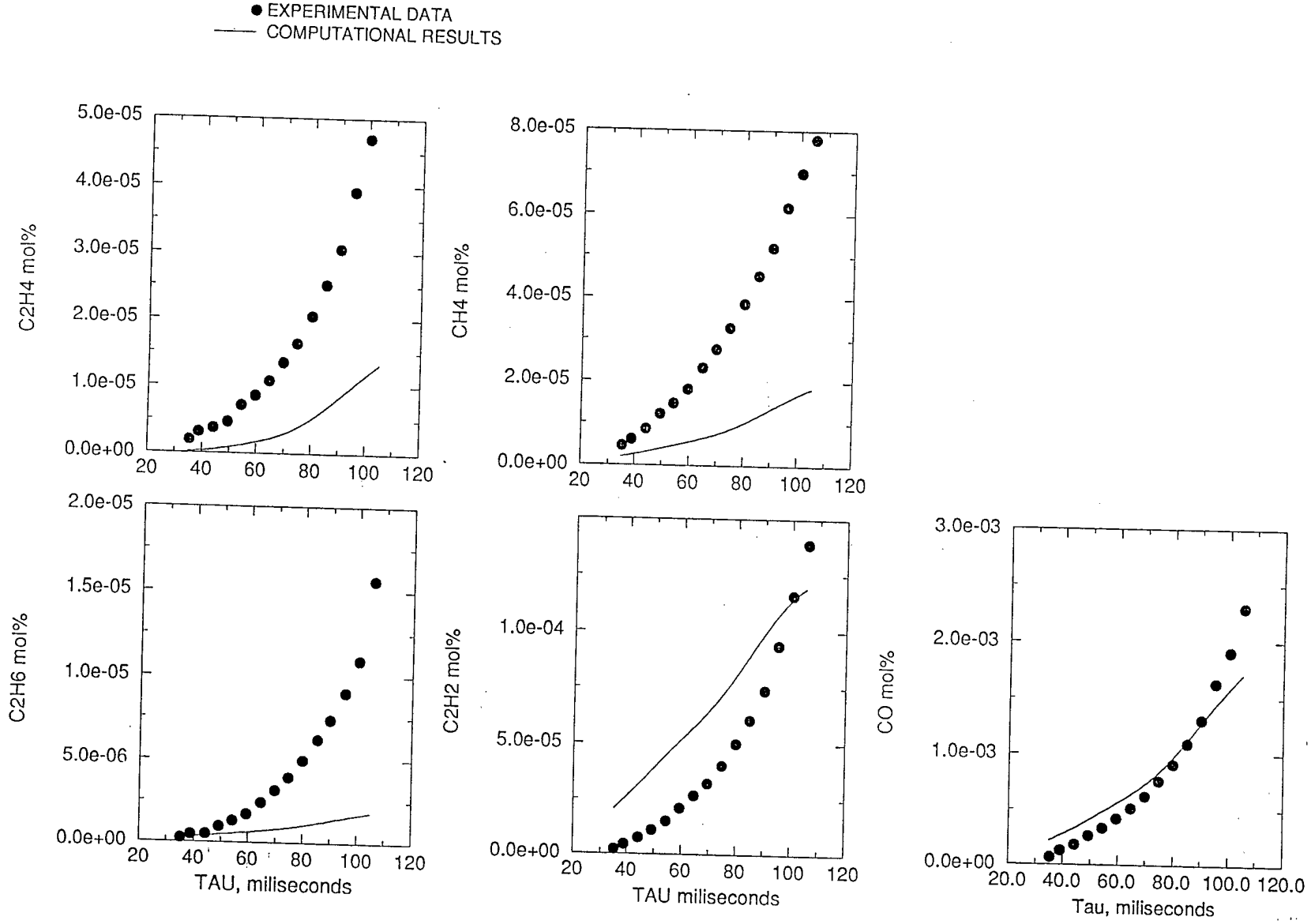

Figure 5.2.4.3
Toluene Stirred Reactor Computational Results
Small Hydrocarbons and CO

The concentrations of styrene were over-predicted by a factor of two whereas the concentrations of ethyl benzene were under-predicted by a factor of 75. This is clearly not sensible and as noted above, this portion of the sub-mechanism requires additional work.

The concentrations of bibenzyl were under-predicted by a factor of 75. As noted by Emdee *et al* [29] it is possible that the benzyl radical could recombine in the probe thus appearing as bibenzyl. If half the concentration of the benzyl radical is added to the predicted concentrations of bibenzyl, the concentration of bibenzyl is under-predicted by a factor of three. Clearly, either the concentration of the benzyl radical is under-predicted by the model or the experimental measurements of bibenzyl are in error. Additional data is necessary to corroborate either hypothesis.

The concentrations of 1,3-butadiene, cyclopentadiene, vinyl acetylene and acetylene are predicted within a factor of two or better. Again, however, the accuracy of the predictions decreases as a function of residence time. The concentration of CO is well predicted, as also reported by Foelsche *et al* [31]. The concentrations of ethane, methane and ethylene are under-predicted by factors between three and four. The under-prediction of methane and ethane is similar to that observed in the *n*-heptane stirred reactor computations as a consequence of uncertainties in reactions rate data. However, the under-prediction of ethylene is indicative that the consumption of some of the intermediate species as predicted by the high temperature sub-mechanism, most likely 1,3-butadiene, is too slow at this temperature.

In general, the toluene stirred reactor combustion sub-mechanism provides adequate predictions of major and some intermediate species profiles. Some improvements in the prediction of the cresols and cyclopentadiene have been made over those reported by Emdee *et al* [29] and Foelsche *et al* [31]. However, may uncertainties, both analytical and experimental, remain in this sub-mechanism and the need for additional work is readily recognised.

6.0 FINAL MECHANISM

Based on the path analysis and validation of the individual sub-mechanisms for *n*-heptane toluene combustion in diffusion flames and stirred reactors, a final sub-mechanism for the combustion of toluene and *n*-heptane in both devices has been assembled. This mechanism includes the C_1-C_4 and cyclic C_6 sub-mechanism of Lindstedt and co-workers. The total mechanism features 649 elementary reactions and 107 individual species. The final mechanism is shown in Table G1 in Appendix G. Systematic reductions of this mechanism will be under-taken in the next phase of the overall analytical programme.

7.0 CONCLUSIONS

Detailed chemical kinetics models for the combustion of *n*-heptane and toluene and blends of these two fuel components have been assembled. Thermochemical and physical properties for chemical species specific to the combustion of *n*-heptane and toluene have been compiled from existing sources or generated using proven techniques. The mechanisms have been systematically validated by quantitative comparison to major and intermediate species profiles reported by several independent experimenters in both diffusion flame and stirred reactor configurations.

An *n*-heptane combustion chemical kinetics mechanism made up of 481 elementary reactions and 86 species was used to compute laminar *n*-heptane counterflow diffusion flames over a wide range of strain rates. Path analyses for the consumption of *n*-heptane and subsequent intermediates and comparison with experimental measurements of major and intermediate species has shown that it is necessary to include both pyrolysis and radical attack reactions in the chemical model in order accurately predict intermediate species profiles. Furthermore, the distribution of intermediate species is highly sensitive to the rates of the pyrolysis steps. The following two reactions are shown to dominate the consumption of *n*-heptane in diffusion flames:

$$C_7H_{16} = C_3H_7(N) + P\text{-}C_4H_9 \quad (410)$$

$$C_7H_{16} = C_2H_5 + 1\text{-}C_5H_{11} \quad (411)$$

It has been shown that reaction rates an order of magnitude slower than those previously reported in the literature had to be utilised in order to accurately predict intermediate species profiles. The slower reaction rates were used to quantitatively predict the structure of six *n*-heptane diffusion flames with an accuracy well within the bounds of experimental error.

A more extensive *n*-heptane combustion mechanism made up of 582 elementary reactions and 93 species was used to model a stirred reactor configuration. A detailed path analyses of *n*-heptane combustion in stirred reactors at low temperature revealed major differences between dominant reaction paths in stirred reactors and diffusion flame configurations. It is thus shown that kinetics mechanisms validated against stirred reactor data and subsequently reduced on the basis of this data cannot be confidently extended to model the reaction kinetics of combustor configurations which are diffusive in nature. The temperature of the stirred reactor model was increased to 2000K and it was generally shown that reactions neglected from the diffusion flame chemical kinetics model become insignificant at high temperatures. However, it was noted that the following *n*-heptane thermal decomposition reaction was of some significance at both high and low temperatures:

$$C_7H_{16} = 1\text{-}C_6H_{13} + CH_3 \quad (412)$$

Thus, the influence of this *n*-heptane consumption path on the overall structure of *n*-heptane diffusion flames was assessed. This reaction does not have a significant effect on the major and measured intermediate profiles of *n*-heptane diffusion flames. However, it did have an effect on the predicted concentrations of 1-butene, the *n*-butyl radical, 1-pentene, the heptyl radicals and

the heptene isomers. Therefore, this reaction and the subsequent decomposition reactions of the 1-hexyl radical have been added to a more general *n*-heptane mechanism also for diffusion flames.

The *n*-heptane stirred reactor combustion kinetics model has been used to predict experimental species profiles with very good quantitative agreement. Any discrepancies observed were only at the lower temperatures. The predictions reported here are as good and/or better than any previously reported in the literature. Particularly excellent results were achieved in the prediction of 1,3-butadiene, a specie generally over-predicted by other analysts. This is clearly due to the excellent C_1-C_4 sub-mechanism developed by Lindstedt and co-workers at Imperial College.

A toluene/*n*-heptane combustion model made up of 441 elementary reactions and 91 species was assembled and used to model the structure of a 60% toluene/40% *n*-heptane diffusion flame. The mechanism was assembled based on the results of the path analyses of toluene and *n*-heptane combustion in diffusion flames of each pure component. Excellent quantitative agreement was shown between analytical predictions and experimental data. This further proves the versatility of the *n*-heptane combustion model and the general reasonableness of the toluene combustion model.

A toluene combustion chemical kinetics model made up of 437 elementary reactions and 86 species was used to compute the structure of a pure toluene diffusion flame. Analytical predictions appear reasonable based on a very limited experimental data set. Although the experimental data is not sufficient on its own to validate the model, these predictions coupled with those for the toluene/*n*-heptane diffusion flame provides credibility to the toluene model. A more extensive toluene combustion sub-mechanism featuring 447 reactions and 87 species was used to model stirred a stirred reactor configuration. Predictions were generally sensible, although areas for improvement were noted. The two sub-mechanisms were then extended to a more general toluene combustion sub-mechanism also for toluene combustion.

Quantitative soot volume fraction predictions were generally shown to be less than predicted by others. At the moment, the soot formation model essentially allows the prediction of soot radiation heat loss in the flame without resorting to a fictitious heat loss factor. Temperature profiles are shown to be predicted within reasonable accuracy. However, the paths of soot formation in the C_7 hydrocarbon flames is clearly an area for future model enhancement.

All the sub-mechanisms were combined into a final sub-mechanism for C_7 hydrocarbon combustion in intermediate to high temperature environments. The final mechanism features 649 elementary reactions and 107 species.

The work presented herein represents the only computations of C_7 hydrocarbons diffusion flames using detailed chemistry which are shown to accurately model both major and intermediate species profiles reported to date. Nearly all available experimental data reported in the literature has been used to validate the mechanisms with very good results. However, additional experimental data including radical and additional intermediate species profiles over a wider range of experimental conditions would be very useful to fully assess the versatility of the model. Nonetheless, the final mechanism represents the best available state-of-the-art model for C_7 hydrocarbon combustion. Thus, systematic reduction of the mechanism and modelling of more

complex configurations will be undertaken in order to ultimately model the chemical kinetics features of a realistic high speed propulsion combustor device. Once the mechanism has been reduced, it will also be possible to model coflow laminar diffusion flames in order to more thoroughly validate the toluene and *n*-heptane combustion chemistry.

8.0 FUTURE PLANS

Plans for follow-on research include the following:

1. Compute the structures of the toluene/methanol/*n*-heptane counterflow diffusion flames studied by Hamins and Seshadri [42] and Hamins [43] to complete the validation of the toluene combustion sub-mechanism. Continue to survey the literature and individual researchers to identify and gather fundamental toluene and *n*-heptane combustion data as it becomes available for additional kinetics model validation.

2. Reduce the detailed chemical kinetics mechanism through systematic methods. This will result in reaction mechanisms which are based on the fundamental rate constants. A range of simplified reaction mechanisms with decreasing numbers of independent scalars will result and the inaccuracies introduced at each step will be quantified.

3. The resulting simplified reaction mechanisms will be used in multi-dimensional laminar flame computations.

4. Turbulent flames for idealised configurations of relevance to the experimental programme [11] will be computed by the used of presumed and transported *pdf* methods. In the turbulent combustion regimes expected under combustor conditions it is likely that direct kinetics effects will dominate. It is, however, recognised that the number of independent scalars which may be used in transported *pdf* methods is currently severely restricted. Thus, the following approach will be pursued:

a. The detailed kinetic mechanisms will initially be utilised for turbulent flame computations via a extended flamelet presumed *pdf* approach to model features for which direct kinetics effects do not dominate.

b. Subsequently, issues of interest to the experimental research programme [11] such as flame stability will be addressed by the use of transported *pdf* methods.

9.0 REFERENCES

[1] Lander, H., and Nixon, A.C., *Journal of Aircraft*, Vol. 8, No. 4, pp. 200-207(1971).

[2] Nixon, A.C., *A Study on Endothermic and High Energy Fuels for Air breathing Engines*, US. Air Force, AFSC/ASD, Air Force Contract F33615-84-C-2410 Final Report(1986)

[3] Mcfarlane, W.R., and Wiese, D.E., *Fuel Options for High Mach Propulsion Vol. I*, WRDC-TR-90-2090(1990).

[4] Spadaccini, L.R., Colkett, M.B., Marteney, P.J., Roback, R., Glickstein, M.R., and Stiles, A.B., *Endothermic Fuel/Catalyst Development and Evaluation, Phase I Interim Report*, AFSC/WL Contract F33615-87-C-2744(1989).

[5] Salooja, K.C., *Combustion and Flame*, 4:117(1960).

[6] Salooja, K.C., *Combustion and Flame*, 5:243(1961).

[7] Salooja, K.C., *Combustion and Flame*, 6:275(1962).

[8] Lefebvre, A.H., *Investigation of Flame Speeds of Endothermic Fuels*, AFWAL-TR-88-2027(1988).

[9] Richards, G.A. and Lefebvre, A.H., *Combustion and Flame*, 78:299(1989).

[10] Richards, G.A. and Sojka, P.E., *Combustion and Flame*, 79:319(1990).

[11] Buckley, P.L., Private Communication, November 1993.

[12] Hussaini, M.Y., Kumar, A. and Voight, R.G., eds., *Major Research Topics in Combustion*, Springer-Verlag, 1992.

[13] Kailasanath, K., Gardner, J.H., Boris, J.P., and Oran, E.S., *Numerical Simulations of Flowfields in a Central-Dump Ramjet Combustor III. Effects of Chemistry*, Naval Research Laboratory, NRL Memorandum Report 6682(1990).

[14] Drake, M.C., and Blint, R.J., *Combustion Science and Technology* 61:187(1988).

[15] Dixon-Lewis, G., David, T., Gaskell, P.H., Fukutani, S., Jinno, H., Miller, J.A., Kee, R.J., Smooke, M.D., Peters, N., Effelsberg, E., Warnatz, J., and Behrendt, F., *Twentieth Symposium (International) on Combustion*, The Combustion Institute, 1984, p. 1893.

[16] Seshadri, K., Trevino, C., and Smooke, M.D., *Combustion and Flame*, 76:111(1989).

[17] Leung, K.M., and Lindstedt, R.P., Internal Report of Mech. Eng., Imperial College, 1990.

[18] Leung, K.M., Lindstedt, R.P., and Jones, W.P., *Combustion and Flame,* 87:289(1989).

[19] Lindstedt, R.P., and Skevis, G., *Formation of Aromatic Compounds and Soot in Flames,* 207th ACS National Meeting, San Diego, CA, Vol. 39, No. 1, pp. 147(1994)

[20] Leung, K.M., and Lindstedt, R.P., *Detailed Kinetic Modelling of C_1-C_3 Alkane Diffusion Flames,* To appear in *Combustion and Flame*(1994).

[21] Leung, K.M., and Lindstedt, R.P., *Benzene Formation in Propane and Acetylene Premixed Flames,* Work in Progress (1994).

[22] Lindstedt, R.P., and Skevis, G, *Detailed Kinetic Modelling of Premixed Benzene Flames,* To Appear in *Combustion and Flame* (1994).

[24] Lindstedt, R.P., and Skevis, G., *PAH Formation Mechanisms in Premixed Acetylene, Propane and Butadiene Flames,* Work in Progress (1994).

[25] Burcat, A., *The 13th International Symposium of Shock Tubes and Waves,* pp. 826-833(1981).

[26] Burcat, A., Pitz, W.J., and Westbrook, C.K., *Shock Tube Ignition of Octanes,* Lawrence Livermore National Laboratory Pre-print #UCRL-102001(1989).

[27] Ciezki, H., and Adomeit, G., *The 16th International Symposium of Shock Tubes and Waves,* pp. 481-486(1987).

[28] Coats, C.M., and Williams, A., *Seventeenth Symposium (International) on Combustion,* The Combustion Institute, 1978, pp. 611-621.

[29] Emdee, J.L., Brezinsky, K., and Glassman, I., *Journal of Physical Chemistry,* 96:2151-2161(1992)

[30] Bittker, D.A., *Detailed Mechanism of Toluene Oxidation and Comparison with Benzene,* NASA Technical Memorandum 100261(1988)

[31] Foelsche, R.O., Keen, J.M. and Solomon, W.C., *A Non-Equilibrium Computational Method for Predicting Fuel Rich Gas Generator Performance and Exhaust Properties - Volume II: Reaction Kinetics and Computational Results",* University of Illinois Report No. AAE9307, UIL93-0507.

[32] Chakir, A., Belliman, M., Boettner, J.C., and Cathonnet, M., *International Journal of Chemical Kinetics,* Vol. 24, 385-410(1992).

[33] McLain, A.G., Jachimowski, C.J., and Wilson, C.H., *Chemical Kinetic Modelling of Benzene and Toluene Behind Shock Waves,* NASA Tech. Paper 1472.

[34] Cavalier, A., *Combustion and Flame,* 93:279(1993).

[35] Burcat, A., Snyder, C., and Brabbs, T., *Ignition Delay of Benzene and Toluene with Oxygen in Argon,* NASA Tech Memo 87312, May (1986)

[36] Halstead, M.P., Kirsch, L.J., and Quinn, C.P., *Combustion and Flame,* 30:45-60(1977).

[37] Muller, U.C., Peters, N., and Linan, A., *Twenty-Fourth Symposium (International) on Combustion,* The Combustion Institute, 1992, p. 777.

[38] Bui-Pham, M., and Seshadri, K., *Combustion Science and Technology* 79:293(1991).

[39] Darahiba, N., Lacas, F., Rolon, J.C., and Candel, S., *Combustion and Flame,* 95:261(1993).

[40] Abdel-Khalik, S.I., Tamaru, T., and El-Wakil, M., *Fifteenth Symposium (International) on Combustion,* The Combustion Institute, 1968, p. 389.

[41] Abdel-Khalik, S.I., *An Investigation of the Diffusion Flame Surrounding a Simulated Liquid Fuel Droplet,* PhD Thesis, University of Wisconsin-Madison, 1973.

[42] Hamins, A., and Seshadri, K., *Combustion and Flame,* 68:295(1987).

[43] Hamins, A., *Diffusion Flame Studies,* PhD Thesis, University of California, San Diego, 1985.

[44] Brezinsky, K., and Dryer, F.L., *Fundamental Semi-Global Kinetic Mechanisms of Hydrocarbon Combustion,* Princeton University DOE Report 40283-1, October 1983.

[45] Brezinsky, K., *Progress in Energy and Combustion Science,* Vol. 12, pp. 1-24(1986).

[46] Brezinsky, K., Litzinger, T.A., and Glassman, I., *International Journal of Chemical Kinetics,* Vol. 16, p.1053(1984)

[47] Lindstedt, R.P., LACDIF, *A Computer Model for Solving Laminar Counterflow Diffusion Flames.*

[48] Kent, J.H., and Honnery, J.H., *Combustion and Flame,* 79:287(1990).

[49] Leung, K.M, Lindstedt, R.P., and Jones, W.P., *Combustion and Flame,* 87:289(1991).

[50] Peters, N., and Kee, R.J., *Combustion and Flame,* 65:137(1987).

[51] Jones, W.P., and Lindstedt, R.P., *Combustion and Flame,* 73:233(1988).

[52] Jones, W.P., and Lindstedt, R.P., *Combustion and Flame,* 73:233(1988).

[53] Jones, W.P., and Lindstedt, R.P., *Combustion Science and Technology* 61:31-49(1988).

[54] Lindstedt, R.P., LAPREM, *A Computer Model For Solving Laminar Premixed Flames.*

[55] Patankar, S.V., and Spalding, D.B., *Heat and Mass Transfer in Boundary Layers, 2nd ed.,* Intertext, London, 1970.

[56] Lindstedt, R.P., *Simplified Reaction Mechanisms for Soot Formation in Non-Premixed Flames,* To Appear in Mechanisms and Models of Soot Formation, Bockhorn, H., ed., Springer-Verlag.

[57] Chakir, A., Cathonnet, M., Boetnner, J.C., and Gailland, F., *Twenty-Second Symposium (International) on Combustion,* The Combustion Institute, 1988, pp. 873-881.

[58] Chakir, A., Cathonnet, M., Boetnner, J.C., and Gailland, F., *Combustion and Flame,* 72:45(1988).

[59] Chakir, A., Cathonnet, M., Boetnner, J.C., and Gailland, F., *Combustion Science and Technology* 65:207(1988).

[60] -, *NIST Chemical Kinetics Database,* National Institute of Standards and Technology, 1992.

[61] Westbrook, C.K., Pitz, W.J. and Warnatz, J., *Twenty-Second Symposium (International) on Combustion,* The Combustion Institute, 1988, pp. 863-871.

[62] Westbrook, C.K., Pitz, W.J. and Warnatz, J., *Twenty-Second Symposium (International) on Combustion,* The Combustion Institute, 1988, pp. 45-62.

[63] Levuch, S.S., Savichenkov, A.Z., Abadzhev, S.S., and Shivechuka, V.U., *Neftekhimiya,* 1970:10:656.

[64] Reid, R.C., Prausnitz, J.M., and Poling, B.E., *The Properties of Gases and Liquids,* McGraw-Hill, Inc., 1987.

[65] Himmelblau, D.M., *Basic Principles and Calculations in Chemical Kinetics,* Prentice-Hall, Inc., NJ, 1974.

[66] *TRC Thermodynamic Tables - Hydrocarbons,* Thermodynamic Research Centre, 1991.

[67] Burcat, A., and McBride, B.J., *1994 Ideal Gas Thermodynamic Data for Combustion and Air Pollution Use,* TAE697, 1993.

[68] Kee, R.J., Rupley, F.M., and Miller, J.A., *The Chemkin Thermodynamic Data Base,* Sandia National Laboratories Report SAND87-8215B(1990)

[69] Benson, S.W., *Thermochemical Kinetics,* John Wiley & Sons, NY, 1976.

[70] McBride, B.J., *PAC91 Properties and Coefficients 1991,* NASA Reference Publication 1271, 1992.

[71] Burcat, A., private communication (1994).

[72] Svehla, R.A., *Estimated Viscosities and Thermal Conductivities of Gases at High Temperatures,* NASA Technical Report R-132, 1962.

[73] Bird, R.B., Stewart, W.E., and Lightfoot, E.N., *Transport Phenomena,* John Wiley & Sons, NY1960.

[74] Tsang, W., *International Journal of Chemical Kinetics,* Vol. 10, 1119(1978).

[75] Westbrook, C.K., Pitz, W.J., Thornton, M.M., and Malte, P.C., *Combustion and Flame,* 72:45(1988).

[76] Chakir, A., Belliman, M., Boettner, J.C., and Cathonnet, M., *Combustion Science and Technology* 77:239(1991).

[77] Dagaut, P., Cathonnet, M., Boettner, J.C., and Gaillard, F., *Combustion Science and Technology* 77:127(1991).

[78] Daugaut, P., Boettner, J.C., and Cathonnet, M., *Combustion Science and Technology* 56:23(1987).

[79] Hochgreb, S., Yetter, Y.A., and Dryer, F.L., *Twenty-Third Symposium (International) on Combustion,* The Combustion Institute, 1990, p. 171.

[80] Bilger, R.W., *Combustion and Flame,* 30:277(1977).

[81] Aldred, J.W., Patel, J.C., and Williams, A., *Combustion and Flame,* 17, 139(1971).

[82] Seery, D.J., and Zabielski, M.F., *Combustion and Flame,* 78:169(1989).

[83] Bilger, R., Starner, S.H., and Kee, R.J., *Combustion and Flame,* 80:135(1990).

[84] Tsuji, H., *Progress in Energy and Combustion Science,* Vol. 8, pp. 93-119(1982).

[85] Tsuji, H., and Yamaoka, I., *Thirteenth Symposium (International) on Combustion,* The Combustion Institute, 1970, p. 723.

[86] Tsuji, H., and Yamaoka, I., *Twelfth Symposium (International) on Combustion,* The Combustion Institute, 1968, p. 997.

[87] Colkett, M.B., Chiappetta, L., Guile, R.W., Zabielski, M.F., and Seery, D.J., *Combustion and Flame,* 44:3(1982).

[88] Gordon, S., and McBride, B.J., *Computer Program for Calculation of Complex Chemical Equilibrium Compositions, Rocket Performance, Incident and Reflected Shocks, and Chapman-Jouguet Detonations,* NASA SP-273 (1976).

[89] Gulder, O.L., *Combustion and Flame,* 78:179(1989).

[90] Gueret, M., Cathonnet, M, and Boettner, J.C., *Twenty-Third Symposium (International) on Combustion,* The Combustion Institute, 1991, p. 211.

[91] Robaugh, D., and Tsang, W., *Journal of Physical Chemistry,* Vol. 90, p. 4159(1986).

[92] Brouwer, L.D., Mueller-Markgraf, W., and Troe, J., *Journal of Physical Chemistry,* Vol. 92, pp. 4905-4914(1988).

[93] Hippler, H., and Troe, J., *Journal of Physical Chemistry,* Vol. 94, pp. 3803-3806(1990).

[94] Tully, F.P., Ravishankana, A.R., Thompson, R.L., Nicovich, J.M., Shah, R.C., Kreutter, N.M., Wine, P.H., *Journal of Physical Chemistry,* Vol. 85, p. 2262(1987).

[95] Pamidimukkhala, K.M., Kern, R.D., Patel, M.R., Wei, H.C., Kiefer, J.H., *Journal of Physical Chemistry,* Vol. 91, p. 2148(1987).

[96] Braun-Unkhoff, M., Frank, P., and Just, T., *Twenty-Second Symposium (International) on Combustion,* The Combustion Institute, 1988, pp. 1053-1061.

[97] Hamins, A., Anderson, D.T. and Miller, J.H, *Combustion Science and Technology* 71:175(1990).

[98] Smith, R.D., *Journal of Physical Chemistry,* Vol. 83, pp. 1553-1563(1979).

[99] Smith, R.D., *Combustion and Flame,* 35:179(1979).

[100] Mizerka, L.J., and Kiefer, J.H., *International Journal of Chemical Kinetics,* Vol. 18, 363(1986).

[101] Hippler, H., Reihs, C., and Troe, J., *Twenty-Third Symposium (International) on Combustion,* The Combustion Institute, 1991, p. 37.

[102] Lin, C-Y., and Lin, M.C., *Journal of Physical Chemistry,* Vol. 90, p. 425(1986).

[103] He, Y.Z., Mallard, W.G., and Tsang, W., *Journal of Physical Chemistry,* Vol. 92, p. 2196(1979).

[104] Nicovich, J.M., Gump, C.A., Ravi-Shankar, A.R., *Journal of Physical Chemistry,* Vol. 86, p. 1684(1982).

[105] Norton, T.S., and Dryer, F.L., *Combustion Science and Technology* 63:107(1989).

[106] Norton, T.S., and Dryer, F.L., *International Journal of Chemical Kinetics,* Vol. 22, 219(1990).

[107] Santoro, R.J., *Mat. Res. Soc. Symp. Proc.*, Vol. 117, pp.157(1988).

[108] Tesner P.A., Tsygankova, E.I., Guilazetdinov, L.P., Zvyev, V.P., and Loshakova, G.V., *Combustion and Flame,* 17:279(1971).

[109] Frenklack, M., Taki, S., and Matula, R.A., *Combustion and Flame,* 49:275(1983).

[110] Olson, D.B., and Madronich, S., *Combustion and Flame,* 60:203(1985).

[111] Buckley, P.L., Fisher, S.A., and Hille, L.W., *A Simulator for a Hydrocarbon Ram rocket Fuel Gas Generator - First Phase Development,* Defence Science and Technology Organisation, Aeronautical Research Laboratory Report # ARL-PROP-R-181(1989).

[112] Hautman, D.J., PhD Thesis, Department of Mechanical and Aerospace Engineering, Princeton University, Princeton, 1980.

APPENDIX A
FULL *n*-HEPTANE MECHANISM

TABLE A1
n-Heptane Mechanism for Diffusion Flames

	ELEMENTARY REACTION	A m^3, Kmol, sec^{-1}	n	E_a J/mol	REF
1	H + O2 = OH + O	0.2000E+12	o	0.7030E+05	20-24
2	O + H2 = OH + H	0.5120E+02	2.67	0.2630E+05	20-24
3	OH + H2 = H2O + H	0.1000E+06	1.6	0.1380E+05	20-24
4	OH + OH = H2O + O	0.1500E+07	1.14	0.4200E+03	20-24
5	O2 + H + M = HO2 + M	0.6165E+14	1.42	0.0000E+00	20-24
6	HO2 + H = OH + OH	0.1680E+12	0	0.3660E+04	20-24
7	HO2 + H = H2 + O2	0.4270E+11	0	0.5900E+04	20-24
8	HO2 + OH = H2O + O2	0.2890E+11	0	0.2080E+04	20-24
9	HO2 + H = H2O + O	0.3000E+11	0	0.7200E+04	20-24
10	HO2 + O = OH + O2	0.3190E+11	0	0.0000E+00	20-24
11	HO2 + HO2 = H2O2 + O2	0.1860E+10	0	0.6440E+04	20-24
12	H2O2 + H = H2O + OH	0.1000E+11	0	0.1500E+05	20-24
13	H2O2 + H = HO2 + H2	0.1700E+10	0	0.1570E+05	20-24
14	H2O2 + O = HO2 + OH	0.6600E+09	0	0.1660E+05	20-24
15	H2O2 + OH = H2O + HO2	0.7830E+10	0	0.5570E+04	20-24
16	H2O2 + M = OH + OH + M	0.1200E+15	0	0.1900E+06	20-24
17	H + H + M = H2 + M	0.1000E+13	1	0.0000E+00	20-24
18	H + H + M = H2 + M	0.9200E+11	0.60	0.0000E+00	20-24
19	H + H + M = H2 + M	0.6000E+14	1.25	0.0000E+00	20-24
20	H + H + M = H2 + M	0.5490E+15	2	0.0000E+00	20-24
21	H + OH + M = H2O + M	0.2200E+17	2	0.0000E+00	20-24
22	O + O + M = O2 + M	0.6170E+10	0.5	0.0000E+00	20-24
23	CO + OH = CO2 + H	0.4400E+04	1.5	0.3100E+04	20-24
24	CO + HO2 = CO2 + OH	0.1500E+12	0	0.9893E+05	20-24
25	CO + O + M = CO2 + M	0.2510E+08	0	0.1901E+05	20-24
26	CO + O2 = CO2 + O	0.2500E+10	0	0.2000E+06	20-24
27	CH + O2 = CHO + O	0.3300E+11	0	0.0000E+00	20-24
28	CH + CO2 = CHO + CO	0.3400E+10	0	0.2900E+04	20-24
29	CH + O = CO + H	0.5700E+11	0	0.0000E+00	20-24
30	CH + OH = CHO + H	0.3000E+11	0	0.0000E+00	20-24
31	CH + H2O = CH2O + H	0.1170E+13	0.75	0.0000E+00	20-24
32	CH + CH2O = C2H2O + H	0.9460E+11	0	0.2160E+04	20-24
33	CH + CH2(T) = C2H2 + H	0.4000E+11	0	0.0000E+00	20-24
34	CH + CH3 = C2H3 + H	0.3000E+11	0	0.0000E+00	20-24
35	CH + CH4 = C2H4 + H	0.6000E+11	0	0.0000E+00	20-24
36	CH + C2H2 = C3H2 + H	0.1000E+12	0	0.0000E+00	20-24
37	CHO + H = CO + H2	0.9000E+11	0	0.0000E+00	20-24
38	CHO + O = CO + OH	0.3000E+11	0	0.0000E+00	20-24
39	CHO + O = CO2 + H	0.3000E+11	0	0.0000E+00	20-24
40	CHO + OH = CO + H2O	0.1000E+12	0	0.0000E+00	20-24
41	CHO + O2 = CO + HO2	0.3000E+10	0	0.0000E+00	20-24
42	CHO + M = CO + H + M	0.1860E+15	1	0.7110E+05	20-24
43	CH2(S) + H2 = CH3 + H	0.7230E+11	0	0.0000E+00	20-24
44	CH2(S) + H = CH + H2	0.1100E+12	0	0.0000E+00	20-24
45	CH2(S) + O = CO + H + H	0.1500E+11	0	0.0000E+00	20-24
46	CH2(S) + O = CO + H2	0.1500E+11	0	0.0000E+00	20-24
47	CH2(S) + OH = CH2O + H	0.3000E+11	0	0.0000E+00	20-24
48	CH2(S) + O2 = CO + OH + H	0.7000E+11	0	0.0000E+00	20-24
49	CH2(S) + CO2 = CH2O + CO	0.3000E+10	0	0.0000E+00	20-24
50	CH2(S) + CH3 = C2H4 + H	0.2000E+11	0	0.0000E+00	20-24

TABLE A1 (CONTINUED)

51	CH2(S) + CH4 = CH3 + CH3	0.4000E+11	0	0.0000E+00	20-24
52	CH2(S) + C2H2 = C3H3 + H	0.2200E+12	0	0.0000E+00	20-24
53	CH2(S) + C2H2O = C2H4 + CO	0.1600E+12	0	0.0000E+00	20-24
54	CH2(S) + C2H4 = C3H6	0.6600E+11	0	0.0000E+00	20-24
55	CH2(S) + C2H6 = C2H5 + CH3	0.1200E+12	0	0.0000E+00	20-24
56	CH2(S) + M = CH2(T) + M	0.1000E+11	0	0.0000E+00	20-24
57	CH2(T) + H2 = CH3 + H	0.3000E+07	0	0.0000E+00	20-24
58	CH2(T) + H = CH + H2	0.3500E+11	0	0.3080E+04	20-24
59	CH2(T) + O = CO + H + H	0.5000E+11	0	0.0000E+00	20-24
60	CH2(T) + O = CO + H2	0.3000E+11	0	0.0000E+00	20-24
61	CH2(T) + OH = CH + H2O	0.1130E+05	2	0.1256E+05	20-24
62	CH2(T) + OH = CH2O + H	0.2500E+11	0	0.0000E+00	20-24
63	CH2(T) + O2 = CO + H + H	0.8600E+08	0	0.2093E+04	20-24
64	CH2(T) + O2 = CO2 + H2	0.6900E+09	0	0.2093E+04	20-24
65	CH2(T) + O2 = CO + H2O	0.1900E+08	0	0.4187E+04	20-24
66	CH2(T) + O2 = CO2 + H + H	0.1600E+10	0	0.4187E+04	20-24
67	CH2(T) + O2 = CH2O + O	0.5000E+11	0	0.3768E+05	20-24
68	CH2(T) + O2 = CHO + OH	0.4300E+08	0	0.2093E+04	20-24
69	CH2(T) + CO2 = CH2O + CO	0.1100E+09	0	0.4187E+04	20-24
70	CH2(T) + CH2(T) = C2H2 + H + H	0.4000E+11	0	0.3320E+04	20-24
71	CH2(T) + CH3 = C2H4 + H	0.4000E+11	0	0.0000E+00	20-24
72	CH2(T) + C2HO = C2H3 + CO	0.3000E+11	0	0.0000E+00	20-24
73	CH2(T) + C2H2 = C3H3 + H	0.1200E+11	0	0.2763E+05	20-24
74	CH2(T) + C2H4 = C3H6	0.1800E+08	0	0.0000E+00	20-24
75	CH2O + H = CHO + H2	0.2288E+08	1.05	0.1370E+05	20-24
76	CH2O + O = CHO + OH	0.4150E+09	0.57	0.1156E+05	20-24
77	CH2O + OH = CHO + H2O	0.3400E+07	1.18	0.1870E+04	20-24
78	CH2O + O2 = CHO + HO2	0.6000E+11	0	0.1700E+06	20-24
79	CH2O + M = CHO + H + M	0.1260E+14	0	0.3260E+06	20-24
80	CH3 + CH3 = C2H5 + H	0.1000E+11	0	0.5654E+05	20-24
81	CH3 + CH3 = C2H6	0.3600E+11	0	0.0000E+00	20-24
82	CH3 + O = CH2O + H	0.8430E+11	0	0.0000E+00	20-24
83	CH3 + OH = CH2OH + H	0.2640E+17	1.80	0.3380E+05	20-24
84	CH3 + OH = CH2(S) + H2O	0.2650E+11	0	0.9211E+04	20-24
85	CH3 + OH = CH2O + H2	0.3190E+10	0.53	0.4526E+05	20-24
86	CH3 + OH = CH3O + H	0.5740E+10	0.23	0.5833E+05	20-24
87	CH3 + O2 = CH3O + O	0.2050E+16	1.57	0.1224E+06	20-24
88	CH3 + O2 = CH2O + OH	0.3300E+09	0	0.3740E+05	20-24
89	CH3 + HO2 = CH3O + OH	0.1800E+11	0	0.0000E+00	20-24
90	CH3 + CHO = CH4 + CO	0.1200E+12	0	0.0000E+00	20-24
91	CH3 + M = CH2(S) + H + M	0.1900E+14	0	0.3824E+06	20-24
92	CH3 + M = CH + H2 + M	0.6900E+12	0	0.3450E+06	20-24
93	CH3O + H = CH2O + H2	0.2000E+11	0	0.0000E+00	20-24
94	CH3O + O = CH2O + OH	0.1000E+11	0	0.0000E+00	20-24
95	CH3O + OH = CH2O + H2O	0.1000E+11	0	0.0000E+00	20-24
96	CH3O + O2 = CH2O + HO2	0.6300E+08	0	0.1088E+05	20-24
97	CH3O + M = CH2O + H + M	0.1000E+12	0	0.1047E+06	20-24
98	CH2OH + H = CH2O + H2	0.2000E+11	0	0.0000E+00	20-24
99	CH2OH + O = CH2O + OH	0.1000E+11	0	0.0000E+00	20-24
100	CH2OH + OH = CH2O + H2O	0.1000E+11	0	0.0000E+00	20-24
101	CH2OH + O2 = CH2O + HO2	0.1480E+11	0	0.6280E+04	20-24
102	CH2OH + M = CH2O + H + M	0.1000E+12	0	0.1047E+06	20-24
103	CH4 = CH3 + H	0.2400E+17	0	0.4388E+06	20-24
104	CH4 + H = CH3 + H2	0.3900E+04	2.11	0.3240E+05	20-24

TABLE A1 (CONTINUED)

105	CH4	+	O	=	CH3	+	OH	0.9033E+06	1.56	0.3550E+05	20-24
106	CH4	+	OH	=	CH3	+	H2O	0.1560E+05	1.83	0.1160E+05	20-24
107	CH4	+	O2	=	CH3	+	HO2	0.3970E+11	0	0.2380E+06	20-24
108	C2H	+	H2	=	C2H2	+	H	0.4050E+03	2.39	0.3617E+04	20-24
109	C2H	+	O	=	CO	+	CH	0.5000E+11	0	0.0000E+00	20-24
110	C2H	+	OH	=	C2HO	+	H	0.2000E+11	0	0.0000E+00	20-24
111	C2H	+	O2	=	CO	+	CO + H	0.3520E+11	0	0.0000E+00	20-24
112	C2H	+	CH3	=	C3H3	+	H	0.2410E+11	0	0.0000E+00	20-24
113	C2HO	+	H	=	CH2(S)	+	CO	0.1500E+12	0	0.0000E+00	20-24
114	C2HO	+	O	=	CO	+	CO + H	0.1500E+12	0	0.0000E+00	20-24
115	C2HO	+	O2	=	CO	+	CO + H	0.8100E+09	0	0.3570E+04	20-24
116	C2HO	+	O2	=	CO2	+	CO + H	0.8100E+09	0	0.3570E+04	20-24
117	C2HO	+	CH	=	C2H2	+	CO	0.5000E+11	0	0.0000E+00	20-24
118	C2HO	+	C2HO	=	C2H2	+	CO +CO	0.1000E+11	0	0.0000E+00	20-24
119	C2HO	+	C2H2	=	C3H3	+	CO	0.1000E+09	0	0.1260E+05	20-24
120	C2H2	+	O	=	CH2(T)	+	CO	0.7810E+01	2.8	0.2100E+04	20-24
121	C2H2	+	O	=	C2HO	+	H	0.1390E+02	2.8	0.2100E+04	20-24
122	C2H2	+	OH	=	C2H	+	H2O	0.2700E+12	0	0.6300E+05	20-24
123	C2H2	+	OH	=	C2H2O	+	H	0.2000E+11	0	0.3000E+05	20-24
124	C2H2	+	OH	=	CH3	+	CO	0.4850E-06	4	0.8400E+04	20-24
125	C2H2	+	O2	=	C2H	+	HO2	0.1200E+11	0	0.3117E+06	20-24
126	C2H2	+	O2	=	C2HO	+	OH	0.2000E+06	1.5	0.1260E+06	20-24
127	C2H2	+	M	=	C2H	+	H + M	0.4200E+14	0	0.4480E+06	20-24
128	C2H2	+	CH3	=	C3H5(S)			0.1610E+38	8.58	0.8512E+05	20-24
129	C2H2O	+	M	=	CH2(T)	+	CO + M	0.3600E+13	0	0.2480E+06	20-24
130	C2H2O	+	H	=	CH3	+	CO	0.1130E+11	0	0.1400E+05	20-24
131	C2H2O	+	H	=	C2HO	+	H2	0.5000E+11	0	0.3350E+05	20-24
132	C2H2O	+	O	=	CO2	+	CH2(T)	0.1750E+10	0	0.5700E+04	20-24
133	C2H2O	+	O	=	C2HO	+	OH	0.1000E+11	0	0.3350E+05	20-24
134	C2H2O	+	OH	=	CH2O	+	CHO	0.7500E+10	0	0.8370E+04	20-24
135	C2H3	+	H	=	C2H2	+	H2	0.4000E+11	0	0.0000E+00	20-24
136	C2H3	+	OH	=	C2H2	+	H2O	0.2000E+11	0	0.0000E+00	20-24
137	C2H3	+	O	=	C2H2O	+	H	0.3000E+11	0	0.0000E+00	20-24
138	C2H3	+	O2	=	CHO	+	CH2O	0.4480E+24	4.55	0.22943+05	20-24
139	C2H2	+	H	=	C2H3			0.5540E+10	0	0.1009E+05	20-24
140	C2H3	+	CH	=	C2H2	+	CH2(T)	0.5000E+11	0	0.0000E+00	20-24
141	C2H3	+	C2H	=	C2H2	+	C2H2	0.3000E+11	0	0.0000E+00	20-24
142	C2H4	+	H	=	C2H3	+	H2	0.1325E+04	2.53	0.5121E+05	20-24
143	C2H4	+	O	=	CH3	+	CHO	0.1320E+06	1.55	0.1788E+04	20-24
144	C2H4	+	OH	=	C2H3	+	H2O	0.1570E+02	2.75	0.1746E+05	20-24
145	C2H4	+	M	=	C2H2	+	H2 + M	0.2600E+15	0	0.3317E+06	20-24
146	C2H4	+	M	=	C2H3	+	H + M	0.3800E+15	0	0.4107E+06	20-24
147	C2H5	+	O2	=	C2H4	+	HO2	0.1020E+08	0	0.9140E+04	20-24
148	C2H5			=	C2H4	+	H	0.4970E+11	0.73	0.1542E+06	20-24
149	C2H6			=	C2H5	+	H	0.8850E+21	1.23	0.4277E+06	20-24
150	C2H6	+	H	=	C2H5	+	H2	0.1445E+07	1.5	0.3100E+05	20-24
151	C2H6	+	O	=	C2H5	+	OH	0.1000E+07	1.5	0.2430E+05	20-24
152	C2H6	+	OH	=	C2H5	+	H2O	0.7226E+04	2.	0.3616E+04	20-24
153	C3H2	+	O	=	C2H	+	CHO	0.6800E+11	0	0.0000E+00	20-24
154	C3H2	+	OH	=	C2H2	+	CHO	0.5000E+11	0	0.0000E+00	20-24
155	C3H2	+	O2	=	C2HO	+	CO + H	0.5000E+11	0	0.0000E+00	20-24
156	C3H3	+	H	=	C3H2	+	H2	0.5000E+11	0	0.1256E+05	20-24
157	C3H3	+	OH	=	C3H2	+	H2O	0.2000E+11	0	0.0000E+00	20-24

TABLE A1 (CONTINUED)

158	C3H3 + O2 = C2H2O + CHO	0.3000E+08	0	0.1200E+05	20-24
159	C3H3 + O = CH2O + C2H	0.2000E+11	0	0.0000E+00	20-24
160	C3H4(A) = C3H4(P)	0.2500E+13	0	0.2470E+06	20-24
161	C3H4(A)+ M = C3H3 + H + M	0.2000E+16	0	0.3350E+06	20-24
162	C3H4(A)+ H = C3H5(T)	0.8500E+10	0	0.8370E+04	20-24
163	C3H4(A)+ H = C3H5(A)	0.4000E+10	0	0.1130E+05	20-24
164	C3H4(A)+ H = C3H3 + H2	0.1000E+10	0	0.6280E+04	20-24
165	C3H4(A)+ O = C2H4 + CO	0.9000E-05	4.61	0.1780E+05	20-24
166	C3H4(A)+ O = C2H2 + CH2O	0.3000E-05	4.16	0.1780E+05	20-24
167	C3H4(A)+ OH = C2H2O + CH3	0.3120E+10	0	0.1660E+04	20-24
168	C3H4(A)+ OH = C3H3 + H2O	0.1445E+11	0	0.1750E+05	20-24
169	C3H4(A)+ O2 = C3H3 + HO2	0.4000E+11	0	0.2575E+06	20-24
170	C3H4(A)+ CH3 = C3H3 + CH4	0.2000E+10	0	0.3220E+05	20-24
171	C3H4(A)+ C2H = C3H3 + C2H2	0.1000E+11	0	0.0000E+00	20-24
172	C3H4(A)+ C3H5(A)= C3H3 + C3H6	0.2000E+10	0	0.3224E+05	20-24
173	C3H4(P) + M = C3H3 + H + M	0.4700E+16	0	0.3350E+06	20-24
174	C3H4(P) = C2H + CH3	0.4200E+17	0	0.4180E+06	20-24
175	C3H4(P)+ H = C3H5(T)	0.6500E+10	0	0.8373E+04	20-24
176	C3H4(P)+ H = C3H5(S)	0.5800E+10	0	0.1298E+05	20-24
177	C3H4(P)+ H = C3H3 + H2	0.1000E+10	0	0.6280E+04	20-24
178	C3H4(P)+ O = C2H3 + CHO	0.3200E+10	0	0.8410E+04	20-24
179	C3H4(P)+ O = C2H4 + CO	0.3200E+10	0	0.8410E+04	20-24
180	C3H4(P)+ O = C2HO + CH3	0.6300E+10	0	0.8410E+04	20-24
181	C3H4(P)+ OH = C2H2O + CH3	0.5000E-06	4.5	0.4187E+04	20-24
182	C3H4(P)+ OH = C3H3 + H2O	0.1500E+01	3.0	0.8370E+04	20-24
183	C3H4(P)+ O2 = C3H3 + HO2	0.2500E+10	0	0.2130E+06	20-24
184	C3H4(P)+ CH3 = C3H3 + CH4	0.2000E+10	0	0.3220E+05	20-24
185	C3H4(P)+ C2H = C3H3 + C2H2	0.1000E+11	0	0.0000E+00	20-24
186	C3H4(P)+ C3H5(A)= C3H3 + C3H6	0.1000E+10	0	0.3224E+05	20-24
187	C3H5(A)+ H = C3H4(A) + H2	0.3333E+10	0	0.0000E+00	20-24
188	C3H5(A)+ O2 = CH2O + CH2O+ CH	0.6310E+09	0	0.7200E+05	20-24
189	C3H5(A)+ CH3 = C3H4(A) + CH4	0.1000E+09	0	0.0000E+00	20-24
190	C3H5(A)+ C2H5 = C2H6 + C3H4(A)	0.4000E+09	0	0.0000E+00	20-24
191	C3H5(A)+ C2H5 = C2H4 + C3H6	0.4000E+09	0	0.0000E+00	20-24
192	C3H5(A)+ C3H5(A)= C3H4(A) + C3H6	0.1000E+10	0	0.0000E+00	20-24
193	C3H5(S) + H = C3H4(A) + H2	0.3333E+10	0	0.0000E+00	20-24
194	C3H5(S) + O2 = CH3 + CO + CH2O	0.4335E+10	0	0.0000E+00	20-24
195	C3H5(S) + CH3 = C3H4(A) + CH4	0.1000E+09	0	0.0000E+00	20-24
196	C3H5(T)+ H = C3H4(P) + H2	0.3333E+10	0	0.0000E+00	20-24
197	C3H5(T)+ O2 = CH3 + CO + CH2O	0.4335E+10	0	0.0000E+00	20-24
198	C3H5(T)+ CH3 = C3H4(P) + CH4	0.1000E+09	0	0.0000E+00	20-24
199	C3H6 = C3H5(A) + H	0.2500E+16	0	0.3627E+06	20-24
200	C3H6 = C2H3 + CH3	0.1100E+22	1.2	0.4088E+06	20-24
201	C3H6 + H = C3H5(A) + H2	0.0864E+03	2.5	0.1043E+05	20-24
202	C3H6 + H = C3H5(S) + H2	0.2048E+03	2.5	0.4098E+05	20-24
203	C3H6 + H = C3H5(T) + H2	0.4018E+03	2.5	0.5139E+05	20-24
204	C3H6 + O = C2H5 + CHO	0.5217E+05	1.57	0.2629E+04	20-24
205	C3H6 + O = C2H4 + CH2O	0.3484E+05	1.57	0.2629E+04	20-24
206	C3H6 + O = CH3 + CH3 + CO	0.6960E+05	1.57	0.2629E+04	20-24
207	C3H6 + OH = C3H5(A) + H2O	0.3120E+04	2	0.1247E+04	20-24
208	C3H6 + OH = C3H5(S) + H2O	0.1110E+04	2	0.6069E+04	20-24
209	C3H6 + OH = C3H5(T) + H2O	0.2138E+04	2	0.1162E+05	20-24
210	C3H6 + O2 = C3H5(A) + HO2	0.1950E+11	0	0.1633E+06	20-24
211	C3H6 + O2 = C3H5(S) + HO2	0.2000E+11	0	0.1993E+06	20-24
212	C3H6 + O2 = C3H5(T) + HO2	0.2000E+11	0	0.1842E+06	20-24
213	C3H6 + CH3 = C3H5(A) + CH4	0.1600E+09	0	0.3680E+05	20-24
214	C3H6 + CH3 = C3H5(S) + CH4	0.3300E+09	0	0.4233E+05	20-24
215	C3H6 + CH3 = C3H5(T) + CH4	0.5000E+08	0	0.3362E+05	20-24
216	C3H7(N)+ H = C3H8	0.2000E+11	0	0.0000E+00	20-24

TABLE A1 (CONTINUED)

217	C3H7(N) + O2 = C3H6 + HO2	0.1000E+10	0	0.2091E+05	20-24
218	C3H7(N) = C2H4 + CH3	0.3000E+15	0	0.1390E+06	20-24
219	C3H7(N) = C3H6 + H	0.1000E+15	0	0.1549E+06	20-24
220	C3H7(I) + H = C3H8	0.2000E+11	0	0.0000E+00	20-24
221	C3H7(I) + O2 = C3H6 + HO2	0.1000E+10	0	0.1250E+05	20-24
222	C3H7(I) = C2H4 + CH3	0.1000E+11	0	0.1235E+06	20-24
223	C3H7(I) = C3H6 + H	0.6000E+14	0	0.1620E+06	20-24
224	C3H8 = C2H5 + CH3	0.2500E+16	0	0.3500E+06	20-24
225	C3H8 + H = C3H7(N) + H2	0.7500E+11	0	0.3350E+05	20-24
226	C3H8 + H = C3H7(I) + H2	0.3100E+11	0	0.3350E+05	20-24
227	C3H8 + O = C3H7(N) + OH	0.3000E+11	0	0.2410E+05	20-24
228	C3H8 + O = C3H7(I) + OH	0.2600E+11	0	0.1870E+05	20-24
229	C3H8 + OH = C3H7(N) + H2O	0.5754E+06	1.4	0.3558E+04	20-24
230	C3H8 + OH = C3H7(I) + H2O	0.4786E+06	1.4	0.3558E+04	20-24
231	C3H8 + CH3 = C3H7(N) + CH4	0.9033E-03	3.65	0.2990E+05	20-24
232	C3H8 + CH3 = C3H7(I) + CH4	0.1505E-02	3.46	0.2290E+05	20-24
233	C2H2 + C2H2 = C4H4	0.1513E+03	0	0.2303E+05	20-24
234	C2H2 + C2H = C4H2 + H	0.0400E+12	0	0.0000E+00	20-24
235	C3H2 + CH2(T) = C4H3(I) + H	0.3000E+11	0	0.0000E+00	20-24
236	C3H3 + CH = C4H3(N) + H	0.7000E+11	0	0.0000E+00	20-24
237	C3H3 + CH = C4H3(I) + H	0.7000E+11	0	0.0000E+00	20-24
238	C3H3 + CH2(T) = C4H4 + H	0.4000E+11	0	0.0000E+00	20-24
239	C3H3 + C3H3 = C6H5L + H	0.3000E+11	0	0.0000E+00	20-24
240	C3H3 + C3H4(A) = C6H6 + H	0.2200E+09	0	0.8370E+04	20-24
241	C4 + H + M = C4H + M	0.1738E+32	5.5	0.0000E+00	20-24
242	C4H + H2 = C4H2 + H	0.4074E+03	2.4	0.8400E+03	20-24
243	C4H + C2H2 = C6H2 + H	0.1200E+12	0	0.0000E+00	20-24
244	C4H + C4H2 = C8H2 + H	0.1200E+12	0	0.0000E+00	20-24
245	C4H2 = C4H + H	0.7800E+15	0	0.5024E+06	20-24
246	C4H2 + C2H = C6H2 + H	0.1200E+12	0	0.0000E+00	20-24
247	C4H2 + C2H = C4H + C2H2	0.1000E+11	0	0.0000E+00	20-24
248	C4H2 + O = C3H2 + CO	0.1200E+10	0	0.0000E+00	20-24
249	C4H2 + OH = C3H2 + CHO	0.6600E+10	0	0.1716E+04	20-24
250	C4H3(N) = C4H2 + H	0.1000E+15	0	0.1507E+06	20-24
251	C4H3(N) + H = C4H2 + H2	0.5000E+11	0	0.0000E+00	20-24
252	C4H3(N) + OH = C4H2 + H2O	0.3000E+11	0	0.0000E+00	20-24
253	C4H3(N) + M = C4H3(I) + M	0.1000E+12	0	0.0000E+00	20-24
254	C4H3(I) = C4H2 + H	0.1000E+15	0	0.2303E+06	20-24
255	C4H3(I) + H = C4H2 + H2	0.5000E+11	0	0.0000E+00	20-24
256	C4H3(I) + O = C2H2O + C2H	0.2000E+11	0	0.0000E+00	20-24
257	C4H3(I) + OH = C4H2 + H2O	0.3000E+11	0	0.0000E+00	20-24
258	C4H3(I) + O2 = C2H2O + C2HO	0.1000E+10	0	0.0000E+00	20-24
259	C4H4 = C4H3(I) + H	0.1580E+16	0	0.4142E+06	20-24
260	C4H4 = C4H2 + H2	0.8300E+09	0	0.1901E+06	20-24
261	C4H4 + H = C4H3(N) + H2	0.2000E+05	2	0.6276E+05	20-24
262	C4H4 + H = C4H3(I) + H2	0.7500E+04	2	0.2092E+05	20-24
263	C4H4 + OH = C4H3(N) + H2O	0.2500E+04	2	0.2092E+05	20-24
264	C4H4 + OH = C4H3(I) + H2O	0.2500E+04	2	0.8360E+04	20-24
265	C4H4 + C2H = C4H3(I) + C2H2	0.3980E+11	0	0.0000E+00	20-24
266	C4H4 + C2H2 = C6H5L + H	0.1000E+07	0	0.1255E+06	20-24
267	C4H4 + C2H3 = C6H6 + H	0.3000E+09	0	0.1256E+05	20-24
268	C4H5(S) = C4H4 + H	0.1000E+15	0	0.2092E+06	20-24
269	C4H5(S) + H = C4H4 + H2	0.3000E+05	2	0.4180E+04	20-24
270	C4H5(S) + OH = C4H4 + H2O	0.2000E+05	2	0.4180E+04	20-24
271	C4H5(S) = C4H5(T)	0.1500E+14	0	0.2835E+06	20-24

TABLE A1 (CONTINUED)

272	C4H5(T)	= C4H4 + H	0.1000E+15	0	0.1549E+06	20-24
273	C4H5(T)	= C2H2 + C2H3	0.1000E+15	0	0.1837E+06	20-24
274	C4H5(T) + H	= C4H4 + H2	0.3000E+05	2	0.4180E+04	20-24
275	C4H5(T) + OH	= C4H4 + H2O	0.2000E+05	2	0.4180E+04	20-24
276	C4H5(T) + M	= C4H5(I) + M	0.1000E+12	0	0.0000E+00	20-24
277	C4H5(I)	= C4H4 + H	0.1000E+15	0	0.2093E+06	20-24
278	C4H5(I) + H	= C4H4 + H2	0.6800E+05	2	0.4180E+04	20-24
279	C4H5(I) + OH	= C4H4 + H2O	0.4000E+05	2	0.4180E+04	20-24
280	C3H3 + CH3	= C4H6(S)	0.5000E+10	0	0.0000E+00	20-24
281	C4H6(S) + H	= C4H5(S) + H2	0.3000E+05	2	0.2512E+05	20-24
282	C4H6(S) + H	= C4H5(I) + H2	0.3000E+05	2	0.2512E+05	20-24
283	C4H6(S) + H	= C2H3 + C2H4	0.4000E+09	0	0.0000E+00	20-24
284	C4H6(S) + OH	= C4H5(S) + H2O	0.2000E+05	2	0.8373E+04	20-24
285	C4H6(S) + OH	= C4H5(I) + H2O	0.2000E+05	2	0.8373E+04	20-24
286	C4H6(S) + CH3	= C4H5(S) + CH4	0.7000E+11	0	0.7746E+05	20-24
287	C4H6(S)	= C4H6(T)	0.1500E+14	0	0.2835E+06	20-24
288	C4H6(T)	= C4H5(T) + H	0.1585E+17	0	0.4606E+06	20-24
289	C4H6(T)	= C4H5(I) + H	0.3500E+16	0	0.4355E+06	20-24
290	C2H3 + C2H3	= C4H6(T)	0.1000E+11	0	0.0000E+00	20-24
291	C4H6(T) + H	= C4H5(T) + H2	0.3000E+05	2	0.5439E+05	20-24
292	C4H6(T) + H	= C4H5(I) + H2	0.3000E+05	2	0.2510E+05	20-24
293	C4H6(T) + H	= C2H3 + C2H4	0.5000E+09	0	0.0000E+00	20-24
294	C4H6(T) + O	= C4H6O	0.6300E+06	1.45	0.3592E+04	20-24
295	C4H6(T) + OH	= C4H5(T) + H2O	0.2000E+05	2	0.2092E+05	20-24
296	C4H6(T) + OH	= C4H5(I) + H2O	0.2000E+05	2	0.8360E+04	20-24
297	C4H6(T) + O2	= C4H5(T) + HO2	0.4000E+11	0	0.2420E+06	20-24
298	C4H6(T) + C2H3	= C4H5(T) + C2H4	0.6310E+11	0	0.6070E+05	20-24
299	C4H6(T) + C2H3	= C4H5(I) + C2H4	0.2000E+11	0	0.6070E+05	20-24
300	C4H6(T) + CH3	= C4H5(T) + CH4	0.7000E+11	0	0.7746E+05	20-24
301	C4H6(T) + C3H3	= C4H5(T) + C3H4(A)	0.1000E+11	0	0.9420E+05	20-24
302	CH2(S) + C3H4(P)	= C4H6(B)	0.2000E+12	0	0.0000E+00	20-24
303	C4H6(B)	= C4H6(T)	0.6000E+14	0	0.1770E+06	20-24
304	C4H6(B)	= C4H6(S)	0.6000E+14	0	0.1830E+06	20-24
305	C4H6(S)	= C4H6(F)	0.0000E+14	0	0.2700E+06	20-24
306	C3H3 + CH3	= C4H6(F)	0.0000E+10	0	0.0000E+00	20-24
307	C4H6(F) + O	= C3H6 + CO	0.0000E+11	0	0.6860E+04	20-24
308	C4H6O	= C3H6 + CO	0.4000E+16	0	0.3180E+06	20-24
309	C4H6O + H	= C3H6 + CHO	0.1500E+14	0	0.3180E+06	20-24
310	C6H5	= C4H3(N) + C2H2	0.4500E+14	0	0.30350+06	20-24
311	C6H5L	= C4H3(N) + C2H2	0.3160E+14	0	0.1800E+06	20-24
312	C4H5(T) + C2H2	= C6H6 + H	0.1900E+05	1.47	0.2056E+05	20-24
313	C6H2 + H	= C6H3	0.5500E+10	0	0.1000E+05	20-24
314	C6H3 + H	= C6H2 + H2	0.2000E+11	0	0.0000E+00	20-24
315	C6H3 + H	= C6H4	0.2000E+11	0	0.0000E+00	20-24
316	C6H4 + H	= C6H3 + H2	0.1500E+12	0	0.4270E+05	20-24
317	C6H4 + H	= C6H5	0.0000E+00	0	0.1000E+05	20-24
318	C6H4 + OH	= C6H3 + H2O	0.7000E+11	0	0.1260E+05	20-24
319	C6H5 + H	= C6H4 + H2	0.0000E+00	0	0.0000E+00	20-24
320	C6H5 + O2	= C6H5O + O	0.5000E+10	0	0.3127E+05	20-24
321	C6H5 + OH	= C6H5O + H	0.5000E+11	0	0.0000E+00	20-24
322	C6H5L	= C6H5	0.1000E+11	0	0.0000E+00	20-24
323	C6H5L	= C6H4 + H	0.6000E+13	0	0.1527E+06	20-24
324	C6H6	= C6H5 + H	0.1300E+17	0	0.4756E+06	20-24
325	C6H6 + H	= C6H5 + H2	0.2500E+12	0	0.6694E+05	20-24
326	C6H6 + O	= C6H5O + H	0.2000E+11	0	0.2050E+05	20-24

TABLE A1 (CONTINUED)

327	C6H6 + O = C6H5 + OH	0.0000E+11	0	0.6152E+05	20-24
328	C6H6 + OH = C6H5 + H2O	0.1630E+06	1.42	0.6069E+04	20-24
329	C6H6 + O2 = C6H5O + OH	0.4000E+11	0	0.1424E+06	20-24
330	C6H6 + CH3 = C6H5 + CH4	0.2000E+10	0	0.6300E+05	20-24
331	C6H5OH = C6H5O + H	0.2000E+17	0	0.3684E+06	20-24
332	C6H6 + OH = C6H5OH + H	0.1320E+11	0	0.4432E+05	20-24
333	C6H5OH + H = C6H5O + H2	0.1150E+12	0	0.5192E+05	20-24
334	C6H5OH + O = C6H5O + OH	0.2810E+11	0	0.3078E+05	20-24
335	C6H5OH + OH = C6H5O + H2O	0.6000E+10	0	0.0000E+00	20-24
336	C6H5O = C5H5 + CO	0.2510E+12	0	0.1837E+06	20-24
337	C6H5OH = C5H6 + CO	0.2670E+14	0	0.3716E+06	20-24
338	C5H5 + H = C5H6	0.6000E+11	0	0.0000E+00	20-24
339	C5H5 + O = C4H5(T) + CO	0.4000E+12	0	0.0000E+00	20-24
340	C5H5 + O = C5H5O	0.1000E+11	0	0.0000E+00	20-24
341	C5H5 + OH = C5H4OH + H	0.3000E+11	0	0.0000E+00	20-24
342	C5H5 + HO2 = C5H5O + OH	0.3000E+11	0	0.0000E+00	20-24
343	C5H6 + O = C5H5 + OH	0.1810E+11	0	0.1287E+05	20-24
344	C5H6 + OH = C5H5 + H2O	0.3430E+07	1.18	0.1870E+04	20-24
345	C5H6 + O2 = C5H5 + HO2	0.2000E+11	0	0.1046E+06	20-24
346	C5H6 + H = C5H5 + H2	0.2190E+06	1.77	0.1255E+05	20-24
347	C5H6 + HO2 = C5H5 + H2O2	0.2000E+10	0	0.4878E+05	20-24
348	C5H5O = C4H5(T) + CO	0.2510E+09	0	0.1837E+06	20-24
349	C5H4OH = C5H4O + H	0.2100E+11	0	0.2008E+06	20-24
350	C5H5 = C5H5(L)	0.5000E+14	0	0.3340E+06	20-24
351	C3H3 + C2H2 = C5H5(L)	0.8000E+08	0.41	0.1686E+05	20-24
352	C5H5(L) + H = C5H6(L)	0.1000E+11	0	0.0000E+00	20-24
353	C5H5(L) + H2 = C5H6(L) + H	0.1000E+11	0	0.0000E+00	20-24
354	C5H6(L) + O = C5H5(L) + OH	0.1000E+11	0	0.0000E+00	20-24
355	C5H6(L) + OH = C5H5(L) + H2O	0.3000E+11	0	0.0000E+00	20-24
356	C5H6(L) + O2 = C5H5(L) + HO2	0.8000E+10	0	0.1495E+06	20-24
357	C5H6 = C5H6(L)	0.0000E+14	0	0.2008E+06	20-24
358	C5H6(L) = C3H3 + C2H3	0.0000E+14	0	0.4810E+06	20-24
359	C6H5L + H = C3H4(A) + C3H2	0.1000E+11	0	0.0000E+00	20-24
360	C5H5(L) = C3H4(A) + C2H	0.0000E+14	0	0.3108E+06	20-24
361	CH2(T) + C4H2 = C5H3(L) + H	0.1300E+10	0	0.1810E+05	20-24
362	CH2(S) + C4H2 = C5H3(L) + H	0.3000E+10	0	0.0000E+00	20-24
363	C5H5(L) + H = C5H4(L) + H2	0.3000E+11	0	0.0000E+00	20-24
364	C5H5(L) + OH = C5H4(L) + H2O	0.1000E+11	0	0.0000E+00	20-24
365	C5H4(L) + H = C5H3(L) + H2	0.6000E+11	0	0.0000E+00	20-24
366	C5H4(L) + OH = C5H3(L) + H2O	0.2000E+11	0	0.8368E+05	20-24
367	C2H2 + C2H2 = C4H3(N) + H	0.1000E+11	0	0.2805E+06	20-24
368	C2H2 + C2H2 = C4H3(I) + H	0.1513E+12	0	0.2345E+06	20-24
369	C2H2 + C2H2 = C4H2 + H2	0.1513E+11	0	0.1788E+06	20-24
370	C5H4O = CO + C4H4	0.1000E+16	0	0.3266E+06	20-24
371	C6H5L + H = C6H4 + H2	0.6000E+11	0	0.0000E+00	20-24
372	C6H5L + OH = C6H4 + H2O	0.3000E+11	0	0.0000E+00	20-24
373	C5H6 + O2 = C5H5O + OH	0.1000E+11	0	0.8666E+05	20-24
374	C5H3(L) + O = C4H3(N) + CO	0.0000E+11	0	0.0000E+00	20-24
375	C2H3 + O2 = C2H2 + HO2	0.6610E+19	3.28	0.2264E+05	20-24
376	C4H6(S) = C4H5(S) + H	0.3000E+16	0	0.3599E+06	20-24
377	C4H6(S) = C4H5(I) + H	0.7000E+15	0	0.3871E+06	20-24
378	1-C4H7 = C4H6(T) + H	0.1200E+15	0	0.2064E+06	31
379	1-C4H7 = C2H4 + C2H3	0.1000E+12	0	0.1549E+06	31
380	1-C4H7 + H = C4H6(T) + H2	0.3160E+11	0	0.0000E+00	31
381	1-C4H7 + O2 = C4H6(T) + HO2	0.1000E+09	0	0.0000E+00	31

TABLE A1 (CONTINUED)

382	1-C4H7 + CH3 = C4H6(T) + CH4	0.1000E+11	0	0.0000E+00	31
383	1-C4H7 + C2H3 = C4H6(T) + C2H4	0.4000E+10	0	0.0000E+00	31
384	1-C4H7 + C2H5 = C4H6(T) + C2H6	0.4000E+10	0	0.0000E+00	31
385	1-C4H7 + C2H5 = 1-C4H8 + C2H4	0.5000E+09	0	0.0000E+00	31
386	1-C4H7 + C3H5(A) = C4H6(T) + C3H6	0.4000E+11	0	0.0000E+00	31
387	1-C4H7 + 1-C4H7 = C4H6(T) + 1-C4H8	0.3160E+10	0	0.0000E+00	31
388	1-C4H8 = 1-C4H7 + H	0.4070E+19	-1	0.4073E+06	31
389	1-C4H8 = C3H5(A) + CH3	0.8000E+17	0	0.3096E+06	57
390	1-C4H8 + O2 = 1-C4H7 + HO2	0.4000E+10	0	0.1674E+06	57
391	1-C4H8 = C2H3 + C2H5	0.2000E+19	-1	0.4049E+06	57
392	1-C4H8 + H = 1-C4H7 + H2	0.5000E+11	0	0.1632E+05	31
393	1-C4H8 + OH = C3H7(N) + CH2O	0.6500E+10	0	0.0000E+00	57
394	1-C4H8 + OH = C2H6 + CH3 + CO	0.1000E+08	0	0.0000E+00	31
395	1-C4H8 + OH = 1-C4H7 + H2O	0.1750E+11	0	0.1280E+05	57
396	1-C4H8 + O = C2H5 + CH3 + CO	0.1625E+11	0	0.3556E+04	57
397	1-C4H8 + O = 1-C4H7 + OH	0.1300E+11	0	0.1883E+05	57
398	1-C4H8 + HO2 = 1-C4H7 + H2O2	0.1000E+09	0	0.7139E+05	57
399	1-C4H8 + CH3 = 1-C4H7 + CH4	0.1000E+09	0	0.3054E+05	31
400	1-C4H8 + C2H5 = 1-C4H7 + C2H6	0.1000E+09	0	0.3347E+05	57
401	1-C4H8 + C3H5(A) = 1-C4H7 + C3H6	0.8000E+08	0	0.5188E+05	57
402	P-C4H9 = C2H5 + C2H4	0.2511E+14	0	0.1205E+06	59
403	P-C4H9 = 1-C4H8 + H	0.1300E+14	0	0.1632E+06	59
404	P-C4H9 + O2 = 1-C4H8 + HO2	0.1000E+10	0	0.8368E+04	59
405	C5H9 = C3H5(A) + C2H4	0.2500E+14	0	0.1255E+06	62
406	C5H9 = C2H3 + C3H6	0.2500E+14	0	0.1255E+06	62
407	C5H9 = C4H6(S) + CH3	0.1000E+14	0	0.1339E+06	58
408	1-C5H10 = C2H5 + C3H5(A)	0.1000E+17	0	0.2989E+06	62
409	1-C5H11 = C3H7(N) + C2H4	0.3200E+14	0	0.1188E+06	62
410	C7H16 = C3H7(N) + P-C4H9	0.1300E+17	0	0.3428E+06	See text
411	C7H16 = C2H5 + 1-C5H11	0.6500E+16	0	0.3433E+06	See text
412	C7H16 = 1-C7H15 + H	0.1000E+16	0	0.4186E+06	32
413	C7H16 = 2-C7H15 + H	0.1000E+16	0	0.4186E+06	32
414	C7H16 = 3-C7H15 + H	0.1000E+16	0	0.4186E+06	32
415	C7H16 = 4-C7H15 + H	0.1000E+16	0	0.4186E+06	32
416	C7H16 + H = 1-C7H15 + H2	0.2810E+05	2	0.3223E+05	32
417	C7H16 + H = 2-C7H15 + H2	0.9100E+04	2	0.2093E+05	32
418	C7H16 + H = 3-C7H15 + H2	0.9100E+04	2	0.2093E+05	32
419	C7H16 + H = 4-C7H15 + H2	0.4500E+04	2	0.2093E+05	32
420	C7H16 + O = 1-C7H15 + OH	0.2300E+04	2.4	0.6656E+04	32
421	C7H16 + O = 2-C7H15 + OH	0.6400E+03	2.5	0.2093E+05	32
422	C7H16 + O = 3-C7H15 + OH	0.6400E+03	2.5	0.2093E+05	32
423	C7H16 + O = 4-C7H15 + OH	0.3200E+03	2.5	0.2093E+05	32
424	C7H16 + OH = 1-C7H15 + H2O	0.1050E+08	0.97	0.6656E+04	32
425	C7H16 + OH = 2-C7H15 + H2O	0.4700E+05	1.61	0.0000E+00	32
426	C7H16 + OH = 3-C7H15 + H2O	0.4700E+05	1.61	0.0000E+00	32
427	C7H16 + OH = 4-C7H15 + H2O	0.4700E+05	1.61	0.0000E+00	32
428	C7H16 + CH3 = 1-C7H15 + CH4	0.3000E+10	0	0.4856E+05	32
429	C7H16 + CH3 = 2-C7H15 + CH4	0.1600E+10	0	0.3977E+05	32
430	C7H16 + CH3 = 3-C7H15 + CH4	0.1600E+10	0	0.3977E+05	32
431	C7H16 + CH3 = 4-C7H15 + CH4	0.8000E+09	0	0.3977E+05	32
432	C7H16 + HO2 = 1-C7H15 + H2O2	0.1120E+11	0	0.8121E+05	32
433	C7H16 + HO2 = 2-C7H15 + H2O2	0.6800E+10	0	0.7116E+05	32
434	C7H16 + HO2 = 3-C7H15 + H2O2	0.6800E+10	0	0.7116E+05	32
435	C7H16 + HO2 = 4-C7H15 + H2O2	0.3420E+10	0	0.7116E+05	32
436	C7H16 + C2H5 = 1-C7H15 + C2H6	0.1000E+09	0	0.5609E+05	32

TABLE A1 (CONCLUDED)

437	C7H16 + C2H5 = 2-C7H15 + C2H6	0.1000E+09	0	0.4353E+05	32
438	C7H16 + C2H5 = 3-C7H15 + C2H6	0.1000E+09	0	0.4353E+05	32
439	C7H16 + C2H5 = 4-C7H15 + C2H6	0.5010E+08	0	0.4353E+05	32
440	C7H16 + C2H3 = 1-C7H15 + C2H4	0.1000E+10	0	0.7535E+05	32
441	C7H16 + C2H3 = 2-C7H15 + C2H4	0.7940E+09	0	0.7033E+05	32
442	C7H16 + C2H3 = 3-C7H15 + C2H4	0.7940E+09	0	0.7033E+05	32
443	C7H16 + C2H3 = 4-C7H15 + C2H4	0.3980E+09	0	0.7033E+05	32
444	C3H5(A) + C7H16 = 1-C7H15 + C3H6	0.3980E+09	0	0.7870E+05	32
445	C3H5(A) + C7H16 = 2-C7H15 + C3H6	0.8000E+09	0	0.7033E+05	32
446	C3H5(A) + C7H16 = 3-C7H15 + C3H6	0.8000E+09	0	0.7033E+05	32
447	C3H5(A) + C7H16 = 4-C7H15 + C3H6	0.4000E+09	0	0.7033E+05	32
448	C7H16 + O2 = 1-C7H15 + HO2	0.2510E+11	0	0.2051E+06	32
449	C7H16 + O2 = 2-C7H15 + HO2	0.3980E+11	0	0.1993E+06	32
450	C7H16 + O2 = 3-C7H15 + HO2	0.4000E+11	0	0.1993E+06	32
451	C7H16 + O2 = 4-C7H15 + HO2	0.2000E+11	0	0.1993E+06	32
452	1-C7H15 = C2H4 + 1-C5H11	0.2520E+14	0	0.1206E+06	32
453	2-C7H15 = C3H6 + P-C4H9	0.1600E+14	0	0.1185E+06	32
454	3-C7H15 = C3H7(N) + 1-C4H8	0.5000E+13	0	0.1218E+06	32
455	4-C7H15 = 1-C5H10 + C2H5	0.1080E+14	0	0.1172E+06	32
456	1-C7H15 = 1-C7H14 + H	0.1000E+14	0	0.1691E+06	32
457	2-C7H15 = 1-C7H14 + H	0.1000E+14	0	0.1691E+06	32
458	2-C7H15 = 2-C7H14 + H	0.1000E+14	0	0.1691E+06	32
459	3-C7H15 = 2-C7H14 + H	0.1000E+14	0	0.1691E+06	32
460	3-C7H15 = 3-C7H14 + H	0.1000E+14	0	0.1691E+06	32
461	4-C7H15 = 3-C7H14 + H	0.1000E+14	0	0.1691E+06	32
462	1-C7H15 = 2-C7H15	0.2000E+12	0	0.4647E+05	32
463	1-C7H15 = 3-C7H15	0.2000E+12	0	0.7577E+05	32
464	1-C7H15 = 4-C7H15	0.1000E+12	0	0.8372E+05	32
465	2-C7H15 = 3-C7H15	0.2000E+12	0	0.8372E+05	32
466	1-C7H15 + O2 = 1-C7H14 + HO2	0.1000E+10	0	0.8372E+04	32
467	2-C7H15 + O2 = 1-C7H14 + HO2	0.1000E+10	0	0.1884E+05	32
468	2-C7H15 + O2 = 2-C7H14 + HO2	0.2000E+10	0	0.1779E+05	32
469	3-C7H15 + O2 = 2-C7H14 + HO2	0.2000E+10	0	0.1779E+05	32
470	3-C7H15 + O2 = 3-C7H14 + HO2	0.2000E+10	0	0.1779E+05	32
471	4-C7H15 + O2 = 3-C7H14 + HO2	0.4000E+10	0	0.1779E+05	32
472	1-C7H14 = C3H5(A) + P-C4H9	0.2520E+17	0	0.2976E+06	32
473	2-C7H14 = C3H7(N) + 1-C4H7	0.1600E+17	0	0.2901E+06	32
474	3-C7H14 = C2H5 + C5H9	0.3600E+16	0	0.2972E+06	32
475†C6H6	= 6C(S) + 3H2	0.7500E+05	0	0.1715E+06	20-24
476†C2H2	= 2-C(S) + H2	0.1000E-11	0	0.1008E+06	20-24
477†C6H6	= 6C(S) + 3H2	0.1000E-11	0	0.1008E+06	20-24
478†C(S) + OH = CO + H		0.1750E+01	0.5	0.0000E+00	20-24
479†C(S) + O = CO		0.1600E+02	0.5	0.9312E+05	20-24
480†C(S) + C(S) +O2 = CO + CO		0.4650E+01	0.5	0.9353E+05	20-24
481†C(S) + H2O = CO + H2		0.2860E-30	0.5	0.6094E+05	20-24

† These reactions are specific to the soot model.

Reaction rates are expressed in the form $K_j=AT^n\exp(-E/RT)$

TABLE A2

Collision Efficiencies for *n*-Heptane Mechanism for Diffusion Flames

ELEMENTARY REACTION NUMBER	M=SPECIE	COLLISION EFFICIENCY
5, 16, 21, 22, 25, 42	H2	2.5
	CO	1.9
	CO2	3.8
	H2O	12.0
	OTHER	1.0
17	H2	0.0
	CO2	0.0
	H2O	0.0
	OTHER	1.0
18	H2	1.0
	OTHER	0
19	H2O	1.0
	OTHER	0.0
20	CO2	1.0
	OTHER	0
56	H	20
	H2O	3
	OTHER	1.0
81, 103, 148, 149	H2	1.1
	N2	1.6
	O2	1.9
	CO	1.9
	CO2	3.3
	H2O	5.7
	OTHER	1.0
139	H2	2.0
	CO	2.0
	CO2	3.0
	H2O	5.0
	OTHER	1.0
253, 273	H	1.0
	OTHER	0.0

TABLE A3
Modifications to *n*-Heptane Sub-mechanism for Stirred Reactors

ELEMENTARY REACTION									A m^3, Kmol, sec^{-1}	n	E_a J/mol	REF
412†	C7H16			=	1-C6H13	+	CH3		0.6600E+17	0	0.3558E+06	32
449	C7H16	+	1-C4H7	=	1-C7H15	+	1-C4H8		0.1000E+10	0	0.8372E+05	32
450	C7H16	+	1-C4H7	=	2-C7H15	+	1-C4H8		0.1580E+09	0	0.7953E+05	32
451	C7H16	+	1-C4H7	=	3-C7H15	+	1-C4H8		0.1580E+09	0	0.7953E+05	32
452	C7H16	+	1-C4H7	=	4-C7H15	+	1-C4H8		0.8000E+08	0	0.7953E+05	32
453	C7H16	+	CH3O	=	1-C7H15	+	CH3OH		0.3160E+09	0	0.2930E+05	32
454	C7H16	+	CH3O	=	2-C7H15	+	CH3OH		0.2190E+10	0	0.2093E+05	32
454	C7H16	+	CH3O	=	3-C7H15	+	CH3OH		0.2190E+10	0	0.2093E+05	32
456	C7H16	+	CH3O	=	4-C7H15	+	CH3OH		0.1090E+09	0	0.2093E+05	32
464	3-C7H15			=	C6H12	+	CH3		0.8000E+13	0	0.1381E+06	32
485	3-C7H14			=	C6H11	+	CH3		0.5300E+17	0	0.3056E+06	32
486	1-C7H14	+	H	=	C7H13	+	H2		0.8000E+11	0	0.1423E+05	32
487	2-C7H14	+	H	=	C7H13	+	H2		0.1600E+12	0	0.1423E+05	32
488	3-C7H14	+	H	=	C7H13	+	H2		0.1600E+12	0	0.1423E+05	32
489	1-C7H14	+	O	=	C7H13	+	OH		0.4000E+11	0	0.1674E+05	32
490	2-C7H14	+	O	=	C7H13	+	OH		0.8000E+11	0	0.1674E+05	32
491	3-C7H14	+	O	=	C7H13	+	OH		0.8000E+11	0	0.1674E+05	32
492	1-C7H14	+	OH	=	C7H13	+	H2O		0.2000E+11	0	0.1088E+05	32
493	2-C7H14	+	OH	=	C7H13	+	H2O		0.4000E+11	0	0.1088E+05	32
494	3-C7H14	+	OH	=	C7H13	+	H2O		0.4000E+11	0	0.1088E+05	32
495	1-C7H14	+	CH3	=	C7H13	+	CH4		0.2000E+09	0	0.2847E+05	32
496	2-C7H14	+	CH3	=	C7H13	+	CH4		0.4000E+09	0	0.2847E+05	32
497	3-C7H14	+	CH3	=	C7H13	+	CH4		0.4080E+09	0	0.2847E+05	32
498	1-C7H14	+	HO2	=	C7H13	+	H2O2		0.5000E+10	0	0.0000E+00	32
499	2-C7H14	+	HO2	=	C7H13	+	H2O2		0.5000E+10	0	0.0000E+00	32
500	3-C7H14	+	HO2	=	C7H13	+	H2O2		0.5000E+10	0	0.0000E+00	32
501	1-C7H14	+	O	=	C2H3	+	1-C5H10	+ OH	0.2820E+11	0	0.2177E+05	32
502	1-C7H14	+	O	=	C3H5(A)	+	1-C4H8	+ OH	0.2820E+11	0	0.2177E+05	32
503	1-C7H14	+	O	=	1-C4H7	+	C3H6	+ OH	0.2820E+11	0	0.2177E+05	32
504	1-C7H14	+	O	=	C5H9	+	C2H4	+ OH	0.5000E+11	0	0.3286E+05	32
505	2-C7H14	+	O	=	C3H5(T)	+	1-C4H8	+ OH	0.2820E+11	0	0.2177E+05	32
506	2-C7H14	+	O	=	1-C4H7	+	C3H6	+ OH	0.2820E+11	0	0.2177E+05	32
507	2-C7H14	+	O	=	C5H9	+	C2H4	+ OH	0.5000E+11	0	0.3286E+05	32
508	3-C7H14	+	O	=	1-C4H7	+	C3H6	+ OH	0.2820E+11	0	0.2177E+05	32
509	3-C7H14	+	O	=	C5H9	+	C2H4	+ OH	0.5000E+11	0	0.3286E+05	32
510	1-C7H14	+	OH	=	C2H3	+	1-C5H10	+ H2O	0.1290E+07	1.25	0.2930E+04	32
511	1-C7H14	+	OH	=	C3H5(A)	+	1-C4H8	+ H2O	0.1290E+07	1.25	0.2930E+04	32
512	1-C7H14	+	OH	=	1-C4H7	+	C3H6	+ H2O	0.1290E+07	1.25	0.2930E+04	32
513	1-C7H14	+	OH	=	C5H9	+	C2H4	+ H2O	0.4270E+07	1.05	0.7577E+04	32
514	2-C7H14	+	OH	=	C3H5(A)	+	1-C4H8	+ H2O	0.1160E+07	1.25	0.2930E+04	32
515	2-C7H14	+	OH	=	1-C4H7	+	C3H6	+ H2O	0.1160E+07	1.25	0.2930E+04	32
516	2-C7H14	+	OH	=	C5H9	+	C2H4	+ H2O	0.4270E+07	1.05	0.7577E+04	32
517	3-C7H14	+	OH	=	1-C4H7	+	C3H6	+ H2O	0.1160E+07	1.25	0.2930E+04	32
518	3-C7H14	+	OH	=	C5H9	+	C2H4	+ H2O	0.4270E+07	1.05	0.2930E+04	32
519	C7H13			=	C3H5(A)	+	1-C4H8		0.2520E+14	0	0.1256E+06	32
520	C7H13			=	C3H4(A)	+	P-C4H9		0.1000E+14	0	0.1256E+06	32
521	C7H13			=	C4H6(S)	+	C3H7(N)		0.1000E+14	0	0.1340E+06	32
522†	1-C6H13			=	2-C6H13				0.2000E+12	0	0.7577E+05	32
523†	1-C6H13			=	C2H4	+	P-C4H9		0.2520E+14	0	0.1206E+06	32
524†	2-C6H13			=	C3H7(N)	+	C3H6		0.1600E+14	0	0.1185E+06	32
525	1-C6H12			=	C3H7(N)	+	C3H5(A)		0.7940E+15	0	0.2976E+06	74
526	1-C6H12			=	C3H6	+	C3H6		0.3980E+13	0	0.2414E+06	74

TABLE A3 (CONCLUDED)

527	1-C6H12	+	H	=	C6H11	+	H2			0.8020E+11	0	0.1423E+05	32
528	1-C6H12	+	O	=	C6H11	+	OH			0.4000E+11	0	0.1674E+05	32
529	1-C6H12	+	OH	=	C6H11	+	H2O			0.2000E+11	0	0.1088E+05	32
530	1-C6H12	+	CH3	=	C6H11	+	CH4			0.2000E+09	0	0.2846E+05	32
531	1-C6H12	+	HO2	=	C6H11	+	H2O2			0.1000E+09	0	0.7141E+05	32
532	1-C6H12	+	O	=	C2H3	+	1-C4H8	+	OH	0.2820E+11	0	0.2177E+05	32
533	1-C6H12	+	O	=	C3H5(A)	+	C3H6	+	OH	0.2820E+11	0	0.2177E+05	32
534	1-C6H12	+	O	=	1-C4H7	+	C2H4	+	OH	0.5010E+11	0	0.3286E+05	32
535	1-C6H12	+	O	=	CHO	+	1-C5H11			0.1000E+09	0	0.0000E+00	32
536	1-C6H12	+	O	=	CH3	+	P-C4H9	+	CO	0.1000E+09	0	0.0000E+00	32
537	1-C6H12	+	OH	=	C2H3	+	1-C4H8	+	H2O	0.6500E+07	1.25	0.2930E+04	32
538	1-C6H12	+	OH	=	C3H5(A)	+	C3H6	+	H_2O	0.6500E+07	1.25	0.2930E+04	32
539	1-C6H12	+	OH	=	1-C4H7	+	C2H4	+	H_2O	0.2150E+08	1.05	0.7577E+04	32
540	1-C6H12	+	OH	=	CH_2O	+	1-C5H11			0.1000E+09	0	0.0000E+00	32
541	1-C6H12	+	OH	=	C2H4O	+	P-C4H9			0.1000E+09	0	0.0000E+00	32
542	1-C6H11			=	C_3H_6	+	C_3H_5(A)			0.5040E+14	0	0.1256E+06	32
543	1-C6H11			=	C_2H_5	+	C_4H_6(T)			0.5000E+13	0	0.1340E+06	32
544	1-C5H11			=	1-C5H10	+	H			0.1300E+14	0	0.1615E+06	75
545	1-C5H10	+	H	=	C5H9	+	H2			0.2800E+11	0	0.1674E+01	61
546	1-C5H10	+	O	=	C5H9	+	OH			0.2540E+03	2.56	-0.4730E+01	61
547	1-C5H10	+	O	=	P-C4H9	+	CHO			0.1000E+09	0	0.0000E+00	61
548	1-C5H10		+ O	=	C3H7(N)	+	C2H3O			0.1000E+09	0	0.0000E+00	75
549	1-C5H10	+	O	=	1-C4H8	+	CH2O			0.8510E+09	0	0.0000E+00	76
550	1-C5H10	+	O	=	C2H4O	+	C3H6			0.8510E+10	0	0.0000E+00	76
551	1-C5H10	+	O	=	C3H5(A)	+	C2H4	+	OH	0.2000E+11	0	0.2930E+01	76
552	1-C5H10	+	O	=	C3H6	+	C2H3	+	OH	0.1000E+11	0	0.2930E+01	76
553	1-C5H10	+	OH	=	C5H9	+	H2O			0.6800E+11	0	0.1281E+01	75
554	1-C5H10	+	OH	=	P-C4H9	+	CH2O			0.1000E+09	0	0.0000E+00	75
555	1-C5H10	+	OH	=	C3H7(N)	+	C2H4O			0.1000E+09	0	0.0000E+00	75
556	1-C5H10	+	OH	=	C3H5(A)	+	C2H4	+	H2O	0.2000E+07	1.20	0.5023E+00	76
557	1-C5H10	+	OH	=	C3H6	+	C2H3	+	H2O	0.1000E+07	1.2	0.5023E+00	76
558	1-C5H10	+	O2	=	C5H9	+	HO2			0.4000E+10	0	0.1674E+03	76
559	1-C5H10	+	CH3	=	C5H9	+	CH4			0.1000E+09	0	0.3056E+02	75
560	1-C4H8	+	OH	=	C2H4O	+	C2H5			0.1000E+09	0	0.0000E+00	57
561	1-C4H8	+	O	=	C3H6	+	CH2O			0.2505E+10	0	0.0000E+00	57
562	1-C4H8	+	O	=	C2H4O	+	C2H4			0.1250E+11	0	0.3556E+04	57
563	C2H4O	+	M	=	CH3	+	CHO	+	M	0.7000E+13	0	0.3425E+06	31
564	C2H4O	+	H	=	C2H3O	+	H2			0.2100E+07	1.16	0.1009E+05	31
565	C2H4O	+	O	=	C2H3O	+	OH			0.5000E+10	0	0.7593E+04	31
566	C2H4O	+	O2	=	C2H3O	+	HO2			0.4000E+11	0	0.1641E+06	31
567	C2H4O	+	OH	=	C2H3O	+	H2O			0.2300E+08	0.73	-0.4698E+04	31
568	C2H4O	+	HO2	=	C2H3O	+	H2O2			0.3000E+10	0	0.4996E+05	31
569	C2H4O	+	CH2(T)	=	C2H3O	+	CH3			0.2500E+10	0	0.1589E+05	31
570	C2H4O	+	CH3	=	C2H3O	+	CH4			0.2000E-08	5.54	0.1029E+05	31
571	C2H3O			=	CH3	+	CO			0.2320E+27	-5	0.7505E+05	31
572	C2H3O	+	H	=	C2H2O	+	H2			0.2000E+11	0	0.0000E+00	31
573	C2H3O	+	CH3	=	C2H6	+	CO			0.5000E+11	0	0.0000E+00	31
574	C2H2O	+	O2	=	CH2O	+	CO2			0.1000E+07	0	0.0000E+00	77
575	CH3OH	+	HO2	=	CH3O	+	H2O2			0.6200E+10	0	0.8109E+05	31
576	CH3OH	+	OH	=	CH3O	+	H2O			0.1000E+11	0	0.7099E+04	31
577	CH3OH	+	O	=	CH3O	+	OH			0.1000E+11	0	0.1960E+05	31
578	CH3OH	+	CH2O	=	CH3O	+	CH3O			0.1530E+10	0	0.3331E+06	31
579	C3H8	+	C2H5	=	C3H7(N)	+	C2H6			0.3160E+09	0	0.5149E+05	78
580	CH2O	+	CH3O	=	CH3OH	+	CHO			0.6000E+09	0	0.1380E+05	31
581	CH2O	+	HO2	=	CHO	+	H2O2			0.2000E+10	0	0.4898E+05	79
582	CH2O	+	CH3	=	CHO	+	CH4			0.8913E-15	7.40	-0.4019E+04	77

† These reactions subsequently added to *n*-heptane mechanism for diffusion flames.

Reaction rates are expressed in the form $K_j=AT^n\exp(-E/RT)$

APPENDIX B
THERMOCHEMICAL AND PHYSICAL PROPERTIES FOR *n*-HEPTANE MECHANISM

TABLE B1
JANNAF Polynomials for *n*-Heptane Diffusion Flame Mechanism Species

C7H16				
0.17470044E+02	0.42134196E-01	-0.16429033E-04	0.29963565E-08	-0.20648765E-12
-0.31665823E+05	-0.64762071E+02	0.11153248E+02	-0.94941543E-02	0.19557118E-03
-0.24975252E-06	0.98487321E-10	-0.26753133E+05	-0.15922774E+02	REF 67
H				
0.25000000E+01	0.00000000E+00	0.00000000E+00	0.00000000E+00	0.00000000E+00
0.25471627E+05	-0.46011763E+00	0.25000000E+01	0.00000000E+00	0.00000000E+00
0.00000000E+00	0.00000000E+00	0.25471627E+05	-0.46011762E+00	REF 20
OH				
0.28827305E+01	0.10139743E-02	-0.22768771E-06	0.21746837E-10	-0.51263053E-15
0.38868879E+04	0.55957122E+01	0.36372659E+01	0.18509105E-03	-0.16761646E-05
0.23872027E-08	-0.84314418E-12	0.36067817E+04	0.13588605E+01	REF 20
O				
0.25420597E+01	-0.27550619E-04	-0.31028033E-08	0.45510674E-11	-0.43680515E-15
0.29230803E+05	0.49203081E+01	0.29464288E+01	-0.16381665E-02	0.24210317E-05
-0.16028432E-08	0.38906963E-12	0.29147644E+05	0.29639949E+01	REF 20
HO2				
0.40721912E+01	0.21312963E-02	-0.53081453E-06	0.61122690E-10	-0.28411647E-14
-0.15797270E+03	0.34760294E+01	0.29799631E+01	0.49966969E-02	-0.37909969E-05
0.23541924E-08	-0.80890242E-12	0.17622739E+03	0.92227239E+01	REF 20
H2				
0.29914234E+01	0.70006441E-03	-0.56338287E-07	-0.92315782E-11	0.15827518E-14
-0.83503399E+03	-0.13551102E+01	0.32981243E+01	0.82494417E-03	-0.81430153E-06
-0.94754343E-10	0.41348722E-12	-0.10125209E+04	-0.32940941E+01	REF 20
H2O				
0.26721456E+01	0.30562929E-02	-0.87302601E-06	0.12009964E-09	-0.63916179E-14
-0.29899209E+05	0.68628168E+01	0.33868425E+01	0.34749825E-02	-0.63546963E-05
0.69685813E-08	-0.25065884E-11	-0.30208113E+05	0.25902328E+01	REF 20
H2O2				
0.45731667E+01	0.43361363E-02	-0.14746888E-05	0.23489037E-09	-0.14316536E-13
-0.18006961E+05	0.50113696E+00	0.33887536E+01	0.65692260E-02	-0.14850126E-06
-0.46258055E-08	0.24715147E-11	-0.17663147E+05	0.67853631E+01	REF 20
O2				
0.36975782E+01	0.61351969E-03	-0.12588419E-06	0.17752815E-10	-0.11364353E-14
-0.12339302E+04	0.31891656E+01	0.32129364E+01	0.11274863E-02	-0.57561505E-06
0.13138772E-08	-0.87685539E-12	-0.10052490E+04	0.60347376E+01	REF 20
CO				
0.30250781E+01	0.14426885E-02	-0.56308278E-06	0.10185813E-09	-0.69109515E-14
-0.14268349E+05	0.61082177E+01	0.32624516E+01	0.15119408E-02	-0.38817552E-05
0.55819442E-08	-0.24749512E-11	-0.14310539E+05	0.48488969E+01	REF 20
CO2				
0.44536228E+01	0.31401687E-02	-0.12784105E-05	0.23939967E-09	-0.16690332E-13
-0.48966961E+05	-0.95539588E+00	0.22757246E+01	0.99220723E-02	-0.10409113E-04
0.68666868E-08	-0.21172801E-11	-0.48373141E+05	0.10188488E+02	REF 20
N2				
0.29266400E+01	0.14879767E-02	-0.56847608E-06	0.10097038E-09	-0.67533513E-14
-0.92279767E+03	0.59805279E+01	0.32986769E+01	0.14082404E-02	-0.39632223E-05
0.56415153E-08	-0.24448549E-11	-0.10208999E+04	0.39503722E+01	REF 20
CH				
0.21962233E+01	0.23403810E-02	-0.70582013E-06	0.90075822E-10	-0.38550401E-14
0.70867234E+05	0.91783733E+01	0.32002025E+01	0.20728756E-02	-0.51344314E-05
0.57338902E-08	-0.19555332E-11	0.70452594E+05	0.33315878E+01	REF 20
CHO				
0.35572712E+01	0.33455728E-02	-0.13350060E-05	0.24705726E-09	-0.17138509E-13
0.39163245E+04	0.55522995E+01	0.28983297E+01	0.61991466E-02	-0.96230842E-05
0.10898249E-07	-0.45748852E-11	0.41599219E+04	0.89836139E+01	REF 20

TABLE B1 (CONTINUED)

CH2(S)				
0.35528886E+01	0.20667882E-02	-0.19141160E-06	-0.11046734E-09	0.20213496E-13
0.49849754E+05	0.16865700E+01	0.39712651E+01	-0.16990887E-03	0.10253688E-05
0.24925508E-08	-0.19812663E-11	0.49893676E+05	0.57532072E-01	REF 20
CH2(T)				
0.36364078E+01	0.19330566E-02	-0.16870163E-06	-0.10098994E-09	0.18082558E-13
0.45341339E+05	0.21565606E+01	0.37622371E+01	0.11598191E-02	0.24895854E-06
0.88008356E-09	-0.73324354E-12	0.45367906E+05	0.17125776E+01	REF 20
CH2O				
0.29956062E+01	0.66813212E-02	-0.26289547E-05	0.47371529E-09	-0.32125175E-13
-0.15320369E+05	0.69125724E+01	0.16527312E+01	0.12631439E-01	-0.18881685E-04
0.20500314E-07	-0.84132371E-11	-0.14865404E+05	0.13784819E+02	REF 20
CH3				
0.28440516E+01	0.61379741E-02	-0.22303452E-05	0.37851608E-09	-0.24521590E-13
0.16437808E+05	0.54526973E+01	0.24304428E+01	0.11124099E-01	-0.16802203E-04
0.16218287E-07	-0.58649526E-11	0.16423781E+05	0.67897939E+01	REF 20
CH3O				
0.37707996E+01	0.78714974E-02	-0.26563839E-05	0.39444314E-09	-0.21126164E-13
0.12783252E+03	0.29295749E+01	0.21062040E+01	0.72165951E-02	0.53384719E-05
-0.73776363E-08	0.20756105E-11	0.97860107E+03	0.13152177E+02	REF 20
CH2OH				
0.63275204E+01	0.36082708E-02	-0.32015473E-06	-0.19387499E-09	0.35097047E-13
-0.44745093E+04	-0.83293657E+01	0.28626285E+01	0.10015272E-01	-0.52854358E-06
-0.51385398E-08	0.22460410E-11	-0.33496787E+04	0.10397937E+02	REF 20
CH4				
0.16834788E+01	0.10237235E-01	-0.38751286E-05	0.67855849E-09	-0.45034231E-13
-0.10080787E+05	0.96233949E+01	0.77874148E+00	0.17476683E-01	-0.27834090E-04
0.30497080E-07	-0.12239307E-10	-0.98252285E+04	0.13722195E+02	REF 20
C2H				
0.44276881E+01	0.22162686E-02	-0.60489526E-06	0.98825170E-10	-0.73511796E-14
0.64392678E+05	-0.11994418E+01	0.30506678E+01	0.60516745E-02	-0.49566342E-05
0.28041591E-08	-0.81933321E-12	0.64759454E+05	0.59543609E+01	REF 20
C2HO				
0.67580728E+01	0.20004003E-02	-0.20276073E-06	-0.10411318E-09	0.19651647E-13
0.19015133E+05	-0.90712623E+01	0.50479651E+01	0.44534779E-02	0.22682828E-06
-0.14820946E-08	0.22507415E-12	0.19658918E+05	0.48184395E+00	REF 20
C2H2				
0.44367704E+01	0.53760391E-02	-0.19128167E-05	0.32863789E-09	-0.21567095E-13
0.25667664E+05	-0.28003383E+01	0.20135622E+01	0.15190446E-01	-0.16163189E-04
0.90789918E-08	-0.19127460E-11	0.26124443E+05	0.88053779E+01	REF 20
C2H2O				
0.60388174E+01	0.58048405E-02	-0.19209538E-05	0.27944846E-09	-0.14588675E-13
-0.85834023E+04	-0.76575813E+01	0.29749708E+01	0.12118712E-01	-0.23450457E-05
-0.64666850E-08	0.39056492E-11	-0.76326367E+04	0.86735525E+01	REF 20
C2H3				
0.59334679E+01	0.40177456E-02	-0.39667395E-06	-0.14412665E-09	0.23786435E-13
0.31854346E+05	-0.85303125E+01	0.24592764E+01	0.73714764E-02	0.21098729E-05
-0.13216421E-08	-0.11847838E-11	0.33352250E+05	0.11556202E+02	REF 20
C2H4				
0.35284188E+01	0.11485184E-01	-0.44183853E-05	0.78446005E-09	-0.52668485E-13
0.44282886E+04	0.22303891E+01	-0.86148798E+00	0.27961628E-01	-0.33886772E-04
0.27851522E-07	-0.97378789E-11	0.55730459E+04	0.24211487E+02	REF 20
C2H5				
0.71904802E+01	0.64840773E-02	-0.64280647E-06	-0.23478794E-09	0.38808773E-13
0.10674549E+05	-0.14780892E+02	0.26907017E+01	0.87191332E-02	0.44198387E-05
0.93387031E-09	-0.39277735E-11	0.12870404E+05	0.12138195E+02	REF 20
C2H6				
0.48259382E+01	0.13840429E-01	-0.45572588E-05	0.67249672E-09	-0.35981614E-13
-0.12717793E+05	-0.52395067E+01	0.14625387E+01	0.15494667E-01	0.57805073E-05
-0.12578319E-07	0.45862671E-11	-0.11239176E+05	0.14432295E+02	REF 20

TABLE B1 (CONTINUED)

C3H2				
0.65308533E+01	0.58703162E-02	-0.17207767E-05	0.21274979E-09	-0.82919105E-14
0.63989143E+05	-0.11227278E+02	0.26910772E+01	0.14803664E-01	-0.32505513E-05
-0.86443634E-08	0.52848776E-11	0.65027725E+05	0.87573910E+01	REF 20
C3H3				
0.80916252E+01	0.37372850E-02	0.13886647E-05	-0.12298604E-08	0.20681585E-12
0.40225525E+05	-0.18204468E+02	0.25097322E+01	0.17103866E-01	-0.45710858E-05
-0.82841574E-08	0.54362287E-11	0.41827799E+05	0.11011264E+02	REF 20
C3H4(A)				
0.57291441E+01	0.12368045E-01	-0.48056267E-05	0.86013641E-09	-0.58128022E-13
0.20129842E+05	-0.94486675E+01	-0.21319687E+00	0.33587135E-01	-0.38048703E-04
0.27458378E-07	-0.86900443E-11	0.21620484E+05	0.20293926E+02	REF 20
C3H4(P)				
0.55110345E+01	0.12469562E-01	-0.48141646E-05	0.85737695E-09	-0.57715612E-13
0.19619674E+05	-0.10794748E+02	0.62714469E+00	0.31161788E-01	-0.37476638E-04
0.29641178E-07	-0.99873816E-11	0.20834927E+05	0.13468796E+02	REF 20
C3H5(S)				
0.79091978E+01	0.12115255E-01	-0.41175863E-05	0.61566796E-09	-0.33235733E-13
0.28739361E+05	-0.19672333E+02	-0.54100400E+00	0.27284101E-01	-0.96365329E-06
-0.19129462E-07	0.98394175E-11	0.30589561E+05	0.26067337E+02	REF 20
C3H5(T)				
0.79091978E+01	0.12115255E-01	-0.41175863E-05	0.61566796E-09	-0.33235733E-13
0.25711457E+05	-0.19672333E+02	-0.54100400E+00	0.27284101E-01	-0.96365329E-06
-0.19129462E-07	0.98394175E-11	0.27570657E+05	0.26067337E+02	REF 20
C3H6				
0.67322569E+01	0.14908336E-01	-0.49498994E-05	0.72120221E-09	-0.37662043E-13
-0.92357031E+03	-0.13313348E+02	0.14933071E+01	0.20925175E-01	0.44867938E-05
-0.16689121E-07	0.71581465E-11	0.10748264E+04	0.16145340E+02	REF 20
C3H7(N)				
0.79782906E+01	0.15761133E-01	-0.51732432E-05	0.74438922E-09	-0.38249782E-13
0.75794023E+04	-0.19356110E+02	0.19225368E+01	0.24789274E-01	0.18102492E-05
-0.17832658E-07	0.85829963E-11	0.97132812E+04	0.13992715E+02	REF 20
C3H7(I)				
0.80633688E+01	0.15744876E-01	-0.51823918E-05	0.74772455E-09	-0.38544221E-13
0.53138711E+04	-0.21926468E+02	0.17132998E+01	0.25426164E-01	0.15808082E-05
-0.18212862E-07	0.88277103E-11	0.75358086E+04	0.12979008E+02	REF 20
C3H8				
0.75252171E+01	0.18890340E-01	-0.62839244E-05	0.91793728E-09	-0.48124099E-13
-0.16464547E+05	-0.17843903E+02	0.89692080E+00	0.26689861E-01	0.54314251E-05
-0.21260007E-07	0.92433301E-11	-0.13954918E+05	0.19355331E+02	REF 20
C4				
0.65001802E+01	0.42286319E-02	-0.17907176E-05	0.34048125E-09	-0.24039784E-13
0.11434008E+06	-0.11488894E+02	0.23430281E+01	0.16429812E-01	-0.15279858E-04
0.73438264E-08	-0.15822742E-11	0.11545384E+06	0.98262043E+01	REF 20
C4H				
0.62428318E+01	0.61936825E-02	-0.20859315E-05	0.30822034E-09	-0.16364825E-13
0.94300187E+05	-0.72108059E+01	0.50232468E+01	0.70923753E-02	-0.60737619E-08
-0.22757522E-08	0.80869941E-12	0.94858125E+05	-0.69425940E-01	REF 20
C4H2				
0.90314074E+01	0.60472526E-02	-0.19487888E-05	0.27548630E-09	-0.13856080E-13
0.52947355E+05	-0.23850677E+02	0.40051918E+01	0.19810002E-01	-0.98658775E-05
-0.66351582E-08	0.60774129E-11	0.54240648E+05	0.18457365E+01	REF 20
C4H3(N)				
-0.54250956E+01	0.48377223E-01	-0.44313267E-04	0.19237426E-07	-0.31617068E-11
0.63425398E+05	0.52638771E+02	0.45429330E+01	0.17431803E-01	-0.84990543E-05
0.86326585E-09	0.37563103E-12	0.60878062E+05	0.20607948E+01	REF 20
C4H3(I)				
0.84874201E+01	0.86908937E-02	-0.28544437E-05	0.41200798E-09	-0.21301093E-13
0.54044069E+05	-0.19018509E+02	0.35539713E+01	0.19461986E-01	-0.48102484E-05
-0.97301225E-08	0.62390535E-11	0.55527377E+05	0.70829868E+01	REF 20

TABLE B1 (CONTINUED)

```
C4H4
  0.88921490E+01  0.10908850E-01 -0.35949597E-05  0.51934190E-09 -0.26808921E-13
  0.29966522E+05 -0.21726944E+02  0.21403370E+01  0.24605047E-01 -0.36391657E-05
 -0.15304014E-07  0.88964608E-11  0.32056170E+05  0.14282477E+02   REF 20
C4H5(S)
  0.15391707E+02 -0.92495698E-02  0.24010575E-04 -0.14486967E-07  0.28812809E-11
  0.31094857E+05 -0.54439987E+02  0.29675217E+01  0.23545934E-01 -0.65876393E-05
 -0.25386384E-08  0.11598502E-11  0.34677902E+05  0.10334459E+02   REF 20
C4H5(T)
  0.15391707E+02 -0.92495698E-02  0.24010575E-04 -0.14486967E-07  0.28812809E-11
  0.36080547E+05 -0.54439987E+02  0.29675217E+01  0.23545934E-01 -0.65876393E-05
 -0.25386384E-08  0.11598502E-11  0.39663590E+05  0.10334459E+02   REF 20
C4H5(I)
  0.15391707E+02 -0.92495698E-02  0.24010575E-04 -0.14486967E-07  0.28812809E-11
  0.34366447E+05 -0.54439987E+02  0.29675217E+01  0.23545934E-01 -0.65876393E-05
 -0.25386384E-08  0.11598502E-11  0.37949492E+05  0.10334459E+02   REF 20
C4H6(T)
  0.77061882E+01  0.15477240E-01 -0.22161657E-05 -0.17662189E-08  0.57283106E-12
  0.96562637E+04 -0.15592457E+02 -0.19918253E+02  0.17644100E+00 -0.35904226E-03
  0.33266232E-06 -0.11036895E-09  0.14322054E+05  0.10893895E+03   REF 20
C4H6(F)
  0.77061882E+01  0.15477240E-01 -0.22161657E-05 -0.17662189E-08  0.57283106E-12
  0.17108752E+05 -0.15592457E+02 -0.19918253E+02  0.17644100E+00 -0.35904226E-03
  0.33266232E-06 -0.11036895E-09  0.21774543E+05  0.10893895E+03   REF 20
C4H6(B)
  0.77061882E+01  0.15477240E-01 -0.22161657E-05 -0.17662189E-08  0.57283106E-12
  0.25267377E+05 -0.15592457E+02 -0.19918253E+02  0.17644100E+00 -0.35904226E-03
  0.33266232E-06 -0.11036895E-09  0.29933167E+05  0.10893895E+03   REF 20
C4H6O
  0.49302578E+01  0.30160125E-01 -0.16567141E-04  0.44492734E-08 -0.46829386E-12
 -0.15047124E+05  0.38153801E+01  0.23550308E+00  0.48366807E-01 -0.44811732E-04
  0.24686299E-07 -0.59726694E-11 -0.13999238E+05  0.26791668E+02   REF 20
1-C4H7
  0.31728544E+01  0.29838428E-01 -0.13844288E-04  0.28778382E-08 -0.21964906E-12
  0.20867799E+05  0.11869112E+02  0.31728544E+01  0.29838428E-01 -0.13844288E-04
  0.28778382E-08 -0.21964906E-12  0.20867799E+05  0.11869112E+02   PW
1-C4H8
  0.20535841E+01  0.34350507E-01 -0.15883197E-04  0.33089662E-08 -0.25361045E-12
 -0.21397231E+04  0.15543201E+02  0.11811380E+01  0.30853380E-01  0.50865247E-05
 -0.24654888E-07  0.11110193E-10 -0.17904004E+04  0.21062469E+02   PW
P-C4H9
  0.27586045E+01  0.36334544E-01 -0.16733120E-04  0.34711582E-08 -0.26472352E-12
  0.56338379E+04  0.14545769E+02  0.27586045E+01  0.36334544E-01 -0.16733120E-04
  0.34711582E-08 -0.26472352E-12  0.56338379E+04  0.14545769E+02   PW
C5H9
  0.37042289E+01  0.39042108E-01 -0.18223191E-04  0.38031742E-08 -0.29095449E-12
  0.17857311E+05  0.11002142E+02  0.37042289E+01  0.39042108E-01 -0.18223191E-04
  0.38031742E-08 -0.29095449E-12  0.17857311E+05  0.11002142E+02   PW
1-C5H11
  0.32912431E+01  0.45529757E-01 -0.21101181E-04  0.43925299E-08 -0.33570976E-12
  0.26192629E+04  0.13674364E+02  0.32912431E+01  0.45529757E-01 -0.21101181E-04
  0.43925299E-08 -0.33570976E-12  0.26192629E+04  0.13674364E+02   PW
1-C5H10
 -0.26194715E+00  0.52521653E-01 -0.27921931E-04  0.52903104E-08  0.22517016E-12
 -0.46336323E+04  0.28551981E+02 -0.26194715E+00  0.52521653E-01 -0.27921931E-04
  0.52903104E-08  0.22517016E-12 -0.46336323E+04  0.28551981E+02   PW
C6H2
  0.12756519E+02  0.80343808E-02 -0.26182151E-05  0.37250603E-09 -0.18788509E-13
  0.80754687E+05 -0.40412628E+02  0.57510853E+01  0.26367199E-01 -0.11667596E-04
 -0.10714498E-07  0.87902975E-11  0.82620125E+05 -0.43355322E+01   REF 20
C6H3
  0.12761181E+02  0.10385573E-01 -0.34791929E-05  0.51097326E-09 -0.26909651E-13
  0.74777062E+05 -0.38917450E+02  0.50070896E+01  0.26928518E-01 -0.59198655E-05
 -0.15272335E-07  0.94083101E-11  0.77132000E+05  0.22256212E+01   REF 20
```

TABLE B1 (CONTINUED)

```
C6H4
  0.10062741E+02  0.16903043E-01 -0.64730457E-05  0.11240806E-08 -0.73075660E-13
  0.56453730E+05 -0.29693100E+02 -0.13004847E+01  0.38664766E-01 -0.36439442E-05
 -0.26685807E-07  0.14509357E-10  0.60029074E+05  0.31249390E+02    REF 20
C6H5
  0.11433509E+02  0.17014805E-01 -0.58358992E-05  0.88020347E-09 -0.47983644E-13
  0.33941625E+05 -0.38578339E+02 -0.22878075E+01  0.42416330E-01 -0.17666744E-05
 -0.31422520E-07  0.16505464E-10  0.38370789E+05  0.35398270E+02    REF 22
C6H5O
  0.14255515E+02  0.16385024E-01 -0.62779554E-05  0.13068588E-08 -0.14999694E-12
 -0.15296846E+04 -0.48636177E+02 -0.39828930E+01  0.69202796E-01 -0.63259053E-04
  0.28673641E-07 -0.51150360E-11  0.34448469E+04  0.45142021E+02    REF 22
C5H5
  0.10844072E+02  0.15392831E-01 -0.55630422E-05  0.90189440E-09 -0.54156619E-13
  0.26950886E+05 -0.35254983E+02 -0.95902849E+00  0.31396777E-01  0.26724050E-04
 -0.68942183E-07  0.33301983E-10  0.30779441E+05  0.29072780E+02    REF 67
C5H5O
  0.73219724E+01  0.26217271E-01 -0.10394357E-04  0.69805534E-09  0.30307525E-12
  0.86725078E+04 -0.13395977E+02 -0.91274900E+01  0.89092843E-01 -0.98929631E-04
  0.55164946E-07 -0.12054646E-10  0.12050769E+05  0.66558670E+02    REF 22
C5H4O
  0.16174722E+01  0.37716053E-01 -0.23935409E-04  0.72674178E-08 -0.84449082E-12
 -0.32129492E+03  0.13399043E+02 -0.33123374E+01  0.54107033E-01 -0.48252157E-04
  0.26132914E-07 -0.68544311E-11  0.10042001E+04  0.38434387E+02    REF 22
C5H4OH
  0.82749834E+01  0.25455624E-01 -0.11891672E-04  0.20921516E-08 -0.16007544E-13
  0.65311050E+04 -0.18165775E+02 -0.75077271E+01  0.86810358E-01 -0.99664867E-04
  0.56890869E-07 -0.12613540E-10  0.97140107E+04  0.58272274E+02    REF 22
C6H5L
  0.71924891E+01  0.32199372E-01 -0.17901912E-04  0.48632285E-08 -0.51723014E-12
  0.66993375E+05 -0.11418365E+02 -0.24493167E+01  0.73556021E-01 -0.84861349E-04
  0.52961994E-07 -0.13371415E-10  0.68822797E+05  0.34488605E+02    REF 22
C8H2
  0.15680213E+02  0.11154614E-01 -0.37243726E-05  0.51978910E-09 -0.23755503E-13
  0.10811225E+06 -0.55714371E+02  0.46304273E+01  0.39370801E-01 -0.11480348E-04
 -0.25622135E-07  0.16707913E-10  0.11082850E+06  0.80774248E+00    REF 20
C5H5(L)
  0.89391508E+01  0.17945170E-01 -0.60922503E-05  0.69252454E-09  0.92676721E-14
  0.61953191E+05  0.37377625E+01 -0.69306135E+00  0.54876648E-01 -0.59586640E-04
  0.35444899E-07 -0.85479774E-11  0.63674488E+05  0.50645664E+02    REF 22
C5H6(L)
  0.68000879E+01  0.23944799E-01 -0.93979561E-05  0.15285305E-08 -0.70547999E-13
  0.29450406E+05  0.16064999E+02  0.12613640E+01  0.43914810E-01 -0.34713252E-04
  0.14560196E-07 -0.22182141E-11  0.30614170E+05  0.43205833E+02    REF 22
C5H4(L)
  0.89391508E+01  0.17945170E-01 -0.60922503E-05  0.69252454E-09  0.92676721E-14
  0.46909410E+05  0.37377625E+01 -0.69306135E+00  0.54876648E-01 -0.59586640E-04
  0.35444899E-07 -0.85479774E-11  0.48630707E+05  0.50645664E+02    REF 22
C5H3(L)
  0.89391508E+01  0.17945170E-01 -0.60922503E-05  0.69252454E-09  0.92676721E-14
  0.69503538E+05  0.37377625E+01 -0.69306135E+00  0.54876648E-01 -0.59586640E-04
  0.35444899E-07 -0.85479774E-11  0.71224885E+05  0.50645664E+02    REF 22
1-C7H15
  0.12660566E+02  0.47893065E-01 -0.19735835E-04  0.37298693E-08 -0.26299814E-12
 -0.64258434E+04 -0.34510489E+02  0.10280414E+02  0.70155356E-03  0.15955135E-03
 -0.20959318E-06  0.83344532E-10 -0.36030731E+04 -0.10315257E+02    REF 67
2-C7H15
  0.66495419E+00  0.77137977E-01 -0.44929548E-04  0.12854724E-07 -0.14434085E-11
 -0.31296282E+04  0.28957718E+02  0.66495419E+00  0.77137977E-01 -0.44929548E-04
  0.12854724E-07 -0.14434085E-11 -0.31296282E+04  0.28957718E+02    PW
3-C7H15
  0.66495419E+00  0.77137977E-01 -0.44929548E-04  0.12854724E-07 -0.14434085E-11
 -0.31296282E+04  0.28957718E+02  0.66495419E+00  0.77137977E-01 -0.44929548E-04
  0.12854724E-07 -0.14434085E-11 -0.31296282E+04  0.28957718E+02    PW
```

TABLE B1 (CONCLUDED)

4-C7H15				
0.66495419E+00	0.77137977E-01	-0.44929548E-04	0.12854724E-07	-0.14434085E-11
-0.31296282E+04	0.28957718E+02	0.66495419E+00	0.77137977E-01	-0.44929548E-04
0.12854724E-07	-0.14434085E-11	-0.31296282E+04	0.28957718E+02	PW
1-C7H14				
0.13952881E+02	0.41712158E-01	-0.16157950E-04	0.29187538E-08	-0.19958112E-12
-0.14853311E+05	-0.43649205E+02	0.19140427E+01	0.58601697E-01	0.16939333E-05
-0.38140418E-07	0.18157007E-10	-0.10616395E+05	0.22793909E+02	PW
2-C7H14				
0.32385807E+01	0.62326781E-01	-0.29207546E-04	0.61119079E-08	-0.46836433E-12
-0.12588305E+05	0.17598330E+02	0.32385807E+01	0.62326781E-01	-0.29207546E-04
0.61119079E-08	-0.46836433E-12	-0.12588305E+05	0.17598330E+02	PW
3-C7H14				
0.32385807E+01	0.62326781E-01	-0.29207546E-04	0.61119079E-08	-0.46836433E-12
-0.12588305E+05	0.17598330E+02	0.32385807E+01	0.62326781E-01	-0.29207546E-04
0.61119079E-08	-0.46836433E-12	-0.12588305E+05	0.17598330E+02	PW
C(S)				
0.16272659E+01	0.13726102E-02	-0.47427392E-06	0.78269058E-10	-0.46932334E-14
-0.75550659E+03	-0.94597750E+01	-0.39358151E+00	0.50322227E-02	0.21335575E-06
-0.44809667E-08	0.22281673E-11	-0.10043521E+03	0.14578543E+01	REF 20

TABLE B2
JANNAF Polynomials for *n*-Heptane Mechanism
Additional Stirred Reactor Species

CH3OH				
0.36012593E+01	0.10243223E-01	-0.35999217E-05	0.57251951E-09	-0.33912719E-13
-0.25997155E+05	0.47056025E+01	0.57153948E+01	-0.15230920E-01	0.65244182E-04
-0.71080873E-07	0.26135383E-10	-0.25642765E+05	-0.15040970E+01	REF 67
C6H11				
0.24938654E+02	0.13258801E-01	-0.23302223E-05	0.00000000E+00	0.00000000E+00
0.51145941E+04	-0.10690338E+03	0.63802451E+00	0.56209452E-01	-0.23047424E-04
0.00000000E+00	0.00000000E+00	0.14624427E+05	0.28133981E+02	REF 67
1-C6H12				
0.18663635E+02	0.20971451E-01	-0.31082809E-05	-0.68651618E-09	0.16023608E-12
-0.13590895E+05	-0.70915860E+02	0.19686203E+01	0.47656231E-01	0.66015373E-05
-0.37148173E-07	0.16922463E-10	-0.77118789E+04	0.20859230E+02	REF 67
1-C6H13				
0.12759770E 02	0.37134279E-01	-0.14256110E-04	0.25052556E-08	-0.16459707E-12
-0.35693750E 04	-0.36999527E 02	0.23062353E 01	0.50200045E-01	0.79387773E-05
-0.41260655E-07	0.18794369E-10	0.10269711E 03	0.20896637E 02	REF 67
2-C6H13				
0.24056369E+03	-0.16540524E+01	0.41218125E-02	-0.38506450E-05	0.11862751E-08
-0.18510320E+05	-0.98342773E+03	0.24056369E+03	-0.16540524E+01	0.41218125E-02
-0.38506450E-05	0.11862751E-08	-0.18510320E+05	-0.98342773E+03	PW
C7H13				
0.20154745E+02	2.94825740E-02	-1.00547928E-05	1.55779043E-09	-9.02420561E-14
5.28806957E+03	-7.55263310E+01	-5.42049681E-01	7.60738062E-02	-4.99213653E-05
1.70382432E-08	-2.39883209E-12	1.26846066E+04	3.63048921E+01	31
C2H4O				
0.54887641E+01	0.12046190E-01	-0.43336931E-05	0.70028311E-09	-0.41949088E-13
-0.91804251E+04	-0.70799605E+01	0.37590532E+01	-0.94412180E-02	0.80309721E-04
-0.10080788E-06	0.40039921E-10	-0.75608143E+04	0.78497475E+01	REF 67
C2H3O				
0.59447731E+01	0.78667205E-02	-0.28865882E-05	0.47270875E-09	-0.28599861E-13
-0.37873075E+04	-0.50136751E+01	0.41634257E+01	-0.23261610E-03	0.34267820E-04
-0.44105227E-07	0.17275612E-10	-0.26574529E+04	0.73468280E+01	REF 67

TABLE B3
Physical Properties for *n*-Heptane Diffusion Flame Mechanism Species

SPECIE	σ	ϵ/κ	C_v	C_z	μ	Mol Wt.
C7H16	0.63575676E+01	0.416E+03	1.0	1.5	0.605E-05	100.205
H	0.27080000E+01	0.370E+02	1.0	1.0	0.749E-05	1.008
OH	0.27500000E+01	0.800E+02	100.0	1.0	0.197E-04	17.008
O	0.27500000E+01	0.800E+02	1000.0	1.0	0.189E-04	16.000
HO2	0.34580000E+01	0.107E+03	3.0	1.0	0.982E-05	33.008
H2	0.28270000E+01	0.597E+02	280.0	1.0	0.892E-05	2.016
H2O	0.26050000E+01	0.572E+03	4.0	1.0	0.110E-04	18.016
H2O2	0.34580000E+01	0.107E+03	3.0	2.0	0.982E-05	34.020
O2	0.34580000E+01	0.107E+03	3.8	2.0	0.206E-04	32.000
CO	0.36500000E+01	0.980E+02	1.8	4.0	0.178E-04	28.011
CO2	0.37630000E+01	0.244E+03	2.1	1.5	0.152E-04	44.011
N2	0.36200000E+01	0.975E+02	4.0	1.0	0.178E-04	28.016
CH	0.27500000E+01	0.800E+02	2.0	1.0	0.155E-04	13.019
CHO	0.35900000E+01	0.498E+03	2.0	1.5	0.1833-04	29.019
SCH2	0.38000000E+01	0.144E+03	13.0	1.0	0.112E-04	14.026
TCH2	0.38000000E+01	0.144E+03	13.0	1.0	0.112E-04	14.026
CH2O	0.35900000E+01	0.498E+03	2.0	1.5	0.183E-04	30.027
CH3	0.38000000E+01	0.144E+03	1.3	1.5	0.112E-04	15.035
CH3O	0.35900000E+01	0.498E+03	2.0	1.5	0.183E-04	31.027
CH2OH	0.35900000E+01	0.498E+03	2.0	1.5	0.183E-04	31.027
CH4	0.37500000E+01	0.141E+03	13.0	1.0	0.112E-04	16.040
C2H	0.41000000E+01	0.209E+03	2.5	1.5	0.104E-04	25.030
C2HO	0.25000000E+01	0.150E+03	2.0	1.5	0.874E-05	41.030
C2H2	0.41000000E+01	0.209E+03	2.5	1.5	0.104E-04	26.038
C2H2O	0.39700000E+01	0.436E+03	2.0	1.5	0.874E-05	42.038
C2H3	0.41000000E+01	0.209E+03	2.0	1.5	0.104E-04	27.046
C2H4	0.39710000E+01	0.281E+03	2.0	1.5	0.102E-04	28.054
C2H5	0.43020000E+01	0.252E+03	2.0	1.5	0.102E-04	29.062
C2H6	0.43020000E+01	0.252E+03	2.0	1.5	0.947E-05	30.070
C3H2	0.41000000E+01	0.209E+03	1.0	1.5	0.886E-05	38.049
C3H3	0.47600000E+01	0.252E+03	1.0	1.5	0.886E-05	39.057
AC3H4	0.47600000E+01	0.252E+03	1.0	1.5	0.886E-05	40.060
P-C3H4	0.47600000E+01	0.252E+03	1.0	1.5	0.886E-05	40.060
AC3H5	0.47600000E+01	0.252E+03	1.0	1.5	0.886E-05	41.073
SC3H5	0.47600000E+01	0.252E+03	1.0	1.5	0.886E-05	41.073
TC3H5	0.47600000E+01	0.252E+03	1.0	1.5	0.886E-05	41.074
C3H6	0.49820000E+01	0.267E+03	1.0	1.5	0.895E-05	42.08
C3H7N	0.49820000E+01	0.267E+03	1.0	1.5	0.827E-05	43.092
C3H7I	0.49820000E+01	0.267E+03	1.0	1.5	0.827E-05	43.092
C3H8	0.49820000E+01	0.267E+03	1.0	1.5	0.827E-05	44.100
C4	0.43000000E+01	0.130E+03	1.0	1.5	0.180E-04	48.044
C4H	0.51800000E+01	0.357E+03	1.0	1.5	0.755E-05	49.044
C4H2	0.51800000E+01	0.357E+03	1.0	1.5	0.755E-05	50.060
C4H3N	0.51800000E+01	0.357E+03	1.0	1.5	0.755E-05	51.070
C4H3I	0.51800000E+01	0.357E+03	1.0	1.5	0.755E-05	51.070
C4H4	0.51800000E+01	0.357E+03	1.0	1.5	0.755E-05	52.070
C4H5S	0.51800000E+01	0.357E+03	1.0	1.5	0.755E-05	53.080
C4H5T	0.51800000E+01	0.357E+03	1.0	1.5	0.755E-05	53.080
C4H5I	0.52800000E+01	0.330E+03	1.0	1.5	0.755E-05	53.080
C4H6S	0.52800000E+01	0.330E+03	1.0	1.5	0.755E-05	54.090
C4H6T	0.52800000E+01	0.330E+03	1.0	1.5	0.755E-05	54.090
C4H6F	0.52800000E+01	0.330E+03	1.0	1.5	0.755E-05	54.090
C4H6B	0.52800000E+01	0.330E+03	1.0	1.5	0.755E-05	70.092
C4H6O	0.54940000E+01	0.374E+03	1.0	1.5	0.718E-05	55.096
1-C4H7	0.51706000E+01	0.310E+03	1.0	1.5	0.789E-04	56.104
1-C4H8	0.52263650E+01	0.323E+03	1.0	1.5	0.764E-04	57.116
P-C4H9	0.53148680E+01	0.327E+03	1.0	1.5	0.740E-04	69.127
C5H9	0.55506260E+01	0.358E+02	1.0	1.5	0.713E-04	

TABLE B3 (CONCLUDED)

1-C5H11	0.56764616E+01	0.352E+02	1.0	1.5	0.698E-04	71.143
1-C5H10	0.56299311E+01	0.358E+03	1.0	1.5	0.698E-04	70.135
C6H2	0.61820000E+01	0.297E+03	1.0	1.5	0.703E-05	74.082
C6H3	0.61820000E+01	0.297E+03	1.0	1.5	0.703E-05	75.030
C6H4	0.53490000E+01	0.412E+03	1.0	1.5	0.763E-05	76.040
C6H5	0.53490000E+01	0.412E+03	1.0	1.5	0.763E-05	77.050
C6H5O	0.53490000E+01	0.412E+03	1.0	1.5	0.763E-05	93.050
C6H6	0.53490000E+01	0.412E+03	1.0	1.5	0.763E-05	78.050
C6H6O	0.53490000E+01	0.412E+03	1.0	1.5	0.763E-05	94.050
C5H6	0.52090000E+01	0.391E+03	1.0	1.5	0.755E-05	66.103
C5H5	0.50290000E+01	0.426E+03	1.0	1.5	0.770E-05	65.095
C5H5O	0.62340000E+01	0.278E+03	1.0	1.5	0.696E-05	81.095
C5H4O	0.62340000E+01	0.278E+03	1.0	1.5	0.691E-05	80.087
C5H4OH	0.62340000E+01	0.278E+03	1.0	1.5	0.696E-05	81.095
C6H5L	0.53490000E+01	0.412E+03	1.0	1.5	0.763E-05	77.050
C8H2	0.60000000E+01	0.500E+02	1.0	1.5	0.600E-05	98.088
C5H5L	0.50290000E+01	0.427E+03	1.0	1.5	0.770E-05	65.095
C5H6L	0.52090000E+01	0.391E+03	1.0	1.5	0.756E-05	66.103
C5H4L	0.50290000E+01	0.427E+03	1.0	1.5	0.770E-05	64.095
C5H3L	0.50290000E+01	0.427E+03	1.0	1.5	0.770E-05	63.095
1-C7H15	0.62866200E+01	0.409E+03	1.0	1.5	0.622E-04	99.197
2-C7H15	0.62866200E+01	0.401E+03	1.0	1.5	0.628E-04	99.197
3-C7H15	0.62866200E+01	0.401E+03	1.0	1.5	0.628E-04	99.197
4-C7H15	0.62866200E+01	0.401E+03	1.0	1.5	0.628E-04	99.197
1-C7H14	0.63965660E+01	0.414E+03	1.0	1.5	0.593E-04	98.190
2-C7H14	0.61428900E+01	0.419E+03	1.0	1.5	0.639E-04	98.190
3-C7H14	0.61428900E+01	0.419E+03	1.0	1.5	0.639E-04	98.190
C(S)	0.33850000E+01	0.306E+02	4.0	1.0	0.170E-04	12.011

σ = Collision Diameter (Armstrongs)

ϵ/κ = Lennard Jones Potential Parameter (K)

C_V = Vibrational Wall Collision Efficiency

C_Z = Rotational Wall Collision Efficiency

μ = viscosity (kg m^{-1} sec^{-1})

TABLE B4
Physical Properties for *n*-Heptane Mechanism
Additional Stirred Reactor Species

SPECIES	σ	ϵ/κ	C_V	C_Z	μ	Mol Wt.
CH3OH	0.36260000E+01	0.482E+03	2.0	1.5	0.982E-05	32.042
C6H11	0.61820000E+01	0.297E+03	1.0	1.5	0.703E-05	83.140
1-C6H12	0.61820000E+01	0.297E+03	1.0	1.5	0.703E-05	84.160
1-C6H13	0.59490000E+01	0.399E+03	1.0	1.5	0.659E-05	85.160
2-C6H13	0.59409000E+01	0.399E+03	1.0	1.5	0.659E-05	85.160
C7H13	0.61428900E+01	0.418E+03	1.0	1.5	0.639E-04	97.170
C2H4O	0.46668875E+01	0.361E+03	2.0	1.5	0.915E-04	44.050
C2H3O	0.46668875E+01	0.361E+03	2.0	1.5	0.915E-04	43.054

APPENDIX C
n-HEPTANE REACTION RATES DATA

Table 3.1.2.1
n-Heptane Consumption in Diffusion Flames

Reaction								FLAME A kmol/m^3/sec	FLAME B kmol/m^3/sec	FLAME C kmol/m^3/sec
410	C7H16		=	C3H7(N)	+	P-C4H9		3.78E-02	2.10E-02	7.69E-02
411	C7H16		=	C2H5	+	1-C5H11		1.82E-02	1.00E-02	3.72E-02
412	C7H16		=	1-C7H15	+	H		4.88E-06	2.71E-06	1.26E-05
413	C7H16		=	2-C7H15	+	H		4.88E-06	2.71E-06	1.26E-05
414	C7H16		=	3-C7H15	+	H		4.88E-06	2.71E-06	1.26E-05
415	C7H16		=	4-C7H15	+	H		4.88E-06	2.71E-06	1.26E-05
416	C7H16	+ H	=	1-C7H15	+	H2		2.14E-02	1.34E-02	4.24E-02
417	C7H16	+ H	=	2-C7H15	+	H2		1.96E-02	1.27E-02	3.81E-02
418	C7H16	+ H	=	3-C7H15	+	H2		1.96E-02	1.27E-02	3.81E-02
419	C7H16	+ H	=	4-C7H15	+	H2		9.71E-03	6.29E-03	1.89E-02
429	C7H16	+ CH3	=	2-C7H15	+	CH4		6.44E-03	4.27E-03	9.80E-03
430	C7H16	+ CH3	=	3-C7H15	+	CH4		6.44E-03	4.27E-03	9.80E-03
428	C7H16	+ CH3	=	1-C7H15	+	CH4		5.26E-03	3.31E-03	7.91E-03
431	C7H16	+ CH3	=	4-C7H15	+	CH4		3.22E-03	2.13E-03	4.90E-03
424	C7H16	+ OH	=	1-C7H15	+	H2O		1.55E-03	6.63E-04	2.46E-03
425	C7H16	+ OH	=	2-C7H15	+	H2O		1.27E-03	5.40E-04	2.01E-03
426	C7H16	+ OH	=	3-C7H15	+	H2O		1.27E-03	5.40E-04	2.01E-03
427	C7H16	+ OH	=	4-C7H15	+	H2O		1.27E-03	5.40E-04	2.01E-03
445	C7H16	+ C3H5(A)	=	2-C7H15	+	C3H6		1.58E-04	1.03E-04	1.71E-04
446	C7H16	+ C3H5(A)	=	3-C7H15	+	C3H6		1.58E-04	1.03E-04	1.71E-04
420	C7H16	+ O	=	1-C7H15	+	OH		1.23E-04	6.79E-06	9.10E-05
447	C7H16	+ C3H5(A)	=	4-C7H15	+	C3H6		7.89E-05	5.17E-05	8.56E-04
437	C7H16	+ C2H5	=	2-C7H15	+	C2H6		6.64E-05	2.29E-04	4.85E-04
438	C7H16	+ C2H5	=	3-C7H15	+	C2H6		6.64E-05	2.29E-04	4.85E-05
444	C7H16	+ C3H5(A)	=	1-C7H15	+	C3H6		3.55E-05	2.32E-05	4.00E-05
439	C7H16	+ C2H5	=	4-C7H15	+	C2H6		3.32E-05	1.15E-04	2.43E-04
433	C7H16	+ HO2	=	2-C7H15	+	H2O2		2.38E-05	2.23E-06	1.70E-05
434	C7H16	+ HO2	=	3-C7H15	+	H2O2		2.38E-05	2.23E-06	1.70E-05
421	C7H16	+ O	=	2-C7H15	+	OH		2.04E-05	1.10E-06	1.56E-05
422	C7H16	+ O	=	3-C7H15	+	OH		2.04E-05	1.10E-06	1.56E-05
441	C7H16	+ C2H3	=	2-C7H15	+	C2H4		1.91E-05	1.88E-05	4.42E-05
442	C7H16	+ C2H3	=	3-C7H15	+	C2H4		1.91E-05	1.88E-05	4.42E-05
436	C7H16	+ C2H5	=	1-C7H15	+	C2H6		1.44E-05	4.55E-05	9.65E-05
440	C7H16	+ C2H3	=	1-C7H15	+	C2H4		1.51E-05	1.47E-05	3.49E-05
423	C7H16	+ O	=	4-C7H15	+	OH		1.02E-05	5.48E-07	7.82E-06
443	C7H16	+ C2H3	=	4-C7H15	+	C2H4		9.58E-06	9.44E-06	2.22E-05
432	C7H16	+ HO2	=	1-C7H15	+	H2O2		1.43E-06	7.28E-07	6.20E-06
435	C7H16	+ HO2	=	4-C7H15	+	H2O2		1.20E-06	1.12E-06	8.54E-06
450	C7H16	+ O2	=	3-C7H15	+	HO2		2.45E-07	1.86E-08	1.27E-07
449	C7H16	+ O2	=	2-C7H15	+	HO2		2.43E-07	1.85E-08	1.26E-07
451	C7H16	+ O2	=	4-C7H15	+	HO2		1.22E-07	9.31E-09	6.34E-08
448	C7H16	+ O2	=	1-C7H15	+	HO2		8.95E-08	6.75E-09	4.68E-08

Table 3.1.2.2
Heptyl Radicals Consumption in Diffusion Flames

Reaction					FLAME A kmol/m^3/sec	FLAME B kmol/m^3/sec	FLAME C kmol/m^3/sec
453	2-C7H15	=	C3H6	+ P-C4H9	3.41E-02	2.18E-02	6.18E-02
452	1-C7H15	=	C2H4	+ 1-C5H11	3.21E-02	2.01E-02	5.87E-02
455	4-C7H15	=	1-C5H10	+ C2H5	1.52E-02	9.69E-03	2.72E-02
454	3-C7H15	=	C3H7(N)	+ 1-C4H8	1.21E-02	7.44E-03	2.23E-02
463	1-C7H15	=	3-C7H15		-8.33E-03	-5.53E-03	1.46E-02
465	2-C7H15	=	3-C7H15		-5.68E-03	-3.70E-03	-1.01E-02
462	1-C7H15	=	2-C7H15		2.25E-03	1.31E-03	4.40E-03
464	1-C7H15	=	4-C7H15		1.59E-03	1.14E-03	2.83E-03
459	3-C7H15	=	2-C7H14	+ H	3.39E-04	1.84E-04	6.88E-04
460	3-C7H15	=	3-C7H14	+ H	3.39E-04	1.83E-04	6.87E-04
458	2-C7H15	=	1-C7H14	+ H	2.15E-04	1.19E-04	4.22E-04
457	2-C7H15	=	1-C7H14	+ H	2.13E-04	1.16E-04	3.12E-04
456	1-C7H15	=	1-C7H14	+ H	1.56E-04	8.42E-05	3.12E-04
461	4-C7H15	=	3-C7H14	+ H	1.26E-04	6.90E-05	2.49E-04
471	4-C7H15 + O2	=	3-C7H14	+ HO2	2.78E-06	1.00E-06	7.76E-06
466	1-C7H15 + O2	=	1-C7H14	+ HO2	2.57E-06	9.13E-07	6.99E-06
469	3-C7H15 + O2	=	2-C7H14	+ HO2	1.60E-06	5.80E-07	4.74E-06
470	3-C7H15 + O2	=	3-C7H14	+ HO2	1.60E-06	5.80E-07	4.74E-06
468	2-C7H15 + O2	=	2-C7H14	+ HO2	1.58E-06	5.70E-07	4.60E-06
467	2-C7H15 + O2	=	1-C7H14	+ HO2	6.43E-07	3.17E-08	1.90E-06

Table 3.1.2.3
Heptene Consumption in Diffusion Flames

Reaction					FLAME A kmol/m^3/sec	FLAME B kmol/m^3/sec	FLAME C kmol/m^3/sec
473	2-C7H14	=	C3H7(N)	+ 1-C4H7	5.95E-04	6.91E-04	1.67E-03
474	3-C7H14	=	C2H5	+ C5H9	5.26E-04	5.12E-04	1.49E-03
472	1-C7H14	=	C3H5(A)	+ P-C4H9	3.94E-04	3.18E-04	9.38E-04

Table 3.1.2.4
1-*Pentyl Radical Consumption in Diffusion Flames*

Reaction					FLAME A kmol/m^3/sec	FLAME B kmol/m^3/sec	FLAME C kmol/m^3/sec
409	1-C5H11	=	C3H7(N)	+ C2H4	4.59E-02	2.54E-02	8.11E-02

Table 3.1.2.5
1-*Pentene Consumption in Diffusion Flames*

Reaction					FLAME A kmol/m^3/sec	FLAME B kmol/m^3/sec	FLAME C kmol/m^3/sec
408	1-C5H10	=	C2H5	+ C3H5 (A)	4.60E-03	2.20E-02	5.26E-02

Table 3.1.2.6
Pentenyl Radical Consumption in Diffusion Flames

	Reaction	FLAME A kmol/m^3/sec	FLAME B kmol/m^3/sec	FLAME C kmol/m^3/sec
405	C5H9 = C3H5(A) + C2H4	4.60E-03	5.32E-03	1.04E-02
406	C5H9 = C2H3 + C3H6	-4.59E-03	-5.43E-03	-1.00E-02
407	C5H9 = C4H6(S) + CH3	4.72E-04	5.43E-04	9.47E-04

Table 3.1.2.7
n-Butyl Radical Consumption in Diffusion Flames

	Reaction	FLAME A kmol/m^3/sec	FLAME B kmol/m^3/sec	FLAME C kmol/m^3/sec
402	P-C4H9 = C2H5 + C2H4	7.16E-02	4.08E-02	1.32E-01
403	P-C4H9 = 1-C4H8 + H	-7.63E-03	-6.60E-03	-1.73E-02
404	P-C4H9 + O2 = 1-C4H8 + HO2	2.68E-05	2.99E-05	2.11E-04

Table 3.1.2.8
1-Butene Consumption in Diffusion Flames

	Reaction	FLAME A kmol/m^3/sec	FLAME B kmol/m^3/sec	FLAME C kmol/m^3/sec
389	1-C4H8 = C3H5(A) + CH3	1.07E-02	-1.78E-02	-4.97E-02
391	1-C4H8 = C2H3 + C2H5	1.62E-04	1.78E-04	4.89E-04
388	1-C4H8 = 1-C4H7 + H	-6.15E-06	-1.75E-05	-5.33E-05
392	1-C4H8 + H = 1-C4H7 + H2	1.09E-02	9.55E-03	2.44E-02
393	1-C4H8 + OH = C3H7(N) + CH2O	2.39E-04	1.48E-04	4.45E-04
395	1-C4H8 + OH = 1-C4H7 + H2O	2.11E-04	1.27E-04	4.04E-04
399	1-C4H8 + CH3 = 1-C4H7 + CH4	8.51E-05	6.83E-05	1.41E-04
401	1-C4H8 + C3H5(A) = 1-C4H7 + C3H6	6.84E-06	6.27E-06	9.35E-06
396	1-C4H8 + O = C2H5 + CH3 + CO	5.40E-06	4.27E-07	4.33E-06
400	1-C4H8 + C2H5 = 1-C4H7 + C2H6	4.46E-06	1.07E-05	2.03E-05
397	1-C4H8 + O = 1-C4H7 + OH	8.44E-07	8.92E-08	9.73E-07
394	1-C4H8 + OH = C2H6 + CH3 + CO	3.68E-07	2.28E-07	6.85E-07
398	1-C4H8 + HO2 = 1-C4H7 + H2O2	2.17E-09	1.53E-10	1.56E-09
390	1-C4H8 + O2 = 1-C4H7 + HO2	4.34E-08	4.90E-09	2.69E-08

Table 3.1.2.9
1-Butene Radical Consumption in Diffusion Flames

	Reaction	FLAME A kmol/m^3/sec	FLAME B kmol/m^3/sec	FLAME C kmol/m^3/sec
378	1-C4H7 = C4H6(T) + H	3.89E-03	2.90E-03	7.89E-03
379	1-C4H7 = C2H4 + C2H3	3.01E-04	2.16E-04	5.80E-04
382	1-C4H7 + CH3 = C4H6(T) + CH4	7.82E-03	7.40E-03	1.85E-02
386	1-C4H7 + C3H5(A) = C4H6(T) + C3H6	2.56E-04	3.11E-04	4.95E-04
380	1-C4H7 + H = C4H6(T) + H2	1.15E-05	1.78E-05	6.17E-05
383	1-C4H7 + C2H3 = C4H6(T) + C2H4	3.49E-06	5.61E-06	1.25E-05
385	1-C4H7 + C2H5 = 1-C4H8 + C2H4	2.19E-06	4.88E-06	7.49E-06
384	1-C4H7 + C2H5 = C4H6(T) + C2H6	1.83E-06	3.95E-06	6.09E-06
387	1-C4H7 + HO2 = C4H6(T) + 1-C4H8	7.33E-08	1.26E-07	1.87E-07
381	1-C4H7 + O2 = C4H6(T) + HO2	3.05E-06	5.14E-07	2.10E-06

Table 3.1.2.10
Additional n-Heptane Diffusion Flame Reaction Rates

	Reaction	FLAME A kmol/m^3/sec
1	H + O2 = OH + O	6.31E-01
2	O + H2 = OH + H	2.51E-01
3	OH + H2 = H2O + H	6.81E-01
4	OH + OH = H2O + O	1.50E-02
5	O2 + H + M = HO2 + M	1.45E-01
6	HO2 + H = OH + OH	6.91E-02
7	HO2 + H = H2 + O2	1.47E-02
8	HO2 + OH = H2O + O2	3.62E-02
9	HO2 + H = H2O + O	9.34E-03
10	HO2 + O = OH + O2	2.80E-02
11	HO2 + HO2 = H2O2 + O2	4.35E-05
12	H2O2 + H = H2O + OH	1.65E-03
13	H2O2 + H = HO2 + H2	2.64E-04
14	H2O2 + O = HO2 + OH	1.30E-04
15	H2O2 + OH = H2O + HO2	4.91E-03
16	H2O2 + M = OH + OH + M	-6.74E-03
17	H + H + M = H2 + M	1.49E-03
18	H + H + M = H2 + M	2.58E-05
19	H + H + M = H2 + M	1.88E-03
20	H + H + M = H2 + M	4.66E-05
21	H + OH + M = H2O + M	6.23E-02
22	O + O + M = O2 + M	5.54E-04
23	CO + OH = CO2 + H	3.89E-01
24	CO + HO2 = CO2 + OH	2.37E-04
25	CO + O + M = CO2 + M	2.27E-03
26	CO + O2 = CO2 + O	1.18E-05
27	CH + O2 = CHO + O	1.90E-02
28	CH + CO2 = CHO + CO	3.03E-02
29	CH + O = CO + H	2.22E-03
30	CH + OH = CHO + H	5.19E-03
31	CH + H2O = CH2O + H	6.89E-02
32	CH + CH2O = C2H2O + H	1.45E-03
33	CH + CH2(T) = C2H2 + H	1.88E-04
34	CH + CH3 = C2H3 + H	1.00E-03
35	CH + CH4 = C2H4 + H	2.87E-03
36	CH + C2H2 = C3H2 + H	5.53E-03
37	CHO + H = CO + H2	3.76E-02
38	CHO + O = CO + OH	1.91E-03
39	CHO + O = CO2 + H	1.91E-03
40	CHO + OH = CO + H2O	2.37E-02
41	CHO + O2 = CO + HO2	2.36E-03
42	CHO + M = CO + H + M	3.30E-01
43	CH2(S) + H2 = CH3 + H	1.45E-03
44	CH2(S) + H = CH + H2	1.00E-02
45	CH2(S) + O = CO + H + H	1.79E-04
46	CH2(S) + O = CO + H2	1.79E-04

Table 3.1.2.10 (CONTINUED)

47	CH2(S)	+	OH	=	CH2O	+	H		1.77E-03
48	CH2(S)	+	O2	=	CO	+	OH	+ H	1.38E-02
49	CH2(S)	+	CO2	=	CH2O	+	CO		1.40E-02
50	CH2(S)	+	CH3	=	C2H4	+	H		3.71E-04
51	CH2(S)	+	CH4	=	CH3	+	CH3		7.43E-04
52	CH2(S)	+	C2H2	=	C3H3	+	H		2.97E-02
53	CH2(S)	+	C2H2O	=	C2H4	+	CO		2.48E-03
54	CH2(S)	+	C2H4	=	C3H6				3.80E-03
55	CH2(S)	+	C2H6	=	C2H5	+	CH3		2.17E-04
56	CH2(S)	+	M	=	CH2(T)	+	M		1.58E-01
57	CH2(T)	+	H2	=	CH3	+	H		-1.85E-05
58	CH2(T)	+	H	=	CH	+	H2		1.04E-01
59	CH2(T)	+	O	=	CO	+	H	+ H	1.55E-02
60	CH2(T)	+	O	=	CO	+	H2		9.30E-03
61	CH2(T)	+	OH	=	CH	+	H2O		1.77E-02
62	CH2(T)	+	OH	=	CH2O	+	H		3.84E-02
63	CH2(T)	+	O2	=	CO	+	H	+ H	5.09E-04
64	CH2(T)	+	O2	=	CO2	+	H2		3.04E-03
65	CH2(T)	+	O2	=	CO	+	H2O		1.30E-04
66	CH2(T)	+	O2	=	CO2	+	H	+ H	6.09E-03
67	CH2(T)	+	O2	=	CH2O	+	O		1.81E-02
68	CH2(T)	+	O2	=	CHO	+	OH		1.90E-04
69	CH2(T)	+	CO2	=	CH2O	+	CO		1.06E-02
70	CH2(T)	+	CH2(T)	=	C2H2	+	H	+ H	1.76E-03
71	CH2(T)	+	CH3	=	C2H4	+	H		2.17E-02
72	CH2(T)	+	C2HO	=	C2H3	+	CO		9.16E-04
73	CH2(T)	+	C2H2	=	C3H3	+	H		6.04E-03
74	CH2(T)	+	C2H4	=	C3H6				3.66E-05
75	CH2O	+	H	=	CHO	+	H2		1.80E-01
76	CH2O	+	O	=	CHO	+	OH		1.23E-02
77	CH2O	+	OH	=	CHO	+	H2O		1.14E-01
78	CH2O	+	O2	=	CHO	+	HO2		5.64E-06
79	CH2O	+	M	=	CHO	+	H	+ M	-1.75E-05
80	CH3	+	CH3	=	C2H5	+	H		-3.20E-04
81	CH3	+	CH3	=	C2H6				2.97E-02
82	CH3	+	O	=	CH2O	+	H		1.18E-01
83	CH3	+	OH	=	CH2OH	+	H		2.10E-02
84	CH3	+	OH	=	CH2(S)	+	H2O		5.07E-03
85	CH3	+	OH	=	CH2O	+	H2		2.26E-05
86	CH3	+	OH	=	CH3O	+	H		-3.06E-05
87	CH3	+	O2	=	CH3O	+	O		9.60E-05
88	CH3	+	O2	=	CH2O	+	OH		8.00E-04
89	CH3	+	HO2	=	CH3O	+	OH		1.92E-04
90	CH3	+	CHO	=	CH4	+	CO		5.68E-03
91	CH3	+	M	=	CH2(S)	+	H	+ M	-4.20E-03
92	CH3	+	M	=	CH	+	H2	+ M	--3.33E-04
93	CH3O	+	H	=	CH2O	+	H2		8.04E-05
94	CH3O	+	O	=	CH2O	+	OH		3.30E-06
95	CH3O	+	OH	=	CH2O	+	H2O		1.75E-05
96	CH3O	+	O2	=	CH2O	+	HO2		1.87E-07
97	CH3O	+	M	=	CH2O	+	H	+ M	1.77E-04
98	CH2OH	+	H	=	CH2O	+	H2		5.48E-03
99	CH2OH	+	O	=	CH2O	+	OH		2.54E-04
100	CH2OH	+	OH	=	CH2O	+	H2O		1.26E-03
101	CH2OH	+	O2	=	CH2O	+	HO2		4.15E-03

Table 3.1.2.10 (CONTINUED)

102	CH2OH	+	M	=	CH2O	+	H	+	M	9.89E-03
103	CH4			=	CH3	+	H			-4.99E-02
104	CH4	+	H	=	CH3	+	H2			5.48E-02
105	CH4	+	O	=	CH3	+	OH			1.09E-02
106	CH4	+	OH	=	CH3	+	H2O			4.41E-02
107	CH4	+	O2	=	CH3	+	HO2			3.08E-06
108	C2H	+	H2	=	C2H2	+	H			-4.23E-03
109	C2H	+	O	=	CO	+	CH			7.01E-04
110	C2H	+	OH	=	C2HO	+	H			1.39E-03
111	C2H	+	O2	=	CO	+	CO	+	H	8.13E-03
112	C2H	+	CH3	=	C3H3	+	H			3.70E-04
113	C2HO	+	H	=	CH2(S)	+	CO			2.17E-01
114	C2HO	+	O	=	CO	+	CO	+	H	2.12E-02
115	C2HO	+	O2	=	CO	+	CO	+	H	2.43E-03
116	C2HO	+	O2	=	CO2	+	CO	+	H	2.43E-03
117	C2HO	+	CH	=	C2H2	+	CO			1.14E-04
118	C2HO	+	C2HO	=	C2H2	+	CO		+CO	1.93E-04
119	C2HO	+	C2H2	=	C3H3	+	CO			3.48E-04
120	C2H2	+	O	=	CH2(T)	+	CO			8.03E-02
121	C2H2	+	O	=	C2HO	+	H			1.43E-01
122	C2H2	+	OH	=	C2H	+	H2O			1.39E-02
123	C2H2	+	OH	=	C2H2O	+	H			1.99E-01
124	C2H2	+	OH	=	CH3	+	CO			6.05E-04
125	C2H2	+	O2	=	C2H	+	HO2			-2.79E-08
126	C2H2	+	O2	=	C2HO	+	OH			7.07E-04
127	C2H2	+	M	=	C2H	+	H	+	M	-7.75E-04
128	C2H2	+	CH3	=	C3H5(S)					-3.22E-03
129	C2H2O	+	M	=	CH2(T)	+	CO	+	M	4.54E-04
130	C2H2O	+	H	=	CH3	+	CO			7.89E-02
131	C2H2O	+	H	=	C2HO	+	H2			8.29E-02
132	C2H2O	+	O	=	CO2	+	CH2(T)			1.64E-03
133	C2H2O	+	O	=	C2HO	+	OH			1.30E-03
134	C2H2O	+	OH	=	CH2O	+	CHO			3.20E-02
135	C2H3	+	H	=	C2H2	+	H2			5.60E-02
136	C2H3	+	OH	=	C2H2	+	H2O			8.51E-03
137	C2H3	+	O	=	C2H2O	+	H			8.89E-04
138	C2H3	+	O2	=	CHO	+	CH2O			5.79E-04
139	C2H2	+	H	=	C2H3					-3.02E-01
140	C2H3	+	CH	=	C2H2	+	CH2(T)			9.10E-05
141	C2H3	+	C2H	=	C2H2	+	C2H2			6.27E-05
142	C2H4	+	H	=	C2H3	+	H2			3.10E-01
143	C2H4	+	O	=	CH3	+	CHO			1.19E-02
144	C2H4	+	OH	=	C2H3	+	H2O			4.74E-02
145	C2H4	+	M	=	C2H2	+	H2	+	M	1.13E-03
146	C2H4	+	M	=	C2H3	+	H	+	M	-7.61E-04
147	C2H5	+	O2	=	C2H4	+	HO2			2.21E-06
148	C2H5			=	C2H4	+	H			1.27E-01
149	C2H6			=	C2H5	+	H			-1.09E-03
150	C2H6	+	H	=	C2H5	+	H2			2.60E-02
151	C2H6	+	O	=	C2H5	+	OH			2.92E-04
152	C2H6	+	OH	=	C2H5	+	H2O			7.29E-03
153	C3H2	+	O	=	C2H	+	CHO			1.14E-03
154	C3H2	+	OH	=	C2H2	+	CHO			7.45E-03
155	C3H2	+	O2	=	C2HO	+	CO	+	H	3.29E-02
156	C3H3	+	H	=	C3H2	+	H2			2.39E-02

Table 3.1.2.10 (CONTINUED)

157	C3H3 + OH	=	C3H2 + H2O	7.54E-03
158	C3H3 + O2	=	C2H2O + CHO	4.51E-05
159	C3H3 + O	=	CH2O + C2H	1.12E-03
160	C3H4(A)	=	C3H4(P)	4.06E-04
161	C3H4(A)+ M	=	C3H3 + H + M	-3.93E-03
162	C3H4(A)+ H	=	C3H5(T)	-2.28E-03
163	C3H4(A)+ H	=	C3H5(A)	3.61E-03
164	C3H4(A)+ H	=	C3H3 + H2	2.48E-03
165	C3H4(A)+ O	=	C2H4 + CO	2.31E-03
166	C3H4(A)+ O	=	C2H2 + CH2O	2.70E-05
167	C3H4(A)+ OH	=	C2H2O + CH3	3.60E-03
168	C3H4(A)+ OH	=	C3H3 + H2O	4.19E-03
169	C3H4(A)+ O2	=	C3H3 + HO2	1.50E-09
170	C3H4(A)+ CH3	=	C3H3 + CH4	1.27E-03
171	C3H4(A)+ C2H	=	C3H3 + C2H2	6.17E-05
172	C3H4(A)+ C3H5(A)	=	C3H3 + C3H6	5.26E-04
173	C3H4(P) + M	=	C3H3 + H + M	-8.60E-04
174	C3H4(P)	=	C2H + CH3	-6.01E-03
175	C3H4(P)+ H	=	C3H5(T)	1.70E-04
176	C3H4(P)+ H	=	C3H5(S)	9.27E-04
177	C3H4(P)+ H	=	C3H3 + H2	2.68E-04
178	C3H4(P)+ O	=	C2H3 + CHO	2.02E-05
179	C3H4(P)+ O	=	C2H4 + CO	2.02E-05
180	C3H4(P)+ O	=	C2HO + CH3	3.97E-05
181	C3H4(P)+ OH	=	C2H2O + CH3	2.64E-05
182	C3H4(P)+ OH	=	C3H3 + H2O	4.66E-04
183	C3H4(P)+ O2	=	C3H3 + HO2	2.78E-10
184	C3H4(P)+ CH3	=	C3H3 + CH4	1.23E-04
185	C3H4(P)+ C2H	=	C3H3 + C2H2	6.65E-06
186	C3H4(P)+ C3H5(A)	=	C3H3 + C3H6	2.46E-05
187	C3H5(A)+ H	=	C3H4(A)+ H2	2.52E-03
188	C3H5(A)+ O2	=	CH2O + CH2O+ CH	1.63E-05
189	C3H5(A)+ CH3	=	C3H4(A)+ CH4	4.62E-04
190	C3H5(A)+ C2H5	=	C2H6 + C3H4(A)	4.99E-05
191	C3H5(A)+ C2H5	=	C2H4 + C3H6	5.01E-05
192	C3H5(A)+ C3H5(A)	=	C3H4(A)+ C3H6	3.17E-03
193	C3H5(S) + H	=	C3H4(A)+ H2	6.91E-08
194	C3H5(S) + O2	=	CH3 + CO + CH2O	3.59E-07
195	C3H5(S) + CH3	=	C3H4(A) + CH4	3.07E-09
196	C3H5(T)+ H	=	C3H4(P) + H2	1.39E-05
197	C3H5(T)+ O2	=	CH3 + CO + CH2O	5.19E-05
198	C3H5(T)+ CH3	=	C3H4(P) + CH4	4.19E-07
199	C3H6	=	C3H5(A)+ H	-1.27E-02
200	C3H6	=	C2H3 + CH3	-5.24E-03
201	C3H6 + H	=	C3H5(A) + H2	9.31E-03
202	C3H6 + H	=	C3H5(S) + H2	2.06E-03
203	C3H6 + H	=	C3H5(T) + H2	1.79E-03
204	C3H6 + O	=	C2H5 + CHO	6.22E-05
205	C3H6 + O	=	C2H4 + CH2O	4.15E-05
206	C3H6 + O	=	CH3 + CH3 + CO	8.29E-05
207	C3H6 + OH	=	C3H5(A) + H2O	2.27E-03
208	C3H6 + OH	=	C3H5(S) + H2O	5.61E-04
209	C3H6 + OH	=	C3H5(T) + H2O	7.08E-04
210	C3H6 + O2	=	C3H5(A) + HO2	5.39E-07
211	C3H6 + O2	=	C3H5(S) + HO2	7.24E-08

Table 3.1.2.10 (CONTINUED)

212	C3H6	+ O2	=	C3H5(T)	+ HO2		1.37E-07
213	C3H6	+ CH3	=	C3H5(A)	+ CH4		2.35E-04
214	C3H6	+ CH3	=	C3H5(S)	+ CH4		3.01E-04
215	C3H6	+ CH3	=	C3H5(T)	+ CH4		9.67E-05
216	C3H7(N)	+ H	=	C3H8			3.31E-07
217	C3H7(N)	+ O2	=	C3H6	+ HO2		1.20E-07
218	C3H7(N)		=	C2H4	+ CH3		1.08E-01
219	C3H7(N)		=	C3H6	+ H		-2.23E-03
220	C3H7(I)	+ H	=	C3H8			5.67E-07
221	C3H7(I)	+ O2	=	C3H6	+ HO2		4.33E-07
222	C3H7(I)		=	C2H4	+ CH3		2.66E-06
223	C3H7(I)		=	C3H6	+ H		1.22E-05
224	C3H8		=	C2H5	+ CH3		-1.27E-04
225	C3H8	+ H	=	C3H7(N)	+ H2		4.71E-05
226	C3H8	+ H	=	C3H7(I)	+ H2		1.89E-05
227	C3H8	+ O	=	C3H7(N)	+ OH		9.64E-08
228	C3H8	+ O	=	C3H7(I)	+ OH		1.22E-07
229	C3H8	+ OH	=	C3H7(N)	+ H2O		1.24E-05
230	C3H8	+ OH	=	C3H7(I)	+ H2O		1.00E-05
231	C3H8	+ CH3	=	C3H7(N)	+ CH4		2.26E-06
232	C3H8	+ CH3	=	C3H7(I)	+ CH4		1.71E-06
233	C2H2	+ C2H2	=	C4H4			2.64E-07
234	C2H2	+ C2H	=	C4H2	+ H		7.48E-03
235	C3H2	+ CH2(T)	=	C4H3(I)	+ H		3.10E-04
236	C3H3	+ CH	=	C4H3(N)	+ H		1.81E-04
237	C3H3	+ CH	=	C4H3(I)	+ H		1.81E-04
238	C3H3	+ CH2(T)	=	C4H4	+ H		2.19E-03
239	C3H3	+ C3H3	=	C6H5L	+ H		3.79E-03
240	C3H3	+ C3H4(A)	=	C6H6	+ H		8.87E-05
241	C4	+ H + M	=	C4H	+ M		5.16E-09
242	C4H	+ H2	=	C4H2	+ H		-3.23E-05
243	C4H	+ C2H2	=	C6H2	+ H		-3.65E-05
244	C4H	+ C4H2	=	C8H2	+ H		-2.30E-08
245	C4H2		=	C4H	+ H		-1.01E-04
246	C4H2	+ C2H	=	C6H2	+ H		9.49E-05
247	C4H2	+ C2H	=	C4H	+ C2H2		3.30E-05
248	C4H2	+ O	=	C3H2	+ CO		1.10E-04
249	C4H2	+ OH	=	C3H2	+ CHO		6.73E-03
250	C4H3(N)		=	C4H2	+ H		7.68E-06
251	C4H3(N)	+ H	=	C4H2	+ H2		3.56E-04
252	C4H3(N)	+ OH	=	C4H2	+ H2O		6.22E-05
253	C4H3(N)	+ M	=	C4H3(I)	+ M		6.81E-04
254	C4H3(I)		=	C4H2	+ H		-2.47E-04
255	C4H3(I)	+ H	=	C4H2	+ H2		4.40E-04
256	C4H3(I)	+ O	=	C2H2O	+ C2H		4.03E-06
257	C4H3(I)	+ OH	=	C4H2	+ H2O		7.095E-05
258	C4H3(I)	+ O2	=	C2H2O	+ C2HO		2.16E-05
259	C4H4		=	C4H3(I)	+ H		-1.16E-03
260	C4H4		=	C4H2	+ H2		-2.59E-05
261	C4H4	+ H	=	C4H3(N)	+ H2		6.16E-04
262	C4H4	+ H	=	C4H3(I)	+ H2		6.37E-03
263	C4H4	+ OH	=	C4H3(N)	+ H2O		4.17E-04
264	C4H4	+ OH	=	C4H3(I)	+ H2O		1.31E-03
265	C4H4	+ C2H	=	C4H3(I)	+ C2H2		8.96E-05
266	C4H4	+ C2H2	=	C6H5L	+ H		-8.63E-06

Table 3.1.2.10 (CONTINUED)

267	C4H4 + C2H3	=	C6H6 + H	3.76E-05
268	C4H5(S)	=	C4H4 + H	1.92E-04
269	C4H5(S) + H	=	C4H4 + H2	4.12E-04
270	C4H5(S) + OH	=	C4H4 + H2O	6.27E-05
271	C4H5(S)	=	C4H5(T)	1.08E-05
272	C4H5(T)	=	C4H4 + H	1.99E-06
273	C4H5(T)	=	C2H2 + C2H3	6.00E-03
274	C4H5(T) + H	=	C4H4 + H2	1.19E-05
275	C4H5(T) + OH	=	C4H4 + H2O	2.90E-06
276	C4H5(T) + M	=	C4H5(I) + M	-1.18E-03
277	C4H5(I)	=	C4H4 + H	1.13E-03
278	C4H5(I) + H	=	C4H4 + H2	1.46E-03
279	C4H5(I) + OH	=	C4H4 + H2O	4.90E-04
280	C3H3 + CH3	=	C4H6(S)	3.09E-03
281	C4H6(S) + H	=	C4H5(S) + H2	8.61E-04
282	C4H6(S) + H	=	C4H5(I) + H2	7.89E-04
283	C4H6(S) + H	=	C2H3 + C2H4	1.79E-05
284	C4H6(S) + OH	=	C4H5(S) + H2O	4.10E-04
285	C4H6(S) + OH	=	C4H5(I) + H2O	3.86E-04
286	C4H6(S) + CH3	=	C4H5(S) + CH4	5.42E-05
287	C4H6(S)	=	C4H6(T)	1.73E-04
288	C4H6(T)	=	C4H5(T) + H	-6.39E-05
289	C4H6(T)	=	C4H5(I) + H	-6.01E-03
290	C2H3 + C2H3	=	C4H6(T)	1.30E-03
291	C4H6(T) + H	=	C4H5(T) + H2	1.73E-03
292	C4H6(T) + H	=	C4H5(I) + H2	1.01E-02
293	C4H6(T) + H	=	C2H3 + C2H4	5.27E-04
294	C4H6(T) + O	=	C4H6O	1.04E-04
295	C4H6(T) + OH	=	C4H5(T) + H2O	2.16E-03
296	C4H6(T) + OH	=	C4H5(I) + H2O	3.51E-03
297	C4H6(T) + O2	=	C4H5(T) + HO2	2.06E-09
298	C4H6(T) + C2H3	=	C4H5(T) + C2H4	5.16E-04
299	C4H6(T) + C2H3	=	C4H5(I) + C2H4	-7.11E-04
300	C4H6(T) + CH3	=	C4H5(T) + CH4	1.45E-03
301	C4H6(T) + C3H3	=	C4H5(T) + C3H4(A)	-1.73E-05
302	CH2(S) + C3H4(P)	=	C4H6(B)	7.11E-05
303	C4H6(B)	=	C4H6(T)	2.20E-03
304	C4H6(B)	=	C4H6(S)	-2.14E-03
305	C4H6(S)	=	C4H6(F)	-1.00E-15
306	C3H3 + CH3	=	C4H6(F)	-1.00E-15
307	C4H6(F) + O	=	C3H6 + CO	-1.00E-15
308	C4H6O	=	C3H6 + CO	1.05E-04
309	C4H6O + H	=	C3H6 + CHO	2.75E-12
310	C6H5	=	C4H3(N) + C2H2	2.97E-04
311	C6H5L	=	C4H3(N) + C2H2	2.72E-05
312	C4H5(T) + C2H2	=	C6H6 + H	7.15E-06
313	C6H2 + H	=	C6H3	9.09E-05
314	C6H3 + H	=	C6H2 + H2	6.13E-05
315	C6H3 + H	=	C6H4	4.21E-05
316	C6H4 + H	=	C6H3 + H2	5.47E-06
317	C6H4 + H	=	C6H5	-1.00E-15
318	C6H4 + OH	=	C6H3 + H2O	5.27E-06
319	C6H5 + H	=	C6H4 + H2	-1.00E-15
320	C6H5 + O2	=	C6H5O + O	2.15E-04
321	C6H5 + OH	=	C6H5O + H	2.08E-03

Table 3.1.2.10 (CONTINUED)

322	C6H5L	=	C6H5	3.40E-03
323	C6H5L	=	C6H4 + H	-3.31E-05
324	C6H6	=	C6H5 + H	-4.90E-03
325	C6H6 + H	=	C6H5 + H2	3.99E-03
326	C6H6 + O	=	C6H5O + H	2.65E-04
327	C6H6 + O	=	C6H5 + OH	-1.00E-15
328	C6H6 + OH	=	C6H5 + H2O	2.16E-03
329	C6H6 + O2	=	C6H5O + OH	6.91E-06
330	C6H6 + CH3	=	C6H5 + CH4	1.51E-05
331	C6H5OH	=	C6H5O + H	-5.15E-04
332	C6H6 + OH	=	C6H5OH + H	1.37E-04
333	C6H5OH + H	=	C6H5O + H2	2.86E-04
334	C6H5OH + O	=	C6H5O + OH	2.91E-05
335	C6H5OH + OH	=	C6H5O + H2O	2.46E-04
336	C6H5O	=	C5H5 + CO	2.42E-03
337	C6H5OH	=	C5H6 + CO	9.59E-07
338	C5H5 + H	=	C5H6	3.01E-03
339	C5H5 + O	=	C4H5(T) + CO	3.03E-03
340	C5H5 + O	=	C5H5O	3.04E-05
341	C5H5 + OH	=	C5H4OH + H	6.36E-07
342	C5H5 + HO2	=	C5H5O + OH	1.44E-05
343	C5H6 + O	=	C5H5 + OH	6.85E-06
344	C5H6 + OH	=	C5H5 + H2O	3.79E-04
345	C5H6 + O2	=	C5H5 + HO2	1.16E-06
346	C5H6 + H	=	C5H5 + H2	2.62E-03
347	C5H6 + HO2	=	C5H5 + H2O2	4.90E-09
348	C5H5O	=	C4H5(T) + CO	7.44E-06
349	C5H4OH	=	C5H4O + H	3.46E-07
350	C5H5	=	C5H5(L)	1.50E-04
351	C3H3 + C2H2	=	C5H5(L)	3.63E-05
352	C5H5(L) + H	=	C5H6(L)	3.37E-05
353	C5H5(L) + H2	=	C5H6(L) + H	-1.34E-05
354	C5H6(L) + O	=	C5H5(L) + OH	8.06E-05
355	C5H6(L) + OH	=	C5H5(L) + H2O	-1.72E-04
356	C5H6(L) + O2	=	C5H5(L) + HO2	-2.49E-05
357	C5H6	=	C5H6(L)	-1.00E-15
358	C5H6(L)	=	C3H3 + C2H3	-3.49E-07
359	C6H5L + H	=	C3H4(A) + C3H2	-2.72E-06
360	C5H5(L)	=	C3H4(A) + C2H	-3.11E-06
361	CH2(T) + C4H2	=	C5H3(L) + H	3.26E-05
362	CH2(S) + C4H2	=	C5H3(L) + H	8.87E-06
363	C5H5(L) + H	=	C5H4(L) + H2	1.01E-04
364	C5H5(L) + OH	=	C5H4(L) + H2O	2.41E-05
365	C5H4(L) + H	=	C5H3(L) + H2	1.82E-04
366	C5H4(L) + OH	=	C5H3(L) + H2O	-2.48E-07
367	C2H2 + C2H2	=	C4H3(N) + H	-3.88E-04
368	C2H2 + C2H2	=	C4H3(I) + H	-7.16E-03
369	C2H2 + C2H2	=	C4H2 + H2	9.34E-05
370	C5H4O	=	CO + C4H4	9.93E-07
371	C6H5L + H	=	C6H4 + H2	1.44E-07
372	C6H5L + OH	=	C6H4 + H2O	1.75E-08
373	C5H6 + O2	=	C5H5O + OH	2.81E-06
374	C5H3(L) + O	=	C4H3(N) + CO	-1.00E-15
375	C2H3 + O2	=	C2H2 + HO2	-1.02E-04
376	C4H6(S)	=	C4H5(S) + H	-6.34E-04

Table 3.1.2.10 (CONCLUDED)

377	C4H6(S)		=	C4H5(I)	+	H	-9.45E-04
475†	C6H6		=	6C(S)	+	3H2	1.92E-07
476†	C2H2		=	2-C(S)	+	H2	6.67E-04
477†	C6H6		=	6C(S)	+	3H2	6.44E-06
478†	C(S)	+ OH	=	CO	+	H	1.46E-06
479†	C(S)	+ O	=	CO			1.20E-11
480†	C(S)	+ C(S) +O2	=	CO	+	CO	1.10E-06
481†	C(S)	+ H2O	=	CO	+	H2	-1.00E-15

† These reactions are specific to the soot model.

Table 3.1.2.11

Effect of Pyrolysis Rates on n-Heptane Consumption in Diffusion Flames

Reaction	Baseline Scheme Tmax = 1930K kmol/m^3/sec	Rxn 410/10 Tmax = 1927K kmol/m^3/sec	Rxn 411/10 Tmax = 1929K kmol/m^3/sec	No Pyrolysis Tmax = 1913K kmol/m^3/sec
410 C7H16 = C3H7(N) + P-C4H9	2.80E-01	5.00E-02	3.60E-01	-
411 C7H16 = C2H5 + 1-C5H11	1.35E-01	2.70E-01	1.72E-02	-
412 C7H16 = 1-C7H15 + H	3.05E-06	7.30E-06	4.30E-06	-
413 C7H16 = 2-C7H15 + H	3.05E-06	7.30E-06	4.30E-06	-
414 C7H16 = 3-C7H15 + H	3.05E-06	7.30E-06	4.30E-06	-
415 C7H16 = 4-C7H15 + H	3.05E-06	7.30E-06	4.30E-06	-
416 C7H16 + H = 1-C7H15 + H2	7.55E-02	7.79E-02	2.69E-02	9.03E-02
417 C7H16 + H = 2-C7H15 + H2	6.97E-02	7.11E-02	7.07E-02	7.16E-02
418 C7H16 + H = 3-C7H15 + H2	6.98E-02	7.11E-02	7.07E-02	7.16E-02
419 C7H16 + H = 4-C7H15 + H2	3.45E-02	3.52E-02	3.50E-02	3.47E-02
429 C7H16 + CH3 = 2-C7H15 + CH4	1.89E-02	1.85E-02	1.87E-02	2.33E-02
430 C7H16 + CH3 = 3-C7H15 + CH4	1.89E-02	1.85E-02	1.87E-02	2.33E-02
428 C7H16 + CH3 = 1-C7H15 + CH4	1.50E-02	1.49E-02	1.49E-02	2.05E-02
431 C7H16 + CH3 = 4-C7H15 + CH4	9.44E-03	9.27E-02	9.37E-02	1.16E-02
424 C7H16 + OH = 1-C7H15 + H2O	3.08E-03	3.55E-03	3.24E-03	9.33E-03
425 C7H16 + OH = 2-C7H15 + H2O	2.51E-03	2.90E-03	2.64E-03	7.74E-03
426 C7H16 + OH = 3-C7H15 + H2O	2.51E-03	2.90E-03	2.64E-03	3.70E-03
427 C7H16 + OH = 4-C7H15 + H2O	2.51E-03	2.90E-03	2.64E-03	7.74E-03
445 C7H16 + C3H5(A) = 2-C7H15 + C3H6	7.59E-05	1.49E-04	9.89E-05	1.45E-03
446 C7H16 + C3H5(A) = 3-C7H15 + C3H6	7.59E-05	1.49E-04	9.89E-05	1.45E-03
420 C7H16 + O = 1-C7H15 + OH	1.00E-04	1.26E-04	1.06E-04	5.99E-04
447 C7H16 + C3H5(A) = 4-C7H15 + C3H6	3.80E-05	7.27E-05	4.95E-05	7.27E-04
437 C7H16 + C2H5 = 2-C7H15 + C2H6	5.54E-04	4.22E-04	5.03E-04	8.41E-05
438 C7H16 + C2H5 = 3-C7H15 + C2H6	5.54E-04	4.22E-04	5.03E-04	8.41E-05
444 C7H16 + C3H5(A) = 1-C7H15 + C3H6	1.74E-05	3.46E-05	2.27E-05	3.52E-04
439 C7H16 + C2H5 = 4-C7H15 + C2H6	2.77E-04	2.12E-04	2.51E-04	4.21E-05
433 C7H16 + HO2 = 2-C7H15 + H2O2	1.70E-05	1.04E-05	1.46E-05	2.03E-06
434 C7H16 + HO2 = 3-C7H15 + H2O2	1.70E-05	1.04E-05	1.46E-05	2.03E-06
421 C7H16 + O = 2-C7H15 + OH	1.57E-05	2.09E-05	1.71E-05	1.28E-04
422 C7H16 + O = 3-C7H15 + OH	1.57E-05	2.09E-05	1.67E-05	1.28E-04
441 C7H16 + C2H3 = 2-C7H15 + C2H4	7.30E-05	7.46E-05	7.35E-05	4.86E-05
442 C7H16 + C2H3 = 3-C7H15 + C2H4	7.30E-05	7.46E-05	7.35E-05	4.86E-05
436 C7H16 + C2H5 = 1-C7H15 + C2H6	1.14E-04	8.76E-05	1.04E-04	1.88E-05
440 C7H16 + C2H3 = 1-C7H15 + C2H4	5.69E-05	5.92E-05	5.82E-05	4.02E-05
423 C7H16 + O = 4-C7H15 + OH	7.87E-06	1.05E-05	8.55E-06	6.40E-05
443 C7H16 + C2H3 = 4-C7H15 + C2H4	3.61E-05	3.74E-05	3.69E-05	2.44E-05
432 C7H16 + HO2 = 1-C7H15 + H2O2	6.19E-06	3.78E-06	5.33E-06	1.34E-06
435 C7H16 + HO2 = 4-C7H15 + H2O2	8.55E-06	5.25E-06	7.34E-06	1.02E-06
450 C7H16 + O2 = 3-C7H15 + HO2	9.13E-08	1.42E-07	1.08E-07	1.17E-06
449 C7H16 + O2 = 2-C7H15 + HO2	9.09E-08	1.43E-07	1.07E-07	1.16E-06
451 C7H16 + O2 = 4-C7H15 + HO2	4.57E-08	7.13E-08	5.40E-08	5.83E-07
448 C7H16 + O2 = 1-C7H15 + HO2	3.33E-08	5.22E-08	3.94E-08	4.54E-07

Table 3.1.4.1
n-Heptane Consumption in Stirred Reactors

	Reaction							T=1000K τ=180 msec rate kmol/m^3/sec	T=2000K τ=180 msec rate kmol/m^3/sec
425	C7H16	+	OH	=	1-C7H15	+	H2O	9.99E-06	1.10E-07
428	C7H16	+	OH	=	4-C7H15	+	H2O	8.28E-06	9.55E-08
426	C7H16	+	OH	=	2-C7H15	+	H2O	8.27E-06	9.55E-08
427	C7H16	+	OH	=	3-C7H15	+	H2O	8.27E-06	9.55E-08
418	C7H16	+	H	=	2-C7H15	+	H2	4.33E-06	5.17E-08
419	C7H16	+	H	=	3-C7H15	+	H2	4.33E-06	5.17E-08
417	C7H16	+	H	=	1-C7H15	+	H2	3.43E-06	8.09E-08
421	C7H16	+	O	=	1-C7H15	+	OH	2.55E-06	3.76E-07
420	C7H16	+	H	=	4-C7H15	+	H2	2.14E-06	2.56E-08
454	C7H16	+	CH3O	=	2-C7H15	+	CH3OH	2.18E-06	-7.90E-16
455	C7H16	+	CH3O	=	3-C7H15	+	CH3OH	2.18E-06	-7.90E-16
430	C7H16	+	CH3	=	2-C7H15	+	CH4	1.72E-06	3.26E-13
431	C7H16	+	CH3	=	3-C7H15	+	CH4	1.72E-06	3.26E-13
434	C7H16	+	HO2	=	2-C7H15	+	H2O2	1.12E-06	8.90E-14
435	C7H16	+	HO2	=	3-C7H15	+	H2O2	1.12E-06	8.90E-14
429	C7H16	+	CH3	=	1-C7H15	+	CH4	1.12E-06	3.60E-13
432	C7H16	+	CH3	=	4-C7H15	+	CH4	8.61E-07	1.62E-13
436	C7H16	+	HO2	=	4-C7H15	+	H2O2	5.62E-07	4.43E-14
433	C7H16	+	HO2	=	1-C7H15	+	H2O2	5.50E-07	8.00E-14
422	C7H16	+	O	=	2-C7H15	+	OH	2.55E-07	9.48E-08
423	C7H16	+	O	=	3-C7H15	+	OH	2.55E-07	9.48E-08
410	C7H16			=	C3H7(N)	+	P-C4H9	2.03E-07	3.82E-05
424	C7H16	+	O	=	4-C7H15	+	OH	1.27E-07	4.74E-08
453	C7H16	+	CH3O	=	1-C7H15	+	CH3OH	1.15E-07	-9.82E-16
456	C7H16	+	CH3O	=	4-C7H15	+	CH3OH	1.09E-07	-9.90E-16
411	C7H16			=	C2H5	+	1-C5H11	9.64E-08	1.86E-05
446	C7H16	+	C3H5(A)	=	2-C7H15	+	C3H6	2.21E-08	-6.89E-16
447	C7H16	+	C3H5(A)	=	3-C7H15	+	C3H6	2.21E-08	-6.89E-16
412	C7H16			=	1-C6H13	+	CH3	2.16E-08	8.86E-06
438	C7H16	+	C2H5	=	2-C7H15	+	C2H6	1.79E-08	-9.94E-16
439	C7H16	+	C2H5	=	3-C7H15	+	C2H6	1.79E-08	-9.94E-16
448	C7H16	+	C3H5(A)	=	4-C7H15	+	C3H6	1.11E-08	-8.45E-16
440	C7H16	+	C2H5	=	4-C7H15	+	C2H6	8.98E-09	-9.97E-16
459	C7H16	+	O2	=	3-C7H15	+	HO2	5.01E-09	6.20E-12
458	C7H16	+	O2	=	2-C7H15	+	HO2	4.99E-09	6.16E-12
445	C7H16	+	C3H5(A)	=	1-C7H15	+	C3H6	4.02E-09	-9.07E-16
437	C7H16	+	C2H5	=	1-C7H15	+	C2H6	3.96E-09	-9.47E-16
460	C7H16	+	O2	=	4-C7H15	+	HO2	2.51E-09	3.10E-12
457	C7H16	+	O2	=	1-C7H15	+	HO2	1.56E-09	2.73E-12
449	C7H16	+	1-C4H7	=	1-C7H15	+	1-C4H8	7.95E-11	-1.00E-15
442	C7H16	+	C2H3	=	2-C7H15	+	C2H4	7.36E-11	3.59E-16
443	C7H16	+	C2H3	=	37H15	+	C2H4	7.36E-11	3.59E-16
441	C7H16	+	C2H3	=	1-C7H15	+	C2H4	5.07E-11	2.65E-16
444	C7H16	+	C2H3	=	4-C7H15	+	C2H4	3.69E-11	-3.19E-16
450	C7H16	+	1-C4H7	=	2-C7H15	+	1-C4H8	2.08E-11	-1.00E-15
451	C7H16	+	1-C4H7	=	3-C7H15	+	1-C4H8	2.08E-11	-1.00E-15
416	C7H16			=	4-C7H15	+	H	1.17E-12	3.09E-08
452	C7H16	+	1-C4H7	=	4-C7H15	+	1-C4H8	1.05E-11	-1.00E-15
413	C7H16			=	1-C7H15	+	H	9.50E-13	3.09E-08
414	C7H16			=	2-C7H15	+	H	9.52E-13	3.09E-08
415	C7H16			=	3-C7H15	+	H	8.03E-13	3.09E-08

Table 3.1.4.2
Heptyl Radicals Consumption in Stirred Reactors

	Reaction	T=1000K τ=180 msec rate kmol/m^3/sec	T=2000K τ=180 msec rate kmol/m^3/sec
462	2-C7H15 = C3H6 + P-C4H9	2.24E-05	1.29E-05
461	1-C7H15 = C2H4 + 1-C5H11	1.79E-05	1.80E-05
465	4-C7H15 = 1-C5H10 + C2H5	1.27E-05	9.41E-06
473	1-C7H15 = 3-C7H15	-5.81E-06	4.26E-07
463	3-C7H15 = C3H7(N) + 1-C4H8	5.57E-06	3.30E-06
475	2-C7H15 = 3-C7H15	-3.48E-06	3.45E-20
472	1-C7H15 = 2-C7H15	2.67E-06	2.48E-06
474	1-C7H15 = 4-C7H15	1.68E-06	1.32E-07
464	3-C7H15 = 1-C6H12 + CH3	1.25E-06	1.98E-06
481	4-C7H15 + O2 = 3-C7H14 + HO2	1.89E-07	1.20E-11
479	3-C7H15 + O2 = 2-C7H14 + HO2	1.56E-07	6.00E-12
480	3-C7H15 + O2 = 3-C7H14 + HO2	1.56E-07	6.00E-12
476	1-C7H15 + O2 = 1-C7H14 + HO2	1.33E-07	5.28E-12
478	2-C7H15 + O2 = 2-C7H14 + HO2	1.31E-07	6.00E-12
477	2-C7H15 + O2 = 1-C7H14 + HO2	5.78E-08	2.82E-12
469	3-C7H15 = 2-C7H14 + H	3.78E-08	3.85E-07
470	3-C7H15 = 3-C7H14 + H	3.78E-08	3.85E-07
467	2-C7H15 = 1-C7H14 + H	3.12E-08	3.85E-07
468	2-C7H15 = 2-C7H14 + H	3.12E-08	3.85E-07
471	4-C7H15 = 3-C7H14 + H	2.28E-08	3.85E-07
466	1-C7H15 = 1-C7H14 + H	2.04E-08	3.85E-07

Table 3.1.4.3
1-Heptene Consumption in Stirred Reactors

	Reaction	T=1000K τ=180 msec rate kmol/m^3/sec	T=2000K τ=180 msec rate kmol/m^3/sec
498	1-C7H14 + HO2 = C7H13 + H2O2	2.26E-07	6.67E-16
482	1-C7H14 = C3H5(A) + P-C4H9	5.12E-09	4.28E-07
486	1-C7H14 + H = C7H13 + H2	4.45E-09	5.40E-11
492	1-C7H14 + OH = C7H13 + H2O	6.93E-10	3.58E-11
510	1-C7H14 + OH = C2H3 + 1-C5H10 + H2O	6.54E-10	5.01E-11
511	1-C7H14 + OH = C3H5(A) + 1-C4H8 + H2O	6.54E-10	5.01E-11
512	1-C7H14 + OH = 1-C4H7 + C3H6 + H2O	6.54E-10	5.01E-11
513	1-C7H14 + OH = C5H9 + C2H4 + H2O	3.11E-10	2.75E-11
489	1-C7H14 + O = C7H13 + OH	4.36E-11	1.36E-11
495	1-C7H14 + CH3 = C7H13 + CH4	4.11E-11	-9.64E-16
501	1-C7H14 + O = C2H3 + 1-C5H10 + OH	1.68E-11	7.12E-12
502	1-C7H14 + O = C3H5(A) + 1-C4H8 + OH	1.68E-11	7.12E-12
503	1-C7H14 + O = 1-C4H7 + C3H6 + OH	1.68E-11	7.12E-12
504	1-C7H14 + O = C5H9 + C2H4 + OH	7.85E-12	7.12E-12

Table 3.1.4.4
2-Heptene Consumption in Stirred Reactors

Reaction									T=1000K τ=180 msec rate kmol/m^3/sec	T=2000K τ=180 msec rate kmol/m^3/sec
499	2-C7H14	+	HO2	=	C7H13	+	H2O2		3.80E-07	-2.15E-16
483	2-C7H14			=	1-C4H7	+	C3H7(N)		-5.04E-08	4.28E-07
487	2-C7H14	+	H	=	C7H13	+	H2		1.51E-08	9.35E-11
493	2-C7H14	+	OH	=	C7H13	+	H2O		2.38E-09	6.21E-11
514	2-C7H14	+	OH	=	C3H5(A)+		1-C4H8	+ H2O	1.01E-09	4.51E-11
515	2-C7H14	+	OH	=	1-C4H7	+	C3H6	+ H2O	1.01E-09	4.51E-11
516	2-C7H14	+	OH	=	C5H9	+	C2H4	+ H2O	5.34E-10	2.75E-11
490	2-C7H14	+	O	=	C7H13	+	OH		1.50E-10	2.36E-11
496	2-C7H14	+	CH3	=	C7H13	+	CH4		1.41E-10	-9.28E-16
505	2-C7H14	+	O	=	C3H5(T) +		1-C4H8	+ OH	2.89E-11	7.12E-12
506	2-C7H14	+	O	=	1-C4H7	+	C3H6	+ OH	2.89E-11	7.12E-12
507	2-C7H14	+	O	=	C5H9	+	C2H4	+ OH	-1.00E-15	-9.99E-16

Table 3.1.4.5
3-Heptene Consumption in Stirred Reactors

Reaction									T=1000K τ=180 msec rate kmol/m^3/sec	T=2000K τ=180 msec rate kmol/m^3/sec
500	3-C7H14	+	HO2	=	C7H13	+	H2O2		3.79E-07	-2.15E-16
488	3-C7H14	+	H	=	C7H13	+	H2		1.50E-08	9.35E-11
494	3-C7H14	+	OH	=	C7H13	+	H2O		2.37E-09	6.21E-11
485	3-C7H14			=	1-C6H11 +		CH3		1.07E-09	5.59E-07
517	3-C7H14	+	OH	=	1-C4H7	+	C3H6	+ H2O	1.01E-09	4.51E-11
518	3-C7H14	+	OH	=	C5H9	+	C2H4	+ H2O	9.30E-10	3.63E-11
484	3-C7H14			=	C2H5	+	C5H9		-2.34E-10	6.28E-08
491	3-C7H14	+	O	=	C7H13	+	OH		1.49E-10	2.36E-11
497	3-C7H14	+	CH3	=	C7H13	+	CH4		1.43E-10	-9.27E-16
508	3-C7H14	+	O	=	1-C4H7	+	C3H6	+ OH	2.88E-11	7.12E-12
509	3-C7H14	+	O	=	C5H9	+	C2H4	+ OH	1.34E-11	6.48E-12

Table 3.1.4.6
Heptene Radical Consumption in Stirred Reactors

Reaction							T=1000K τ=180 msec rate kmol/m^3/sec	T=2000K τ=180 msec rate kmol/m^3/sec
519	C7H13	=	C3H5(A) +	1-C4H8			6.65E-07	1.33E-05
520	C7H13	=	C3H4(A) +	P-C4H9			2.64E-07	3.27E-06
521	C7H13	=	C4H6(S) +	C3H7(N)			9.64E-08	3.19E-06

Table 3.1.4.7
Hexyl Radicals Consumption in Stirred Reactors

Reaction							T=1000K τ=180 msec rate kmol/m^3/sec	T=2000K τ=180 msec rate kmol/m^3/sec
522	1-C6H13	=	2-C6H13				-5.07E-07	2.10E-06
523	1-C6H13	=	C2H4	+	P-C4H9		2.25E-07	1.80E-05
524	2-C6H13	=	C3H7(N) +	C3H6			1.04E-08	1.29E-05

Table 3.1.4.8
1-Hexene Consumption in Stirred Reactors

	Reaction									T=1000K τ=180 msec rate kmol/m^3/sec	T=2000K τ=180 msec rate kmol/m^3/sec
537	1-C6H12	+	OH	=	C2H3	+	1-C4H8	+	H2O	7.52E-08	2.78E-11
538	1-C6H12	+	OH	=	C3H5(A)	+	C3H6	+	H_2O	7.52E-08	2.78E-11
527	1-C6H12	+	H	=	1-C6H11	+	H2			6.36E-08	3.69E-12
525	1-C6H12			=	C3H7(N)	+	C3H5(A)			3.69E-08	1.48E-08
539	1-C6H12	+	OH	=	1-C4H7	+	C2H4	+	H_2O	3.57E-08	1.52E-11
526	1-C6H12			=	C3H6	+	C3H6			1.60E-08	2.19E-10
529	1-C6H12	+	OH	=	1-C6H11	+	H2O			1.58E-08	3.92E-12
531	1-C6H12	+	HO2	=	1-C6H11	+	H2O2			1.58E-08	-9.99E-16
528	1-C6H12	+	O	=	1-C6H11	+	OH			9.96E-09	1.49E-11
530	1-C6H12	+	CH3	=	1-C6H11	+	CH4			9.39E-09	-9.61E-16
533	1-C6H12	+	O	=	C3H5(A)	+	C3H6	+	OH	3.84E-09	7.84E-12
540	1-C6H12	+	OH	=	CH_2O	+	1-C5H11			2.93E-09	3.81E-13
541	1-C6H12	+	OH	=	C2H4O	+	P-C4H9			2.92E-09	3.81E-13
532	1-C6H12	+	O	=	C2H3	+	1-C4H8	+	OH	1.93E-10	7.84E-12
535	1-C6H12	+	O	=	CHO	+	1-C5H11			1.86E-10	1.02E-13
536	1-C6H12	+	O	=	CH3	+	P-C4H9	+	CO	1.86E-10	1.02E-13
534	1-C6H12	+	O	=	1-C4H7	+	C2H4	+	OH	1.80E-09	7.15E-12

Table 3.1.4.9
1-Hexene Radical Consumption in Stirred Reactors

	Reaction						T=1000K τ=180 msec rate kmol/m^3/sec	T=2000K τ=180 msec rate kmol/m^3/sec
542	1-C6H11	=	C3H6	+	C3H5(A)		9.65E-08	2.66E-05
543	1-C6H11	=	C2H5	+	C4H6(T)		3.51E-09	1.59E-06

Table 3.1.4.10
1-Pentyl Radical Consumption in Stirred Reactors

	Reaction					T=1000K τ=180 msec rate kmol/m^3/sec	T=2000K τ=180 msec rate kmol/m^3/sec
409	1-C5H11	=	C3H7(N)	+	C2H4	2.12E-05	3.87E-05
544	1-C5H11	=	1-C5H10	+	H	-2.28E-06	1.21E-06

Table 3.1.4.11
1-Pentene Consumption Stirred Reactors

	Reaction								T=1000K τ=180 msec rate kmol/m^3/sec	T=2000K τ=180 msec rate kmol/m^3/sec
553	1-C5H10	+	OH	=	C5H9	+	H2O		1.87E-06	8.59E-10
408	1-C5H10			=	C2H5	+	C3H5 (A)		1.63E-06	1.24E-06
545	1-C5H10	+	H	=	C5H9	+	H2		1.15E-06	1.20E-10
556	1-C5H10	+	OH	=	C3H5(A)+		C2H4	+ H2O	9.59E-07	4.85E-10
557	1-C5H10	+	OH	=	C3H6	+	C2H3	+ H2O	4.80E-07	2.43E-10
546	1-C5H10	+	O	=	C5H9	+	OH		1.75E-07	7.01E-10
549	1-C5H10	+	O	=	1-C4H8	+	CH2O		6.94E-08	6.27E-11
550	1-C5H10	+	O	=	C2H4O	+	C3H6		6.94E-08	6.27E-11
559	1-C5H10	+	CH3	=	C5H9	+	CH4		1.60E-08	-8.75E-16
554	1-C5H10	+	OH	=	P-C4H9	+	CH2O		1.28E-08	2.73E-12
555	1-C5H10	+	OH	=	C3H7(N)	+	C2H4O		1.21E-08	2.73E-12
551	1-C5H10	+	O	=	C3H5(A)	+	C2H4	+ OH	4.81E-09	2.53E-11
552	1-C5H10	+	O	=	C3H6	+	C2H3	+ OH	2.41E-09	1.27E-11
558	1-C5H10	+	O2	=	C5H9	+	HO2		1.29E-09	1.07E-14
547	1-C5H10	+	O	=	P-C4H9	+	CHO		8.15E-10	7.36E-13
548	1-C5H10	+	O	=	C3H7(N)	+	C2H3O		8.15E-10	7.36E-13

Table 3.1.4.12
Pentenyl Radical Consumption in Stirred Reactors

	Reaction					T=1000K τ=180 msec rate kmol/m^3/sec	T=2000K τ=180 msec rate kmol/m^3/sec
405	C5H9	=	C3H5(A)	+	C2H4	1.61E-06	1.32E-05
406	C5H9	=	C2H3	+	C3H6	1.48E-06	1.32E-05
407	C5H9	=	C4H6(S)	+	CH3	1.24E-07	3.20E-06

Table 3.1.4.13
n-Butyl Radical Consumption in Stirred Reactors

	Reaction							T=1000K τ=180 msec rate kmol/m^3/sec	T=2000K τ=180 msec rate kmol/m^3/sec
402	P-C4H9		=	C2H5	+	C2H4		2.53E-05	2.43E-05
403	P-C4H9		=	1-C4H8	+	H		2.27E-06	9.67E-07
404	P-C4H9	+ O2	=	1-C4H8	+	HO2		1.43E-07	7.14E-12

Table 3.1.4.14
1-Butene Consumption

	Reaction									T=1000K τ=180 msec rate kmol/m^3/sec	T=2000K τ=180 msec rate kmol/m^3/sec
389	1-C4H8			=	C3H5(A)	+	CH3			-6.45E-06	9.91E-07
392	1-C4H8	+	H	=	1-C4H7	+	H2			3.08E-06	4.43E-11
393	1-C4H8	+	OH	=	C3H7(N)	+	CH2O			1.19E-06	3.38E-11
395	1-C4H8	+	OH	=	1-C4H7	+	H2O			6.85E-07	4.16E-11
396	1-C4H8	+	O	=	C2H5	+	CH3	+	CO	1.23E-07	1.84E-11
560	1-C4H8	+	OH	=	C2H4O	+	C2H5			-1.00E-07	5.19E-13
562	1-C4H8	+	O	=	C2H4O	+	C2H4			9.48E-08	1.42E-11
561	1-C4H8	+	O	=	C3H6	+	CH2O			2.91E-08	3.51E-12
390	1-C4H8	+	O2	=	1-C4H7	+	HO2			-2.46E-08	1.24E-15
399	1-C4H8	+	CH3	=	1-C4H7	+	CH4			2.28E-08	-9.76E-16
397	1-C4H8	+	O	=	1-C4H7	+	OH			1.57E-08	5.81E-12
400	1-C4H8	+	C2H5	=	1-C4H7	+	C2H6			4.26E-09	-9.99E-16
401	1-C4H8	+	C3H5(A)	=	1-C4H7	+	C2H6			-4.26E-09	-9.99E-16
388	1-C4H8			=	1-C4H7	+	H			-2.62E-09	3.78E-11
394	1-C4H8	+	OH	=	C2H6	+	CH3	+	CO	1.83E-09	5.10E-14
398	1-C4H8	+	HO2	=	1-C4H7	+	H2O2			1.20E-09	-9.99E-16
391	1-C4H8			=	C2H3	+	C2H5			-9.25E-17	4.04E-11

Table 3.1.4.15
1-Butene Radical Consumption in Stirred Reactors

	Reaction									T=1000K τ=180 msec rate kmol/m^3/sec	T=2000K τ=180 msec rate kmol/m^3/sec
381	1-C4H7	+	O2	=	C4H6(T)	+	HO2			3.35E-06	8.73E-13
378	1-C4H7			=	C4H6(T)	+	H			2.39E-07	4.92E-07
379	1-C4H7			=	C2H4	+	C2H3			1.05E-07	9.05E-09
386	1-C4H7	+	C3H5(A)	=	C4H6(T)	+	C3H6			5.70E-08	-6.38E-16
382	1-C4H7	+	CH3	=	C4H6(T)	+	CH4			1.15E-08	8.91E-15
380	1-C4H7	+	H	=	C4H6(T)	+	H2			1.78E-09	5.04E-11
384	1-C4H7	+	C2H5	=	C4H6(T)	+	C2H6			1.25E-09	-9.99E-16
385	1-C4H7	+	C2H5	=	1-C4H8	+	C2H4			1.56E-10	-9.99E-16
387	1-C4H7	+	HO2	=	C4H6(T)	+	1-C4H8			5.27E-11	-1.00E-15
383	1-C4H7	+	C2H3	=	C4H6(T)	+	C2H4			1.52E-11	-8.18E-16

Table 3.1.4.16
Propane Consumption in Stirred Reactors

	Reaction									T=1000K τ=180 msec rate kmol/m^3/sec	T=2000K τ=180 msec rate kmol/m^3/sec
224	C3H8			=	C2H5	+	CH3			-2.00E-08	1.82E-09
229	C3H8	+	OH	=	C3H7(N)	+	H2O			2.61E-09	5.95E-11
230	C3H8	+	OH	=	C3H7(I)	+	H2O			2.17E-09	4.00E-11
225	C3H8	+	H	=	C3H7(N)	+	H2			1.25E-09	1.41E-11
226	C3H8	+	H	=	C3H7(I)	+	H2			3.80E-10	4.71E-12
228	C3H8	+	O	=	C3H7(I)	+	OH			7.69E-11	5.64E-12
227	C3H8	+	O	=	C3H7(N)	+	OH			4.64E-11	5.82E-12
231	C3H8	+	CH3	=	C3H7(N)	+	CH4			4.64E-11	-8.34E-16
232	C3H8	+	CH3	=	C3H7(I)	+	CH4			4.51E-11	-9.00E-16
579	C3H8	+	C2H5	=	C3H7(N)	+	C2H6			-1.76E-12	-1.00E-15

Table 3.1.4.17
Acetaldehyde Consumption in Stirred Reactors

	Reaction								T=1000K τ=180 msec rate kmol/m^3/sec	T=2000K τ=180 msec rate kmol/m^3/sec
560	1-C4H8	+	OH	=	C2H4O	+	C2H5		-1.00E-07	5.19E-13
564	C2H4O	+	H	=	C2H3O	+	H2		9.09E-09	6.46E-11
568	C2H4O	+	HO2	=	C2H3O	+	H2O2		5.21E-09	-7.40E-16
570	C2H4O	+	CH3	=	C2H3O	+	CH4		2.38E-09	9.85E-15
566	C2H4O	+	O2	=	C2H3O	+	HO2		3.08E-10	9.38E-14
565	C2H4O	+	O	=	C2H3O	+	OH		2.56E-10	1.55E-11
563	C2H4O	+	M	=	CH3	+	CHO	+ M	2.26E-12	2.54E-13
569	C2H4O	+	CH2(T)	=	C2H3O	+	CH3		1.07E-13	5.42E-16
567	C2H4O	+	OH	=	C2H3O	+	H2O		-9.99E-16	-1.00E-15

Table 3.1.4.18
Acetyl Radical Consumption in Stirred Reactors

	Reaction							T=1000K τ=180 msec rate kmol/m^3/sec	T=2000K τ=180 msec rate kmol/m^3/sec
571	C2H3O			=	CH3	+	CO	2.50E-08	7.91E-08
573	C2H3O	+	CH3	=	C2H6	+	CO	4.44E-13	4.86E-14
572	C2H3O	+	H	=	C2H2O	+	H2	7.72E-15	8.26E-12

Table 3.1.4.19
Ketene Consumption in Stirred Reactors

	Reaction							T=1000K τ=180 msec rate kmol/m^3/sec	T=2000K τ=180 msec rate kmol/m^3/sec
574	C2H2O	+	O2	=	CH2O	+	CO2	1.18E-07	7.99E-09
130	C2H2O	+	H	=	CH3	+	CO	4.17E-10	7.10E-06
134	C2H2O	+	OH	=	CH2O	+	CHO	2.11E-10	1.94E-05
131	C2H2O	+	H	=	C2HO	+	H2	1.15E-10	9.39E-06
129	C2H2O	+	M	=	CH2(T)	+	CO + M	-5.07E-11	6.70E-06
132	C2H2O	+	O	=	CO2	+	CH2(T)	4.64E-12	1.06E-06
133	C2H2O	+	O	=	C2HO	+	OH	9.36E-13	1.10E-06
53	CH2(S)	+	C2H2O	=	C2H4	+	CO	7.19E-14	2.04E-09

Table 3.1.4.20
Methyl Alcohol Consumption in Stirred Reactors

	Reaction							T=1000K τ=180 msec rate kmol/m^3/sec	T=2000K τ=180 msec rate kmol/m^3/sec
576	CH3OH	+	OH	=	CH3O	+	H2O	4.66E-07	-1.87E-12
575	CH3OH	+	HO2	=	CH3O	+	H2O2	-1.05E-07	-2.35E-14
578	CH3OH	+	CH2O	=	CH3O	+	CH3O	-7.95E-09	-1.00E-15
577	CH3OH	+	O	=	CH3O	+	OH	6.99E-09	7.87E-13

Table 3.1.4.21
Formaldehyde Consumption in Stirred Reactors

Reaction	T=1000K τ=180 msec rate kmol/m^3/sec	T=2000K τ=180 msec rate kmol/m^3/sec
75 CH2O + H = CHO + H2	5.25E-06	4.74E-05
77 CH2O + OH = CHO + H2O	5.17E-06	1.05E-04
581CH2O + HO2 = CHO + H2O2	6.85E-07	3.55E-11
582CH2O + CH3 = CHO + CH4	3.94E-07	3.04E-09
580CH2O + CH3O = CH3OH + CHO	1.71E-07	3.65E-14
76 CH2O + O = CHO + OH	1.18E-07	1.49E-05
32CH + CH2O = C2H2O + H	8.14E-09	4.44E-09
78 CH2O + O2 = CHO + HO2	3.89E-08	1.94E-08
79 CH2O + M = CHO + H + M	-4.90E-12	2.39E-07

APPENDIX D
TOLUENE/*n*-HEPTANE AND TOLUENE SUB-MECHANISMS

TABLE D1
Toluene/*n*-Heptane Sub-mechanism for Diffusion Flames

	ELEMENTARY REACTION								A m^3, Kmol, sec^{-1}	n	E_a J/mol	REF
375	C7H8L			=	C7H8				0.3000E+11	0	0.0000E+00	19,22
376	C7H8	+	O	=	C7H7	+	OH		0.3190E+07	1.21	0.1048E+05	19,22
377	C7H8	+	OH	=	C7H7	+	H2O		0.1260E+11	0	0.1081E+05	94
378	C7H8	+	H	=	C7H7	+	H2		0.5000E+12	0	0.5230E+05	96
379	C7H8	+	H	=	C6H6	+	CH3		0.1200E+11	0	0.2143E+05	91
380	C7H8			=	C6H5	+	CH3		0.1400E+17	0	0.4176E+06	29
381	C7H8			=	C7H7	+	H		0.6310E+16	0	0.3780E+06	93
382	C7H8	+	C6H5	=	C6H6	+	C7H7		0.2100E+10	0	0.1842E+05	29
383	C7H8	+	CH3	=	CH4	+	C7H7		0.3160E+09	0	0.3977E+05	29
384	C7H8	+	O	=	OC7H7	+	H		0.1630E+11	0	0.1430E+05	29
385	C7H7	+	O	=	C7H6O	+	H		0.2500E+12	0	0.0000E+00	29
386	C7H7	+	O	=	C6H5	+	CH2O		0.8000E+11	0	0.0000E+00	29
387	C7H7	+	OH	=	C7H7OH				0.6000E+11	0	0.0000E+00	29
388	C7H7OH	+	H	=	C7H6O	+	H2	+ H	0.8000E+11	0	0.3447E+05	29
389	C7H6O	+	OH	=	C6H5CO	+	H2O		0.1710E+07	1.18	-0.1871E+04	29
390	C7H6O	+	H	=	C6H5CO	+	H2		0.5000E+11	0	0.2063E+05	29
391	C7H6O	+	H	=	C6H6	+	CHO		0.1200E+11	0	0.2155E+05	29
392	C7H6O			=	C6H5	+	CHO		0.1000E+17	0	0.3432E+06	29
393	OC7H7	+	H	=	HOC7H7				0.2500E+12	0	0.0000E+00	29
394	OC7H7			=	C6H6	+	H	+ CO	0.2510E+12	0	0.1837E+06	29
395	HOC7H7	+	OH	=	OC7H7	+	H2O		0.6000E+10	0	0.0000E+00	29
396	HOC7H7	+	H	=	OC7H7	+	H2		0.1150E+12	0	0.5190E+05	29
397	HOC7H7	+	H	=	C7H8	+	OH		0.2210E+11	0	0.3311E+05	29
398	HOC7H7	+	H	=	C6H5OH	+	CH3		0.1200E+11	0	0.2155E+05	29
399	C6H5CO			=	C6H5	+	CO		0.3980E+15	0	0.1231E+06	29
400	C7H7			=	C7H7L				0.3160E+13	0	0.3567E+06	19,22
401	C7H7L			=	C5H5(L)	+	C2H2		0.1000E+13	0	0.1464E+06	19,22
402	1-C4H7			=	C4H6(T)	+	H		0.1200E+15	0	0.2064E+06	31
403	1-C4H7			=	C2H4	+	C2H3		0.1000E+12	0	0.1549E+06	31
404	1-C4H7	+	CH3	=	C4H6(T)	+	CH4		0.1000E+11	0	0.0000E+00	31
405	1-C4H7	+	C3H5(A)	=	C4H6(T)	+	C3H6		0.4000E+11	0	0.0000E+00	31
406	1-C4H8			=	C3H5(A)	+	CH3		0.8000E+17	0	0.3096E+06	55
407	1-C4H8	+	H	=	1-C4H7	+	H2		0.5000E+11	0	0.1632E+05	31
408	P-C4H9			=	C2H5	+	C2H4		0.2511E+14	0	0.1205E+06	57
409	P-C4H9			=	1-C4H8	+	H		0.1300E+14	0	0.1632E+06	57
410	1-C5H10			=	C2H5	+	C3H5(A)		0.1000E+17	0	0.2989E+06	60
411	1-C5H11			=	C3H7(N)	+	C2H4		0.3200E+14	0	0.1188E+06	60
412	C7H16			=	C3H7(N)	+	P-C4H9		0.1300E+17	0	0.3428E+06	See text
413	C7H16			=	C2H5	+	1-C5H11		0.6500E+16	0	0.3433E+06	See text
414	C7H16	+	H	=	1-C7H15	+	H2		0.2810E+05	2	0.3223E+05	32
415	C7H16	+	H	=	2-C7H15	+	H2		0.9100E+04	2	0.2093E+05	32
416	C7H16	+	H	=	3-C7H15	+	H2		0.9100E+04	2	0.2093E+05	32
417	C7H16	+	H	=	4-C7H15	+	H2		0.4500E+04	2	0.2093E+05	32
418	C7H16	+	OH	=	1-C7H15	+	H2O		0.1050E+08	0.97	0.6656E+04	32
419	C7H16	+	OH	=	2-C7H15	+	H2O		0.4700E+05	1.61	0.0000E+00	32
420	C7H16	+	OH	=	3-C7H15	+	H2O		0.4700E+05	1.61	0.0000E+00	32
421	C7H16	+	OH	=	4-C7H15	+	H2O		0.4700E+05	1.61	0.0000E+00	32
422	C7H16	+	CH3	=	1-C7H15	+	CH4		0.3000E+10	0	0.4856E+05	32
423	C7H16	+	CH3	=	2-C7H15	+	CH4		0.1600E+10	0	0.3977E+05	32
424	C7H16	+	CH3	=	3-C7H15	+	CH4		0.1600E+10	0	0.3977E+05	32
425	C7H16	+	CH3	=	4-C7H15	+	CH4		0.8000E+09	0	0.3977E+05	32
426	1-C7H15			=	C2H4	+	1-C5H11		0.2520E+14	0	0.1206E+06	32

TABLE D1 (CONCLUDED)

427	2-C7H15	=	C3H6	+	P-C4H9			0.1600E+14	0	0.1185E+06	32
428	3-C7H15	=	C3H7(N)	+	1-C4H8			0.5000E+13	0	0.1218E+06	32
429	4-C7H15	=	1-C5H10	+	C2H5			0.1080E+14	0	0.1172E+06	32
430	1-C7H15	=	2-C7H15					0.2000E+12	0	0.4647E+05	32
431	1-C7H15	=	3-C7H15					0.2000E+12	0	0.7577E+05	32
432	1-C7H15	=	4-C7H15					0.1000E+12	0	0.8372E+05	32
433	2-C7H15	=	3-C7H15					0.2000E+12	0	0.8372E+05	32

Reaction rates are expressed in the form $K_j=AT^n\exp(-E/RT)$

TABLE D2
Toluene Sub-mechanism for Diffusion Flames

	ELEMENTARY REACTION									A m^3,Kmol,sec^{-1}	n	E_a J/mol	REF
378	C6H6	+	CH2(S)	=	C7H8L					0.1000E+11	0	0.3567E+05	19,22
379	C7H8L			=	C7H8					0.3000E+11	0	0.0000E+00	19,22
380	C7H8	+	O	=	C7H7	+	OH			0.3190E+07	1.2	0.1048E+05	19,22
381	C7H8	+	OH	=	C7H7	+	H2O			0.1260E+11	0	0.1081E+05	92
382	C7H8	+	O2	=	C7H7	+	HO2			0.3000E+12	0	0.1733E+06	29
383	C7H8	+	H	=	C7H7	+	H2			0.5000E+12	0	0.5230E+05	96
384	C7H8	+	H	=	C6H6	+	CH3			0.1200E+11	0	0.2143E+05	91
385	C7H8			=	C6H5	+	CH3			0.1400E+17	0	0.4176E+06	29
386	C7H8			=	C7H7	+	H			0.6310E+16	0	0.3780E+06	93
387	C7H8	+	C6H5	=	C6H6	+	C7H7			0.2100E+10	0	0.1842E+05	29
388	C7H8	+	CH3	=	C7H7	+	CH4			0.3160E+09	0	0.3977E+05	29
389	C7H8	+	O	=	OC7H7	+	H			0.1630E+11	0	0.1431E+05	29
390	C6H5OH	+	C7H7	=	C6H5O	+	C7H8			0.1050E+09	0	0.3977E+05	29
391	HOC7H7	+	C7H7	=	OC7H7	+	C7H8			0.1050E+09	0	0.3977E+05	29
392	C7H7	+	O	=	C7H6O	+	H			0.2500E+12	0	0.0000E+00	29
393	C7H7	+	O	=	C6H5	+	CH2O			0.8000E+11	0	0.0000E+00	29
394	C7H7	+	HO2	=	C7H6O	+	H	+	OH	0.2500E+12	0	0.0000E+00	29
395	C7H7	+	HO2	=	C6H5	+	CH2O	+	OH	0.8000E+11	0	0.0000E+00	29
396	C7H7	+	C7H7	=	C14H14					0.2510E+09	0.4	0.0000E+00	29
397	C8H10			=	C7H7	+	CH3			0.3090E+14	0	0.2510E+06	100
398	C7H7	+	OH	=	C7H7OH					0.6000E+11	0	0.0000E+00	29
399	C7H7OH	+	O2	=	C7H6O	+	HO2	+	H	0.2000E+12	0	0.1733E+06	29
400§	C7H7OH	+	OH	=	C7H7O	+	H2O			0.5000E+10	0	0.0000E+00	101
401	C7H7OH	+	H	=	C7H6O	+	H2	+	H	0.8000E+11	0	0.3447E+05	29
402	C7H7OH	+	H	=	C6H6	+	CH2OH			0.1200E+11	0	0.2155E+05	29
403	C7H7OH	+	C7H7	=	C7H6O	+	C7H8	+	H	0.2110E+09	0	0.3977E+05	29
404	C7H7OH	+	C6H5	=	C7H6O	+	C6H6	+	H	0.1400E+10	0	0.1842E+05	29
405	C7H6O	+	O2	=	C6H5CO	+	HO2			0.1020E+11	0	0.1630E+06	29
406	C7H6O	+	OH	=	C6H5CO	+	H2O			0.1710E+07	1.18	-0.1871E+04	29
407	C7H6O	+	H	=	C6H5CO	+	H2			0.5000E+11	0	0.2063E+05	29
408	C7H6O	+	H	=	C6H6	+	CHO			0.1200E+11	0	0.2155E+05	29
409	C7H6O	+	O	=	C6H5CO	+	OH			0.9040E+10	0	0.1289E+05	29
410	C7H6O	+	C7H7	=	C7H8	+	C6H5CO			0.2770E+01	2.81	0.2417E+05	29
411	C7H6O	+	CH3	=	C6H5CO	+	CH4			0.2770E+01	2.81	0.2417E+05	29
412	C7H6O	+	C6H5	=	C6H5CO	+	C6H6			0.7010E+09	0	0.1842E+05	29
413	C7H6O	+	HO2	=	C6H5CO	+	H2O2			0.1000E+12	0	0.2093E+05	30
414	C7H6O			=	C6H5	+	CHO			0.1000E+17	0	0.3433E+06	30
415	C8H10	+	OH	=	C8H8	+	H2O	+	H	0.8430E+10	0	0.1081E+05	29

TABLE D2 (CONCLUDED)

416	C8H10	+ H	=	C8H8	+	H2	+ H	0.8000E+11	0	0.3447E+05	29
417	C8H10	+ O2	=	C8H8	+	HO2	+ H	0.2000E+12	0	0.1733E+06	29
418	OC7H7	+ H	=	HOC7H7				0.2500E+12	0	0.0000E+00	29
419	OC7H7		=	C6H6	+	H	+ CO	0.2510E+12	0	0.1838E+06	29
420	HOC7H7	+ OH	=	OC7H7	+	H2O		0.6000E+10	0	0.0000E+00	29
421	HOC7H7	+ H	=	OC7H7	+	H2		0.1150E+12	0	0.5191E+05	29
422	HOC7H7	+ H	=	C7H8	+	OH		0.2210E+11	0	0.3311E+05	29
423	HOC7H7	+ H	=	C6H5OH	+	CH3		0.1200E+11	0	0.2155E+05	29
424	C6H5CO		=	C6H5	+	CO		0.3980E+15	0	0.1231E+06	29
425	C6H5	+ C6H5	=	C12H10				0.1000E+10	0	0.0000E+00	30
426	C7H7		=	C7H7L				0.3160E+13	0	0.3567E+06	19,22
427	C7H7L		=	C5H5(L)	+	C2H2		0.1000E+13	0	0.1464E+06	19,22
428	C7H7L		=	C4H4	+	C3H3		0.2000E+13	0	0.3490E+06	19,22
429	C7H7L		=	C3H3	+	C2H2	+ C2H2	0.1780E+11	0	0.3549E+06	19,22
430§	C7H7O		=	C7H6O	+	H		0.1270E+15	0	0.4614E+04	101

§ Specific to diffusion flames

Reaction rates are expressed in the form $K_j = AT^n \exp(-E/RT)$

TABLE D3
Changes to Toluene Diffusion Flames Sub-Mechanism for Stirred Reactors

ELEMENTARY REACTION								A m^3, Kmol, sec^{-1}	n	E_a J/mol	REF
273	C4H5(T)		=	C2H2	+	C2H3		0.4000E+13	0	0.1920E+06	24
317	C6H5		=	C6H4	+	H		0.3000E+14	0	0.3724E+06	24
323	C6H5L		=	C6H4L	+	H		0.8000E+12	0	0.1536E+06	24
326	C6H6	+ O	=	C6H5O	+	H		0.2780E+11	0	0.2054E+05	104
331	C6H5O	+ H	=	C6H5OH				0.2500E+12	0	0.0000E+00	103
336	C6H5O		=	C5H5	+	CO		0.1590E+12	0	0.1837E+06	102
339	C5H5	+ O	=	C4H5(T)	+	CO		0.5000E+11	0	0.0000E+00	29, See Text
371	C6H5L	+ H	=	C6H4L	+	H2		0.1000E+12	0	0.0000E+00	24
372	C6H5L	+ OH	=	C6H4L	+	H2O		0.2000E+11	0	0.0000E+00	24
373	C5H6	+ O2	=	C5H5O	+	OH		0.0000E+11	0	0.8666E+05	Removed, See Text
380	C7H8	+ O	=	C7H7	+	OH		0.3190E+07	1.21	0.1048E+05	Removed, See Text
386	C7H7	+ H	=	C7H8				0.1800E+12	0	0.0000E+00	29
394	OC7H7		=	C6H6	+	H	+ CO	0.7900E11	0	0.18740E+06	102, See Text
401	C7H7OH	+ H	=	C7H6O	+	H2	+ H	0.8000E+11	0	0.3447E+05	Removed, See Text
414	C7H6O		=	C6H5	+	CHO		0.1000E+17	0	0.3433E+06	Removed, See Text
420	HOC7H7	+ OH	=	OC7H7	+	H2O		0.6000E+10	0	0.0000E+00	Removed, See Text
431	CH2O	+ HO2	=	CHO	+	H2O2		0.1990E+10	0	0.4879E+05	106
432	CH2O	+ CH3	=	CHO	+	CH4		0.5540E+01	2.81	0.2453E+05	1060
433	CH4	+ HO2	=	CH3	+	H2O2		0.1810E+09	0	0.7774E+05	105
434	C4H6(T)	+ O	=	C2H2O	+	C2H4		0.1000E+10	0	0.0000E+00	31
435	C4H6(T)	+ O	=	C3H4(P)	+	CH2O		0.1000E+10	0	0.0000E+00	31
436	C5H6	+ C6H5O	=	C6H5OH	+	C5H5		0.3160E+09	0	0.3347E+05	29
437	C6H5	+ OH	=	C6H4	+	H2O		0.2000E+11	0	0.0000E+00	24
438	C6H5	+ O2	=	C6H4	+	HO2		0.2610E+11	0	0.2561E+05	24
439	C6H5	+ O2	=	C6H5O	+	O		0.2090E+10	0	0.3125E+05	102
440	C6H5OH	+ C2H3	=	C6H5O	+	C2H4		0.6000E+10	0	0.0000E+00	29
441	C6H5OH	+ C6H5	=	C6H5O	+	C6H6		0.4910E+10	0	0.1841E+05	29

APPENDIX E
THERMOCHEMICAL AND PHYSICAL PROPERTIES FOR TOLUENE/*n*-HEPTANE AND TOLUENE SUB-MECHANISMS

TABLE E1
JANNAF Polynomials for Toluene Sub-mechanism Species

```
C7H8
  0.14234929E+02  0.23072029E-01 -0.54616157E-05 -0.97171848E-09  0.52401985E-12
  0.74657373E+03 -0.49325272E+02  0.14234929E+02  0.23072029E-01 -0.54616157E-05
 -0.97171848E-09  0.52401985E-12  0.74657373E+03 -0.49325272E+02   REF 67
C6H5CO
 -0.76918614E+00  0.55455726E-01 -0.34664368E-04  0.88063610E-08 -0.43666034E-12
  0.11143146E+05  0.32024105E+02 -0.76918614E+00  0.55455726E-01 -0.34664368E-04
  0.88063610E-08 -0.43666034E-12  0.11143146E+05  0.32024105E+02   PW
C7H8L
 -0.13757692E+02  0.11484089E+00 -0.12106851E-03  0.66261705E-07 -0.14455333E-10
  0.23941000E+05  0.87316025E+02 -0.13757692E+02  0.11484089E+00 -0.12106851E-03
  0.66261705E-07 -0.14455333E-10  0.23941000E+05  0.87316025E+02   REF 22
C7H7
  0.14043980E+02  0.23493873E-01 -0.85375367E-05  0.13890841E-08 -0.83614420E-13
  0.18564203E+05 -0.51665589E+02  0.48111540E+00  0.38512832E-01  0.32861492E-04
 -0.76972721E-07  0.35423068E-10  0.23307027E+05  0.23548820E+02   REF 67
C7H7L
 -0.14231613E+02  0.16832972E+00 -0.28957374E-03  0.23736918E-06 -0.69394046E-10
  0.20246734E+05  0.66954346E+02 -0.14231613E+02  0.16832972E+00 -0.28957374E-03
  0.23736918E-06 -0.69394046E-10  0.20246734E+05  0.66954346E+02   REF 22
OC7H7
 -0.29244521E+01  0.72308660E-01 -0.52679799E-04  0.18029228E-07 -0.22330289E-11
 -0.14259766E+03  0.36648621E+02 -0.29244521E+01  0.72308660E-01 -0.52679799E-04
  0.18029228E-07 -0.22330289E-11 -0.14259766E+03  0.36648621E+02   PW
HOC7H7
 -0.32751951E+01  0.77922545E-01 -0.60354632E-04  0.23376813E-07 -0.35583873E-11
 -0.17551484E+05  0.40368690E+02 -0.32751951E+01  0.77922545E-01 -0.60354632E-04
  0.23376813E-07 -0.35583873E-11 -0.17551484E+05  0.40368690E+02   PW
C7H6O
 -0.15328401E+01  0.58126155E-01 -0.33953951E-04  0.75374835E-08 -0.98655486E-13
 -0.62751094E+04  0.34853806E+02 -0.15328401E+01  0.58126155E-01 -0.33953951E-04
  0.75374835E-08 -0.98655486E-13 -0.62751094E+04  0.34853806E+02   PW
C7H7OH
 -0.27946572E+01  0.68989187E-01 -0.44636494E-04  0.13176090E-07 -0.12568589E-11
 -0.14001355E+05  0.41228657E+02 -0.27946572E+01  0.68989187E-01 -0.44636494E-04
  0.13176090E-07 -0.12568589E-11 -0.14001355E+05  0.41228657E+02   PW
C8H8
  0.57468890E+01  0.48250760E-01 -0.25794920E-04  0.65860550E-08 -0.65297670E-12
  0.13434980E+05 -0.60621620E+01  0.11784510E+01  0.35972650E-01  0.63202020E-04
 -0.12341850E-06  0.57205890E-10  0.15406210E+05  0.22145280E+02   REF 67
C8H10
  0.38789780E+01  0.58100590E-01 -0.31963800E-04  0.84489930E-08 -0.86948250E-12
 -0.50249220E+03  0.38370990E+01 -0.72668450E+01  0.10030890E+00 -0.96517150E-04
  0.55659080E-07 -0.14533700E-10  0.19872900E+04  0.58577460E+02   REF 67
C12H10
  0.24289017E 02  0.34006648E-01 -0.11722408E-04  0.17729298E-08 -0.96812532E-13
  0.10287000E 05 -0.10802374E 03 -0.40739527E 01  0.86973310E-01 -0.42353613E-05
 -0.64564460E-07  0.34150169E-10  0.19405965E 05  0.44741348E 02   REF 67
C14H14
 -0.88047981E+01  0.13876630E+00 -0.98184872E-04  0.32592112E-07 -0.38599458E-11
  0.14423895E+05  0.70463058E+02 -0.88047981E+01  0.13876630E+00 -0.98184872E-04
  0.32592112E-07 -0.38599458E-11  0.14423895E+05  0.70463058E+02   PW
C7H7O
 -0.27946572E+01  0.68989187E-01 -0.44636494E-04  0.13176090E-07 -0.12568589E-11
 -0.14001355E+05  0.41228657E+02 -0.27946572E+01  0.68989187E-01 -0.44636494E-04
  0.13176090E-07 -0.12568589E-11 -0.14001355E+05  0.41228657E+02   PW
```

TABLE E2
Physical Properties for Toluene Sub-mechanism Species

SPECIES	σ	ϵ/κ	C_v	C_z	μ	Mol Wt.
C7H8	0.60890000E+01	0.352E+03	1.0	1.5	0.692E-05	92.141
C6H5CO	0.58813000E+01	0.501E+03	1.0	1.5	0.707E-04	105.077
C7H8L	0.59550000E+01	0.499E+03	1.0	1.5	0.604E-05	92.141
C7H7	0.60890000E+01	0.352E+03	1.0	1.5	0.688E-05	91.133
C7H7L	0.59320000E+01	0.510E+03	1.0	1.5	0.595E-05	91.133
OC7H7	0.69596000E+01	0.491E+03	1.0	1.5	0.480E-04	107.140
HOC7H7	0.56860000E+01	0.541E+03	1.0	1.5	0.688E-04	108.140
C7H6O	0.57343265E+01	0.535E+03	1.0	1.5	0.674E-04	106.124
C7H7OH	0.60053000E+01	0.555E+03	1.0	1.5	0.639E-04	108.140
C7H7O	0.58064000E+01	0.474E+03	1.0	1.5	0.703E-04	107.077
C8H8	0.58420000E+01	0.473E+03	1.0	1.5	0.669E-04	104.152
C8H10	0.60590000E+01	0.475E+03	1.0	1.5	0.564E-04	106.168
C12H10	0.66759620E+01	0.608E+03	1.0	1.5	0.563E-04	154.212
C14H14	0.68409000E+01	0.577E+03	1.0	1.5	0.598E-04	182.266
C7H7O	0.58064000E+01	0.474E+03	1.0	1.5	0.703E-04	107.077

σ = Collision Diameter (Armstrongs)
ϵ/κ = Lennard Jones Potential Parameter (K)
C_V = Vibrational Wall Collision Efficiency
C_Z = Rotational Wall Collision Efficiency
μ = viscosity (kg m^{-1} sec^{-1})

APPENDIX F
TOLUENE/*n*-HEPTANE REACTION RATES DATA

Table 4.1.2.1
Toluene Consumption in Toluene/n-Heptane Diffusion Flame

ELEMENTARY REACTION								a=50 max rate kmol/m^3/sec Tmax=1819K	Reaction ranking in pure toluene diffusion flame
381	C7H8			=	C7H7	+	H	-3.11E-01	1
378	C7H8	+	H	=	C7H7	+	H2	2.40E-01	2
377	C7H8	+	OH	=	C7H7	+	H2O	7.46E-02	3
379	C7H8	+	H	=	C6H6	+	CH3	4.22E-02	4
376	C7H8	+	O	=	C7H7	+	OH	1.95E-02	5
380	C7H8			=	C6H5	+	CH3	-1.17E-02/6.23E-04	6
384	C7H8	+	O	=	OC7H7	+	H	7.76E-03	7
383	C7H8	+	CH3	=	CH4	+	C7H7	7.27E-03	9
382	C7H8	+	C6H5	=	C6H6	+	C7H7	2.77E-03	8

Table 4.1.2.2
Benzyl Radical Consumption in Toluene/n-Heptane Diffusion Flame

ELEMENTARY REACTION								a=50 max rate kmol/m^3/sec Tmax=1793K	Reaction ranking in pure toluene diffusion flame
387	C7H7	+	OH	=	C7H7OH			1.55E-02	1
385	C7H7	+	O	=	C7H6O	+	H	5.65E-03	2
386	C7H7	+	O	=	C6H5	+	CH2O	1.81E-03	3

Table 4.1.2.3
Linear C_7H_7 Radical Production in Toluene/n-Heptane Diffusion Flame

ELEMENTARY REACTION				a=50 max rate kmol/m^3/sec Tmax=1819K	pure toluene flame max rate kmol/m^3/sec Tmax=1855K
401	C7H7	=	C7H7L	8.49E-05	4.16E-04

Table 4.1.2.4
Linear C_7H_7 Radical Consumption in Toluene/n-Heptane Diffusion Flame

ELEMENTARY REACTION						a=50 max rate kmol/m^3/sec Tmax=1819K	pure toluene flame max rate kmol/m^3/sec Tmax=1855K
402	C7H7L	=	C5H5(L)	+	C2H2	8.49E-05	4.16E-04

Table 4.1.2.5
Benzyl Alcohol Consumption in Toluene/n-Heptane Diffusion Flame

ELEMENTARY REACTION									a=50 max rate kmol/m^3/sec Tmax=1819K	pure toluene flame max rate kmol/m^3/sec Tmax=1855K
388	C7H7OH	+	H	=	C7H6O	+	H2	+	H	1.55E-02	4.61E-02

Table 4.1.2.6
Benzaldehyde Consumption in Toluene/n-Heptane Diffusion Flame

ELEMENTARY REACTION									a=50 max rate kmol/m^3/sec Tmax=1819K	Reaction ranking in pure toluene diffusion flame
392	C7H6O			=	C6H5	+	CHO		1.86E-02	1
389	C7H6O	+	OH	=	C6H5CO	+	H2O		8.80E-04	2
390	C7H6O	+	H	=	C6H5CO	+	H2		7.97E-04	3
391	C7H6O	+	H	=	C6H6	+	CHO		1.80E-04	4

Table 4.1.2.7
Cresoxy radical Consumption in Toluene/n-Heptane Diffusion Flame

ELEMENTARY REACTION									a=50 max rate kmol/m^3/sec Tmax=1819K	Reaction ranking in pure toluene diffusion flame
393	OC7H7	+	H	=	HOC7H7				6.61E-03	1
394	OC7H7			=	C6H6	+	H	+ CO	5.41E-03	2

Table 4.1.2.8
Cresol Consumption in Toluene/n-Heptane Diffusion Flame

ELEMENTARY REACTION									a=50 max rate kmol/m^3/sec Tmax=1793K	Reaction ranking in pure toluene diffusion flame
396	HOC7H7	+	OH	=	OC7H7	+	H2O		2.67E-03	1
397	HOC7H7	+	H	=	OC7H7	+	H2		1.44E-03	2
399	HOC7H7	+	H	=	C6H5OH	+	CH3		1.14E-03	3
398	HOC7H7	+	H	=	C7H8	+	OH		9.27E-04	4

Table 4.1.2.9
Benzoyl Radical Consumption in Toluene/n-Heptane Diffusion Flame

ELEMENTARY REACTION									a=50 max rate kmol/m^3/sec Tmax=1819K	pure toluene flame max rate kmol/m^3/sec Tmax=1855K
400	C6H5CO			=	C6H5	+	CO		1.61E-03	1.50E-03

Table 4.1.2.10
Benzene Consumption in Toluene/n-Heptane Diffusion Flame

ELEMENTARY REACTION									a=50 max rate kmol/m^3/sec Tmax=1819K	Reaction ranking in pure toluene diffusion flame
328	C6H6	+	OH	=	C6H5	+	H2O		4.11E-02	1
325	C6H6	+	H	=	C6H5	+	H2		2.99E-02	2
324	C6H6			=	C6H5	+	H		-2.03E-02	3
326	C6H6	+	O	=	C6H5O	+	H		7.36E-03	4
332	C6H6	+	OH	=	C6H5OH	+	H		6.27E-03	5
330	C6H6	+	CH3	=	C6H5	+	CH4		7.85E-04	7
329	C6H6	+	O2	=	C6H5O	+	OH		6.38E-04	6
240	C3H3	+	C3H4(A)	=	C6H6	+	H		7.11E-05	11
267	C4H4	+	C2H3	=	C6H6	+	H		4.77E-06/-5.58E-05	8
374	C6H6	+	CH2(S)	=	C7H8L				1.87E-05	10
312	C4H5(T)	+	C2H2	=	C6H6	+	H		3.74E-07	9
327	C6H6	+	O	=	C6H5	+	OH		-1.00E-15	12

Table 4.1.2.11
Linear C_7H_8 Consumption in Toluene/n-Heptane Diffusion Flame

ELEMENTARY REACTION							a=50 max rate kmol/m^3/sec Tmax=1819K	pure toluene flame max rate kmol/m^3/sec Tmax=1855K
375	C7H8L		=	C7H8			3.00E-05	3.00E-05

Table 4.1.2.12
Phenyl Radical Consumption in Toluene/n-Heptane Diffusion Flame

ELEMENTARY REACTION							a=50 max rate kmol/m^3/sec Tmax=1793K	Reaction ranking in pure toluene diffusion flame
321	C6H5	+	OH	=	C6H5O	+ H	2.96E-02	1
322	C6H5L			=	C6H5		1.42E-03/-1.94E-02	3
310	C6H5			=	C4H3(N)	+ C2H2	1.43E-02	2
320	C6H5	+	O2	=	C6H5O	+ O	4.17E-03	4
317	C6H4	+	H	=	C6H5		-1.00E-15	5
319	C6H5	+	H	=	C6H4	+ H2	-1.00E-15	6

Table 4.1.2.13
Linear C_6H_5 Consumption in Toluene/n-Heptane Diffusion Flame

ELEMENTARY REACTION							a=50 max rate kmol/m^3/sec Tmax=1819K	Reaction ranking in pure toluene diffusion flame
322	C6H5L			=	C6H5		1.42E-03/-1.94E-02	1
239	C3H3	+	C3H3	=	C6H5L	+ H	1.95E-03/-1.77E-02	2
311	C6H5L			=	C4H3(N)	+ C2H2	1.68E-03	4
323	C6H5L			=	C6H4	+ H	1.664E-03	3
266	C4H4	+	C2H2	=	C6H5L	+ H	-2.11E-05	5

Table 4.1.2.14
Phenoxy radical Consumption in Toluene/n-Heptane Diffusion Flame

ELEMENTARY REACTION							a=50 max rate kmol/m^3/sec Tmax=1819K	Reaction ranking in pure toluene diffusion flame
336	C6H5O			=	C5H5	+ CO	4.57E-02	1
331	C6H5OH			=	C6H5O	+ H	6.01E-03/-1.16E-03	2

Table 4.1.2.15
Phenyl Alcohol Consumption in Toluene/n-Heptane Diffusion Flame

ELEMENTARY REACTION							a=50 max rate kmol/m^3/sec Tmax=1819K	Reaction ranking in pure toluene diffusion flame
331	C6H5OH			=	C6H5O	+ H	6.01E-03	4
335	C6H5OH	+	OH	=	C6H5O	+ H2O	1.73E-03	1
333	C6H5OH	+	H	=	C6H5O	+ H2	8.04E-04	2
334	C6H5OH	+	O	=	C6H5O	+ OH	3.07E-04	3

Table 4.1.2.16
n-Heptane Consumption in Toluene/n-Heptane Diffusion Flame

ELEMENTARY REACTION								a=50 max rate kmol/m^3/sec Tmax=1819K	Reaction ranking in pure *n*-heptane diffusion flame
413	C7H16		=	C3H7(N)	+	P-C4H9		5.50E-02	1
414	C7H16		=	C2H5	+	1-C5H11		2.68E-02	2
424	C7H16	+	CH3 =	2-C7H15	+	CH4		5.32E-03	7
425	C7H16	+	CH3 =	3-C7H15	+	CH4		5.32E-03	8
423	C7H16	+	CH3 =	1-C7H15	+	CH4		4.50E-03	9
415	C7H16	+	H =	1-C7H15	+	H2		3.08E-03	3
416	C7H16	+	H =	2-C7H15	+	H2		2.78E-03	4
417	C7H16	+	H =	3-C7H15	+	H2		2.78E-03	5
426	C7H16	+	CH3 =	4-C7H15	+	CH4		2.66E-03	10
418	C7H16	+	H =	4-C7H15	+	H2		1.37E-03	6
419	C7H16	+	OH =	1-C7H15	+	H2O		4.76E-04	11
420	C7H16	+	OH =	2-C7H15	+	H2O		3.88E-04	12
421	C7H16	+	OH =	3-C7H15	+	H2O		3.88E-04	13
422	C7H16	+	OH =	4-C7H15	+	H2O		3.88E-04	14

Table 4.1.2.17
Heptyl Radicals Consumption in Toluene/n-Heptane Diffusion Flame

ELEMENTARY REACTION							a=50 max rate kmol/m^3/sec Tmax=1819K	Reaction ranking in pure *n*-heptane diffusion flame
428	2-C7H15	=	C3H6	+	P-C4H9		1.06E-02	1
427	1-C7H15	=	C2H4	+	1-C5H11		9.96E-03	2
430	4-C7H15	=	1-C5H10	+	C2H5		4.82E-03	3
429	3-C7H15	=	C3H7(N)	+	1-C4H8		3.89E-03	4
432	1-C7H15	=	3-C7H15				-2.71E-03/2.95E-07	5
434	2-C7H15	=	3-C7H15				-1.84E-03	6
433	1-C7H15	=	4-C7H15				4.60E-04	8
431	1-C7H15	=	2-C7H15				3.01E-04	7

Table 4.1.2.18
1-Pentyl Radical Consumption in Toluene/n-Heptane Diffusion Flame

ELEMENTARY REACTION							a=50 max rate kmol/m^3/sec Tmax=1819K	pure *n*-heptane flame max rate kmol/m^3/sec Tmax=1738K
412	1-C5H11	=	C3H7(N)	+	C2H4		3.27E-02	2.54E-02

Table 4.1.2.19
1-Pentene Radical Consumption in Toluene/n-Heptane Diffusion Flame

ELEMENTARY REACTION							a=50 max rate kmol/m^3/sec Tmax=1819K	pure *n*-heptane flame max rate kmol/m^3/sec Tmax=1738K
411	1-C5H10	=	C2H5	+	C3H5(A)		5.67E-03	2.20E-02

Table 4.1.2.20
n-Butyl Radical Consumption in Toluene/n-Heptane Diffusion Flame

	ELEMENTARY REACTION							a=50 max rate kmol/m^3/sec Tmax=1819K	Reaction ranking in pure *n*-heptane diffusion flame
409	P-C4H9		=	C2H5	+	C2H4		-4.44E-06/5.99E-02	1
410	P-C4H9		=	1-C4H8	+	H		-1.62E-04/5.38E-04	2

Table 4.1.2.21
1-Butene Consumption in Toluene/n-Heptane Diffusion Flame

	ELEMENTARY REACTION							a=50 max rate kmol/m^3/sec Tmax=1819K	Reaction ranking in pure *n*-heptane diffusion flame
407	1-C4H8		=	C3H5(A)	+	CH3		-4.70E-03/8.55E-03	1
408	1-C4H8	+ H	=	1-C4H7	+	H2		8.42E-04	2

Table 4.1.2.22
1-Butene Radical Consumption in Toluene/n-Heptane Diffusion Flame

	ELEMENTARY REACTION							a=50 max rate kmol/m^3/sec Tmax=1819K	Reaction ranking in pure *n*-heptane diffusion flame
403	1-C4H7		=	C4H6(T)	+	H		7.58E-04	1
404	1-C4H7		=	C2H4	+	C2H3		4.90E-05	2
406	1-C4H7	+ C3H5(A)	=	C4H6(T)	+	C3H6		3.13E-05	3
405	1-C4H7	+ CH3	=	C4H6(T)	+	CH4		1.24E-05	4

APPENDIX G
TOLUENE REACTION RATES DATA

Table 5.1.2.1
Toluene Consumption in Toluene Diffusion Flame

	ELEMENTARY REACTION									a=50 max rate kmol/m^3/sec Tmax=1855K
386	C7H8			=	C7H7	+	H			-3.85E-01
383	C7H8	+	H	=	C7H7	+	H2			2.97E-01
381	C7H8	+	OH	=	C7H7	+	H2O			1.08E-01
384	C7H8	+	H	=	C6H6	+	CH3			4.87E-02
380	C7H8	+	O	=	C7H7	+	OH			3.39E-02
385	C7H8			=	C6H5	+	CH3			2.66E-02
389	C7H8	+	O	=	OC7H7	+	H			1.32E-02
387	C7H8	+	C6H5	=	C6H6	+	C7H7			5.36E-03
388	C7H8	+	CH3	=	C7H7	+	CH4			1.29E-03
382	C7H8	+	O2	=	C7H7	+	HO2			4.33E-03

Table 5.1.2.2
Benzyl Radical Consumption in Toluene Diffusion Flame

	ELEMENTARY REACTION									a=50 max rate kmol/m^3/sec Tmax=1855K
398	C7H7	+	OH	=	C7H7OH					4.61E-02
392	C7H7	+	O	=	C7H6O	+	H			1.44E-02
393	C7H7	+	O	=	C6H5	+	CH2O			4.59E-03
396	C7H7	+	C7H7	=	C14H14					-3.09E-03/2.80E-03
394	C7H7	+	HO2	=	C7H6O		H	+	OH	3.38E-03
395	C7H7	+	HO2	=	C6H5	+	CH2O	+	OH	1.08E-03
397	C8H10			=	C7H7	+	CH3			-2.82E-04/2.56E-09
390	C6H5OH	+	C7H7	=	C6H5O	+	C7H8			1.33E-06
391	HOC7H7	+	C7H7	=	OC7H7	+	C7H8			-4.18E-06/6.80E-07

Table 5.1.2.3
Linear C_7H_7 Radical Production in Toluene Diffusion Flame

	ELEMENTARY REACTION			a=50 max rate kmol/m^3/sec Tmax=1855K
426	C7H7	=	C7H7L	4.16E-04

Table 5.1.2.4
Linear C_7H_7 Radical Consumption in Toluene Diffusion Flame

	ELEMENTARY REACTION							a=50 max rate kmol/m^3/sec Tmax=1855K
427	C7H7L	=	C5H5(L)	+	C2H2			4.16E-04
428	C7H7L	=	C4H4	+	C3H3			8.64E-10
429	C7H7L	=	C3H3	+	C2H2	+	C2H2	5.65E-12

Table 5.1.2.5
Benzyl Alcohol Consumption in Toluene Diffusion Flame

	ELEMENTARY REACTION									a=50 max rate kmol/m^3/sec Tmax=1855K
401	C7H7OH	+	H	=	C7H6O	+	H2	+	H	4.61E-02
404	C7H7OH	+	C6H5	=	C7H6O	+	C6H6	+	H	6.48E-08
403	C7H7OH	+	C7H7	=	C7H6O	+	C7H8	+	H	4.07E-08
402	C7H7OH	+	H	=	C6H6	+	CH2OH			3.07E-08
399	C7H7OH	+	O2	=	C7H6O	+	HO2	+	H	8.63E-09
400	C7H7OH	+	OH	=	C7H7O	+	H2O			1.53E-10

Table 5.1.2.6
Benzaldehyde Consumption in Toluene Diffusion Flame

	ELEMENTARY REACTION							a=50 max rate kmol/m^3/sec Tmax=1855K
414	C7H6O			=	C6H5	+	CHO	5.77E-02
406	C7H6O	+	OH	=	C6H5CO	+	H2O	1.28E-03
410	C7H6O	+	C7H7	=	C7H8	+	C6H5CO	1.27E-03
407	C7H6O	+	H	=	C6H5CO	+	H2	9.62E-04
408	C7H6O	+	H	=	C6H6	+	CHO	2.17E-04
411	C7H6O	+	CH3	=	C6H5CO	+	CH4	1.64E-04
409	C7H6O	+	O	=	C6H5CO	+	OH	8.52E-05
412	C7H6O	+	C6H5	=	C6H5CO	+	C6H6	1.57E-05
413	C7H6O	+	HO2	=	C6H5CO	+	H2O2	8.72E-06
405	C7H6O	+	O2	=	C6H5CO	+	O2	4.08E-07

Table 5.1.2.7
Ethyl Benzene Consumption in Toluene Diffusion Flame

	ELEMENTARY REACTION									a=50 max rate kmol/m^3/sec Tmax=1855K
397	C8H10			=	C7H7	+	CH3			-4.13E-04
416	C8H10	+	H	=	C8H8	+	H2	+	H	2.82E-04
417	C8H10	+	O2	=	C8H8	+	HO2	+	H	-1.35E-06
415	C8H10	+	OH	=	C8H8	+	H2O	+	H	3.19E-09

Table 5.1.2.8
Cresoxy radical Consumption in Toluene Diffusion Flame

	ELEMENTARY REACTION									a=50 max rate kmol/m^3/sec Tmax=1855K
419	OC7H7			=	C6H6	+	H	+	CO	1.00E-02
418	OC7H7	+	H	=	HOC7H7					7.77E-03

Table 5.1.2.9
Cresol Consumption in Toluene Diffusion Flame

	ELEMENTARY REACTION								a=50 max rate kmol/m^3/sec Tmax=1855K
420	HOC7H7	+	OH	=	OC7H7	+	H2O		3.47E-03
421	HOC7H7	+	H	=	OC7H7	+	H2		1.60E-03
423	HOC7H7	+	H	=	C6H5OH	+	CH3		1.17E-03
422	HOC7H7	+	H	=	C7H8	+	OH		9.72E-04

Table 5.1.2.10
Benzoyl Radical Consumption in Toluene Diffusion Flame

	ELEMENTARY REACTION					a=50 max rate kmol/m^3/sec Tmax=1855K
424	C6H5CO	=	C6H5	+	CO	1.50E-03

Table 5.1.2.11
Benzene Consumption in Toluene Diffusion Flame

	ELEMENTARY REACTION								a=50 max rate kmol/m^3/sec Tmax=1855K
328	C6H6	+	OH	=	C6H5	+	H2O		7.37E-02
325	C6H6	+	H	=	C6H5	+	H2		4.57E-02
324	C6H6			=	C6H5	+	H		-3.38E-02
326	C6H6	+	O	=	C6H5O	+	H		1.48E-02
332	C6H6	+	OH	=	C6H5OH	+	H		1.22E-02
329	C6H6	+	O2	=	C6H5O	+	OH		2.00E-03
330	C6H6	+	CH3	=	C6H5	+	CH4		1.05E-03
267	C4H4	+	C2H3	=	C6H6	+	H		-1.14E-04
312	C4H5(T)	+	C2H2	=	C6H6	+	H		4.24E-08/-1.64E-05
378	C6H6	+	CH2(S)	=	C7H8L				2.98E-05
240	C3H3	+	C3H4(A)	=	C6H6	+	H		2.66E-06
327	C6H6	+	O	=	C6H5	+	OH		-1.00E-15

Table 5.1.2.12
Linear C_7H_8 Consumption in Toluene Diffusion Flame

	ELEMENTARY REACTION			a=50 max rate kmol/m^3/sec Tmax=1855K
379	C7H8L	=	C7H8	3.00E-05

Table 5.1.2.13
Phenyl Radical Consumption in Toluene Diffusion Flame

	ELEMENTARY REACTION								a=50 max rate kmol/m^3/sec Tmax=1855K
321	C6H5	+	OH	=	C6H5O	+	H		5.74E-02
310	C6H5			=	C4H3(N)	+	C2H2		5.31E-02
322	C6H5L			=	C6H5				-4.95E-02/1.27E-04
320	C6H5	+	O2	=	C6H5O	+	O		1.55E-02
425	C6H5	+	C6H5	=	C12H10				4.59E-04
317	C6H4	+	H	=	C6H5				-1.00E-15
319	C6H5	+	H	=	C6H4	+	H2		-1.00E-15

Table 5.1.2.14
Linear C_6H_5 Consumption in Toluene Diffusion Flame

	ELEMENTARY REACTION								a=50 max rate kmol/m^3/sec Tmax=1855K
322	C6H5L			=	C6H5				-4.95E-02/1.27E-04
239	C3H3	+	C3H3	=	C6H5L	+	H		-3.93E-02
323	C6H5L			=	C6H4	+	H		8.34E-03
311	C6H5L			=	C4H3(N)	+	C2H2		7.73E-03
266	C4H4	+	C2H2	=	C6H5L	+	H		-4.46E-05
371	C6H5L	+	H	=	C6H4	+	H2		4.48E-06
372	C6H5L	+	OH	=	C6H4	+	H2O		2.44E-06
359	C6H5L	+	H	=	C3H4(A)	+	C3H2		4.93E-07

Table 5.1.2.15
Phenoxy radical Consumption in Toluene Diffusion Flame

	ELEMENTARY REACTION								a=50 max rate kmol/m^3/sec Tmax=1855K
336	C6H5O			=	C5H5	+	CO		9.04E-02
331	C6H5OH			=	C6H5O	+	H		1.19E-02

Table 5.1.2.16
Phenyl Alcohol Consumption in Toluene Diffusion Flame

	ELEMENTARY REACTION								a=50 max rate kmol/m^3/sec Tmax=1855K
335	C6H5OH	+	OH	=	C6H5O	+	H2O		1.58E-03
333	C6H5OH	+	H	=	C6H5O	+	H2		6.99E-04
334	C6H5OH	+	O	=	C6H5O	+	OH		3.36E-04
337	C6H5OH			=	C5H6	+	CO		2.35E-05

Table 5.1.2.17
Methoxy Phenyl Radical Consumption in Toluene Diffusion Flame

	ELEMENTARY REACTION								a=50 max rate kmol/m^3/sec Tmax=1738K
430	C7H7O			=	C7H6O	+	H		6.67E-02

Table 5.1.3.1a
Toluene Consumption in Toluene Stirred Reactor

ELEMENTARY REACTION	T=1188K τ=75 msec rate kmol/m^3/sec	T=2000K τ=75 msec rate kmol/m^3/sec
381 C7H8 + OH = C7H7 + H2O	3.77E-05	1.04E-05
383 C7H8 + H = C7H7 + H2	1.66E-05	9.03E-06
389 C7H8 + O = OC7H7 + H	1.69E-05	8.56E-06
384 C7H8 + H = C6H6 + CH3	9.48E-06	1.39E-06
382 C7H8 + O2 = C7H7 + HO2	9.18E-06	1.98E-07
387 C7H8 + C6H5 = C6H6 + C7H7	3.95E-06	5.27E-11
391 HOC7H7+ C7H7 = OC7H7 + C7H8	-6.07E-07	-5.40E-14
388 C7H8 + CH3 = C7H7 + CH4	1.45E-07	2.39E-12

Table 5.1.3.1b
Toluene Production in Toluene Stirred Reactor

ELEMENTARY REACTION	T=1188K τ=75 msec rate kmol/m^3/sec	T=2000K τ=75 msec rate kmol/m^3/sec
386 C7H7 + H = C7H8	1.13E-05	-1.96E-05
403 C7H7OH + C7H7 = C7H6O + C7H8 +H	4.97E-08	-7.24E-16
385 C7H8 = C6H5 + CH3	-2.44E-07	7.22E-05
410 C7H6O + C7H7 = C7H8 + C6H5CO	7.76E-06	1.48E-11
390 C6H5OH + C7H7 = C6H5O + C7H8	1.31E-08	1.24E-15

Table 5.1.3.2
Benzyl Radical Consumption in Toluene Stirred Reactor

ELEMENTARY REACTION	T=1188K τ=75 msec rate kmol/m^3/sec	T=2000K τ=75 msec rate kmol/m^3/sec
394 C7H7 + HO2 = C7H6O + H + OH	2.07E-05	1.12E-08
386 C7H7 + H = C7H8	1.13E-05	-1.96E-05
392 C7H7 + O = C7H6O + H	1.01E-05	2.97E-05
395 C7H7 + HO2 = C6H5 + CH2O + OH	6.62E-06	3.59E-09
397 C8H10 = C7H7 + CH3	-4.40E-06	8.65E-09
393 C7H7 + O = C6H5 + CH2O	3.24E-06	9.51E-06
403 C7H7 + OH = C7H7OH	2.75E-06	8.09E-09
391 HOC7H7 + C7H7 = OC7H7 + C7H8	-6.07E-07	-5.40E-14
396 C7H7 + C7H7 = C14H14	2.52E-08	-1.72E-06
390 C6H5OH + C7H7 = C6H5O + C7H8	1.31E-08	1.24E-15

Table 5.1.3.3
Linear C_7H_7 Radical Production in Toluene Stirred Reactor

ELEMENTARY REACTION	T=1188K τ=75 msec rate kmol/m^3/sec	T=2000K τ=75 msec rate kmol/m^3/sec
426 C7H7 = C7H7L	6.11E-11	3.55E-08

Table 5.1.3.4
Linear C_7H_7 Radical Consumption in Toluene Stirred Reactor

	ELEMENTARY REACTION	T=1188K τ=75 msec rate kmol/m^3/sec	T=2000K τ=75 msec rate kmol/m^3/sec
427	C7H7L = C5H5(L) + C2H2	3.66E-10	1.50E-07
428	C7H7L = C4H4 + C3H3	-1.21E-14	1.55E-12
429	C7H7L = C3H3 + C2H2 + C2H2	-1.00E-15	8.64E-15

Table 5.1.3.5
Benzyl Alcohol Consumption in Toluene Stirred Reactor

	ELEMENTARY REACTION	T=1188K τ=75 msec rate kmol/m^3/sec	T=2000K τ=75 msec rate kmol/m^3/sec
400	C7H7OH + OH = C7H6O + H2O + H	3.84E-07	6.65E-09
402	C7H7OH + H = C6H6 + CH2OH	1.44E-07	1.31E-09
399	C7H7OH + O2 = C7H6O + HO2 + H	1.53E-07	1.22E-10
403	C7H7OH + C7H7 = C7H6O + C7H8 + H	4.97E-08	-7.25E-16
404	C7H7OH + C6H5 = C7H6O + C6H6 + H	4.46E-08	3.46E-14

Table 5.1.3.6
Benzaldehyde Consumption in Toluene Stirred Reactor

	ELEMENTARY REACTION	T=1188K τ=75 msec rate kmol/m^3/sec	T=2000K τ=75 msec rate kmol/m^3/sec
410	C7H6O + C7H7 = C7H8 + C6H5CO	7.76E-06	1.48E-11
406	C7H6O + OH = C6H5CO + H2O	6.71E-06	1.92E-05
407	C7H6O + H = C6H5CO + H2	3.69E-06	4.89E-06
409	C7H6O + O = C6H5CO + OH	9.29E-07	4.47E-06
408	C7H6O + H = C6H6 + CHO	8.07E-07	1.11E-06
411	C7H6O + CH3 = C6H5CO + CH4	2.34E-07	9.32E-11
412	C7H6O + C6H5 = C6H5CO + C6H6	1.25E-07	1.51E-11
405	C7H6O + O2 = C6H5CO + O2	1.24E-07	9.78E-09

Table 5.1.3.7
Ethyl Benzene Consumption in Toluene Stirred Reactor

	ELEMENTARY REACTION	T=1188K τ=75 msec rate kmol/m^3/sec	T=2000K τ=75 msec rate kmol/m^3/sec
416	C8H10 + H = C8H8 + H2 + H	4.34E-06	1.69E-06
415	C8H10 + OH = C8H8 + H2O + H	9.43E-09	1.71E-11
417	C8H10 + O2 = C8H8 + HO2 + H	3.74E-09	3.13E-13

Table 5.1.3.8
Cresoxy radical Consumption in Toluene Stirred Reactor

	ELEMENTARY REACTION	T=1188K τ=75 msec rate kmol/m^3/sec	T=2000K τ=75 msec rate kmol/m^3/sec
419	OC7H7 = C6H6 + H + CO	1.16E-05	8.33E-06
418	OC7H7 + H = HOC7H7	4.46E-06	4.28E-07
391	HOC7H7 + C7H7 = OC7H7 + C7H8	-6.07E-06	-5.40E-14

Table 5.1.3.9
Cresol Consumption in Toluene Stirred Reactor

	ELEMENTARY REACTION	T=1188K τ=75 msec rate kmol/m^3/sec	T=2000K τ=75 msec rate kmol/m^3/sec
423	HOC7H7 + H = C6H5OH + CH3	3.31E-07	1.33E-07
422	HOC7H7 + H = C7H8 + OH	1.47E-07	9.25E-08
421	HOC7H7 + H = OC7H7 + H2	4.91E-08	2.02E-07

Table 5.1.3.10
Benzoyl Radical Consumption in Toluene Stirred Reactor

	ELEMENTARY REACTION	T=1188K τ=75 msec rate kmol/m^3/sec	T=2000K τ=75 msec rate kmol/m^3/sec
424	C6H5CO = C6H5 + CO	1.96E-05	2.35E-05

Table 5.1.3.11
Benzene Consumption in Toluene Stirred Reactor

	ELEMENTARY REACTION	T=1188K τ=75 msec rate kmol/m^3/sec	T=2000K τ=75 msec rate kmol/m^3/sec
326	C6H6 + O = C6H5O + H	2.43E-06	9.46E-06
328	C6H6 + OH = C6H5 + H2O	1.40E-06	3.57E-06
325	C6H6 + H = C6H5 + H2	1.38E-07	1.56E-06
312	C4H5(T) + C2H2 = C6H6 + H	5.18E-08	-1.69E-07
324	C6H6 = C6H5 + H	-2.67E-08	-1.37E-05
327	C6H6 + O = C6H5 + OH	2.77E-08	5.48E-07
332	C6H6 + OH = C6H5OH + H	2.35E-08	1.22E-06
330	C6H6 + CH3 = C6H5 + CH4	1.96E-08	-5.68E-11
267	C4H4 + C2H3 = C6H6 + H	6.05E-10	-9.30E-09
329	C6H6 + O2 = C6H5O + OH	-6.51E-10	1.72E-10
378	C6H6 + CH2(S) = C7H8L	2.90E-12	-3.13E-09

Table 5.1.3.12
Linear C_7H_8 Consumption in Toluene Stirred Reactor

ELEMENTARY REACTION	T=1188K τ=75 msec rate kmol/m^3/sec	T=2000K τ=75 msec rate kmol/m^3/sec
379 C7H8L = C7H8	7.01E-13	-3.13E-09

Table 5.1.3.13
Phenyl Radical Consumption in Toluene Stirred Reactor

ELEMENTARY REACTION	T=1188K τ=75 msec rate kmol/m^3/sec	T=2000K τ=75 msec rate kmol/m^3/sec
320 C6H5 + O2 = C6H5O + O	2.60E-05	3.30E-06
322 C6H5L = C6H5	-8.27E-07	-2.49E-05
438 C6H5 + O2 = C6H4 + HO2	3.14E-07	5.70E-05
385 C7H8 = C6H5 + CH3	-2.44E-07	7.22E-05
322 C6H5 + OH = C6H4 + H	2.45E-08	1.53E-05
317 C6H5 = C6H4 + H	-5.30E-09	9.63E-07
319 C6H5 + H = C6H4 + H2	-4.15E-10	9.03E-08

Table 5.1.3.14
Linear C_6H_5 Radical Consumption in Toluene Stirred Reactor

ELEMENTARY REACTION	T=1188K τ=75 msec rate kmol/m^3/sec	T=2000K τ=75 msec rate kmol/m^3/sec
322 C6H5L = C6H5	-8.27E-07	-2.49E-05
323 C6H5L = C6H4L + H	-1.40E-09	3.49E-06
266 C4H4 + C2H2 = C6H5L + H	-6.95E-10	-1.20E-08
239 C3H3 + C3H3 = C6H5L + H	-2.48E-10	-1.74E-05
311 C6H5L = C4H3(N) + C2H2	-2.53E-13	3.95E-06
371 C6H5L + H = C6H4L + H2	7.06E-14	5.59E-09
372 C6H5L + OH = C6H4L + H2O	1.74E-14	4.23E-09

Table 5.1.3.15
Phenoxy Radical Consumption in Toluene Stirred Reactor

ELEMENTARY REACTION	T=1188K τ=75 msec rate kmol/m^3/sec	T=2000K τ=75 msec rate kmol/m^3/sec
336 C6H5O = C5H5 + CO	2.67E-05	2.22E-05
331 C6H5O + H = C6H5OH	3.70E-06	-8.70E-06

Table 5.1.3.16
Phenyl Alcohol Consumption Consumption in Toluene Stirred Reactor

ELEMENTARY REACTION								T=1188K τ=75 msec rate kmol/m^3/sec	T=2000K τ=75 msec rate kmol/m^3/sec
335	C6H5OH	+	OH	=	C6H5O	+	H2O	1.54E-06	4.05E-07
441	C6H5OH	+	C6H5	=	C6H5O	+	C6H6	2.74E-07	5.31E-12
334	C6H5OH	+	O	=	C6H5O	+	OH	1.59E-07	2.50E-07
333	C6H5OH	+	H	=	C6H5O	+	H2	1.16E-07	9.04E-08
440	C6H5OH	+	C2H3	=	C6H5O	+	C2H4	9.83E-08	3.16E-13
390	C6H5OH	+	C7H7	=	C6H5O	+	C7H8	1.31E-08	1.24E-15
337	C6H5OH			=	C5H6	+	CO	3.58E-10	9.25E-08

Table 5.1.3.17
Cyclopentadiene Consumption in Toluene Stirred Reactor

ELEMENTARY REACTION								T=1188K τ=75 msec rate kmol/m^3/sec	T=2000K τ=75 msec rate kmol/m^3/sec
345	C5H6	+	O2	=	C5H5	+	HO2	1.33E-05	6.90E-10
344	C5H6	+	OH	=	C5H5	+	H2O	2.30E-06	4.62E-08
346	C5H6	+	H	=	C5H5	+	H2	1.70E-06	2.90E-08
343	C5H6	+	O	=	C5H5	+	OH	3.18E-07	1.07E-08
436	C5H5	+	C6H5O	=	C5H5	+	C6H5OH	1.81E-08	-8.53E-16
347	C5H6	+	HO2	=	C5H5	+	H2O2	1.90E-09	4.64E-14

Table 5.1.3.18
Cyclopentadienyl Consumption in Toluene Stirred Reactor

ELEMENTARY REACTION								T=1188K τ=75 msec rate kmol/m^3/sec	T=2000K τ=75 msec rate kmol/m^3/sec
338	C5H5	+	H	=	C5H6			1.96E-05	-5.39E-09
342	C5H5	+	HO2	=	C5H5O	+	OH	8.07E-06	-2.92E-09
339	C5H5	+	O	=	C4H5(T)	+	CO	6.58E-06	1.04E-05
341	C5H5	+	OH	=	C5H4OH	+	H	5.20E-06	4.25E-06
340	C5H5	+	O	=	C5H5O			1.30E-06	1.54E-06
350	C5H5			=	C5H5L			3.11E-08	6.11E-06

APPENDIX H
FINAL *n*-HEPTANE AND TOLUENE SUB-MECHANISM

TABLE H1
n-Heptane and Toluene Sub-mechanism for Diffusion Flames and Stirred Reactors

	ELEMENTARY REACTION										A m^3, Kmol, sec^{-1}	n	E_a J/mol	REF
273	C4H5(T)			=	C2H2	+	C2H3				0.4000E+13	0	0.1920E+06	24
317	C6H5			=	C6H4	+	H				0.3000E+14	0	0.3724E+06	24
323	C6H5L			=	C6H4L	+	H				0.8000E+12	0	0.1536E+06	24
326	C6H6	+	O	=	C6H5O	+	H				0.2780E+11	0	0.2054E+05	104
331	C6H5O	+	H	=	C6H5OH						0.2500E+12	0	0.0000E+00	103
336	C6H5O			=	C5H5	+	CO				0.1590E+12	0	0.1837E+06	102
339	C5H5	+	O	=	C4H5(T)	+	CO				0.5000E+11	0	0.0000E+00	29, See Text
371	C6H5L	+	H	=	C6H4L	+	H2				0.1000E+12	0	0.0000E+00	24
372	C6H5L	+	OH	=	C6H4L	+	H2O				0.2000E+11	0	0.0000E+00	24
373	C5H6	+	O2	=	C5H5O	+	OH				0.0000E+11	0	0.8666E+05	Removed, See Text
378	C6H6	+	CH2(S)	=	C7H8L						0.1000E+11	0	0.3567E+05	19,22
379	C7H8L			=	C7H8						0.3000E+11	0	0.0000E+00	19,22
380	C7H8	+	OH	=	C7H7	+	H2O				0.1260E+11	0	0.1081E+05	92
381	C7H8	+	O2	=	C7H7	+	HO2				0.3000E+12	0	0.1733E+06	29
382	C7H8	+	H	=	C7H7	+	H2				0.5000E+12	0	0.5230E+05	96
383	C7H8	+	H	=	C6H6	+	CH3				0.1200E+11	0	0.2143E+05	91
384	C7H8			=	C6H5	+	CH3				0.1400E+17	0	0.4176E+06	29
385	C7H7	+	H	=	C7H8						0.1800E+12	0	0.0000E+00	29
386	C7H8	+	C6H5	=	C6H6	+	C7H7				0.2100E+10	0	0.1842E+05	29
387	C7H8	+	CH3	=	C7H7	+	CH4				0.3160E+09	0	0.3977E+05	29
388	C7H8	+	O	=	OC7H7	+	H				0.1630E+11	0	0.1431E+05	29
389	C6H5OH	+	C7H7	=	C6H5O	+	C7H8				0.1050E+09	0	0.3977E+05	29
390	HOC7H7	+	C7H7	=	OC7H7	+	C7H8				0.1050E+09	0	0.3977E+05	29
391	C7H7	+	O	=	C7H6O	+	H				0.2500E+12	0	0.0000E+00	29
392	C7H7	+	O	=	C6H5	+	CH2O				0.8000E+11	0	0.0000E+00	29
393	C7H7	+	HO2	=	C7H6O	+	H	+	OH		0.2500E+12	0	0.0000E+00	29
394	C7H7	+	HO2	=	C6H5	+	CH2O	+	OH		0.8000E+11	0	0.0000E+00	29
395	C7H7	+	C7H7	=	C14H14						0.2510E+09	4	0.0000E+00	29
396	C8H10			=	C7H7	+	CH3				0.3090E+14	0	0.2510E+06	100
397	C7H7	+	OH	=	C7H7OH						0.6000E+11	0	0.0000E+00	29
398	C7H7OH	+	O2	=	C7H6O	+	HO2	+	H		0.2000E+12	0	0.1733E+06	29
399	C7H7OH	+	OH	=	C7H6O	+	H2O	+	H		0.8430E+10	0	0.1081E+05	29
400	C7H7OH	+	H	=	C7H6O	+	H2	+	H		0.8000E+11	0	0.3447E+05	29
401	C7H7OH	+	C7H7	=	C7H6O	+	C7H8	+	H		0.2110E+09	0	0.3977E+05	29
402	C7H7OH	+	C6H5	=	C7H6O	+	C6H6	+	H		0.1400E+10	0	0.1842E+05	29
403	C7H6O	+	O2	=	C6H5CO	+	HO2				0.1020E+11	0	0.1630E+06	29
404	C7H6O	+	OH	=	C6H5CO	+	H2O				0.1710E+07	1.18	-0.1871E+04	29
405	C7H6O	+	H	=	C6H5CO	+	H2				0.5000E+11	0	0.2063E+05	29
406	C7H6O	+	H	=	C6H6	+	CHO				0.1200E+11	0	0.2155E+05	29
407	C7H6O	+	O	=	C6H5CO	+	OH				0.9040E+10	0	0.1289E+05	29
408	C7H6O	+	C7H7	=	C7H8	+	C6H5CO				0.2770E+01	2.81	0.2417E+05	29
409	C7H6O	+	CH3	=	C6H5CO	+	CH4				0.2770E+01	2.81	0.2417E+05	29
410	C7H6O	+	C6H5	=	C6H5CO	+	C6H6				0.7010E+09	0	0.1842E+05	29
411	C7H6O	+	HO2	=	C6H5CO	+	H2O2				0.1000E+12	0	0.2093E+05	30
412	C7H6O			=	C6H5	+	CHO				0.1000E+17	0	0.3433E+06	30

TABLE H1 (CONTINUED)

413	C8H10	+	H	=	C8H8	+	H2	+	H	0.8000E+11	0	0.3447E+05	29
414	C8H10	+	O2	=	C8H8	+	HO2	+	H	0.2000E+12	0	0.1733E+06	29
415	OC7H7	+	H	=	HOC7H7					0.2500E+12	0	0.0000E+00	29
416	OC7H7			=	C6H6	+	H	+	CO	0.7900E+11	0	0.18740E+06	102, See Text
417	HOC7H7	+	OH	=	OC7H7	+	H2O			0.6000E+10	0	0.0000E+00	29
418	HOC7H7	+	H	=	C7H8	+	OH			0.2210E+11	0	0.3311E+05	29
419	HOC7H7	+	H	=	C6H5OH	+	CH3			0.1200E+11	0	0.2155E+05	29
420	C6H5CO			=	C6H5	+	CO			0.3980E+15	0	0.1231E+06	29
421	C6H5	+	C6H5	=	C12H10					0.1000E+10	0	0.0000E+00	30
422	C7H7			=	C7H7L					0.3160E+13	0	0.3567E+06	19,22
423	C7H7L			=	C5H5(L)	+	C2H2			0.1000E+13	0	0.1464E+06	19,22
424	C7H7L			=	C4H4	+	C3H3			0.2000E+13	0	0.3490E+06	19,22
425	C7H7L			=	C3H3	+	C2H2	+	C2H2	0.1780E+11	0	0.3549E+06	19,22
426	C7H7O			=	C7H6O	+	H			0.1270E+15	0	0.4614E+04	101
427	CH2O	+	HO2	=	CHO	+	H2O2			0.1990E+10	0	0.4879E+05	106
428	CH2O	+	CH3	=	CHO	+	CH4			0.5540E+01	2.81	0.2453E+05	1060
429	CH4	+	HO2	=	CH3	+	H2O2			0.1810E+09	0	0.7774E+05	105
430	C4H6(T)	+	O	=	C2H2O	+	C2H4			0.1000E+10	0	0.0000E+00	31
431	C4H6(T)	+	O	=	C3H4(P)	+	CH2O			0.1000E+10	0	0.0000E+00	31
432	C5H6	+	C6H5O	=	C6H5OH	+	C5H5			0.3160E+09	0	0.3347E+05	29
433	C6H5	+	OH	=	C6H4	+	H2O			0.2000E+11	0	0.0000E+00	24
434	C6H5	+	O2	=	C6H4	+	HO2			0.2610E+11	0	0.2561E+05	24
435	C6H5	+	O2	=	C6H5O	+	O			0.2090E+10	0	0.3125E+05	102
436	C6H5OH	+	C2H3	=	C6H5O	+	C2H4			0.6000E+10	0	0.0000E+00	29
437	C6H5OH	+	C6H5	=	C6H5O	+	C6H6			0.4910E+10	0	0.1841E+05	29
438	1-C4H7			=	C4H6(T)	+	H			0.1200E+15	0	0.2064E+06	31
439	1-C4H7			=	C2H4	+	C2H3			0.1000E+12	0	0.1549E+06	31
440	1-C4H7	+	H	=	C4H6(T)	+	H2			0.3160E+11	0	0.0000E+00	31
441	1-C4H7	+	O2	=	C4H6(T)	+	HO2			0.1000E+09	0	0.0000E+00	31
441	1-C4H7	+	CH3	=	C4H6(T)	+	CH4			0.1000E+11	0	0.0000E+00	31
443	1-C4H7	+	C2H3	=	C4H6(T)	+	C2H4			0.4000E+10	0	0.0000E+00	31
444	1-C4H7	+	C2H5	=	C4H6(T)	+	C2H6			0.4000E+10	0	0.0000E+00	31
445	1-C4H7	+	C2H5	=	1-C4H8	+	C2H4			0.5000E+09	0	0.0000E+00	31
446	1-C4H7	+	C3H5(A)	=	C4H6(T)	+	C3H6			0.4000E+11	0	0.0000E+00	31
447	1-C4H7	+	1-C4H7	=	C4H6(T)	+	1-C4H8			0.3160E+10	0	0.0000E+00	31
448	1-C4H8			=	1-C4H7	+	H			0.4070E+19	-1	0.4073E+06	31
449	1-C4H8			=	C3H5(A)	+	CH3			0.8000E+17	0	0.3096E+06	57
450	1-C4H8	+	O2	=	1-C4H7	+	HO2			0.4000E+10	0	0.1674E+06	57
451	1-C4H8			=	C2H3	+	C2H5			0.2000E+19	-1	0.4049E+06	57
452	1-C4H8	+	H	=	1-C4H7	+	H2			0.5000E+11	0	0.1632E+05	31
453	1-C4H8	+	OH	=	C3H7(N)	+	CH2O			0.6500E+10	0	0.0000E+00	57
454	1-C4H8	+	OH	=	C2H6	+	CH3	+	CO	0.1000E+08	0	0.0000E+00	31
455	1-C4H8	+	OH	=	1-C4H7	+	H2O			0.1750E+11	0	0.1280E+05	57
456	1-C4H8	+	O	=	C2H5	+	CH3	+	CO	0.1625E+11	0	0.3556E+04	57
457	1-C4H8	+	O	=	1-C4H7	+	OH			0.1300E+11	0	0.1883E+05	57
458	1-C4H8	+	HO2	=	1-C4H7	+	H2O2			0.1000E+09	0	0.7139E+05	57
459	1-C4H8	+	CH3	=	1-C4H7	+	CH4			0.1000E+09	0	0.3054E+05	31
460	1-C4H8	+	C2H5	=	1-C4H7	+	C2H6			0.1000E+09	0	0.3347E+05	57
461	1-C4H8	+	C3H5(A)	=	1-C4H7	+	C3H6			0.8000E+08	0	0.5188E+05	57
462	P-C4H9			=	C2H5	+	C2H4			0.2511E+14	0	0.1205E+06	59
463	P-C4H9			=	1-C4H8	+	H			0.1300E+14	0	0.1632E+06	59
464	P-C4H9	+	O2	=	1-C4H8	+	HO2			0.1000E+10	0	0.8368E+04	59
465	C5H9			=	C3H5(A)	+	C2H4			0.2500E+14	0	0.1255E+06	62
466	C5H9			=	C2H3	+	C3H6			0.2500E+14	0	0.1255E+06	62
467	C5H9			=	C4H6(S)	+	CH3			0.1000E+14	0	0.1339E+06	58
468	1-C5H10			=	C2H5	+	C3H5(A)			0.1000E+17	0	0.2989E+06	62
469	1-C5H11			=	C3H7(N)	+	C2H4			0.3200E+14	0	0.1188E+06	62

TABLE H1 (CONTINUED)

470	C7H16			=	C3H7(N)	+	P-C4H9	0.1300E+17	0	0.3428E+06	See text
471	C7H16			=	C2H5	+	1-C5H11	0.6500E+16	0	0.3433E+06	See text
472	C7H16			=	1-C6H13	+	CH3	0.6600E+16	0	0.3558E+06	See Text
473	C7H16			=	1-C7H15	+	H	0.1000E+16	0	0.4186E+06	32
474	C7H16			=	2-C7H15	+	H	0.1000E+16	0	0.4186E+06	32
475	C7H16			=	3-C7H15	+	H	0.1000E+16	0	0.4186E+06	32
476	C7H16			=	4-C7H15	+	H	0.1000E+16	0	0.4186E+06	32
477	C7H16	+	H	=	1-C7H15	+	H2	0.2810E+05	2	0.3223E+05	32
478	C7H16	+	H	=	2-C7H15	+	H2	0.9100E+04	2	0.2093E+05	32
479	C7H16	+	H	=	3-C7H15	+	H2	0.9100E+04	2	0.2093E+05	32
480	C7H16	+	H	=	4-C7H15	+	H2	0.4500E+04	2	0.2093E+05	32
481	C7H16	+	O	=	1-C7H15	+	OH	0.2300E+04	2.4	0.6656E+04	32
482	C7H16	+	O	=	2-C7H15	+	OH	0.6400E+03	2.5	0.2093E+05	32
483	C7H16	+	O	=	3-C7H15	+	OH	0.6400E+03	2.5	0.2093E+05	32
484	C7H16	+	O	=	4-C7H15	+	OH	0.3200E+03	2.5	0.2093E+05	32
485	C7H16	+	OH	=	1-C7H15	+	H2O	0.1050E+08	0.97	0.6656E+04	32
486	C7H16	+	OH	=	2-C7H15	+	H2O	0.4700E+05	1.61	0.0000E+00	32
487	C7H16	+	OH	=	3-C7H15	+	H2O	0.4700E+05	1.61	0.0000E+00	32
488	C7H16	+	OH	=	4-C7H15	+	H2O	0.4700E+05	1.61	0.0000E+00	32
489	C7H16	+	CH3	=	1-C7H15	+	CH4	0.3000E+10	0	0.4856E+05	32
490	C7H16	+	CH3	=	2-C7H15	+	CH4	0.1600E+10	0	0.3977E+05	32
491	C7H16	+	CH3	=	3-C7H15	+	CH4	0.1600E+10	0	0.3977E+05	32
492	C7H16	+	CH3	=	4-C7H15	+	CH4	0.8000E+09	0	0.3977E+05	32
493	C7H16	+	HO2	=	1-C7H15	+	H2O2	0.1120E+11	0	0.8121E+05	32
494	C7H16	+	HO2	=	2-C7H15	+	H2O2	0.6800E+10	0	0.7116E+05	32
495	C7H16	+	HO2	=	3-C7H15	+	H2O2	0.6800E+10	0	0.7116E+05	32
496	C7H16	+	HO2	=	4-C7H15	+	H2O2	0.3420E+10	0	0.7116E+05	32
497	C7H16	+	C2H5	=	1-C7H15	+	C2H6	0.1000E+09	0	0.5609E+05	32
498	C7H16	+	C2H5	=	2-C7H15	+	C2H6	0.1000E+09	0	0.4353E+05	32
499	C7H16	+	C2H5	=	3-C7H15	+	C2H6	0.1000E+09	0	0.4353E+05	32
500	C7H16	+	C2H5	=	4-C7H15	+	C2H6	0.5010E+08	0	0.4353E+05	32
501	C7H16	+	C2H3	=	1-C7H15	+	C2H4	0.1000E+10	0	0.7535E+05	32
502	C7H16	+	C2H3	=	2-C7H15	+	C2H4	0.7940E+09	0	0.7033E+05	32
503	C7H16	+	C2H3	=	3-C7H15	+	C2H4	0.7940E+09	0	0.7033E+05	32
504	C7H16	+	C2H3	=	4-C7H15	+	C2H4	0.3980E+09	0	0.7033E+05	32
505	C3H5(A)	+	C7H16	=	1-C7H15	+	C3H6	0.3980E+09	0	0.7870E+05	32
506	C3H5(A)	+	C7H16	=	2-C7H15	+	C3H6	0.8000E+09	0	0.7033E+05	32
507	C3H5(A)	+	C7H16	=	3-C7H15	+	C3H6	0.8000E+09	0	0.7033E+05	32
508	C3H5(A)	+	C7H16	=	4-C7H15	+	C3H6	0.4000E+09	0	0.7033E+05	32
509	C7H16	+	O2	=	1-C7H15	+	HO2	0.2510E+11	0	0.2051E+06	32
510	C7H16	+	O2	=	2-C7H15	+	HO2	0.3980E+11	0	0.1993E+06	32
511	C7H16	+	O2	=	3-C7H15	+	HO2	0.4000E+11	0	0.1993E+06	32
512	C7H16	+	O2	=	4-C7H15	+	HO2	0.2000E+11	0	0.1993E+06	32
513	1-C7H15			=	C2H4	+	1-C5H11	0.2520E+14	0	0.1206E+06	32
514	2-C7H15			=	C3H6	+	P-C4H9	0.1600E+14	0	0.1185E+06	32
515	3-C7H15			=	C3H7(N)	+	1-C4H8	0.5000E+13	0	0.1218E+06	32
516	4-C7H15			=	1-C5H10	+	C2H5	0.1080E+14	0	0.1172E+06	32
517	1-C7H15			=	1-C7H14	+	H	0.1000E+14	0	0.1691E+06	32
518	2-C7H15			=	1-C7H14	+	H	0.1000E+14	0	0.1691E+06	32
519	2-C7H15			=	2-C7H14	+	H	0.1000E+14	0	0.1691E+06	32
520	3-C7H15			=	2-C7H14	+	H	0.1000E+14	0	0.1691E+06	32
521	3-C7H15			=	3-C7H14	+	H	0.1000E+14	0	0.1691E+06	32
522	4-C7H15			=	3-C7H14	+	H	0.1000E+14	0	0.1691E+06	32
523	1-C7H15			=	2-C7H15			0.2000E+12	0	0.4647E+05	32
524	1-C7H15			=	3-C7H15			0.2000E+12	0	0.7577E+05	32
525	1-C7H15			=	4-C7H15			0.1000E+12	0	0.8372E+05	32
526	2-C7H15			=	3-C7H15			0.2000E+12	0	0.8372E+05	32

TABLE H1 (CONTINUED)

527	1-C7H15	+	O2	=	1-C7H14	+	HO2				0.1000E+10	0	0.8372E+04	32
528	2-C7H15	+	O2	=	1-C7H14	+	HO2				0.1000E+10	0	0.1884E+05	32
529	2-C7H15	+	O2	=	2-C7H14	+	HO2				0.2000E+10	0	0.1779E+05	32
530	3-C7H15	+	O2	=	2-C7H14	+	HO2				0.2000E+10	0	0.1779E+05	32
531	3-C7H15	+	O2	=	3-C7H14	+	HO2				0.2000E+10	0	0.1779E+05	32
532	4-C7H15	+	O2	=	3-C7H14	+	HO2				0.4000E+10	0	0.1779E+05	32
533	1-C7H14			=	C3H5(A)	+	P-C4H9				0.2520E+17	0	0.2976E+06	32
534	2-C7H14			=	C3H7(N)	+	1-C4H7				0.1600E+17	0	0.2901E+06	32
535	3-C7H14			=	C2H5	+	C5H9				0.3600E+16	0	0.2972E+06	32
536	C7H16	+	1-C4H7	=	1-C7H15	+	1-C4H8				0.1000E+10	0	0.8372E+05	32
537	C7H16	+	1-C4H7	=	2-C7H15	+	1-C4H8				0.1580E+09	0	0.7953E+05	32
538	C7H16	+	1-C4H7	=	3-C7H15	+	1-C4H8				0.1580E+09	0	0.7953E+05	32
539	C7H16	+	1-C4H7	=	4-C7H15	+	1-C4H8				0.8000E+08	0	0.7953E+05	32
540	C7H16	+	CH3O	=	1-C7H15	+	CH3OH				0.3160E+09	0	0.2930E+05	32
541	C7H16	+	CH3O	=	2-C7H15	+	CH3OH				0.2190E+10	0	0.2093E+05	32
542	C7H16	+	CH3O	=	3-C7H15	+	CH3OH				0.2190E+10	0	0.2093E+05	32
543	C7H16	+	CH3O	=	4-C7H15	+	CH3OH				0.1090E+09	0	0.2093E+05	32
544	3-C7H15			=	C6H12	+	CH3				0.8000E+13	0	0.1381E+06	32
545	3-C7H14			=	C6H11	+	CH3				0.5300E+17	0	0.3056E+06	32
546	1-C7H14	+	H	=	C7H13	+	H2				0.8000E+11	0	0.1423E+05	32
547	2-C7H14	+	H	=	C7H13	+	H2				0.1600E+12	0	0.1423E+05	32
548	3-C7H14	+	H	=	C7H13	+	H2				0.1600E+12	0	0.1423E+05	32
549	1-C7H14	+	O	=	C7H13	+	OH				0.4000E+11	0	0.1674E+05	32
550	2-C7H14	+	O	=	C7H13	+	OH				0.8000E+11	0	0.1674E+05	32
551	3-C7H14	+	O	=	C7H13	+	OH				0.8000E+11	0	0.1674E+05	32
552	1-C7H14	+	OH	=	C7H13	+	H2O				0.2000E+11	0	0.1088E+05	32
553	2-C7H14	+	OH	=	C7H13	+	H2O				0.4000E+11	0	0.1088E+05	32
554	3-C7H14	+	OH	=	C7H13	+	H2O				0.4000E+11	0	0.1088E+05	32
555	1-C7H14	+	CH3	=	C7H13	+	CH4				0.2000E+09	0	0.2847E+05	32
556	2-C7H14	+	CH3	=	C7H13	+	CH4				0.4000E+09	0	0.2847E+05	32
557	3-C7H14	+	CH3	=	C7H13	+	CH4				0.4080E+09	0	0.2847E+05	32
558	1-C7H14	+	HO2	=	C7H13	+	H2O2				0.5000E+10	0	0.0000E+00	32
559	2-C7H14	+	HO2	=	C7H13	+	H2O2				0.5000E+10	0	0.0000E+00	32
560	3-C7H14	+	HO2	=	C7H13	+	H2O2				0.5000E+10	0	0.0000E+00	32
561	1-C7H14	+	O	=	C2H3	+	1-C5H10	+	OH		0.2820E+11	0	0.2177E+05	32
562	1-C7H14	+	O	=	C3H5(A)	+	1-C4H8	+	OH		0.2820E+11	0	0.2177E+05	32
563	1-C7H14	+	O	=	1-C4H7	+	C3H6	+	OH		0.2820E+11	0	0.2177E+05	32
564	1-C7H14	+	O	=	C5H9	+	C2H4	+	OH		0.5000E+11	0	0.3286E+05	32
565	2-C7H14	+	O	=	C3H5(T)	+	1-C4H8	+	OH		0.2820E+11	0	0.2177E+05	32
566	2-C7H14	+	O	=	1-C4H7	+	C3H6	+	OH		0.2820E+11	0	0.2177E+05	32
567	2-C7H14	+	O	=	C5H9	+	C2H4	+	OH		0.5000E+11	0	0.3286E+05	32
568	3-C7H14	+	O	=	1-C4H7	+	C3H6	+	OH		0.2820E+11	0	0.2177E+05	32
569	3-C7H14	+	O	=	C5H9	+	C2H4	+	OH		0.5000E+11	0	0.3286E+05	32
570	1-C7H14	+	OH	=	C2H3	+	1-C5H10	+	H2O		0.1290E+07	1.25	0.2930E+04	32
571	1-C7H14	+	OH	=	C3H5(A)	+	1-C4H8	+	H2O		0.1290E+07	1.25	0.2930E+04	32
572	1-C7H14	+	OH	=	1-C4H7	+	C3H6	+	H2O		0.1290E+07	1.25	0.2930E+04	32
573	1-C7H14	+	OH	=	C5H9	+	C2H4	+	H2O		0.4270E+07	1.05	0.7577E+04	32
574	2-C7H14	+	OH	=	C3H5(A)	+	1-C4H8	+	H2O		0.1160E+07	1.25	0.2930E+04	32
575	2-C7H14	+	OH	=	1-C4H7	+	C3H6	+	H2O		0.1160E+07	1.25	0.2930E+04	32
576	2-C7H14	+	OH	=	C5H9	+	C2H4	+	H2O		0.4270E+07	1.05	0.7577E+04	32
577	3-C7H14	+	OH	=	1-C4H7	+	C3H6	+	H2O		0.1160E+07	1.25	0.2930E+04	32
578	3-C7H14	+	OH	=	C5H9	+	C2H4	+	H2O		0.4270E+07	1.05	0.2930E+04	32
579	C7H13			=	C3H5(A)	+	1-C4H8				0.2520E+14	0	0.1256E+06	32
580	C7H13			=	C3H4(A)	+	P-C4H9				0.1000E+14	0	0.1256E+06	32
581	C7H13			=	C4H6(S)	+	C3H7(N)				0.1000E+14	0	0.1340E+06	32
582	1-C6H13			=	2-C6H13						0.2000E+12	0	0.7577E+05	32
583	1-C6H13			=	C2H4	+	P-C4H9				0.2520E+14	0	0.1206E+06	32
584	2-C6H13			=	C3H7(N)	+	C3H6				0.1600E+14	0	0.1185E+06	32
585	1-C6H12			=	C3H7(N)	+	C3H5(A)				0.7940E+15	0	0.2976E+06	74
586	1-C6H12			=	C3H6	+	C3H6				0.3980E+13	0	0.2414E+06	74
587	1-C6H12	+	H	=	C6H11	+	H2				0.8020E+11	0	0.1423E+05	32
588	1-C6H12	+	O	=	C6H11	+	OH				0.4000E+11	0	0.1674E+05	32

TABLE H1 (CONCLUDED)

589	1-C6H12	+	OH	=	C6H11	+	H2O			0.2000E+11	0	0.1088E+05	32
590	1-C6H12	+	CH3	=	C6H11	+	CH4			0.2000E+09	0	0.2846E+05	32
591	1-C6H12	+	HO2	=	C6H11	+	H2O2			0.1000E+09	0	0.7141E+05	32
592	1-C6H12	+	O	=	C2H3	+	1-C4H8	+	OH	0.2820E+11	0	0.2177E+05	32
593	1-C6H12	+	O	=	C3H5(A)	+	C3H6	+	OH	0.2820E+11	0	0.2177E+05	32
594	1-C6H12	+	O	=	1-C4H7	+	C2H4	+	OH	0.5010E+11	0	0.3286E+05	32
595	1-C6H12	+	O	=	CHO	+	1-C5H11			0.1000E+09	0	0.0000E+00	32
596	1-C6H12	+	O	=	CH3	+	P-C4H9	+	CO	0.1000E+09	0	0.0000E+00	32
597	1-C6H12	+	OH	=	C2H3	+	1-C4H8	+	H2O	0.6500E+07	1.25	0.2930E+04	32
598	1-C6H12	+	OH	=	C3H5(A)	+	C3H6	+	H_2O	0.6500E+07	1.25	0.2930E+04	32
599	1-C6H12	+	OH	=	1-C4H7	+	C2H4	+	H_2O	0.2150E+08	1.05	0.7577E+04	32
600	1-C6H12	+	OH	=	CH_2O	+	1-C5H11			0.1000E+09	0	0.0000E+00	32
601	1-C6H12	+	OH	=	C2H4O	+	P-C4H9			0.1000E+09	0	0.0000E+00	32
602	1-C6H11			=	C_3H_6	+	C_3H_5(A)			0.5040E+14	0	0.1256E+06	32
603	1-C6H11			=	C_2H_5	+	C_4H_6(T)			0.5000E+13	0	0.1340E+06	32
604	1-C5H11			=	1-C5H10	+	H			0.1300E+14	0	0.1615E+06	75
605	1-C5H10	+	H	=	C5H9	+	H2			0.2800E+11	0	0.1674E+01	61
606	1-C5H10	+	O	=	C5H9	+	OH			0.2540E+03	2.56	-0.4730E+01	61
607	1-C5H10	+	O	=	P-C4H9	+	CHO			0.1000E+09	0	0.0000E+00	61
608	1-C5H10		+ O	=	C3H7(N)	+	C2H3O			0.1000E+09	0	0.0000E+00	75
609	1-C5H10	+	O	=	1-C4H8	+	CH2O			0.8510E+09	0	0.0000E+00	76
610	1-C5H10	+	O	=	C2H4O	+	C3H6			0.8510E+10	0	0.0000E+00	76
611	1-C5H10	+	O	=	C3H5(A)	+	C2H4	+	OH	0.2000E+11	0	0.2930E+01	76
612	1-C5H10	+	O	=	C3H6	+	C2H3	+	OH	0.1000E+11	0	0.2930E+01	76
613	1-C5H10	+	OH	=	C5H9	+	H2O			0.6800E+11	0	0.1281E+01	75
614	1-C5H10	+	OH	=	P-C4H9	+	CH2O			0.1000E+09	0	0.0000E+00	75
615	1-C5H10	+	OH	=	C3H7(N)	+	C2H4O			0.1000E+09	0	0.0000E+00	75
616	1-C5H10	+	OH	=	C3H5(A)	+	C2H4	+	H2O	0.2000E+07	1.2	0.5023E+00	76
617	1-C5H10	+	OH	=	C3H6	+	C2H3	+	H2O	0.1000E+07	1.2	0.5023E+00	76
618	1-C5H10	+	O2	=	C5H9	+	HO2			0.4000E+10	0	0.1674E+03	76
619	1-C5H10	+	CH3	=	C5H9	+	CH4			0.1000E+09	0	0.3056E+02	75
620	1-C4H8	+	OH	=	C2H4O	+	C2H5			0.1000E+09	0	0.0000E+00	57
621	1-C4H8	+	O	=	C3H6	+	CH2O			0.2505E+10	0	0.0000E+00	57
622	1-C4H8	+	O	=	C2H4O	+	C2H4			0.1250E+11	0	0.3556E+04	57
623	C2H4O	+	M	=	CH3	+	CHO	+	M	0.7000E+13	0	0.3425E+06	31
624	C2H4O	+	H	=	C2H3O	+	H2			0.2100E+07	1.26	0.1009E+05	31
625	C2H4O	+	O	=	C2H3O	+	OH			0.5000E+10	0	0.7593E+04	31
626	C2H4O	+	O2	=	C2H3O	+	HO2			0.4000E+11	0	0.1641E+06	31
627	C2H4O	+	OH	=	C2H3O	+	H2O			0.2300E+08	0.73	-0.4698E+04	31
628	C2H4O	+	HO2	=	C2H3O	+	H2O2			0.3000E+10	0	0.4996E+05	31
629	C2H4O	+	CH2(T)	=	C2H3O	+	CH3			0.2500E+10	0	0.1589E+05	31
630	C2H4O	+	CH3	=	C2H3O	+	CH4			0.2000E-08	5.54	0.1029E+05	31
631	C2H3O			=	CH3	+	CO			0.2320E+27	-5	0.7505E+05	31
632	C2H3O	+	H	=	C2H2O	+	H2			0.2000E+11	0	0.0000E+00	31
633	C2H3O	+	CH3	=	C2H6	+	CO			0.5000E+11	0	0.0000E+00	31
634	C2H2O	+	O2	=	CH2O	+	CO2			0.1000E+07	0	0.0000E+00	77
635	CH3OH	+	HO2	=	CH3O	+	H2O2			0.6200E+10	0	0.8109E+05	31
636	CH3OH	+	OH	=	CH3O	+	H2O			0.1000E+11	0	0.7099E+04	31
637	CH3OH	+	O	=	CH3O	+	OH			0.1000E+11	0	0.1960E+05	31
638	CH3OH	+	CH2O	=	CH3O	+	CH3O			0.1530E+10	0	0.3331E+06	31
639	C3H8	+	C2H5	=	C3H7(N)	+	C2H6			0.3160E+09	0	0.5149E+05	78
640	CH2O	+	CH3O	=	CH3OH	+	CHO			0.6000E+09	0	0.1380E+05	31
641	CH2O	+	HO2	=	CHO	+	H2O2			0.2000E+10	0	0.4898E+05	79
642	CH2O	+	CH3	=	CHO	+	CH4			0.8913E-15	7.4	-0.4019E+04	77
643	C6H6			=	6C(S)	+	3H2			0.7500E+05	0	0.1715E+06	20-24
644	C2H2			=	2-C(S)	+	H2			0.1000E-11	0	0.1008E+06	20-24
645	C6H6			=	6C(S)	+	3H2			0.1000E-11	0	0.1008E+06	20-24
646	C(S)	+ OH		=	CO	+	H			0.1750E+01	0.5	0.0000E+00	20-24
647	C(S)	+ O		=	CO					0.1600E+02	0.5	0.9312E+05	20-24
648	C(S)	+ C(S)	+O2	=	CO	+	CO			0.4650E+01	0.5	0.9353E+05	20-24
649	C(S)	+ H2O		=	CO	+	H2			0.2860E-30	0.5	0.6094E+05	20-24